

---

# An Electrochemical System for DNA Microarray Fabrication

RYAN DAVID EGELAND  
LINCOLN COLLEGE  
UNIVERSITY OF OXFORD

## ABSTRACT

This work demonstrates a new method for making oligonucleotide microarrays by synthesis *in situ*. The method uses conventional DNA synthesis chemistry with an electrochemical deblocking step. Acid is delivered to specific regions on a glass slide, thus allowing nucleotide addition only at chosen sites. Deblocking is complete in a few seconds, when competing side-product reactions are minimal. Results demonstrate the successful synthesis of 17-mers and discrimination of single-base pair mismatched hybrids. Features generated in this study are 40  $\mu\text{m}$  wide, with sharply defined edges. The synthetic technique may be applicable to fabrication of other molecular arrays.

The acid used for synthesis is produced by electrochemical oxidation of a reversible redox couple at microelectrodes. This work explores, in detail, the nature and pattern of the induced chemical change, and its dependence on the nature of the electrolyte and the strength and duration of current applied to the microelectrodes. Under suitable conditions, the active species is confined to micron-sized features and diffusion does not obscure the surface pattern produced. Experimental results, theoretical analysis, and digital simulation identify a chemical annihilation process critical to ensuring high feature resolution.

The microelectrodes used for synthesis are designed to sustain high currents, chemical attack, and mechanical wear so that many hundreds of syntheses can be performed with the same microelectrode set. Software, custom electronics, and a sealed piston and cylinder fluidics chamber allow synthesis automation. The electrochemical and mechanical system is robust and may be adapted to a range of other biomolecule syntheses.

---

# An Electrochemical System for DNA Microarray Fabrication

Ryan David Egeland  
Lincoln College  
University of Oxford

A thesis  
presented to the University of Oxford  
in fulfilment of the  
thesis requirement for the degree of  
Doctor of Philosophy  
in  
Biochemistry  
(with Support also from the  
Department of Engineering)

Oxford, England  
Trinity Term, 2003



---

## **Declaration**

I hereby declare that I am the sole author of this thesis.

I authorise the University of Oxford to lend this thesis to other institutions or individuals for the purpose of scholarly research.

Signature

I further authorise the University of Oxford to reproduce this thesis by photocopying or by other means, in total or in part, at the request of other institutions or individuals for the purpose of scholarly research.

Signature



---

## Acknowledgements

A team of supportive and encouraging individuals enabled the work presented in this thesis. Their kind attention to teaching, training, education, and above all, the excitement of science, created an enormously enjoyable and enriching learning experience for me at Oxford. I was continuously delighted to participate in a scientific and engineering team like none I had ever experienced. Far into the future, I am certain I will treasure the scientific pearls of experience, judgement and insight I have collected in the laboratory and at the chalkboard over the last few years. To those who cultivated these treasures, I owe an immeasurable debt of gratitude.

First, my supervisor and mentor, **Prof. Ed Southern**, has been the largest contributor to this endeavour. His kind invitation to join the group marked the beginning of an unbelievably enriching experience for me as a student. In the sense that this thesis marks the end of that phase, I regret to leave it behind. His many productive years as a scientist provided me with the historical context of my work. His creative spirit was contagious. His gentle stewardship probed neither too little nor too much. His ability to provide general direction, while leaving enough uncharted territory to me, ensured I never got lost, but never quite knew exactly where I was. The balance, I learned, is the essence of science. Ed's patience, wisdom, kindness, and most importantly, his enthusiasm made this work the journey of a lifetime.

I am forever grateful, also, to **Prof. Peter Dobson** of the Department of Engineering. He not only enabled my initial introduction to Ed's lab, but also provided an enormous amount of support in the engineering aspects of the work. His unlimited kindness and generosity, coupled with a tremendous depth of experience and command of the literature made him the first point of contact for all things engineering. All the microelectrodes I created in this work were fabricated in the **Engineering** clean-room; the resources Pete provided in this regard were of immeasurable value to the project's success. I cannot imagine a more helpful individual.

**Dr. Tim Fell** was the engineer who physically guided me into the challenging multi-disciplinary field of DNA microarray fabrication. His introduction to highly specialised clean-room techniques and equipment constituted a tremendous asset to the microelectrode fabrication part of my work. Certainly a year or more could have been wasted simply "getting up to speed" in the clean-room without Tim's help. His guidance also in overcoming the challenges involved in joining a new lab and style of education were critical to my sanity.

If tallied, the number of questions **Dr. Peter Leigh** (Dept. of Engineering) answered for me about clean-room work would probably number in the thousands. The daily operation of the clean-room was largely in his hands, and he could help with nearly any process. A large part of the fabrication process development is owed to Pete. **Martin Johnson** is equally commended for all his help with laboratory equipment, machining work, and general contributions to any scientific apparatus construction requirements in Biochemistry. **Dr. Frank Marken** (Dept of Physical Chemistry) aided with the theoretical electrochemistry; it is likely I would still be trying to decipher the electrochemical literature without his kind contributions. **Dr. John Elder** provided help on the electrochemical modelling work, and his careful proofreading was matched by none.

**Dr. Misha Shchepinov** and **Dr. Kalim Mir**, also of Ed's "oligo group," provided me with the largest staple of day-to-day support through their scientific tutorship, encouragement, and friendship. No student can survive the research process without good friends, and I am very fortunate to count Misha and Kalim as such. Lastly, I thank the **Rhodes Scholarship Trust** for the generous scholarship enabling my Oxford tenure.

---

## Abstract

This work demonstrates a new method for making oligonucleotide microarrays by synthesis *in situ*. The method uses conventional DNA synthesis chemistry with an electrochemical deblocking step. Acid is delivered to specific regions on a glass slide, thus allowing nucleotide addition only at chosen sites. Deblocking is complete in a few seconds, when competing side-product reactions are minimal. Results demonstrate the successful synthesis of 17-mers and discrimination of single-base pair mismatched hybrids. Features generated in this study are 40  $\mu\text{m}$  wide, with sharply defined edges. The synthetic technique may be applicable to fabrication of other molecular arrays.

The acid used for synthesis is produced by electrochemical oxidation of a reversible redox couple at microelectrodes. This work explores, in detail, the nature and pattern of the induced chemical change, and its dependence on the nature of the electrolyte and the strength and duration of current applied to the microelectrodes. Under suitable conditions, the active species is confined to micron-sized features and diffusion does not obscure the surface pattern produced. Experimental results, theoretical analysis, and digital simulation identify a chemical annihilation process critical to ensuring high feature resolution.

The microelectrodes used for synthesis are designed to sustain high currents, chemical attack, and mechanical wear so that many hundreds of syntheses can be performed with the same microelectrode set. Software, custom electronics, and a sealed piston and cylinder fluidics chamber allow synthesis automation. The electrochemical and mechanical system is robust and may be adapted to a range of other biomolecule syntheses.

---

*Dedicated to Mike Herron, Dr. Deborah Brooks-Golden, Dr. Pierce Flemming,  
and David and Jean Egeland for their support of a child's curiosity.*

---

## Table of Contents

Declaration .....	i
Acknowledgements .....	ii
Abstract.....	iii
Table of Contents.....	v
Chapter 1 Introduction.....	1
1.1 DNA Microarray Applications.....	1
1.2 Microarray Formats .....	2
1.3 Existing Microarray Fabrication Methods.....	3
1.4 Fabrication and Design Challenges .....	5
1.5 Electrochemical Patterning.....	6
1.6 <i>In situ</i> Electrochemical Biopolymer Synthesis.....	8
1.7 <i>In Situ</i> Electrochemical Microarray Fabrication .....	9
1.8 Organisation of this Thesis.....	10
Chapter 2 An Electrochemical System for Surface Patterning.....	13
2.1 Abstract .....	13
2.2 Introduction.....	14
2.3 Experimental Section .....	17
2.3.1 Materials.....	17
2.3.2 Microelectrode Array .....	18
2.3.3 Preparation of Glass Substrate .....	19
2.3.4 Reagent Delivery and Substrate Positioning .....	20
2.3.5 Acid Generation and Current Measurement.....	20
2.3.6 Acetylation and Fluorescent Reporter.....	21
2.3.7 Fluorescence Detection .....	21
2.3.8 Cyclic Voltammetry.....	22
2.4 Results and Discussion.....	22
2.4.1 Interaction of Acid at the Surface.....	22
2.4.2 Acid Generation .....	23
2.5 Conclusions.....	30
2.6 Acknowledgement .....	31
2.7 Figures .....	32

---

Chapter 3 A Microelectrode Array Device for High-Resolution <i>In Situ</i> Biomolecule Synthesis On Surfaces.....	40
3.1 Abstract .....	40
3.2 Introduction.....	41
3.3 Materials and Methods .....	44
3.3.1 Microelectrode Fabrication .....	44
3.3.2 Electronic Control and Measurement .....	47
3.3.3 Substrate Positioning and Fluidics .....	48
3.3.4 Computer Interface and Software.....	49
3.3.5 Reagents and Chemical Synthesis .....	50
3.3.6 Oligonucleotide Synthesiser and Interface .....	51
3.4 Results and Discussion.....	52
3.4.1 Microelectrode Arrays.....	52
3.4.2 Synthetic Control and Monitoring .....	55
3.4.3 Substrate Positioning and Reagent Delivery.....	56
3.4.4 Chemical Synthesis .....	57
3.5 Conclusions.....	60
3.6 Figures .....	62
3.7 Acknowledgements.....	72
Chapter 4 Electrochemically Directed Synthesis of Oligonucleotides for DNA Microarray Fabrication .....	73
4.1 Abstract .....	73
4.2 Introduction.....	74
4.3 Results.....	77
4.3.1 Electrochemical generation of acid by arrays of microelectrodes and interaction with an apposed substrate .....	78
4.3.2 Synthesis of oligonucleotides using electrochemical deblocking.....	80
4.3.3 Rates of deblocking and depurination and synthesis yields .....	81
4.4 Discussion.....	84
4.5 Methods.....	86
4.5.1 Electrode and reaction chamber assembly .....	86
4.5.2 Synthesis chemistry .....	87
4.5.3 Hybridisation to synthesised probes.....	88
4.6 Acknowledgements.....	89
4.7 Figures .....	90
Chapter 5 Discussion I Electrochemical Microarray Fabrication: Outcomes and Comparison with Existing Methods.....	96
5.1 Review .....	96
5.2 Uniformity, Consistency, and Reproducibility.....	98

---

---

5.2.1 Spotting Arrays .....	98
5.2.2 Electrochemical Arrays.....	99
5.3 Fidelity of Synthesis and Length of Probes .....	100
5.3.1 Relevance of Probe Length.....	100
5.3.2 Photolithographic Arrays .....	100
5.3.3 Ink-Jet Arrays .....	101
5.3.4 Electrochemical Arrays.....	101
5.4 Density of Probes .....	102
5.4.1 Spotting and Ink-Jet Arrays .....	103
5.4.2 Photolithographic Arrays .....	103
5.4.3 Electrochemical Arrays.....	104
5.5 Ease of Fluidics and System Integration .....	106
5.5.1 Challenges in Fluid Handling.....	106
5.5.2 Ink-Jet and Photolithographic Arrays .....	107
5.5.3 Electrochemical Arrays.....	108
5.6 Simplicity of Fabrication.....	110
5.7 Customisation of Probe Design.....	111
5.8 Range of Applications .....	113
5.9 Medical Applications .....	114
Chapter 6 Discussion II Diffusion, Annihilation, and Resolution: Theoretical Considerations and Digital Simulation.....	116
6.1 Context .....	116
6.2 Electrochemical Patterning.....	119
6.2.1 Existing Techniques and Limitations .....	119
6.2.2 The Utility of Annihilation.....	120
6.3 Annihilation Physics and Chemistry .....	121
6.4 Limits of Theory .....	125
6.5 A Computer Simulation .....	127
6.5.1 Setup.....	128
6.5.2 Simulation.....	129
6.5.3 Experimental Verification .....	133
6.6 Fundamental Physical Limits .....	135
6.7 Conclusions.....	137
6.8 Figures .....	138
Appendix A Microarrays in Biology and Medicine: A Review of Current Progress and Future Prospects .....	152
A.1 Abstract .....	152
A.2 Applications .....	153
A.3 Cancer .....	154

---

---

A.4 Functional Analysis.....	157
A.5 Drug Development.....	158
A.6 Toxicology.....	159
A.7 Infectious Disease.....	160
A.8 Further Topics.....	163
Appendix B Simulation of Electrochemically Activated Confined Chemical Patterning of Surfaces Using an Array of Microband Electrodes.....	164
Appendix C Tritylisation of Pyrene, Perylene and Coronene: A New Family of Switchable Fluorescent Labels.....	166
Appendix D Supplementary Confocal Image Data .....	173
Appendix E An Electrochemical Redox Couple Activated by Microelectrodes for Confined Chemical Patterning of Surfaces.....	186
Appendix F Microelectronics .....	194
Appendix G Mechanical Diagrams.....	202
Appendix H Oligonucleotide Synthesiser Modification and Control .....	207
Appendix I Software.....	218
Appendix J Current Measurements .....	243
References.....	253

---

*At the atomic level, we have new kinds of forces and new kinds of possibilities, new kinds of effects. The problems of manufacture and reproduction of materials will be quite different. I am, as I said, inspired by the biological phenomena in which chemical forces are used in repetitious fashion to produce all kinds of weird effects (one of which is the author).*

-R.P. Feynman, 1959



# Chapter 1

## Introduction

*This introduction briefly surveys the DNA microarray field and state of the art, with a primary discussion of fabrication technology and electrochemical patterning, the focus of this thesis.*

### 1.1 DNA Microarray Applications

High-throughput analytical techniques have recently revolutionised the discovery, investigation, and analysis of genetic information. DNA microarrays and DNA chip devices, used to perform DNA and RNA hybridisation analysis in a highly parallel, miniaturised fashion, have been applied to a wide range of applications in the context of basic biology and human disease<sup>a</sup>. At present, DNA microarray devices are used most extensively for large-scale gene expression<sup>1-3</sup> and single nucleotide polymorphism<sup>4,5</sup> analysis, but other applications include optimisation of antisense oligonucleotides<sup>6</sup>, basic studies of molecular hybridisation<sup>7,8</sup>, resequenc-

---

<sup>a</sup> For a review of DNA microarray applications in biology and medicine, see **Appendix A**.

ing genes to identify mutations<sup>9-11</sup>, and analysing DNA-protein interactions<sup>12</sup>. DNA microarrays have found uses in genetic, infectious disease, and cancer diagnosis, pharmacogenomics-based screening, environmental research, and forensic analysis. The use of DNA microarrays in these, and other unforeseen applications, will continue to propel revolutionary discovery and practical applications in biology and medicine.

## 1.2 Microarray Formats

DNA microarrays are made by attaching DNA probes to a solid substrate, generally glass, silicon dioxide, or plastic. The probes, typically synthetic oligonucleotides, amplicons, or larger DNA or RNA fragments, are attached to the substrate through covalent or non-covalent means. In the case of oligonucleotides, the many probes are either synthesised in-place on the substrate through stepwise base addition (termed “*in situ* arrays”), or prepared individually and then each deposited to the substrate separately (so-called “spotting arrays”). In either case, placing a different probe in each of hundreds or thousands of defined regions on the substrate allows a single chip to simultaneously perform many analyses, on each of many targets.

The analytical utility of microarray devices is driven by a number of important design characteristics. First, increasing the number of probes per chip in-

creases the number of analyses available per test. Second, increasing the density at which the probes are attached decreases the reaction time and the quantity of target analyte required per test. Third, ensuring fidelity and purity of the probes maximises resolvability and precision of hybridisation results. Fourth, the ability to use long probes allows maximisation of the probe-target hybridisation interaction (especially useful in expression analysis). Fifth, the flexibility to design any probe sequence at any location allows construction of comprehensive probe libraries (especially useful in resequencing or single nucleotide polymorphism analyses). Sixth, flexibility in the synthetic chemistry allows for the use of different chemistries so that probes can be made with different backbones and bases. Seventh, integration of target sample preparation and hybridisation detection with the rest of the device radically decreases the number of manual steps required for analysis (critical in any point-of-care or clinical setting). Achieving all these requirements in a single platform has been the goal of much microarray technology research. At present, achieving this goal has proved elusive.

### **1.3 Existing Microarray Fabrication Methods**

A wide range of chemical and engineering approaches have been devised to make arrays. The challenges in accurately attaching thousands of high-quality probes to a microscopic surface area, perhaps less than a square millimetre, have repre-

sented an active area of research, investigation, and development for at least a decade (several recent reviews<sup>13-15</sup> comprehensively survey the work). At present, intense research and development in the field, combined with diverse approaches to fabrication have created a wide variation in device capabilities and characteristics. Continued rapid evolution and persisting technologically heterogeneous approaches to array fabrication demonstrate that no single methodology has yet proven ideal.

Several means are presently used for microarray fabrication. One set of methods deposits spots of presynthesised nucleic acids on the surface of the support<sup>3</sup>, or on microbeads<sup>16</sup>. In others, probes are synthesised *in situ*<sup>17-20</sup>. Each method has its strengths and weaknesses. A photolithographic method provides high spatial resolution<sup>18</sup> and has proven successful for repeat manufacture of the same oligonucleotide sets. But as each oligonucleotide set requires a new mask set, the method is less suitable for custom designs. A new light-directed method<sup>21</sup>, which uses programmable microarrays of mirrors rather than masks, may eliminate this problem, and new photolabile protecting groups may improve coupling yields<sup>22</sup>, which are currently reported to be lower than in conventional oligonucleotide synthesis<sup>23</sup>. Physical masking<sup>24</sup> using mechanical flow cells and conventional synthetic chemistry gives high coupling yields and also provides high resolution, but is best used for sets of probes with related sequences, such as all sequences of a predetermined length, or tiling paths of all oligonucleotides

complementary to a gene of known sequence<sup>25</sup>. Ink jet fabrication is rapid, highly flexible and has a high throughput<sup>26-28</sup>. However, the accuracy in aiming droplets of reagents and their subsequent surface spread upon impact limits resolution<sup>20</sup>.

## 1.4 Fabrication and Design Challenges

Productive development of array fabrication techniques necessitates integration of chemical synthesis, automation, miniaturisation, microfluidics, quality control, basic biochemistry and molecular biology, and data collection and analysis techniques. This integration places high demands on device performance. Chemical synthesis methods must be developed allowing selective placement of oligonucleotides at specific locations on a solid material, combined with a means for permanent attachment or immobilisation. The enormous number of chemical steps involved makes automation of the process, through robotic or other digital means, absolutely necessary. Achieving high densities requires microscopic precision in manufacturing; technology adapted from the semiconductor industry provides useful solutions in this respect. However, as these techniques have conventionally been optimised for solid-phase and thin-film materials, means to apply the processes to solution-phase reactions require development of novel fluid handling and microfluidics systems. Ensuring high-fidelity over the complete, enormous set of probes is only accomplished through careful monitoring

and control of each of the thousands of chemical steps involved, and therefore, quality control of the manufacturing processes is critical. When ultimately applied to the interrogation of genetic material, devices must have characteristics which are compatible with molecular biology and biochemical protocols. Lastly, a convenient and efficient means must be developed to detect and record the results obtained from hybridisation of targets to the microarray device. Ideally, any means of array fabrication should also be inexpensive, flexible, and rapid.

This thesis describes novel solutions to these problems in the context of a fundamentally new electrochemical approach to *in situ* microarray fabrication.

## 1.5 Electrochemical Patterning

Frequently, electrochemical systems have been investigated in the context of analytical applications. Since Nernst pioneered descriptions of the relationship between electrical potential and thermodynamic properties of a chemical system in 1889, a wide range of theoretical analyses, techniques, and applications have produced a very large body of literature and specialised knowledge of all types of electrochemical processes. Indeed, electroanalytical techniques are applicable to almost every element in the periodic table<sup>29</sup>. Although less well-documented, electrochemistry has also been used for various steps in synthetic chemistry since the time of Faraday. Since then, hundreds of electro-organic synthesis processes

have been developed including, for example, the Kolbe reaction, reductive dimerisation, hydrogenation of heterocycles, fluorination, methoxylation, epoxidation, oxidation of aromatic hydrocarbons, and others<sup>30</sup> in bulk industrial scales.

More recently, synthetic electrochemical processes have been used in small-scale surface patterning. First pioneered by Alan Bard and colleagues a decade ago<sup>31</sup>, the typical format involves writing patterns with an active electrode “pen.” Termed “scanning electrochemical microscopy” (SECM), the electrode pen oxidises or reduces a metal on a surface as it is moved about to “draw” lines. Although recently-developed means of controlling diffusion<sup>32</sup> allow very high-resolution features, the method is impractical for array manufacture. Moving the tool to hundreds or thousands of probe locations on a surface and maintaining critical registration and alignment across many fabrication steps would make writing arrays by SECM tedious if not impossible.

Although not used in synthesising array probes, electrochemical processes have been used to perform single chemical steps relevant to microarray fabrication. Livache and colleagues have demonstrated electrochemically directed copolymerisation of pyrrole and pre-synthesised oligonucleotides containing electroactive substituents<sup>33,34</sup>. By selectively controlling the polymerisation at individually-addressed electrodes, electronic circuitry and software directed attachment of the oligonucleotides to up to 128 electrode pads. Other work has used microelectrodes to immobilise active enzymes<sup>35</sup> or a small array of peptides<sup>36</sup>, also

using redox products to initiate polymerisation reactions. In these demonstrations, custom electrochemically-active reagents allowed covalent probe attachment to the polymer matrix. Parallel synthesis of many probes is not possible with these techniques, as each oligonucleotide to be attached must be prepared individually. Furthermore, each electrode set can be used for only one array; the polymerisation process is not reversible.

## 1.6 *In situ* Electrochemical Biopolymer Synthesis

Although a recent literature review identified no publications describing microelectrode devices used to perform serial stepwise chemical steps in the context of *in situ* synthesis, it is likely that such work is underway<sup>5,37</sup>. It may be possible to perform chemical synthesis directly on microelectrode surfaces. A polymer coating on the microelectrodes provides a matrix on which covalent attachment of chemical moieties is performed electrochemically<sup>5,38</sup>. Several problems may arise with this approach. First, diffusion of redox products away from the immediate vicinity of the microelectrodes, and subsequent reduction of product concentration, may limit the maximum resolution. Generally the rate of spread of products in solution is inversely proportional to dimensions; patterning surfaces with solution-based chemistry becomes challenging below about 100  $\mu\text{m}$  if the synthetic reaction is not nearly instantaneous. Second, highly reactive redox products, in-



cluding free radicals, radical ions, and unstable intermediate products are produced at the solution-electrode interface<sup>30,39,40</sup>. These species may react to destroy the desired oligonucleotide or other synthetic product being made directly on the electrode surface. Third, as the synthetic product must be immobilised on a polymer in contact with the electrodes, the polymer itself must be compatible with the chemical synthesis, and with subsequent means of analysis. Fourth, synthesis of products on a matrix directly attached to the microelectrodes precludes reusing the microelectrodes for fabricating multiple arrays with the same electrode set. As such microelectrode devices are presently custom-made, fabrication expense could prove prohibitive.

## **1.7 *In Situ* Electrochemical Microarray Fabrication**

This thesis describes a new method for directing the synthesis of oligonucleotides on the surface of a solid support, which uses electrode arrays to induce electrochemical reactions in highly localised regions. The microarray of synthons is made on a planar substrate of either glass or silicon dioxide, the face of which is placed against the electrode array for the duration of synthesis. At each step of synthesis, acid is produced in confined regions by application of current to individual electrodes, directing patterned removal of protecting groups on the adjacent substrate. The electrochemical reaction used is reversible, compatible with

high-yield oligonucleotide synthesis, and confined to distinct regions without significant diffusion problems. This approach minimises the problems of other electrochemical approaches, yet has advantages of parallel synthesis flexibility in the synthetic chemistry.

## 1.8 Organisation of this Thesis

As typical of microarray technology in general, this work required the integration of techniques from a range of disciplines including materials science, engineering, chemistry, biology, electronics, and computer science. Presented as a series of publications or manuscripts, the description of the results is roughly divided into five sections as follows:

1. **Chapter 2. Electrochemical patterning:** investigation, characterisation, and optimisation of an electrochemical system compatible with the microelectrode characteristics and high-resolution surface patterning.
2. **Chapter 3. Materials, microelectronics, and engineering:** manufacture of suitable, robust microelectrodes, and development of a programmed power supply to deliver predetermined potential to each electrode independently for a preset duration with means to measure

current at each electrode, and construction of a computer-controlled and automated reaction system including a sealed chamber in which to carry out the electrochemistry and nucleotide coupling reactions.

3. **Chapter 4. Oligonucleotide synthesis:** optimisation and demonstration of oligonucleotide synthesis in high yield, and successful application to single-base mismatches detected with a 17 nucleotide base probe.
4. **Chapter 5. Discussion I:** summary and integration of the work as a whole in the context of other methods of array fabrication, and analysis and interpretation of aspects of this work not extensively covered in the manuscripts.
5. **Chapter 6. Discussion II:** theoretical considerations and digital simulations exploring the relationships between diffusion, annihilation, and pattern resolution.

Each manuscript in chapters 2, 3, and 4 is briefly introduced and reproduced in this thesis, with modification only in style. At a possible cost in some repetition of introductory remarks, this format affords the stylistic efficiency and brevity typical of scientific communications. The concluding **Discussion I** and **Discussion II** sections integrate the work as a whole and allow for further commentary and analysis not included in the manuscripts. **Appendix A** briefly highlights

some of the potential long-range applications of this work in a biological and medical context. **Appendix B** is a short paper resulting from extension of the topics presented in **Chapter 6**. **Appendix C** is a paper incorporating methods developed in this work including a demonstration of localised acid production in real-time using a pH-sensitive reporter. **Appendix D** is **Chapter 2** in reprint format. **Appendix E** presents interesting results not included elsewhere, with brief descriptions and commentary. **Appendices F-J** provide further complete engineering and experimental data not presented in the body of the thesis.

## Chapter 2

# An Electrochemical System for Surface Patterning

*This chapter focuses on the chemistry and electrochemistry components of this work. It was published as a full paper<sup>b</sup> in Analytical Chemistry in 2002 (a reprint is included in Appendix E). Frank Marken assisted in the cyclic voltammetry work as shown in Figure 3. All other experimental work and writing was conducted primarily by the author of this thesis.*

### 2.1 Abstract

Microelectrodes, printed as an array on the surface of a silicon chip, generate chemically active species in a solution of electrolyte held between the electrode array and a glass plate. The active species induce chemical change in molecules coupled to the surface of the glass plate, which is separated from the electrode array by a gap of several microns. This communication explores the nature and

---

<sup>b</sup> Paper authors: Ryan D. Egeland (corresponding), Frank Marken, Edwin M. Southern.

pattern of the induced chemical change, and its dependence on the nature of the electrolyte and the strength and duration of current applied to the microelectrodes. We show that under suitable conditions the active species is confined to micron-sized features and diffusion does not obscure the surface pattern produced.

## 2.2 Introduction

The techniques which revolutionised the manufacture of electronic components have recently been applied to biological and chemical systems. Small devices carrying molecules of DNA<sup>19,25,36,41-43</sup> or peptides<sup>44</sup> have been fabricated on glass, silicon and plastic substrates. These chemical and biological chips have been used in genomic analysis<sup>45,46</sup>, gene expression profiling<sup>47</sup>, drug analysis<sup>48,49</sup>, and in environmental and biological sample analysis<sup>50-54</sup>. Although several *in situ* fabrication techniques have been used to make these devices, there remain many significant technical challenges<sup>17,23</sup>.

There are two requirements for any *in situ* molecular fabrication method. First, it must be able to apply the methods of chemical synthesis to make molecules of defined structure on a solid substrate. Second, it must be capable of creating the molecular features in spatially defined regions. Many organic syntheses follow stepwise pathways in which an active group is exposed by removal of a

protecting group and then coupled with an active reagent<sup>55-57</sup>. Nucleic acid and peptide syntheses utilise this approach<sup>58</sup>; these chemistries were first adapted to solid-state synthesis and then to patterned synthesis on planar substrates. In these and other syntheses, protecting groups are typically removed by acid or base.

Methods that have been used for patterned *in situ* synthesis include ink-jet application of deprotection agents<sup>28</sup>, application of precursors by physical masking<sup>8,24,59</sup> or ink-jet printing<sup>26,27,60,61</sup>, application of physical masks by photolithography<sup>62</sup>, and removal of photo-labile protecting groups by photomasking<sup>17,18</sup>. Although these methods have proven useful, each has certain disadvantages. Physical masking is only suitable when the synthetic pattern may be formed by overlapping placements of the mask; the resolution of the ink-jet method is limited by the accuracy in aiming droplets of reagents and by surface spread on the surface; the photolithographic methods require special photosensitive reagents and expensive mask set fabrication for each pattern produced.

In this work, we explore a method of patterning a surface using electrochemically generated reagents. Electrochemically produced reagents include acids, bases, radicals, reactive gases or ions, metals, and many types of reducing and oxidizing species<sup>30,39,40,63-66</sup>. The amount and reactivity of reagents is controlled by the choice of electrolyte solution or the applied voltage. This fine regulation of

the chemical conditions may thus permit a degree of reaction control not possible with other fabrication methods.

Electrochemical methods described previously use single active electrodes<sup>40</sup> and are not suitable for creating large numbers of small features. We describe a new approach using an array of individually-addressable electrodes placed in close proximity to the treated surface. The electrodes generate active reagent which reacts with molecules on the surface. In the examples described here, active reagent is an acid, generated at anodes.

The elements of the microelectrode array are individually addressable, so independent pattern features may be generated in parallel. Furthermore, using anodes and cathodes in close proximity introduces a means of controlling reactant diffusion. In systems utilizing a single isolated electrode to generate an active species, such as scanning electrochemical microscopy (SECM), reactants diffuse rapidly from the vicinity of the electrode. A number of electrical and chemical means have been used to confine the reagents generated at the microelectrode<sup>67,68</sup>, but diffusion is intrinsic to any reagent in solution. For example, a small 1.7  $\mu\text{m}$  electrode generates a 250  $\mu\text{m}$  pattern after 20 s which grows to the relatively macroscopic dimension of 400  $\mu\text{m}$  after 80 s<sup>69</sup>. Such diffusion clearly limits creating many small features in close proximity. We have designed a chemical system which limits these effects.



A cathode-generated quenching reagent destroys acid everywhere but in regions close to the anode that generated it. This constraining effect of the counterelectrodes creates features which approach the size of the microelectrodes themselves. Unlike methods such as scanning electrochemical microscopy patterning where the tool must be physically manipulated to write a surface feature, this method allows rapid printing on a surface, with the printed pattern determined simply by microelectrode arrangement.

## 2.3 Experimental Section

### 2.3.1 Materials

Silicon wafers were used for creating the microelectrodes and as the solid supports for the electrochemical patterning. Wafers were purchased from AUREL GmbH (Landsberg, Germany) as P-type (boron doped), <100> orientation, 7-21 ohm cm resistivity, 100mm diameter, 518-532  $\mu\text{m}$  thick, "CZ Silicon Prime Wafers, SEMI standard." The wafers were thermally oxidised to yield a  $124 \pm 0.4$  nm surface thickness of silicon dioxide. Glycidoxypropyltrimethoxysilane (Sigma-Aldrich, Poole, England) was used as supplied. Polyethylene glycol (200 avg. mol. wt., Sigma-Aldrich) was used without further purification. Benzoquinone, hydroquinone, and tetrabutylammonium hexafluorophosphate

(Sigma-Aldrich) were dissolved in anhydrous acetonitrile (supplied as “phosphoramidite diluent,” Cruachem, Glasgow) under dry argon immediately before use. Dimethoxytrityl (DMT) was attached to the substrate as a thymidine  $\beta$ -cyanoethyl phosphoramidite (Cruachem) using standard DNA synthesis reagents (Cruachem). Equal volumes of acetic anhydride and dimethylaminopyridine (Cruachem) were used in solution for the acetylation. “Cy5 phosphoramidite” used for fluorescent reporting was purchased from Amersham Pharmacia Biotech (Buckinghamshire, England), and diluted with anhydrous acetonitrile (100mg/ml) before use. Iridium metal used for microelectrodes was 99.9% purity (Johnson Matthey Noble Metals, London).

### **2.3.2 Microelectrode Array**

The fabrication of a microelectrode array resistant to reduction, oxidation, chemical attack, and mechanical destruction presented certain challenges and will be described in detail elsewhere. Briefly, 96 linear electrodes were fabricated by electron-beam evaporation of 50nm iridium metal onto silicon wafers previously patterned with an organic photoresist using conventional UV-light photolithography. After removing the photoresist in acetone, the iridium was annealed by heating at 350° C for 30 minutes in air, and then cleaned by reactive ion etching (in oxygen and argon). The resulting microelectrodes, each measuring

$40 \pm 0.1 \mu\text{m}$  wide by  $750 \mu\text{m}$  long and separated by  $40 \mu\text{m}$  gaps, were connected to separate printed circuit board tracks via  $20 \mu\text{m}$  gold wire bonds.

### 2.3.3 Preparation of Glass Substrate

Polished, oxidised silicon wafers were used as the patterned surface supports. Before electrochemical patterning, the wafer surface was functionalised with a linker molecule to which the organic reagents were attached<sup>70</sup>. Wafers were placed in a 18.1 L vacuum furnace chamber with an ampoule containing 5 mL glycidoxypropyltrimethoxysilane. After heating the furnace to  $185^\circ\text{C}$ , the ampoule was heated to  $205^\circ\text{C}$  and the chamber evacuated to 25-30 mBar. After approximately 2.5 mL of the silane had evaporated, the chamber was allowed to cool under vacuum ( $10^{-3}$  Torr). A linker molecule was attached by immersing the glycidoxypropyltrimethoxysilane-derivatised wafers in 200 mL polyethylene glycol containing 100  $\mu\text{L}$  sulphuric acid. DMT-containing phosphoramidite was then covalently attached to the free hydroxyl on the polyethylene glycol by conventional oligonucleotide synthesis techniques<sup>58,71</sup> employing 3% dichloroacetic acid deblocking. The wafer substrate surface thus prepared was cut into 1 cm squares for use in patterning.

### 2.3.4 Reagent Delivery and Substrate Positioning

Reagents used for the electrochemically-directed synthetic steps were flushed across the entire substrate surface in an apparatus designed to hold the substrate a specified distance ( $20 \pm 1 \mu\text{m}$  in these experiments) from the microelectrode set (**Figure 1**). This distance could be increased by adjusting a digital micrometer head piston to allow large volumes of solvent or other reagent through the system as appropriate, and then re-established during the electrochemical acid generation.

### 2.3.5 Acid Generation and Current Measurement

A custom electronic circuit applied current in a parallel fashion to each of the electrodes independently and is described in detail elsewhere. Any electrode could be disconnected from the voltage source (made floating) by analogue multiplex switch integrated circuits. Voltages were applied at the anodes with respect to the cathodes (the electrochemical system is a two-electrode cell). As the current delivered to each individual electrode was very small (nanoamps), instrumentation amplifiers were employed in its measurement. A computer software program controlled this electronic circuit, and also automated delivery of reagents to the substrate.

### 2.3.6 Acetylation and Fluorescent Reporter

The loss of the acid-sensitive trityl protecting group on conventional phosphoramidites indicated regions where acid reached the substrate during the electrochemical deblocking step. After electrochemical patterning of a microscope slide coated with trityl-containing phosphoramidite, the entire surface was treated with a mixture of equal volumes of acetic anhydride and dimethylaminopyridine using an ABI 394 DNA synthesiser. This reagent renders the regions previously subject to acids unreactive towards further chemical modification. Remaining trityl groups were removed by treating the whole surface with dichloroacetic acid (DCA) and a subsequent final modification of the entire surface with Cy5 phosphoramidite resulted in fluorescence everywhere except those regions patterned by electrochemically generated acids.

### 2.3.7 Fluorescence Detection

Fluorescent molecules were detected using a Leica TCS NT confocal microscope. Confocal microscopy allowed examination of fluorescence in a single focal plane, thus eliminating background fluorescence while observing the monolayer. Before each measurement, the focal plane was adjusted to the height of the substrate on the microscope stage, and the photomultiplier tube (PMT) voltage adjusted to maximum sensitivity without saturation. The fluorescent units recorded for each

image are arbitrary and not directly comparable across experiments, as microscope adjustments were independent for each sample.

### 2.3.8 Cyclic Voltammetry

Voltammetric experiments were performed with an Autolab potentiostat system (Eco Chemie, The Netherlands) in a conventional three electrode cell with a platinum gauze counter electrode and a saturated Calomel (SCE) reference electrode. The cyclic voltammograms were obtained for the reduction and oxidation of an acetonitrile solution (0.1 M  $\text{NBu}_4\text{PF}_6$ ) of 2.5 mM benzoquinone and 2.5 mM hydroquinone at a 1 mm platinum disc electrode ( $T=22^\circ\text{C}$ ).

## 2.4 Results and Discussion

### 2.4.1 Interaction of Acid at the Surface

As an example of a step used widely in organic synthesis, we chose to study the thermodynamically and kinetically favourable removal of a dimethoxytrityl (DMT) group by mild acid to form a primary hydroxyl (an overall depiction of the process is shown in **Figure 2**). A glass chip was first derivatised with a linker to which a deoxyribo-thymidine (dT) phosphotriester was attached by conventional phosphoramidite coupling<sup>58</sup>. The dT carried a DMT group on the

5'-hydroxyl. We had previously verified that the DMT group could be removed efficiently by dilute sulphuric acid in acetonitrile.

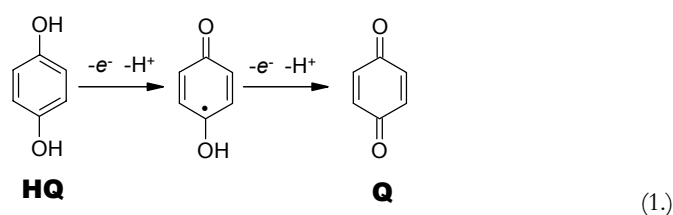
The objective was to remove this group using acid generated at the anodes of a microelectrode array placed against the glass chip by a substrate positioning apparatus allowing fine control of the distance between the electrodes and chip (**Figure 1**), and to acetylate the hydroxyl groups in the exposed regions by treatment of the whole surface with acetic anhydride. The DMT groups not removed by the electrochemical step were then removed by treating the whole surface with a solution of dichloroacetic acid in dichloromethane. The hydroxyl groups thus exposed were coupled to Cy5, a fluorescent dye, so that the pattern produced by the electrochemical generation of acid was revealed by observing the fluorescence of the Cy5 in a confocal microscope.

In the following sections, we discuss the processes which generate active species at the electrodes, the reaction which takes place on the substrate and the interactions which take place in the solution between the electrodes to destroy the species generated at the anode and cathode. We discuss the stoichiometry and kinetics of these processes.

### **2.4.2 Acid Generation**

We have explored the effects of varying the electrolyte solution and the results presented here were obtained with an electrolyte system optimised for the acety-

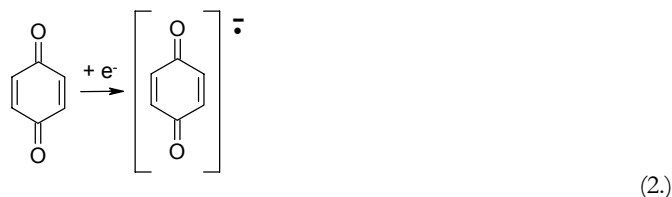
lation patterning process. Acid was generated at the anode by the oxidation of hydroquinone (HQ) to benzoquinone (Q) in acetonitrile. Although the mechanism was subject to some controversy in the early literature<sup>72-77</sup>, the oxidation half-reaction yields a clean source of protons at the anodes, as shown below:



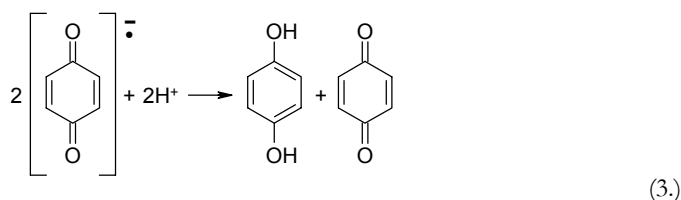
This oxidation of hydroquinone and the reduction of benzoquinone in these experiments was characterised by cyclic voltammetry in bulk electrolyte solution (see **Figure 3**). The two main processes detected under these conditions are the oxidation of hydroquinone ( $\text{P2}_{\text{ox}}$ ) at + 1.2 V *vs.* saturated Calomel electrode (SCE) peak potential (equation 1) and the reduction of benzoquinone ( $\text{P1}_{\text{red}}$ , equation 2 below) at -0.47 V *vs.* SCE peak potential. Two minor signals in the voltammogram may be attributed to the oxidation of hydroquinone in the deprotonated state ( $\text{P4}_{\text{ox}}$ ) and the reduction of benzoquinone in the presence of electrogenerated acid ( $\text{P3}_{\text{red}}$ ). Overall the reaction scheme is complex but in agreement with previous reports<sup>73</sup>.

The process at the cathodes is the reduction of benzoquinone, and yields a radical anion as follows<sup>78</sup>:





The radical anion is relatively stable, but may undergo follow-up chemical reactions in the presence of protons. We therefore speculated that acid in solution would be consumed by the cathodic radical anion as follows:



As the radical anion and proton are of opposite charge, we considered that electric field effects in depleted concentrations of supporting electrolyte may also act to enhance the annihilation of acid<sup>79</sup>.

We speculated that the acid generated in the anodic process (P2) would be strong enough to remove the acid labile DMT group. The voltage (applied at the anodes with respect to the cathodes) required to establish the pH gradient was expected to be between 0.9 V (difference between potentials for reduction P1 and oxidation P4) and 1.67 V (difference between reduction P1 and oxidation P2). Observations described below support this prediction and demonstrate that the rate of production of acid at the anodes and the rate of diffusion across the gap to the surface leads to complete removal of the DMT in a few seconds.

### 2.4.2.1 Stoichiometry and Kinetics

The rate of the patterning reaction is determined by the probability that protons in solution reach the immobilised DMT at the surface. We therefore found it instructive to compare the total number of hydroquinone molecules in solution to the number of DMT groups on the surface.

Before voltage is applied, the amount of DMT on the glass chip is ca. 10 pmol per mm<sup>2</sup> surface area<sup>80</sup>. The quantity of hydroquinone in a 20 µm depth of electrolyte solution overlying the surface is 500 pmol per mm<sup>2</sup>. Thus, oxidation of all the hydroquinone in this area would result in a 100-fold molar excess of acid assuming all protons transverse the electrode-surface gap and arrive evenly over the chip surface.

A true estimate of the number of protons generated at the anode can be obtained from measurement of the current. The number of protons ( $N_p$ ) produced during patterning of duration  $t$  is equal to the number of electrons ( $N_e$ ) removed from the anodes by the external voltage source, and was calculated from the applied current ( $i$ ) as follows:

$$N_p = N_e = \frac{\int_0^t i \cdot dt}{F} \quad (4.)$$

Where  $F$  is Faraday's constant (we assumed 100% current efficiency for these calculations). We designed an amplifier circuit to record current at each of the

microelectrodes to nanoamp precision, with negligible measured background current. We then used the electrodes to generate patterns and considered the amount of acid produced under various conditions.

We applied a range of DC potentials to anodes (with respect to cathodes) which were 7.5 mm long by 40  $\mu\text{m}$  wide and separated from adjacent cathodes by 40  $\mu\text{m}$  (the significance of the electrode arrangement is discussed later), with a depth of solution of 20  $\mu\text{m}$  between the electrode array and substrate. The rate of protons generated is very small at cell potentials below 1.2 V and increases exponentially above 1.3 V (**Figure 4**), with a corresponding increase in the rate of the patterning at the substrate (**Figure 5**). The current is high directly after the voltage is applied while the hydroquinone near the anodes is oxidised (as in a potential step experiment). It then reaches a diffusion-limited steady state near 1  $\mu\text{A}$  for a cell potential of 1.33 V after approximately 2 seconds, when the rate of anodic hydroquinone oxidation is balanced by its regeneration from benzoquinone and protons at the cathode.

We consider here the total amount of acid generated over an anode *vs.* the amount required to pattern the surface in a time course experiment where the electrodes were 7500  $\mu\text{m}$  long by 40  $\mu\text{m}$  wide and separated from adjacent cathodes by 40  $\mu\text{m}$ , with a depth of solution of 20  $\mu\text{m}$  between the electrode array and the substrate. At 1.33 V,  $2.0 \pm 0.1$  pmol protons are generated at each anode in 0.2 s, rising to  $800 \pm 40$  pmol in 80 s. This total quantity of acid generated

after 80 s is in vast excess to the DMT groups in the region of the substrate opposite the anode.

Analysis of the reaction at the surface of the substrate shows that reaction is essentially complete after about 4 s at 1.33 V, resulting in a 75  $\mu\text{m}$  wide pattern (**Figure 6**) and the complete detritylation of 30 pmol DMT. **Figure 7** shows stoichiometry calculated from replicates of the experiment in **Figure 6**, where  $N_r$  was calculated by measuring the surface area of the completely reacted stripe and multiplying by the known initial density of unreacted DMT on the surface, as described above. The amount of acid generated after 4s is  $40 \pm 2$  pmol. Some of this acid does not reach the substrate because it is consumed by an interaction with products diffusing locally from the cathode into the region between the electrodes.

#### 2.4.2.2 Diffusion and Proton Neutralisation

We believe the electrode arrangement presented in this communication causes consumption of anode-generated protons near the cathodes by the reaction shown in equation 3. Because we used cathodes situated only 40  $\mu\text{m}$  from the anodes, the products liberated at the cathodes diffuse rapidly to mix with the protons generated at the anodes allowing regeneration of hydroquinone and benzoquinone in the solution between the electrodes (complete reaction system as mentioned previously in **Figure 2**). These products can then diffuse into the re-

gion of the electrodes where they will take place in further electrochemical reactions.

**Figure 8** is a dramatic demonstration of this effect; a single cathode placed between two adjacent anodes prevents any acid from reaching the surface in its vicinity upon application of 1.33 V for 20 s. Subsequent removal of the cathode allows protons to flood the area.

That the width of the line in **Figure 6** does not increase with prolonged generation of acid demonstrates the confinement of protons over very long time periods. As the patterning technique presented here uses free protons in solution, the lines generated at the surface would become wider if protons were free to diffuse over time. For example, an unconfined collection of 40 pmol protons released from the 40  $\mu\text{m}$ -wide anodes would reach the surface to produce a stripe over 400  $\mu\text{m}$  wide after 40 s. **Figure 6** shows that this does not occur; the radical anions near the cathode consume protons in this region and thus limit the stripe to about 75  $\mu\text{m}$ , and even after 80 s the width of the stripe is unchanged.

The ability to deliver sharp pH gradients over a long time period provides significant advantages in inducing chemical reactions to completion on a surface. Although this particular reaction was relatively fast so that the surface was patterned after ca. 4 s, less kinetically favourable reactions may be driven to completion by delivering anodic products to confined regions for any duration required, without diffusion outside the regions.

## 2.5 Conclusions

In this work we have demonstrated a number of advantages of the use of arrays of microelectrodes for performing synthetic reactions on a surface.

First, the proximity of anodes and cathodes restricts diffusion of the active species generated at one electrode by interaction with the products of the electrode of opposite charge. Thus, the pattern of change induced on the substrate closely mirrors the pattern of the electrode array, and features with dimensions of a few microns are readily generated.

Second, fine control of the reaction is permitted by regulating the voltage and duration of the pulse, and by measurement of current.

Third, a high degree of parallelism permits many different reaction conditions to be applied to different regions of the substrate surface; the number is limited only by the number of electrodes in the array.

We illustrate the method by the removal of an acid labile protecting group which is commonly used in organic synthesis. Elsewhere we will describe the extension of this reaction to the synthesis of oligonucleotides, but the method has wider potential. Electrochemical methods can be used to generate acids and bases or other reactants of different strengths by changing the electrolyte, solvent or applied potential. There are many examples of organic synthesis steps which use acids, bases, or other reactants which could be generated at electrodes. Thus the method could be applied to a very diverse collection of chemical syntheses.

## 2.6 Acknowledgement

We especially thank Prof. P. Dobson and Dr. P. Leigh of Oxford Dept. of Engineering for invaluable fabrication advice and resources. Mr. M. Johnson helped with apparatus construction, and Drs. M. Shchepinov and K. Mir provided kind encouragement. R.D.E. thanks the Rhodes Scholarship for enabling his Oxford tenure. F.M. thanks the Royal Society for the award of a University Research Fellowship. This work was supported by the U.K. Medical Research Council.

## 2.7 Figures

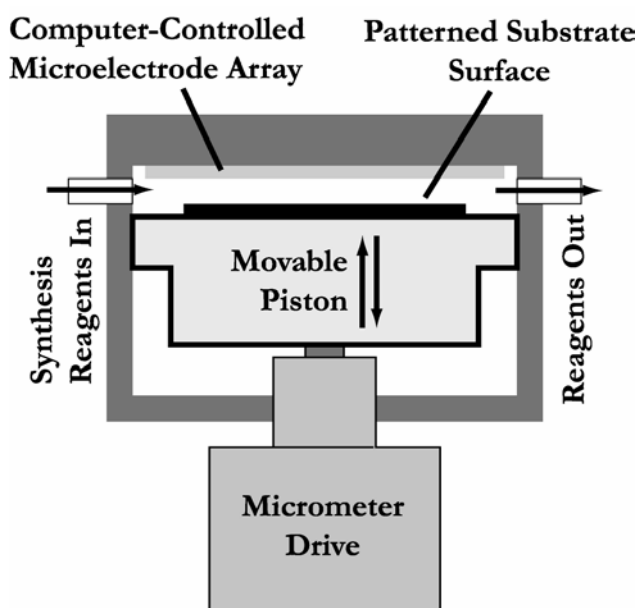


**Figure 1** Chemical patterning reactions on a surface were carried out in an enclosed chamber through which appropriate reagents could be delivered. A digital micrometer head precisely manipulated a gap between a microelectrode array and the surface so that chemical products generated at the microelectrodes could diffuse to the patterned surface, where synthetic chemical steps were performed. A custom designed computer control board controlled the flow of reagents, applied external potentials to each of 96 individual microelectrodes, and measured the resulting currents.



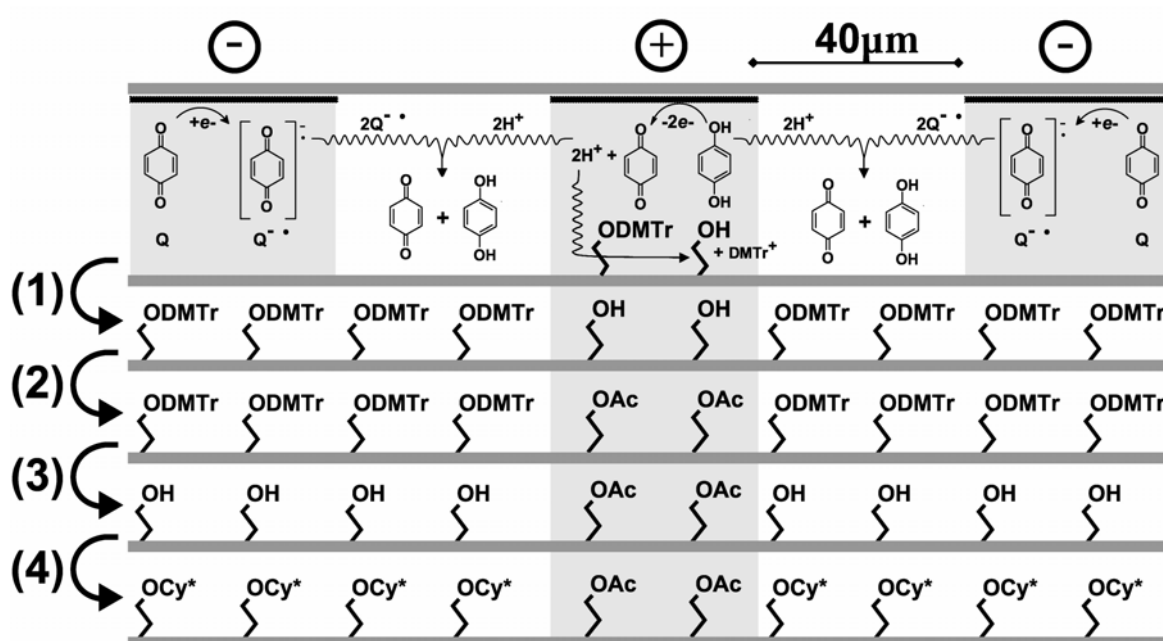


**Figure 2** The electrochemical oxidation of hydroquinone at the anodes (+) on an array of microelectrodes delivers acid to localised regions on a surface (the grey shading symbolises surface regions near the anode). The acid removes a dimethoxytrityl (DMTr) group (1) to expose a primary hydroxyl (OH), which is then exposed to an acetylating reagent (2) to attach an acetyl group (Ac). Subsequent treatment of the entire surface with an acid solution (3) followed by coupling of a fluorescent (Cy\*) dye (4) allows imaging by confocal microscopy so that regions of acetylation are revealed by diminished fluorescence. The counter-electrode process at the adjacent cathodes (–) is the reduction of benzoquinone, which yields a radical anion reactive with protons, thus acting to deplete acid in the cathode region and regenerate hydroquinone.

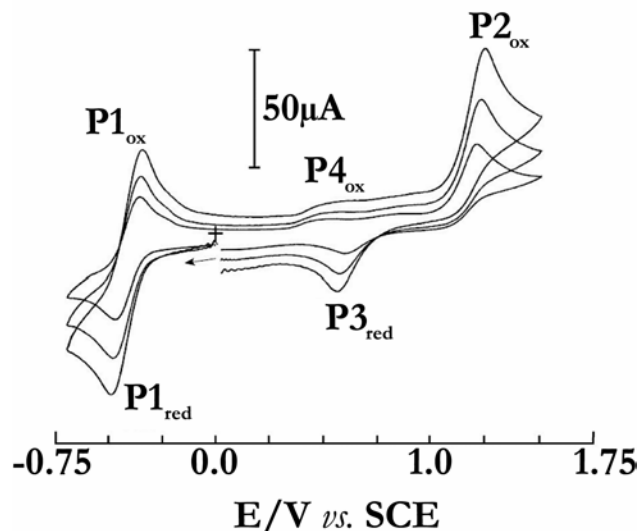


**Figure 3** The chemical system comprising the reversible oxidation of hydroquinone and reduction of benzoquinone generates well defined, electrochemically induced pH-gradients, with proton generation at the anode and proton consumption at the cathode. This figure shows cyclic voltammograms for the reduction and oxidation of an acetonitrile solution (0.1 M  $NBu_4PF_6$ ) of 2.5 mM benzoquinone and 2.5 mM hydroquinone at a 1 mm platinum disc electrode (scan rates 200, 500, 1000  $mV s^{-1}$ ,  $T=22^\circ C$ ). The peak  $P1_{red}$  corresponds to the reversible reduction of benzoquinone to yield a radical anion and  $P2_{ox}$  corresponds to the oxidation of hydroquinone. Minor signals  $P4_{ox}$  and  $P3_{red}$  have been assigned tentatively to the oxidation of deprotonated hydroquinone and the reduction of protonated benzoquinone, respectively.

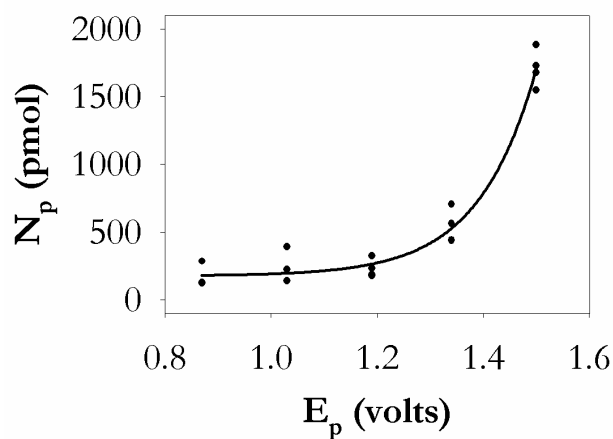


**Figure 4** The number of protons ( $N_p$ ) produced was calculated from electrical current measurements. This figure shows the total protons liberated after 20 s as a function of the applied electrical potential ( $E_p$ ). The voltage and microelectrode geometry for these experiments is as shown in Figure 5. The plot shows that  $N_p$  varies exponentially with potential. Thus, the rate of acid production and therefore surface patterning may be manipulated by small changes in applied potential. The total number of protons liberated at high voltages exceeds 1000 pmol (the maximum amount that can generated without regeneration of reactant), thus demonstrating the regeneration of hydroquinone from benzoquinone and free protons in solution.

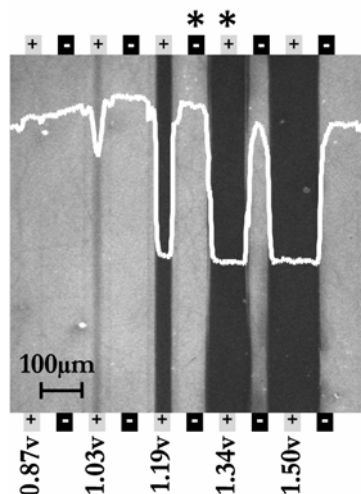


**Figure 5** Fluorescent image of a surface after patterning with electrochemically generated acid. White (fluorescence) appears where the surface was left unchanged by the acid generated at the anodes; dark areas represent formation of an ester bond at the surface where the dimethoxytrityl was removed. The active patterning reagents are generated at the anodes ( + ) and confined by the cathodes ( - ). The potential applied to the microelectrodes greatly affects the surface patterning reaction. Five different potentials were applied for 20 s to electrodes 20  $\mu\text{m}$  from the surface. A potential of 0.87 V generated insufficient quantities of acid for reaction at the surface. At 1.03 V, reaction is detectable but incomplete. In contrast, at 1.50 V, reaction is complete everywhere inside the flanking cathodes. The overlying white plot indicates average fluorescent intensity (arbitrary units) across the image.

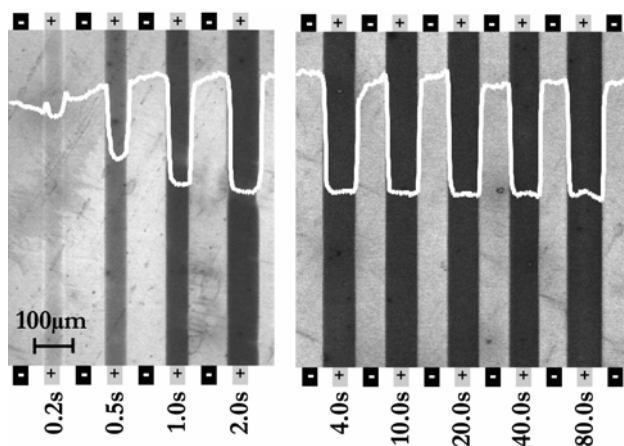


**Figure 6** The extent of reaction at the surface may be controlled and investigated by delivering timed applications of current to the electrodes; the patterning reagent is confined to the anodic region over very long times. This image shows the patterns formed over a time course, using a fixed potential of 1.33 V applied to electrodes 20  $\mu\text{m}$  from the surface. Diffusion does not blur the edges of the stripe formed after 80 s. Instead, the sharply defined stripes are limited to regions between the cathodes and show that patterning reagents may be directed to strictly confined areas. After 0.2 s, detritylation is incomplete; it is near completion at 1.0 s and complete by 2.0 s. With longer times, the width of the stripe increases slightly until it is stable at ca 10 s. There is no detectable change between 10 and 80 s, when the reaction was terminated.

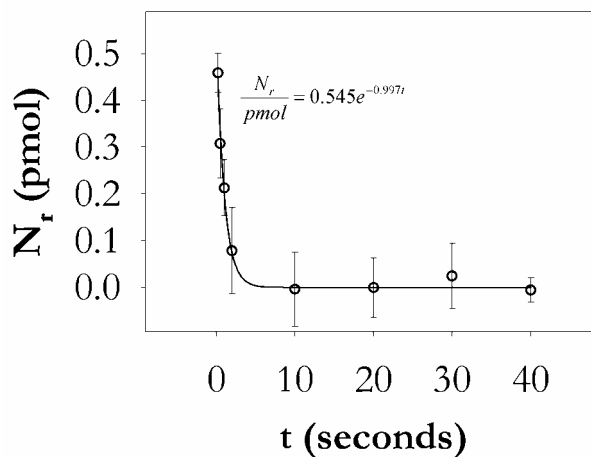


**Figure 7** The initial extent and rate of the chemical reaction at the surface is determined by the amount of acid reaching the surface. This plot shows the rate of patterning reaction, measured as the consumption of unreacted surface molecules ( $N_r$ ), and is taken from area measurements of the stripes in replicates of the experiment shown in Figure 6. In these experiments, protons were liberated at the anode at a measured, constant rate of 10 pmol/s. The reaction rate at the surface is determined by both this rate of proton production and the proportion these protons which reach the patterned surface. If the protons reach the surface, they act to remove remaining DMT groups; if they travel elsewhere, they are consumed by the cathodic products (reaction shown in Figure 2). The plot shows that reaction is complete by about 4 s (additional protons liberated after this time elicit no further chemical change).

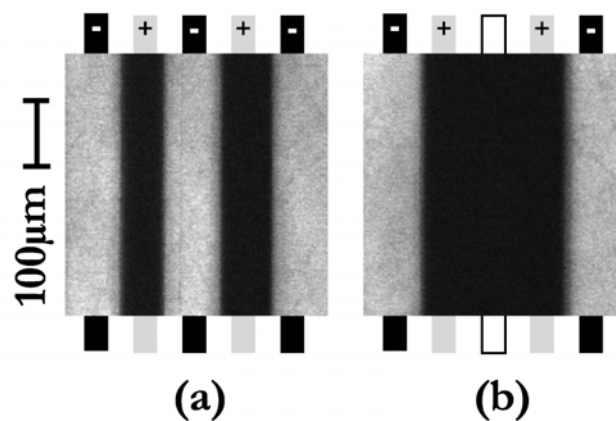


**Figure 8** This image shows the ability to confine the acid by the cathodes. (a) Current (fixed at 1.33 V for 16 s) applied to two anodes and three cathodes produced two dark stripes. (b) Without a cathode separating the anodes (outline shows where the cathode was disconnected from the circuit), anodic products flood the middle area, resulting in a single, wide stripe. The patterned surface was 40 μm from the electrodes in this experiment.

## Chapter 3

# A Microelectrode Array Device for High-Resolution *In Situ* Biomolecule Synthesis On Sur- faces

*This chapter focuses on the microelectrode fabrication, engineering, electronics, and software components of this work. It was submitted for publication as a full paper<sup>c</sup> in Biosensors and Bioelectronics in September 2003. All experimental work and writing were conducted primarily by the author of this thesis.*

### 3.1 Abstract

An array of independent iridium electrodes, prepared by thin-film techniques, is used to induce localised redox reactions in an electrolyte. The microelectrodes are designed to sustain high currents, chemical attack, and mechanical wear so

---

<sup>c</sup> Manuscript authors: Ryan D. Egeland (corresponding) and Edwin M. Southern.



that the redox reactions can be used to perform multiple chemical syntheses on a solid surface placed against the microelectrode array. A computer controls application of voltage to the array of electrodes, and an amplifier circuit measures current used for each synthetic step. The extent of the chemical modification at the surface is thereby monitored and controlled in real time to optimise yields. Synthesis reagent delivery and precise positioning of the surface are achieved by a piston and cylinder reaction chamber, in which the surface to be modified is attached to the end of the piston and the electrode array is placed at the end-face of the cylinder. Reagents are introduced and removed through ports in the sides of the cylinder. The microelectrodes are used in parallel to synthesise multiple oligonucleotides *in situ* on silicon dioxide, but the electrochemistry may be adapted to a range of other biomolecule syntheses. This communication describes the device fabrication and instrumentation in detail.

## 3.2 Introduction

Microfabrication techniques which revolutionised the electronics industry have recently been applied to chemical and biological applications<sup>81,82</sup>. With micron-sized features, devices made with such techniques may be used to manipulate and analyse extremely small quantities of samples in highly parallel manner impossible in larger scale devices. Physical laws at such small dimensions often permit per-

formance characteristics vastly superior to those of larger-scale equivalents<sup>83,84</sup>, or enable entirely new applications. A wide range of components have been incorporated into these devices to perform fluid handling, reagent delivery, mixing, separation, chemical analysis, fluorescent detection, or chemical modification at a microscopic scale, on a range of biological materials. Many of these functions rely upon microelectrodes as a component of their design.

Microelectrodes have most often been used in biochemistry to perform three classes of functions. In the first class, often used in analytical applications, biological molecules in solution are measured and characterised by observing variation in current upon application of potential (through cyclic voltammetry or its variants). Small electrodes in these applications allow high sensitivities, but as the currents are commensurately small, multiple electrodes must be combined in parallel<sup>52</sup> to increase the signal. In a second class of functions, microelectrodes create an electric field which may induce electrophoretic migration of ions in solution; this phenomenon can move minute quantities of fluids<sup>85</sup> or a biomolecule of interest<sup>82,86</sup>. In addition, this class of function can be used to alter the ionic environment near the microelectrodes for optimisation of analytical conditions<sup>87</sup>. In the third class of functions, used in attachment applications, electrochemical redox products from microelectrodes can drive the capture of DNA<sup>33,34,88</sup>, antibodies<sup>89</sup>, peptides<sup>90,91</sup>, and enzymes<sup>92</sup> on an electrode surface for a range of analytical applications<sup>93</sup>.

In this paper, we present a new use of microelectrodes in a device which synthesises DNA on surfaces separated from the electrodes. In contrast to electrochemical devices designed for attachment of pre-synthesised molecules, this device permits synthesis of DNA *in situ*. The economy of synthetic steps afforded by the combinatorial *in situ* method is remarkable, as  $4^n$  distinct sequences of length  $n$  may be generated in only  $4 \times n$  chemical steps.

The device uses an array of iridium microelectrodes to generate acids in a confined space within an organic electrolyte. The acid is used in a chemical reaction<sup>94</sup> to modify a surface (the “substrate”) held against the microelectrodes at a specified distance in a specifically defined, and easily modified, pattern. In the application described here, the patterning process is repeated and automated for stepwise oligonucleotide synthesis. *In situ* synthesis of many oligonucleotides in the context of DNA microarray fabrication is one potential application, but a diversity of electrochemical reaction systems could be exploited through similar means for synthetic attachment of many molecular types.

To create an array of oligonucleotides with different sequences at each location, numerous deblocking reactions must be carried out in each reaction cycle. The array configuration of the microelectrodes allows these steps to be performed in parallel, thus greatly reducing total fabrication times. Software drives an electronic interface to the electrodes. Thus, a simple computer data table can control a particular combinatorial synthesis. A mechanically-controlled reaction

chamber delivers reagents and positions the substrate at a precise distance from the microelectrodes. An instrumentation amplifier circuit designed to measure current at each microelectrode monitors and adjusts the extent of the DNA synthesis reaction in real-time. The microelectrodes are durable and reusable so that hundreds or thousands of DNA or other biomolecule chips may be produced using the same microelectrode set. This communication describes the fabrication and features of the microelectrode device, the accompanying electronics, and the fluidics housing in detail, and presents a brief demonstration of oligonucleotide synthesis using the described device.

### 3.3 Materials and Methods

#### 3.3.1 Microelectrode Fabrication

A brief outline of the microelectrode fabrication process is shown in **Figure 11**. Silicon wafers provided the insulating material on which the microelectrodes were fabricated. The wafers were purchased from AUREL GmbH (Landsberg, Germany) as P-type (boron doped), <100> orientation, 7-21 ohm-cm resistivity, 100mm diameter, 518-532  $\mu\text{m}$  thick, “CZ Silicon Prime Wafers, SEMI standard,” and thermally oxidised to yield a  $124 \pm 0.4$  nm surface thickness of silicon dioxide (performed by Dept. of Electronics and Computer Science, Southampton

University). After baking at 120 °C for 25 minutes and cooling for 5 minutes approximately 4 ml of a positive organic photoresist dilution was applied (four parts “BPRS 150 photoresist,” OCG Microelectronics Materials, West Patterson, NJ with one part “Waycoat LSI positive resist thinner,” Olin Hunt Specialty Products, Norwalk, CT). After a two minute settling time, the wafers were spun at 3000 RPM for 30 seconds and the resulting thin photoresist layer baked for 20 minutes at 90 °C in air.

After exposing the wafers to a UV light source (UVP Inc., San Gabriel, CA) at 10 mW/cm<sup>2</sup> ( $\lambda=365$  nm) for 4.5 seconds through a chrome-coated quartz photomask (manufactured by Compugraphics Intl., Glenrothes, Scotland) on a photomask aligner (“Emhart Dynaport MAS 12”), the wafer was immersed in developer for 2 minutes (one part “PLSI Positive Resist Developer,” Olin Microelectronic Materials, Norwalk, CT with four parts deionised water). The wafer was washed with deionised water, baked at 100°C for 20 minutes, and “descummed” by reactive ion etching at 25 W in 37 sccm oxygen and immediately placed in a vacuum evaporator for iridium patterning.

Iridium metal (99.9% purity) was purchased as 2 mm rod stock from Johnson Matthey (London). Four 3 mm-long segments were placed into a graphite crucible (approx. 2.5 mL in volume) in a vacuum evaporator (BOC Edwards, Crawley England) used for metallisation. Two or three wafers situated approximately 20 cm from the crucible were coated with 50 nm iridium (measured with a crystal

thickness meter during evaporation) by pumping the chamber to  $3 \times 10^{-6}$  Torr and heating the metal with an electron-beam gun set to 300 mA at 5 KV for approximately 3 minutes.

Before photoresist removal, 75 nm of aluminium was applied to the microelectrode connection pads for later wire bonding; the entire wafer surface, except the pads, was masked with aluminium foil and then placed in a tungsten-filament vacuum evaporator. Approximately 75 nm of aluminium (99.99% purity) was deposited onto the wafers.

The wafer was placed in an ultrasonic acetone bath for 30 minutes to dissolve the photoresist and reveal the microelectrodes. The electrodes were annealed at 350 °C in air for 1 hour to promote adhesion with the wafer surface, cleaned by reactive ion etching (100 W in 37 sccm oxygen and 17 sccm argon for 2 minutes), and washed with deionised water. A strip of adhesive polyimide tape 7.5 mm wide was placed across the middle of the electrode pattern, and the bonding pads were similarly masked in preparation for coating with a silicon dioxide insulating layer. Silicon dioxide was deposited onto the wafers by an RF magnetron sputter deposition system (Nordiko “NM200,” Havant, UK) in argon (32 sccm, 9 mTorr,  $8 \times 10^{-7}$  mbar base pressure) at 150 W and 800 V for 1 h (the target was cleaned for 15 minutes at 150 W prior to deposition).

The wafer was glued to a printed circuit board (0.006 inch track widths, manufactured by RAK Printed Circuit Boards, Saffron Walden, England) pat-

terned with 96 gold-plated conductor tracks. Gold electroplating of the tracks enabled direct connection of the microelectrodes to the PCB by wire-bonding; plating was performed by applying  $0.3 \text{ A/dm}^2$  to the copper PCB tracks for 2 h in a solution containing 25 g KAuC<sub>N</sub>, 1280 mL “Aural 292 make-up solution” (Lea-Ronal, Buxton, England), and 1.7 L deionised water, yielding a 0.001 inch-thick layer. Wire bonds using 22  $\mu\text{m}$  gold wire connected each of the aluminium-coated microelectrode pads to a separate PCB track.

### 3.3.2 Electronic Control and Measurement

Application and measurement of current at each individual microelectrode presented difficult circuitry challenges precluding an off-the-shelf solution. A circuit including a series of digitally controlled multiplexer switches was designed to drive the microelectrodes, allowing each microelectrode to be connected to either ground or a fixed voltage source, or disconnect from the current path entirely in a floating mode. In other words, any of the microelectrodes could be switched at will during the course of the experiment to act as cathode or anode; alternatively, they could be switched to an inactive state. Voltages were applied by a computer control board (described below) to very low input offset-voltage, low drift operational amplifier (LF411, National Semiconductor) driver circuits (**Figure 12A**), ensuring accuracy to  $\pm 10 \text{ mV}$  at the microelectrodes.

Current was detected as a voltage drop across a resistor in series with the current path output to each individual microelectrode, with appropriate feedback circuits (**Figure 12B**). As current at each individual electrode was very small (typically between 10 and 1000 nA), a very high common-mode rejection ratio instrumentation amplifier integrated circuit (AD620AN, Analog Devices, Norwood, MA) ensured an accurate, noise free interface with the digital signal sampling.

Upon testing and optimisation of the described circuits on a breadboard prototype, a permanent printed circuit board was designed according to optimised schematics with the aid of “Protel” CAD software (Altium Ltd., Frenchs Forest, Australia). Twelve independent and identical control and analysis circuits on the PCB allowed switching and measuring twelve microelectrodes in parallel. By switching this bank of twelve to each of eight banks of microelectrodes from the full set of 96 as appropriate, each individual microelectrode on the microelectrode chip could be controlled and monitored independently throughout the course of a synthetic trial.

### 3.3.3 Substrate Positioning and Fluidics

Precise and accurate control of the gap between the microelectrode array and the substrate was achieved by a high-precision digital micrometer head (Mitutoyo model 164-172, Andover, UK) and accompanying microfluidics flow cell consist-



ing of a cylinder and piston device, depicted in **Figure 14**. This flow cell device was fabricated from PTFE (to ensure resistance to chemical interaction with reagents) using a precision lathe and conventional machining techniques. The piston, to which the substrate was attached, was moved by action of the micrometer, such that the substrate could be positioned at any measured distance relative to the microelectrodes. A fluid inlet and outlet in the cylinder of the flow cell allowed DNA synthesis reagents and electrolyte solutions to be introduced in the gap between the substrate and microelectrodes.

Moving the substrate approximately 1 mm away from the microelectrodes minimised hydrodynamic resistance during large-volume flow-cell flushing between synthetic steps. During electrochemical steps, the gap was set between 5-180  $\mu\text{m}$  so the acid generated at the microelectrodes would reach the substrate. The micrometer was controlled manually, with its final reading automatically recorded ( $\pm 1 \mu\text{m}$ ) digitally at each step.

### 3.3.4 Computer Interface and Software

Software designed in “Labview” (National Instruments, Austin TX, USA) switched the microelectrodes, collected and digitised output from the current measurement circuitry, and synchronised delivery of reagents to the flow cell by a DNA synthesiser (see below). The software was interfaced to the electronics through a PCI interface card (Model No. PCI-6025E, National Instruments),

which provided 16 analogue inputs and two analogue voltage outputs to the circuitry.

### 3.3.5 Reagents and Chemical Synthesis

Volumes of freshly prepared electrolyte (25 mM hydroquinone and 25 mM benzoquinone with 25 mM tetrabutylammonium hexafluorophosphate in anhydrous acetonitrile), phosphoramidite solution (0.1 M with 0.5 M tetrazole activator solution in anhydrous acetonitrile, Cruachem), oxidizing solution (0.1 M iodine in 20% pyridine, 10% water, and 70% tetrahydrofuran; Cruachem), and washing solvent (acetonitrile), were delivered to the reaction chamber as described below. For conventional deblocking 3% dichloroacetic acid in dichloromethane was used in place of the electrolyte solution.

The solid support used for synthesis was a glass chip derivatised with (3-glycidoxypropyl)-trimethoxysilane and a polyethylene glycol linker<sup>70</sup>. Hexamer synthesis was the sequence CGCATC (in typical 3' to 5' synthesis direction), with detection by a complementary, Cy5-labeled target. Direct fluorescent derivatisation of the substrate was through covalent attachment of Cy5 phosphoramidite (Amersham). Fluorescence images were obtained by a Leica TCS NT confocal microscope with maximal pinhole aperture, in photon counting mode (photomultiplier tube voltages adjusted for maximum dynamic range).

### 3.3.6 Oligonucleotide Synthesiser and Interface

Reagent delivery to the microfluidics flow cell was performed by a modified ABI 394 oligonucleotide synthesiser (Applied Biosystems, Foster City, CA). Reagent lines were redirected to the fluid inlet and outlet ports of the flow cell, and the sequence and timing of reagent delivery was customised according to flow cell volume and flow characteristics. The synthesiser provided relay output signals, which were interfaced to the computer software for synchronisation with the microelectrode driver software.

The synthesiser program, considerably different from standard protocols, was devised to ensure complete rinsing with short cycle times. As this program required careful development in the context of electrochemical deblocking and flow cell volume, it is summarised as follows here (all reagents delivered to inlet port of column, except “reverse flush,” where argon was applied to the outlet port to drive liquid retrograde to waste): (1) Acetonitrile flush 14 s. (2) Reverse flush 0.5 s, acetonitrile 1.5 s. Repeat x 5. (3) Electrolyte solution 15 s. (4) Wait 1 s, Electrolyte solution 1 s. Repeat x 5. (5) Signal for micrometer adjustment to electrochemical gap distance. (6) Wait 30 s (while fluid mixing dissipates). (7) Signal computer to activate microelectrodes, and wait until finished. (8) Open chamber argon vent, signal for micrometer adjustment to flushing gap distance. (9) Repeat steps 1 and 2. (10) Reverse flush 20 s. (11) Phosphoramidite solution 3.5 s, tetrazole 1.5 s. Repeat x 3. (12) Wait 5 s, tetrazole 0.5 s. Repeat x 5. (13)

Reverse flush 15 s. (14) Oxidiser 18 s, reverse flush 1 s. (15) Oxidiser 2s, reverse flush 1 s. Repeat x 7. (16) Reverse flush 20 s, acetonitrile 15 s, reverse flush 15 s, 30 s acetonitrile. (17) Reverse flush 0.5 s, acetonitrile 1.5 s. Repeat x 5. (18) Reverse flush 15 s. (19) Dichloromethane 20 s, reverse flush 20 s. (20) Acetonitrile 20 s, reverse flush 20 s. (21) Acetonitrile 10 s, reverse flush 1 s. Repeat x 6. (22) Reverse flush 60 s. (23) Repeat entire cycle for each additional base addition. Total cycle time was less than 20 minutes per base addition.

## 3.4 Results and Discussion

### 3.4.1 Microelectrode Arrays

The microelectrodes used to generate reagents for oligonucleotide synthesis were subject to approximately 300 N of clamping force and a harsh chemical environment which we have found to damage or dissolve many conventional electrode and conductor materials. More conventional biosensor or other microelectrode applications use low currents and potentials compared to those we found necessary to generate reagents for *in-situ* oligonucleotide synthesis. This application therefore required highly conductive, corrosion resistant, and mechanically robust electrodes.

A number of conventional electrode materials were patterned onto silicon wafers using a range of thin film photolithographic techniques but failed to survive when used in DNA synthesis. Gold was soluble in the iodine solutions used for an oxidation step. Aluminium, well-characterised, inexpensive, and used routinely in semiconductor manufacture, participated in an electrochemical redox reaction upon application of potentials greater than about 0.6 V, resulting in rapid destruction of the electrode array (**Figure 9**). Platinum did not adhere well to the wafer surface, and was not durable enough for these experiments. Silver, although very conductive, also dissolved upon application of potential.

Iridium, an inert platinum-group metal frequently used in electroanalytical applications<sup>95</sup>, was found to suffer none of these deficits. Its high conductivity ( $188.679 \text{ m}\Omega^{-1}\text{cm}^{-1}$ ) and chemical inertness (the most corrosion-resistant metal known) have provided great advantages in microelectrode applications. However, its high melting point (2457 °C) made metallisation and patterning procedures difficult and its chemical inertness initially prevented adhesion to the silicon wafer on which the electrodes were produced. We addressed these problems by employing electron-beam evaporation, aluminium deposition on the microelectrode connector pads, annealing steps, and silicon dioxide dielectric coating of the electrodes.

A range of heat annealing procedures in both inert (95% argon with 5% hydrogen) and oxidizing (100% oxygen) atmospheres (at temperatures ranging from

100-2000 °C) were attempted to strengthen the adhesion of the iridium to the silicon dioxide wafer. Surprisingly, a relatively mild heat annealing in air at 350 °C for one hour generated very strong microelectrodes, resistant even to scratching with a steel scalpel blade. This was presumably due to relief of interfacial tension, formation of an iridium-oxide adhesion layer between the silicon dioxide and iridium metal, and possibly iridium inter-diffusion into the silicon dioxide surface upon heating. Conductivity of the iridium microelectrodes was unchanged by the annealing procedure, resulting in a resistance of approximately 5 k $\Omega$  measured across each electrode track length (ca. 3 cm). At the nanoamp currents employed in these experiments, this resistance generated insignificant potential drops in each of the electrodes (less than 1 mV with 1-2 V applied), so that the electrochemical reactions would be uniform across their lengths.

A number of microelectrode arrays with different geometries were made using this process. We initially produced a range of electrode dimensions from 5  $\mu\text{m}$  (see **Figure 10**) to 80  $\mu\text{m}$ , and found that 40  $\mu\text{m}$  electrodes were the most reliably produced using our photolithographic equipment. For the experiments described here, we used an array of 96 independent linear electrode tracks, each 40  $\mu\text{m}$  wide on 120  $\mu\text{m}$  centres, and 7.5 mm long. A 3 mm wide fan-out to aluminium-coated connection pads allowed strong connection of each electrode to printed circuit board, which contained the electronics used to apply voltages and measure current at each microelectrode in a parallel fashion.

### 3.4.2 Synthetic Control and Monitoring

One advantage of using an electrochemical method to produce reagents used for synthesis is that the reaction can be monitored and controlled electronically. The flexibility afforded becomes particularly important if the strength of reagents used in a given synthetic step must be tightly controlled to avoid incomplete reaction or competing side-reactions. The acid deblocking step in the phosphoramidite method of oligonucleotide synthesis (discussed later) is a good example of this type of sensitivity: the reaction must be driven to completion by sufficiently strong acid, but the range for error is small, as excessive acid, or overextended treatment will result in a depurination reaction that diminishes yields<sup>96</sup>. We therefore designed a circuit permitting fine electronic control and monitoring of the microelectrodes during this delicate acid deblocking step.

The rate of the electrochemical reaction was controlled by manipulating the potential at the microelectrodes. The resulting current is a direct measure of the amount of acid generated (calculated as the integrated current divided by Faraday's constant). We designed a circuit which could deliver independently controlled voltages ( $\pm 5$  V AC or DC) to any of 96 microelectrodes simultaneously (see **Figure 12**). The resulting electrochemical current at each microelectrode was too small to measure using conventional techniques, so custom circuitry employed high-sensitivity components and careful design allowing a large measurable dynamic range (approx. 5-2000 nA) at each electrode. The most important

part of the measurement circuitry was a high common mode rejection ratio instrumentation amplifier, used to cancel noise (see **Figure 12B**). Any remaining offset biases in the measurement circuitry were corrected by software, so the measurements were accurate to within  $\pm 4$  nA (over the typical 100-1000 nA operating range).

Using the described circuitry and microelectrodes, we applied a range of voltages to 10  $\mu\text{m}$ , 20  $\mu\text{m}$ , 40  $\mu\text{m}$ , and 80  $\mu\text{m}$  electrodes bathed in a hydroquinone and acetonitrile electrolyte. We examined the generation of acid by either a pH-sensitive fluorescent dye, or by covalently attaching an acid-sensitive fluorescent molecule to a microscope slide, placing the slide on the microelectrodes, and observing destruction of the fluorophore by the acid (see **Figure 17**). We quickly verified through this fluorescent system that not only the voltage, but also the distance between the microelectrodes and the slide affected the shape and intensity of the fluorescent patterns produced. As this distance was not easily controlled in the arrangement, we realised that reproducible synthesis on a substrate required accurate control of the gap between electrode array and substrate.

### 3.4.3 Substrate Positioning and Reagent Delivery

The synthesis of oligonucleotides required one electrochemical deblocking step at each synthesis cycle. During electrochemical deblocking, the substrate was moved very close to the microelectrodes to expose it to the acid. At other steps in the



cycle, the gap was enlarged to provide enough space to flush reagents. A mechanical positioning device (**Figure 12**) was engineered to maintain alignment of the substrate with the microelectrodes, so that each deblocking step used to attach another residue to the growing oligonucleotide occurred in its proper location.

A micrometer head actuated a piston to which the substrate was attached. A cylinder housing this piston was clamped to the microelectrode wafer surface to create a sealed reaction chamber through which electrolyte and synthesis reagents were delivered from a conventional oligonucleotide synthesiser adapted to the volume of the chamber and synchronised to the microelectrode activation by computer. This system automated the hundreds of chemical delivery, washing, electrode activation, and substrate positioning steps necessary for oligonucleotide synthesis; it enabled us to test many synthesis conditions, requiring thousands of chemical steps, with relative ease.

#### 3.4.4 Chemical Synthesis

The chemical protocol we used with the microelectrode device borrowed many steps from the well-developed phosphoramidite method for oligonucleotide synthesis; however, we used the microelectrodes to generate acid during the deblocking step, replacing conventional deblocking by dichloroacetic acid. This step is very sensitive to the acid used and the reaction time. Significant losses result if it

is not carefully optimised. Indeed, early literature reports document numerous optimisation trials using a range of acid strengths, many with only moderate success<sup>71,96-98</sup>. We anticipated similar difficulties, as we sought to perform the deblocking using electrochemically-generated acids uncharacterised in the context of oligonucleotide synthesis. However, exploiting the flexibility inherent in the electronic control of the microelectrodes and substrate positioning, we were quickly able to establish conditions generating high synthesis yields.

We considered that the oxidation of hydroquinone in acetonitrile would liberate free protons; initial experiments indicated the possibility of generating a wide range of acidities confined to regions near the anode<sup>94</sup>, so we used this electrolyte system while examining the effects of other reaction parameters. The size and shape of the microelectrodes can be varied; we used an array of 40  $\mu\text{m}$  linear electrodes for a detailed investigation of other synthesis conditions.

In early experiments, we observed effects of acid at the substrate by simply (covalently) coating the substrate with an acid-sensitive fluorescent reporter substrate and observing its destruction in low pH (as in **Figure 17**). Subsequent techniques relied on a single, acid mediated deblocking step of a 5'-dimethoxythymidine coated substrate; after deblocking, the resulting free hydroxyl groups were acetylated and the remaining blocking groups removed by treating the entire surface with dichloroacetic acid. In this system, the pattern of electrochemical deblocking was revealed by treating the surface with a fluorescently-labelled

phosphoramidite so that fluorescence would be present only in regions *unaffected* by the electrochemically generated acid.

Using this simple one step synthetic process, we examined the effect of over 200 different combinations of voltages (from 0.3-1.9 V) and substrate-microelectrode gap distances (from 1  $\mu\text{m}$  to 180  $\mu\text{m}$ ). An abridged set of these results is shown in **Figure 17**, where the dark regions represent areas of electrochemical deblocking. These experiments demonstrated that deblocking was complete and well-confined by the microelectrodes using potentials ranging from 1.18-1.5 V. Surprisingly, varying gap distances from 2-180  $\mu\text{m}$  had little effect on the pattern produced (to be discussed elsewhere).

From this exploration, we selected a range of mild conditions which removed blocking groups in high yield and then used these specific conditions to perform five electrochemical deblocking steps in building a six-base oligonucleotide. Yields of the hexanucleotide were determined by hybridisation to a fluorescently-labelled complementary oligonucleotide, known to bind only to a complete six-nucleotide sequence. We performed 80 different syntheses using this test; the abbreviated results are shown in **Figure 18**, where white regions indicate areas where five rounds of both electrochemical deblocking and subsequent base addition were successful. This result demonstrates a promising approach to *in situ* DNA synthesis using microelectrodes, and will be described in detail elsewhere.

This study illustrates the advantages of the flexible, electronically controlled, highly parallel features of the microelectrode device. Indeed, the parallel features of the device were used here to quickly optimise the sensitive deblocking step for oligonucleotide synthesis. The array configuration of the electrodes lends itself to the combinatorial fabrication of large libraries of biomolecules or other products.

### 3.5 Conclusions

Oligonucleotide synthesis, in confined regions of a substrate, at high yields was achieved using electrochemically generated acids at microelectrodes held near a substrate. The ease with which synthesis conditions were modified electronically demonstrates the flexibility of the technique. As many chemical syntheses proceed by alternating steps of coupling and deprotection the method should be generally applicable to fabrication of arrays of other types of molecules. Other uses for the method could include etching, polymer deposition, or generally many types of surface modifications.

Connecting each of the microelectrodes to a separate conductor limits the number of microelectrodes that can be connected in an array. A more elegant alternative would be to generate, switch, and measure the electrode activity by CMOS transistor logic on the microelectrode array itself. Such devices have been

made for analytical applications, but the higher current required for synthesis could present materials compatibility problems. Furthermore, moving from linear electrodes to “pixels” or spots would require careful adjustment of the synthesis conditions to maintain high resolution and reasonable yields. Should such a large-scale fabrication process be feasible, only a few connections to input digital logic and power would be necessary to drive synthesis by a very large array of small microelectrodes; the density of the electrodes would be limited only by the smallest sizes achievable by photolithography (presently better than 0.12  $\mu\text{m}$ ).

### 3.6 Figures

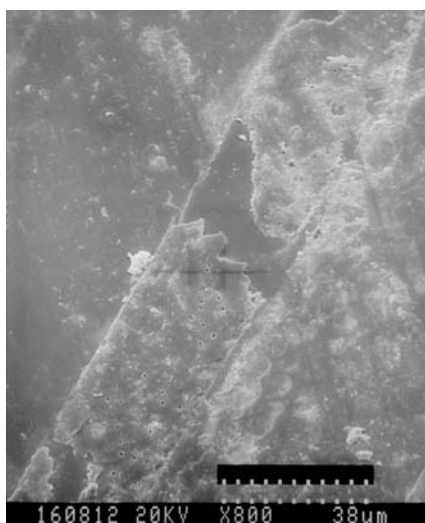


**Figure 9** Conventional thin-film materials destroyed during attempted synthesis of oligonucleotides. This electrode would be suitable for low-current analytical or electrophoretic applications, but proved unstable under the relatively high current densities required for *in-situ* DNA synthesis. This scanning electron micrograph shows the destruction of aluminium microelectrodes after applying the 1.33 V for 10 s necessary for synthesis. Platinum, although electrochemically inert, was not suitably adherent and durable for repeated use.

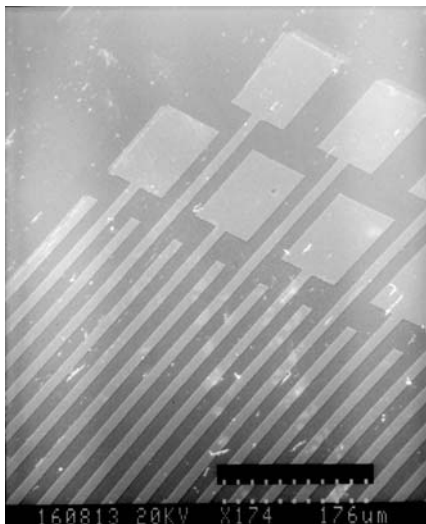


**Figure 10** Iridium microelectrodes fabricated using a photolithographic procedure (shown in **Figure 11**). The electrodes were electrochemically inert, conductive, stable to oligonucleotide synthesis reagents, and adherent to silicon dioxide. This scanning-electron micrograph shows 5  $\mu\text{m}$  iridium microelectrodes after approx. 100 electrochemical oxidation steps at the same voltage and duration as for the aluminium electrodes shown in **Figure 9**. There are no signs of deterioration.

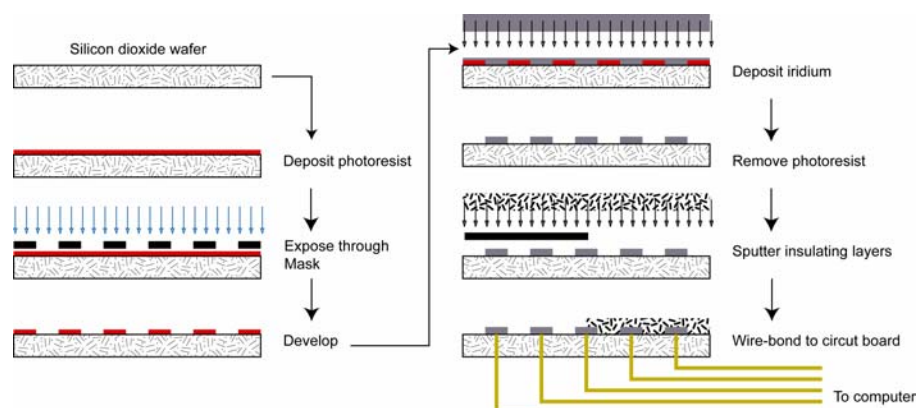


**Figure 11** The relatively simple, 9 step, two layer, thin-film lift-off process developed for fabricating the iridium microelectrodes. Conventional positive-photoresist patterning, followed by electron-beam iridium deposition, silicon dioxide dielectric deposition, annealing (not shown) and wire bonding resulted in inert, adherent, and very durable iridium microelectrodes. See text for details.



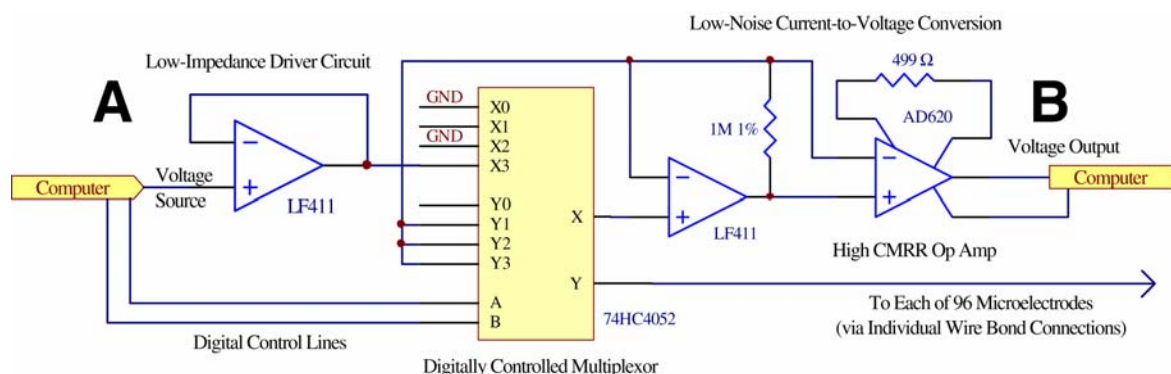


**Figure 12** The electronic circuitry used to apply potential to each of 96 independent microelectrodes. Precise software-controlled voltages were delivered by low output impedance, low drift operational amplifiers (**A**) switched by digitally-controlled analogue-switch multiplexers (digital signals at A and B switched the X0..3 and Y0..3 inputs to X and Y outputs) shown in this abbreviated schematic. The current-to-voltage instrumentation amplifier circuit (**B**) delivered very low-noise microelectrode current measurements to a computer. Amplification levels were digitally-controlled (not shown) for full dynamic range; noise was measured as less than 1% RMS with typical 100-1000 nA microelectrode currents.

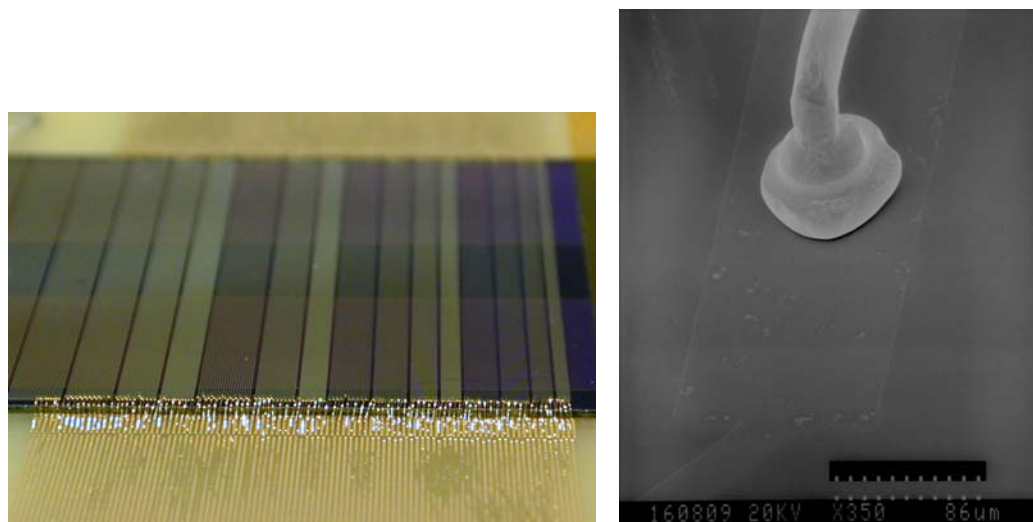


**Figure 13** Example microelectrodes. Each of 96 linear microelectrodes were connected to the computer-controlled circuitry by 22  $\mu\text{m}$  gold wire bonds on an aluminium padding. The left figure shows an example device with various electrode widths and pitches (enlarged view at right). Unlike typical electroanalytical microelectrode configurations, the separate connections to each iridium microelectrode allowed individualised control for parallel *in situ* synthesis. In essence, each of the microelectrodes was connected to a separate output as shown in **Figure 11** and **Figure 12** during activation.

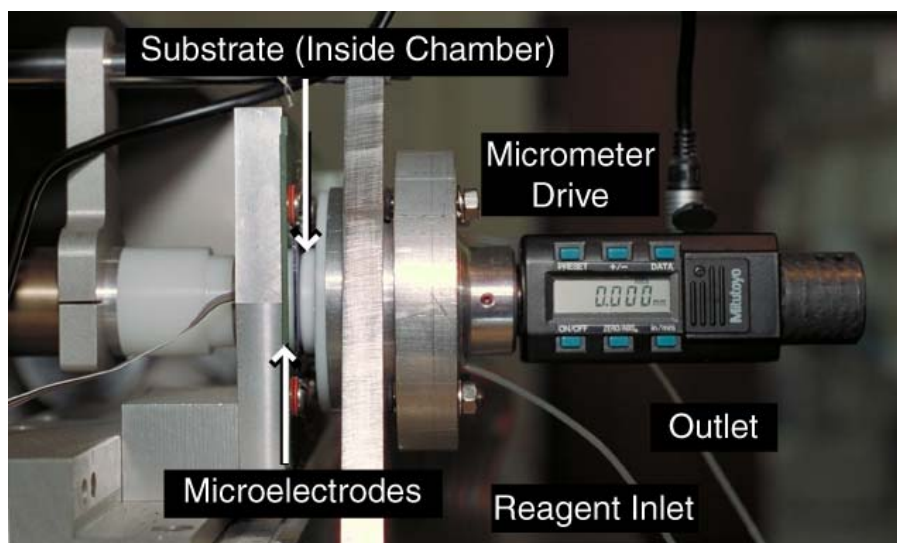


**Figure 14** The piston and cylinder microfluidics flow cell used for *in-situ* synthesis on a substrate. The cylinder of the flow cell was clamped against the face of the microelectrodes, and the substrate was attached to a movable piston inside the cylinder (not visible). Manipulation of the micrometer drive moved the piston, thus placing the substrate at any measured distance from the microelectrodes.

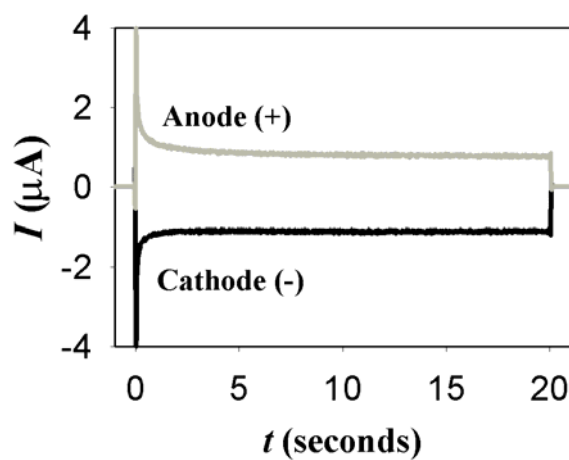


**Figure 15** An example of current measurements at a single anode (1.35 v) with two flanking (grounded) cathodes. Noise and drift minimisation by the circuit in **Figure 12** allowed relatively accurate and precise measurements. This plot shows that current reaches a steady state after about 2.5 s. At the anode, each electron removed from solution yields one proton. Thus, the total number of protons liberated during a given step may be calculated from these measurements (detailed in **Figure 16**).

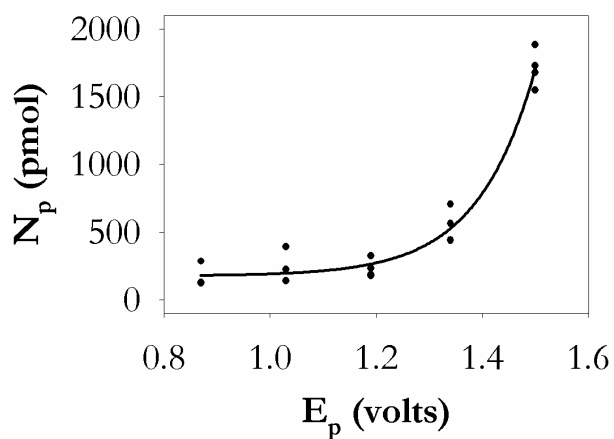


**Figure 16** Total measured quantity of acid produced ( $N_p$ ) during a synthesis step at various voltages. The current measurements taken at each electrode (as shown in **Figure 14**) are directly related to the amount of acid produced. Monitoring the current thus permits direct observation of the synthetic process in real-time.  $N_p$  was calculated simply as the integration of the current over time divided by Faraday's constant. The graph represents three replicate measurements from 40  $\mu\text{m}$  microelectrodes, with voltages applied for 20 s. The patterns produced from these conditions are shown in **Figure 17**.

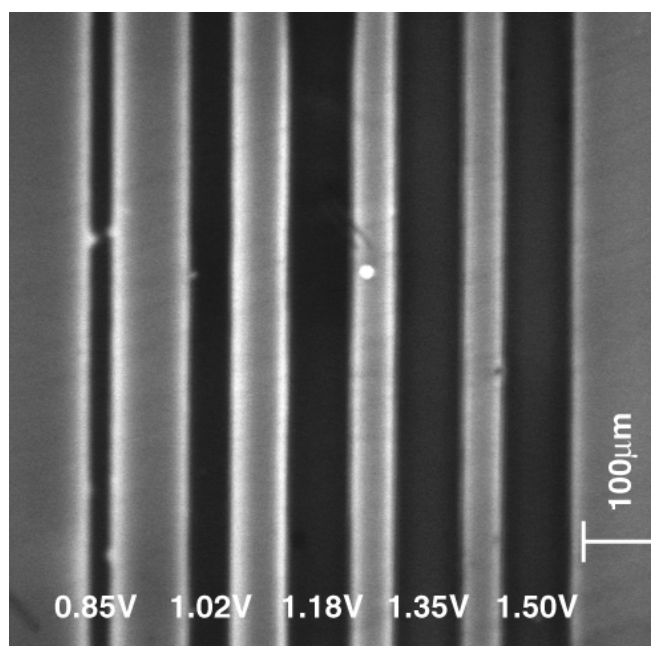


**Figure 17** Effects of microelectrode-generated acid on a surface (the “substrate”) held near the microelectrodes. The dark bands on the confocal-micrograph shown here signify locations where acid from the underlying microelectrodes reached the substrate to destroy a previously attached, acid-sensitive fluorescent molecule (detected by the microscope). Individual control of each electrode allowed simultaneous application of current at controlled voltages (as labelled). Current measurements for these experiments are shown in **Figure 16**.

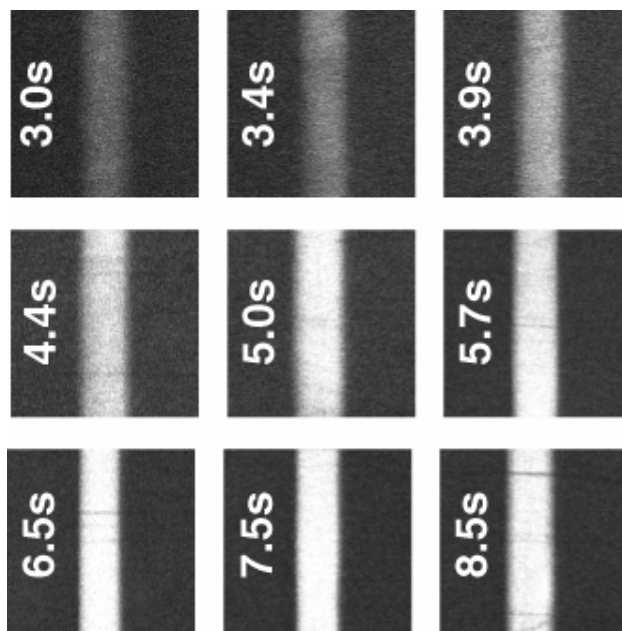


**Figure 18** Demonstration of oligonucleotide synthesis using the microelectrode device. In this image, a complementary, fluorescently-labelled oligonucleotide reporter indicated five successful steps of electrochemical deblocking and coupling. The white areas represent regions where acid was generated for synthesis. The increasing fluorescent intensity with increasing time (identical for each of the 5 synthetic steps) demonstrates the ability to regulate the extent of chemical reaction electronically.

### 3.7 Acknowledgements

We thank Prof. Peter Dobson and Dr. Peter Leigh of the Oxford Dept. of Engineering for invaluable microfabrication advice, instruction, and resources, and Dr. Tim Fell for introductory clean-room instruction. R.D.E thanks the Rhodes Scholarship for enabling his Oxford tenure. This work was supported by the UK Medical Research Council.



## Chapter 4

# Electrochemically Directed Synthesis of Oligonucleotides for DNA Microarray Fabrica- tion

*This chapter focuses on the DNA synthesis and microarray application components of this work. It was submitted for publication as a full paper<sup>d</sup> in Nucleic Acids Research in September 2003. With the exception of the data in **Figure 24**, which was performed in collaboration with Tim Fell, all experimental work and writing was conducted primarily by the author of this thesis.*

### 4.1 Abstract

We demonstrate a new method for making oligonucleotide microarrays by synthesis *in situ*. The method uses conventional DNA synthesis chemistry with an

---

<sup>d</sup> Manuscript authors: Ryan D. Egeland (corresponding) and Edwin M. Southern.

electrochemical deblocking step. Acid is delivered to specific regions on a glass slide, thus allowing nucleotide addition only at chosen sites. The acid is produced by electrochemical oxidation controlled by an array of independent microelectrodes. Deblocking is complete in a few seconds, when competing side-product reactions are minimal. We demonstrate the successful synthesis of 17-mers and discrimination of single-base pair mismatched hybrids. Features generated in this study are 40  $\mu\text{m}$  wide, with sharply defined edges. The synthetic technique may be applicable to fabrication of other molecular arrays.

## 4.2 Introduction

DNA microarrays are increasingly used in the biological sciences to help interpret the data emerging from large-scale genome sequencing. They are used for the analysis and comparison of gene expression levels<sup>1-3</sup>, resequencing genes to identify mutations<sup>9-11</sup>, analysis of sequence polymorphism on a large scale<sup>4,99</sup>, optimisation of antisense oligonucleotides<sup>6</sup>, basic studies of molecular hybridisation<sup>7,8</sup> and analysing DNA-protein interactions<sup>12</sup>. Several methods have been developed to fabricate arrays. One set of methods deposits spots of presynthesised nucleic acids on the surface of the support<sup>3</sup>, or on microbeads<sup>16</sup>. In others, probes are synthesised *in situ*<sup>17-20</sup>. Each method has its strengths and weaknesses. An ideal method of array fabrication would be rapid so that an array could be designed

and made within a few hours; would have high spatial resolution to reduce the size and hence the amounts of reagents used in hybridisation; would allow the use of different chemistries so that probes could be made with different backbones and bases; would allow 3' or 5' attachment so probes could be used in enzymatic extension as well as hybridisation based tests; would be programmable so that a computer file would direct defined sequences to defined sites on the array. No existing method of array fabrication meets all these criteria. A photolithographic method provides high spatial resolution<sup>18</sup> and has proven successful for repeat manufacture of the same oligonucleotide sets. But as each oligonucleotide set requires a new mask set, the method is less suitable for custom designs. A new light-directed method<sup>21</sup>, which uses programmable microarrays of mirrors rather than masks, may eliminate this problem and new photolabile protecting groups may improve coupling yields<sup>22</sup>, which are reported to be lower than conventional oligonucleotide synthesis yields at present<sup>23</sup>. Physical masking using mechanical flow cells and conventional synthetic chemistry gives high coupling yields and also provides high resolution, but is best used for sets of probes with related sequences, such as all sequences of a predetermined length<sup>24</sup>, or tiling paths of all oligonucleotides complementary to a gene of known sequence<sup>25</sup>. Ink jet fabrication is rapid, highly flexible and has a high throughput<sup>26-28</sup>. However, its resolution is limited by the accuracy in aiming droplets of reagents and by their spread upon surface impact<sup>20</sup>.

Ideally, all molecules at each location in an array should have the same predefined base sequence. For *in situ* synthesis, whereby nucleotides are coupled one at a time to the growing chain, non-quantitative yield at any nucleotide addition results in a defective oligonucleotide probe at that location on the array. This problem places heavy demands on the chemistry for oligonucleotide synthesis, which must have high stepwise yields with a minimum of side reactions for each chemical step required to add a nucleotide.

In this paper we describe a new method for directing the synthesis of oligonucleotides on the surface of a solid support, which uses electrode arrays to induce electrochemical reactions in highly localised regions. The microarray ("DNA chip") is made on a planar substrate of either glass or silicon dioxide, the face of which is placed against the electrode array for the duration of synthesis. At each step of synthesis, acid is produced in confined regions by application of current to individual electrodes, directing patterned removal of protecting groups on the adjacent substrate. We demonstrate the rapid synthesis of 17-mers, in small, confined regions and show discrimination of single base mismatches by hybridisation.

### 4.3 Results

Others have made arrays by attaching presynthesised nucleic acids to electrodes<sup>36</sup>, and it is possible to make arrays by *in situ* synthesis on electrodes<sup>37</sup>. In these systems, the array of electrodes becomes incorporated into the nucleic acid array. However, oligonucleotides synthesised directly on electrode surfaces may be subject to destructive electrolysis products, and there are advantages to using an electrode array as a printing tool so that one such tool can make many arrays. Our objective was to make a device similar to a printing tool, with addressable, individually controlled, electrodes, so that the same tool could make arrays with different sets of oligonucleotides.

To evaluate this method of making microarrays we addressed five areas:

- manufacture of suitable, robust microelectrodes
- development of a programmed power supply to deliver predetermined potential to each electrode independently for a preset duration with means to measure current at each electrode
- construction of an automated reaction system including a sealed chamber in which to carry out the electrochemistry and nucleotide coupling reactions
- choice of electrolyte
- optimisation of reaction parameters.

The apparatus and its construction (summarised in **Figure 19**) will be described in detail elsewhere. The most important element of the apparatus is the array of metallic electrodes. These corrosion-resistant electrodes were linear, 40  $\mu\text{m}$  wide, separated by 40  $\mu\text{m}$  gaps, and fabricated by thin-film photolithography. The accompanying control circuitry allowed independent addressing and current measurement at each electrode. The electrodes were durable, and used for over 500 cycles without mechanical or electrical deterioration (as determined by scanning electron microscopy and resistivity measurements). This paper is mainly concerned with the choice of reaction conditions to give the maximum oligonucleotide yield in well-defined microscopic areas on a glass or silicon support.

#### **4.3.1 Electrochemical generation of acid by arrays of microelectrodes and interaction with an apposed substrate**

Oxidation of an electrolyte solution after application of current to microelectrodes liberates acid at the anodes; concomitant reduction at the cathodes consumes acid (**Figure 20**). The ions and radicals generated by these redox reactions at the electrode surfaces move away from the electrodes and to the substrate through a combination of diffusion, migration, and convection effects. During this transit time the electrode products may further react. Once the primary or

secondary products reach the substrate, they may either react to remove protecting groups (deblock), facilitating coupling of the next nucleotide or depurinate and thereby destroy the oligonucleotides already synthesised. This complex nature of the system precludes modelling without unreasonable assumptions and so we have developed an empirical approach, which allows us to see the end result of acid reacting with groups on the surface of a glass substrate placed against the electrode array.

We used fluorescent dyes as reporter groups. In an extensive set of experiments, fluorescent Cy5 groups were attached to any regions where the electrochemical reactions exposed free hydroxyl residues using otherwise conventional DNA synthesis chemistry. These preliminary experiments (results not shown) allowed us to find a range of conditions which gave high deblocking yields in well defined regions. They also established the basic shapes and dimensions of the patterns of deblocking on the adjacent surface, and showed the effects of varying the voltage, the duration of the pulse, the spacing between electrodes and the distance separating the microelectrode array and the surface of the substrate. One unexpected result of this series of experiments was the high edge definition of the pattern generated by the action of the protons on the substrate surface. We have shown that this effect is due to annihilation of protons by the electrode products of the cathodes which flank the anodes<sup>94</sup>. Another desirable outcome of

this effect is that diffusion of reactive protons to adjacent regions is suppressed to an insignificant level.

The total yield of oligonucleotide on the surface is likely to be of the order of 1-10 pmol per mm<sup>2</sup> - too small to measure via direct methods or via high pressure liquid chromatography analysis (HPLC) after cleavage from the surface<sup>100</sup>. To overcome this measurement difficulty, we estimated the synthesis yield of oligonucleotides, and hence the extent of the electrochemical reactions, from the level of hybridisation to a complementary fluorescent probe. For semi-quantitative analysis, we took three sets of measurements for each experiment at different photomultiplier tube (PMT) voltages so as to view all intensity values of the sample in a linear response region of the PMT. This approach was sufficient to optimise stepwise coupling yield, as it was easy to determine which set of conditions produced the highest yield. An indirect approach to estimating the rates of deblocking and depurination is described in the next section.

### 4.3.2 Synthesis of oligonucleotides using electrochemical deblocking

The yield and quality of oligonucleotides are of great importance for any *in situ* method of making oligonucleotide arrays. In the method presented here, only the deblocking step differs from conventional phosphoramidite oligonucleotide synthesis chemistry. Coupling yields are close to quantitative for synthesis on col-



umns of controlled pore glass, with moderate excess of reagent over the large number of active sites on the solid support<sup>71</sup>. For the planar glass substrate used in this work, the excess is orders of magnitude larger. We therefore assume 100% coupling efficiency and consider how the overall yield of oligonucleotide is affected by incomplete deblocking and losses due to depurination. In a series of experiments, a six base sequence, 3' CGCATC 5' was synthesised on top of a lawn of dA<sub>10</sub>, introduced to maximise detection of any electrochemically induced depurination (dA is the most acid-depurination sensitive base<sup>101</sup>). Only the last two bases were coupled electrochemically. In one set of range-finding experiments, time was varied over a wide range (e.g. **Figure 22**), and in another experimentation set, the voltage was varied (results not shown). The synthesis of the hexanucleotide was observed by hybridising to a Cy5-labeled target containing the complement of the above sequence (detailed in methods section where the two nucleotides were added as shown in **Figure 21b**). This target hybridises only to the full six base sequence of the probe; absence of any one of the six bases abolishes hybridisation.

#### 4.3.3 Rates of deblocking and depurination and synthesis yields

Deblocking in the region of the substrate opposite the anode is rapid. The distribution of hybridisation intensity produced by electrochemically deblocking for three to five seconds (**Figure 22**) suggests acid has reached the substrate surface

as a cylindrical diffusion layer “wave front.” At 3 seconds, the intensity at the centre of the stripe is higher than the intensity at the edges. The overall intensity has increased at 5 seconds, and by 8.5 seconds the profile has a flat top, indicating complete deblocking. After 11.1 seconds, the intensity in the middle of the stripe decreases, indicating loss of oligonucleotide by depurination in this region most exposed to acid.

After 11.1 seconds deblocking for each of two steps, fluorescent intensity in the middle decreased by 4.2%, relative to the *peak* edge intensity, which we assume to represent complete deblocking. This analysis suggests a small average loss of yield of ca. 2% per step in the middle of the stripe at 11 seconds. Losses by depurination at earlier times, when deblocking is complete, are much smaller, as the rates of both deblocking and depurination accelerate rapidly over the early time period as acid begins to reach the surface. Thus, loss of oligonucleotide in the middle of the stripe is not detectable at 8.5 seconds, is 4.2 % at 11.1 seconds, 50% at 24.3 seconds, and nearly 100% at 41.0 seconds.

Other experiments show that losses in the middle of the stripes, where acid is strongest, are less than 1% for conditions that give complete deblocking over the width of the stripe. Syntheses of the 6-mer (**Figure 21**) and a 17-mer (**Figure 23**), with nine seconds of electrochemical deblocking at each step, show no measurable intensity losses in the middle of the stripes. If there were 1% loss at each step, there should have been 6% and 15% cumulative losses during the five

and 16 deblocking steps used in the synthesis of the 6-mer and 17-mer, respectively. Such high losses would produce stripes with decreased intensity in the middle, resembling those seen in the later images from the time course experiment (described above and **Figure 22**). However, the intensity across the 6-mer and 17-mer stripes is uniform, showing that the loss during nine seconds of deblocking must be less than 1% and may be less than 0.5%.

In addition to demonstrating minimal depurination, these syntheses confirm that deblocking is essentially complete at nine seconds. If deblocking were incomplete in the multi-step synthesis of the 6-mer and the 17-mer, accumulated low yields would produce profiles with low, rounded tops and diffuse edges, similar to those seen in the early steps of the time course experiment (**Figure 22**, 3.0-5.8s). Instead, the intensity profiles have flat tops and sharp boundaries (**Figure 21** and **Figure 23**) indicating that deblocking is essentially complete in each of the steps.

Finally, these results show that diffusion of acid into adjacent regions is confined by the cathodes. As the overall width of the stripe continues to increase with time (a manifestation of the cylindrical “wave front” mentioned above), the effects of the cathodes maintain the sharpness of the edges; these effects, discussed in detail elsewhere<sup>94</sup>, result from the efficient annihilation of protons by species produced at the cathodes and act to prevent synthesis cross contamination between adjacent electrodes.

## 4.4 Discussion

This study explored the potential of a novel method for generating patterned surfaces by an electrochemical printing process. The printing tool was an array of microelectrodes patterned on the surface of a silicon chip. By directing the current to selected electrodes, chemical reactions were induced on the surface of a substrate held close to the electrode array.

The deblocking step in oligonucleotide synthesis demands precise control. Too much or too little deblocking over multiple couplings has a dramatic effect on yields of long sequences. The independent control of the electrodes of the array and the adjustable reaction synthesis chamber apparatus allowed us to explore multiple conditions such as separation between electrode array and substrate, voltage, and duration of pulse. We were quickly able to establish a set of conditions which gave well defined stripes of chemical transformation on the substrate, with near complete deblocking and without serious depurination. Creating a 17-mer in good yield illustrates that this system is capable of precise and reproducible control.

The electrodes used in this study were directly connected to a switchable power supply. This configuration lends itself well to preliminary studies described here. We aim to adapt standard fabrication methods, for example those that have been used in the manufacture of visual displays and demonstrated in related electrochemical applications<sup>102</sup>, to develop a system in which the elec-

trodes form a two dimensional array of small points, each switchable by indirect addressing. This will allow for random access, with flexible addressing so that the design of the array can be rapidly and easily changed from one run to another. The sharpness of the edges of the chemical image suggests that 10-20  $\mu\text{m}$  features should not be difficult to achieve. In addition, in other experiments we have made features as small as 2  $\mu\text{m}$  using a multilayer electrode (**Figure 24**).

A number of features distinguish this new method from alternative ways of patterning surfaces such as photolithography, ink-jet printing, or the use of stencil masks. As there is potentially no movement of parts between coupling steps, loss of registration between the printing tool and the printed surface does not lead to degradation of the chemical image. The method uses standard chemistries, so it is fast and can be applied to the synthesis of oligonucleotides in either chemical orientation or to nucleotide analogues for which standard reagents are available. Electrochemical processes can generate a variety of active species, including ions, radicals, and radical ions, depending on the electrolyte. In this study, we chose an electrolyte which generates acid and used this reaction to remove an acid-labile protecting group during the synthesis of oligonucleotides. However, the method is not limited to this application and could be used to generate arrays of other types of molecules and to pattern materials by etching or deposition.

## 4.5 Methods

### 4.5.1 Electrode and reaction chamber assembly

Electrode materials were chosen to exhibit high conductivity and chemical stability under the harsh redox conditions employed during deblocking. Positive resist photolithography was used to produce iridium metal (50 nm thickness) electrodes on oxidised high-resistivity silicon wafers. After heat annealing and cleaning, each electrode was individually connected by ultrasonic gold wire bonding to a printed circuit board, where digitally controlled analogue switch integrated circuits activated electrodes chosen for a given deblocking step. Currents were applied as constant voltage sources regulated by independent operational amplifiers. Parallel Low-noise instrumentation amplifier feedback circuits continuously measured nanoamp-precision current at each of the electrodes. A computer, programmed for this work, controlled all voltages, timing, and electrode switching, and collected current measurement data.

The piston and cylinder of the synthesis chamber assembly was machined from PTFE, chosen to provide a good seal against the atmosphere and be resistant to chemical attack by the harsh reagents used during synthesis. A fixed force of 500 N, applied to the synthesis chamber assembly with a stepper motor-driven clamp, sealed the reaction chamber assembly against the electrode array before each experiment.

### 4.5.2 Synthesis chemistry

A modified DNA Synthesiser (ABI 394 DNA Synthesiser, ABI) delivered all reagents to the synthesis chamber assembly. Delivered volumes of freshly prepared electrolyte (25 mM hydroquinone and 25 mM benzoquinone with 25 mM tetrabutylammonium hexafluorophosphate in anhydrous acetonitrile), phosphoramidite solution (0.1 M with 0.5 M tetrazole activator solution; Cruachem), oxidizing solution (0.1 M iodine in 20% pyridine, 10% water, and 70% tetrahydrofuran; Cruachem), and washing solvent (acetonitrile), were individually optimised to completely fill and rinse the reaction chamber cavity and allow sufficient time for complete chemical reaction. The piston was routinely separated 800  $\mu\text{m}$  from the electrode during delivery of all reagents. For nucleotides added using conventional deblocking, 3% dichloroacetic acid in dichloromethane was used in place of the electrolyte solution.

The solid support used for synthesis was a glass chip derivatised with (3-glycidoxypropyl)-trimethoxysilane and a polyethylene glycol linker<sup>70</sup>. An initial DMT protected dA residue was then added across the entire support surface to present a DMT group to the first deblocking step.

Preliminary experiments established that, holding all other variables constant, decreasing the voltage at the electrodes, shortening the current application time, or increasing the separation between the electrode array and substrate decreased the quantity of acid reaching the substrate. In optimising the acid exposure for

all work described here, we fixed the voltage of the anodes at 1.33 V with respect to the cathodes and maintained a separation distance of 40  $\mu\text{m}$ , while varying only current application time (ranging from 0.5 to 90 seconds).

### 4.5.3 Hybridisation to synthesised probes

Probes were deprotected according to the method of Polushin<sup>103</sup> by immersing the entire substrate in a 50% aminoethanol, 50% ethanol solution for 25 minutes at 60 deg C. Hybridisation targets were 5' labelled with Cy5 (Amersham) and purified by HPLC. Hybridisation reactions were carried out at 25 deg C in solutions (5  $\mu\text{l}$ ) containing 50 pmol/ $\mu\text{l}$  target, 0.1% w/v ficoll, 0.1% w/v polyvinylpyrrolidone, 0.1% bovine serum albumin pentax fraction V, 20 mM Tris HCl, 50 mM KCl, 10 mM MgCl<sub>2</sub>, and 1 mM EDTA, in distilled water, (pH 8.3) by introducing the solution between a glass coverslip and the substrate. A brief, room temperature wash in hybridisation buffer was used to remove any non-specific interactions without significant dissociation of the target. Hybridisation to the substrate was analysed by a Leica TCS NT confocal microscope with maximal pinhole aperture, in photon counting mode. As substrate alignment in the microscope focal plane is difficult to achieve, but important to measured readings, each signal was maximised by adjusting the microscope stage before measurement. Because the full range of hybridisation signals exceeded the dynamic range of the microscope, each sample was observed with three or more PMT voltages to ensure measure-



ment of the full signal range of each sample. Images from the confocal microscope were captured in a digital format and quantified using “The Image Processing Toolkit” (Reindeer Software) in Adobe Photoshop 6.0.

## 4.6 Acknowledgements

We especially thank Prof. P. Dobson and Dr. P. Leigh of Oxford Dept. of Engineering, and Dr. F. Marken of Oxford Dept. of Phys. Chem., and Dr. T. Fell of Oxford Dept. of Biochemistry for invaluable advice. Mr. M. Johnson helped with apparatus construction, and Drs. M. Shchepinov and K. Mir provided kind encouragement. RDE thanks the Rhodes Scholarship which enabled his Oxford tenure. This work was supported by the U.K. Medical Research Council.

## 4.7 Figures

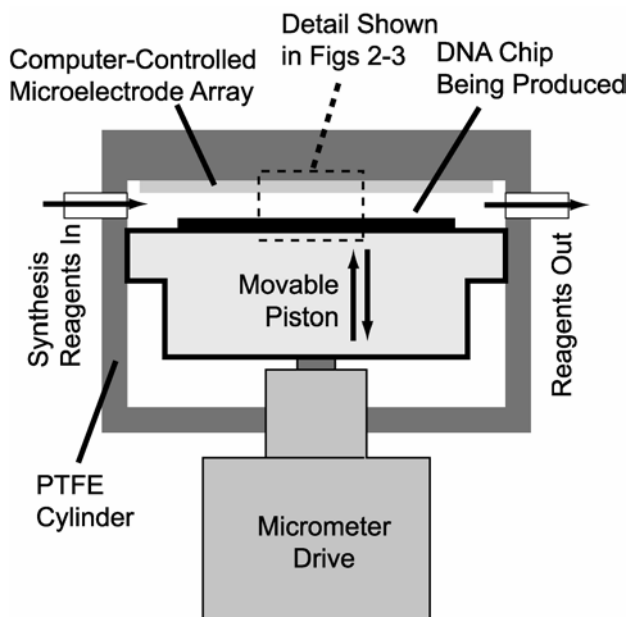


**Figure 19** Apparatus used for electrochemical treatment and oligonucleotide synthesis. Synthesis is accomplished in a reaction chamber in which an array of electrodes directs acid deblocking to confined regions on a solid support, a glass chip. The surface of the electrode array is sealed against the end of a PTFE cylinder to create a cavity. The glass chip is mounted on the end of a PTFE piston positioned by a micrometer drive. During the electrochemical deblocking step, the chip is presented to the electrode array by moving the piston forward to a 40  $\mu\text{m}$  gap. The piston is then moved back to widen the gap to 800  $\mu\text{m}$  to allow the cavity to be flushed with solvent, electrolyte, or solutions of reagents at the different stages of oligonucleotide synthesis, delivered from an ABI 394 DNA Synthesiser. A computer coordinates and controls the overall process: delivery of reagents from the synthesiser and application, switching, and measurement of current to the electrodes. Oligonucleotides of predetermined sequence can be made at any desired positions on the chip by appropriate programming of the electrochemical deblocking and nucleotide coupling steps.

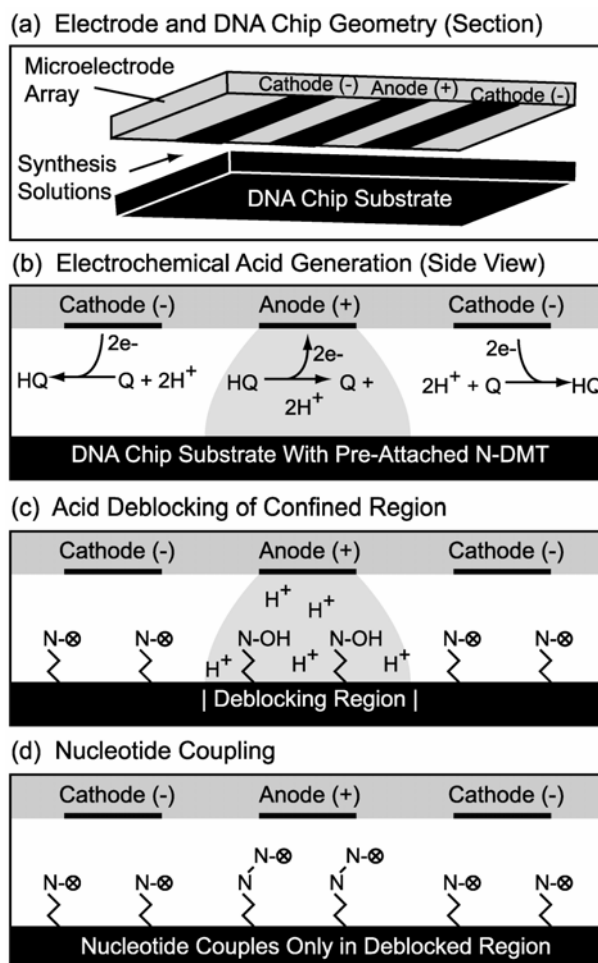


**Figure 20** Chemical reaction cycle. *(a)* Alternating electrodes of the array were connected as cathodes and anodes and placed adjacent to a glass chip with the apparatus in Fig. 1. *(b)* The electrolyte held between the surface of the chip and the electrode array comprises a solution of hydroquinone (HQ) and benzoquinone (Q) in acetonitrile. Oxidation at the anode produces acid (in the shaded region) and regenerates the benzoquinone consumed by cathodic reduction. Acid ( $H^+$ ) migrates away from the anode. Acid which migrates sideways reacts with cathodic products. *(c)* Acid which migrates downwards will meet the surface of the chip where it induces deblocking (removal of the dimethoxytrityl group ( $\otimes$ ) from the end of the oligonucleotide chain) thus selectively determining where the next nucleotide ( $N-\otimes$ ) additions will occur *(d)*. The amount of reactant produced and therefore the extent of modification of the surface depends on the strength and duration of the current.

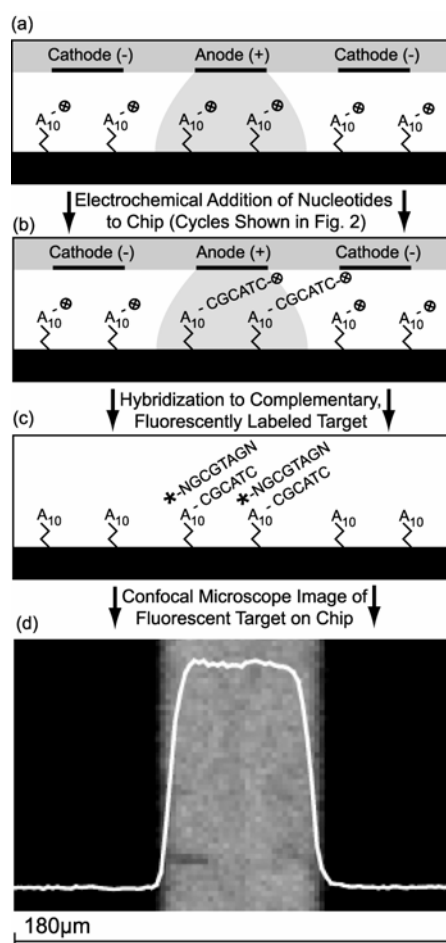


**Figure 21** Evaluation of electrochemical deblocking by hybridisation to a fluorescent complementary hexamer. **(a)** The hexamer was synthesised by adding six bases on to a presynthesised “lawn” of ten dA nucleotides (dA is the residue most sensitive to acid depurination) to maximise sensitivity to depurination reactions. **(b)** Electrochemical deblocking, followed by base addition was repeated six times (for the result shown) to produce the hexamer. **(c)** This electrochemically synthesised oligonucleotide was detected by hybridising to a complementary target known to hybridise in high yield only to the complete hexamer probe sequence. **(d)** The resulting fluorescent image of the complementary target; the high signal of the complementary target with respect to background fluorescence shows that synthesis of the hexamer was in high yield, even under the adverse conditions of a purine-rich “lawn.” The shaded region shows where electrochemical deblocking was performed as in **Figure 20b-c** and the white plot indicates fluorescent intensity across the image (arbitrary units).

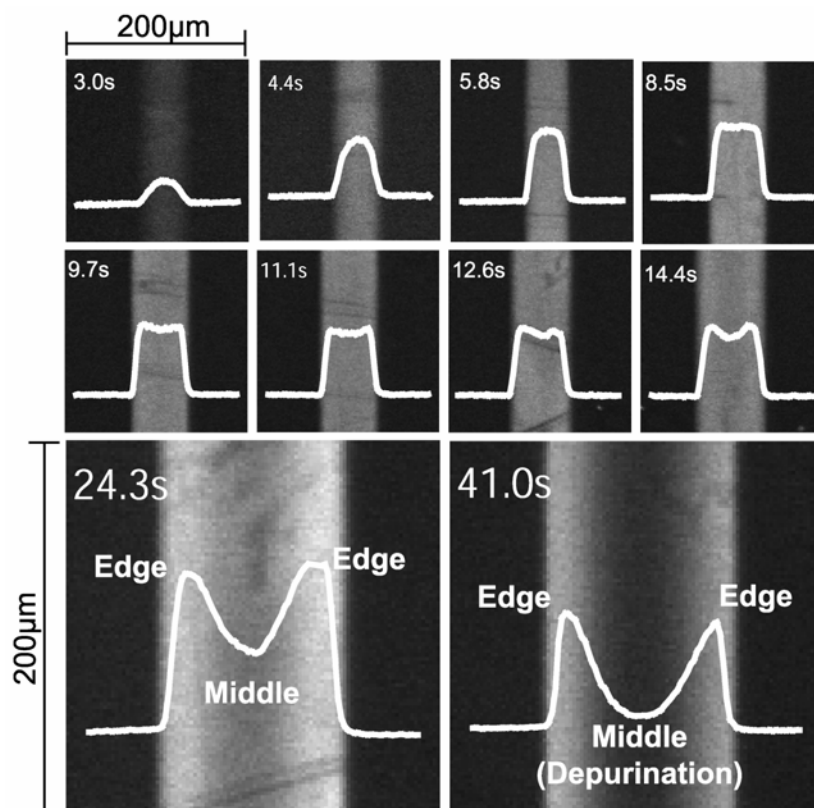


**Figure 22** A time course experiment with synthetic steps as shown in Fig. 3. The images show hybridisation to stripes of hexadecanucleotide, AAAAAAAAAACGCATC, made by coupling the first fourteen nucleotides over the whole surface. For the final two couplings, deblocking was carried out electrochemically. In each image, the duration for each deblocking step (in seconds) is shown in the upper left. The white plot indicates fluorescent intensity across each image; the units are arbitrary but consistent for all images.

At short times (approximately three seconds at each of the electrochemical deblocking reactions) the yield is low, because deblocking is incomplete. Intensity of hybridisation increases to a maximum between 5.8 and 8.5 s. With prolonged exposure to acid, depurination becomes more pronounced in the middle of the stripe where acid is most concentrated (11.1 s-24.3 s), but the edges still show high intensity, indicative of quantitative yield. Only after extremely long exposure to acid (41.0 s, bottom) does edge intensity decrease, after almost all of the middle has been depurinated. Even after such long exposures to acid, the edges remain sharp, indicating that the acid generated at each electrode is strictly confined and demonstrating minimal cross-talk between adjacent electrodes.

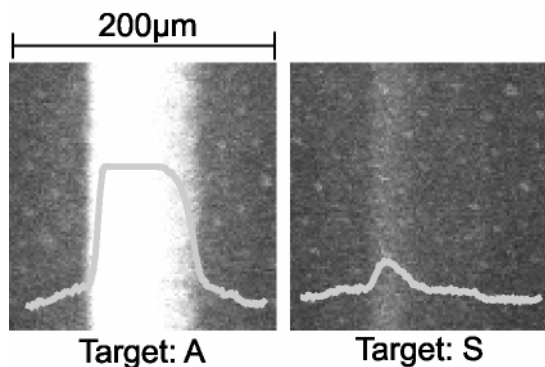


**Figure 23** Hybridisation of fluorescently-labelled wild-type “A” human  $\beta$ -globin oligonucleotides to electrochemically synthesised 17-mers. This confocal micrograph shows images of hybridisation to the matched target “A” human haemoglobin mRNA (left) and mismatched target “S” type sickle cell mutant mRNA (right). All 17 residues in the probe were coupled after electrochemically deblocking the previous residue. The peak signal for the matched target on the left is about 4.5 times that of the mismatch on the right. These images demonstrate high fluorescent intensity with good discrimination indicating high synthetic yields in these preliminary experiments.

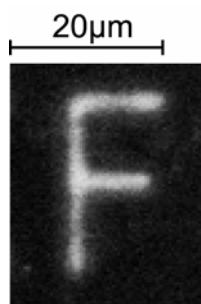


**Figure 24** Demonstration of small feature sizes. A multi-layer microelectrode device with 2 micron microelectrodes was used to attach a single fluorescently-labelled phosphoramidite to a solid surface using the electrochemical deblocking methods as shown in **Figure 20**. Confocal microscopy of the fluorescent molecule reveals features approximating the size and shape (the letter “F”) of the microelectrode used for synthesis. The relatively sharp and small features demonstrate the potential of electrochemical syntheses for high-density molecular array fabrication.

## Chapter 5

### Discussion I

# Electrochemical Microarray Fabrication: Outcomes and Comparison with Existing Methods

*This chapter highlights and discusses the electrochemical microarray fabrication techniques developed in this work. Particular attention is focused on comparison with other array fabrication methods. The chapter integrates discussion of this work as a whole.*

## 5.1 Review

The manuscripts contained within this thesis have discussed in detail the design and construction of a microelectrode and fluidics system used for *in situ* oligonucleotide synthesis for DNA microarray fabrication. First, the development of the hydroquinone and benzoquinone electrolyte and demonstration of the control of



diffusion through the reversible redox annihilation process at the zone between anodes and cathodes (**Chapter 2**) permitted spatially-confined, high-density, multi-step syntheses. Second, the fabrication of the microelectrodes and design of the fluidics and positioning system and accompanying electronics and software (**Chapter 3**) enabled subsequent highly-parallel experiments exploring effects of electrolyte composition and electronic parameters such as voltage, current, and pulse timing on patterns produced on the substrate. Exploration and optimisation of this surface patterning method in the context of oligonucleotide synthesis (**Chapter 4**) enabled successful and reproducible electrochemical construction of six-base sequences in high yield. Seventeen base sequences were synthesised as a final demonstration of the entire system, with discrimination of single-base mismatches detected in the human haemoglobin gene sequence.

As the electrochemical systems and techniques introduced in this thesis are new, evaluation of the results can be considered in the context of other existing micropatterning methods, with a focus on synthetic oligonucleotide DNA microarrays in particular. As mentioned, the immense number of distinct chemical steps involved in production of a single DNA microarray device brings unique mechanical, fluidics handling, synthetic chemistry, and quality control challenges; the apparatus and systems presented in this thesis go far in solving these. That no single microarray fabrication system has yet proven best for all circumstances,

despite a decade of intensive research, demonstrates the challenges and continuing evolution in this fast-moving scientific field.

Ultimately, the practical utility of a device made with the electrochemical methods presented in this thesis will be determined by its suitability in particular biological applications. Although different applications exploit specific device capabilities to various degrees, certain characteristics are universally desirable, and the electrochemical method presented here may be usefully evaluated in the context of these characteristics.

## **5.2 Uniformity, Consistency, and Reproducibility**

### **5.2.1 Spotting Arrays**

Array analytical sensitivity is important, given the biological significance of subtle variations in messenger RNA (mRNA) levels in gene expression analyses, or of single-nucleotide mismatches in genomic analyses. The method used by many laboratories, spotting pre-synthesised oligonucleotides or expressed copy DNA (cDNA)<sup>3,104</sup> on glass, is prone to a number of problems. Non-uniform spots, scratches, dye separation, and clumps commonly introduce significant error<sup>105,106</sup>, decreasing the power of the analysis. These problems are compounded when the probes are cDNAs, as the process of making the probes, by growing clones or

polymerase chain reaction (PCR) amplification, often leads to replacement of the desired probe by a contaminant<sup>107-109</sup>. Error rates as high as 40% have been reported when multiple error-prone methods are combined<sup>110,111</sup>. Furthermore, as the state of bound DNA is ill-defined for cDNA probes<sup>104</sup>, hybridisation to the target may be unpredictable and difficult to control. The ink-jet and photolithographic arrays, given that each probe is designed synthetically, are much more uniform than the spotting arrays.

### 5.2.2 Electrochemical Arrays

The electrochemical method, in contrast, allows specific direction of probe synthesis *in situ*. The electrochemically directed deprotection reaction is driven by solution chemistry and electronic switching of microelectrodes, rather than mechanical means of moving and depositing liquids. Because any inconsistency in the electrolyte solution or electronic circuitry will be recognised through significant current fluctuations, the current measured at each microelectrode gives a useful check of chemical yields. Notably, this quality-control check occurs in real-time; any deviations in the array fabrication process are noticed as the array is made, rather than after hybridisation experiments reveal flawed probes.

## 5.3 Fidelity of Synthesis and Length of Probes

### 5.3.1 Relevance of Probe Length

Some applications, such as the analysis of single nucleotide polymorphisms (SNPs), exploit minor variations in probe sequence to detect target sequence variation. For these applications, maximal sensitivity is achieved with short probes, as they show relatively large changes in hybridisation yields with only single base variations. In other applications, such as expression analysis, the probes are used primarily to quantify total levels of relatively dissimilar targets. Although short probes may be suitable for some of these applications<sup>1</sup>, longer probes minimise effects of site-specific interactions and melting temperature, and ensure high complementarity to target, thus maximising detection sensitivity<sup>112</sup>.

### 5.3.2 Photolithographic Arrays

Existing photolithographic *in situ* fabrication methods rely on a photo-deblocking step that is inefficient relative to conventional solution-phase 5'-dimethoxytrityl deblocking in acid. The resulting low stepwise yields, reported to range from 81-94% depending on the nucleoside and its substituents<sup>23</sup>, restrict the maximum oligonucleotide length on these photolithographic arrays to less than 25 nucleotides. More efficient photolabile blocking groups<sup>22</sup>, or other photolithographic processes, including the use of photochemically-generated acids to deprotect

conventional dimethoxytrityl (DMT) groups<sup>19</sup>, may increase yields. Nonetheless, at present, it seems doubtful that any of the photo-deblocking methods will reach the nearly quantitative yields<sup>71</sup> now routine with conventional solution-phase oligonucleotide synthesis. Indeed, the persistence of “descumming” steps (required to remove residual photoresist after exposure and development steps) in conventional microelectronics photolithography, where there are no complex DNA synthesis challenges, indicates the inherent difficulty of achieving quantitative yields with even simple photochemical reaction systems.

### 5.3.3 Ink-Jet Arrays

In contrast to the photolithographic arrays, ink-jet based arrays rely upon conventional oligonucleotide synthesis chemistry, resulting in correspondingly higher yields. High-quality short probes may be produced for analysis of variation, or probes in excess of 50 nucleotides may be used for expression analysis<sup>20,28</sup>. The ink-jet methods require precise mechanical alignment of the print head, process monitoring, and atmospheric control systems to ensure high-fidelity synthesis.

### 5.3.4 Electrochemical Arrays

This thesis demonstrates the electrochemical synthesis of 17-mers in high yield with a hand-made prototype device. Measured coupling yields are high (likely greater than 98%). Only the deblocking step, which is performed with an elec-

trochemically generated acid in acetonitrile, differs from conventional oligonucleotide synthesis. The concentration of the acid generated was easily controllable by manipulating the gap distance, applied voltage, or application time; a series of optimisation experiments exploited this flexibility to reach high deblocking efficiencies quickly. As the acid is generated in solution-phase, the deblocking step may be driven to completion by maintaining high acid concentrations. Using excess reactant in this fashion to increase product yields is a commonly used technique in organic chemistry, but has no direct equivalent in the case of photochemical reactions.

## 5.4 Density of Probes

Fundamental physical dimensions (the diameter of double-stranded DNA is 2.4 nm and 0.34 nm from base to base) place an lower bound on the smallest array feature size. Existing array fabrication techniques, however, do not approach this limit, although it is possible to perform manipulation and hybridisation of DNA at a molecular level in the limited scale of individually interrogated probes<sup>113,114</sup>. Thus, there is much room for improvement in array fabrication technology before molecular dimensions are reached; until that time, the primary impediments to increased density are more those of practical engineering concerns than fundamental physics.

### 5.4.1 Spotting and Ink-Jet Arrays

As cDNA-based arrays typically use a limited number of probes and are fabricated by hand or robotically driven pins, most spotting arrays are fabricated on a macroscopic scale. However, higher-density cDNA arrays can be made by more precise piezoelectric driven “pens,” or by ink-jet based methods. The ink-jet based methods typically achieve the smallest features (whether used for spotting cDNA or synthesising oligonucleotide probes in-situ), but imprecision of the ink jet printing head and spread of drops when they hit the surface limits ink-jet array densities to about 10-100 probes per mm<sup>2</sup> (feature sizes greater than 100 μm)<sup>28</sup>.

### 5.4.2 Photolithographic Arrays

Photolithographic arrays have a density of 1000-2000 probes per mm<sup>2</sup> (feature sizes around 20 μm). However, because the photolithographic arrays contain short probes, between 30 and 40 probes must be used per target in a redundant fashion<sup>1,112,115</sup>, offsetting the advantage of high probe density. Thus, the overall number of analysed targets per surface area is about the same for ink-jet and photolithographic arrays. Whereas mechanical precision limits the density of ink-jet arrays, diffraction, scatter, and internal reflection in the glass substrate blur the edges of the probes in photolithographic arrays; nonetheless, the sub-micron feature sizes realised through advanced techniques in the microelectronics industry demonstrate the potential for further miniaturisation.

### 5.4.3 Electrochemical Arrays

The smallest single-step feature demonstrated through the electrochemical method presented in this thesis is 3  $\mu\text{m}$  (representing a theoretical probe density greater than 100,000 per  $\text{mm}^2$ ), but the lower limit has not been aggressively pursued. The mechanical alignment of the substrate during reagent flushing, not diffusion or size of the microelectrodes, limited the smallest synthesised oligonucleotide probe to 40  $\mu\text{m}$ , with 120  $\mu\text{m}$  centre-to-centre distance. Assuming a large library of probes deposited at this feature size, the equivalent probe density (70-600 probes per  $\text{mm}^2$ ) compares favourably with ink-jet and photolithographic arrays. Nonetheless, both the ability to make very small electrodes and the diffusion-driven nature of the electrochemical process will limit the maximum densities possible through this electrochemical method.

#### 5.4.3.1 Microelectrode Engineering Considerations

Multiple experiments presented in this thesis show that feature sizes on the substrate correspond to the dimensions of the microelectrodes. As the microelectrodes used in these experiments were made through conventional clean-room techniques, there is no inherent reason high-tolerance equipment already used routinely in semiconductor manufacture could not be adapted to the process. Fabrication of 5  $\mu\text{m}$  microelectrodes was accomplished in this work with dated processes and equipment. Although clean-room capabilities limited device com-



plexity to a relatively modest design of 96 linear, passively switched electrodes, further integration of switching and measurement circuitry on the electrode device itself could readily enable hundreds or thousands of switchable microelectrode elements<sup>116,117</sup>. Thus, the challenges of electrode design in this work did not, and in principle should not, impede further attempts to increase array density.

The high currents necessary to drive the deblocking reaction to completion required special microelectrode materials. Iridium microelectrodes were most successful in these experiments, but as the electrolyte composition, applied current, electrode materials, and electrode geometry all influence the rate of acid reaching the surface, it may be possible to alter the most accessible of these parameters in future device designs. For example, exploring various electrolyte formulations could be continued further than in this work; adding chemical substituents to the benzoquinone, varying the concentration of background electrolyte, or even using a different solvent could improve compatibility with more conventional electrode materials.

#### 5.4.3.2 Fundamental Theoretical Limits

The 40  $\mu\text{m}$  microelectrode size used in this work was chosen only for convenience of manufacture in the clean room. Simple, single-step electrochemical patterns, with sizes below 5  $\mu\text{m}$ , were created using this technique. Although ex-

perimentally difficult to explore synthesis at very small dimensions, a comprehensive theoretical analysis aided by a detailed computer model evaluates the question of density and resolution for this technique. Presented in **Discussion II**, the analysis suggests feature sizes below 2  $\mu\text{m}$  are not unreasonable using the same chemical and electrochemical parameters as routine in this work. Computer simulations strongly suggest that sub-micron features may be possible with higher current, or a slightly modified electrolyte. Although the practical obstacles to manufacturing and controlling a device at that scale may prove severe, theory and simulation suggest that only engineering skill, and not fundamental physics will limit the technique's ultimate potential.

## 5.5 Ease of Fluidics and System Integration

### 5.5.1 Challenges in Fluid Handling

Oligonucleotide synthesis, whether performed through photolithographic or conventional deblocking chemistry, requires the delivery of reactive solutions and solvents including acetonitrile, dichloroacetic acid in dichloromethane, iodine, tetrahydrofuran (THF) and pyridine, acetic anhydride, N-methyl imidazole, and lutidine to a solid support (usually glass). Glass materials do not degrade on exposure to these reagents, but other materials used in constructing the fluidics

chambers, delivery lines, valves, and seals of a fluidics delivery system must withstand these harsh chemical conditions. Such design challenges limit the utility of microfluidics techniques developed for non-reactive, aqueous liquid handling. Furthermore, the coupling step during synthesis must be performed under anhydrous conditions; it is therefore necessary that fluid handling systems be impervious to outside air, or conducted under inert atmosphere.

### 5.5.2 Ink-Jet and Photolithographic Arrays

Only relevant to the *in situ* fabrication methods, various systems have been devised to deliver synthesis reagents for array construction. The ink-jet method, as mentioned earlier, relies upon the movement of a mechanical printing head to direct synthesis precursors on a substrate with localised hydrophobic and hydrophilic regions<sup>81</sup> to minimise spread of droplets when they hit the surface; the substrate is then taken to a liquid handling station for treatment with the oxidising and deprotecting reagents. One photolithographic system<sup>118</sup> requires the assembly and disassembly of chrome masks at each base addition step, representing the need for 100 chrome masks for arrays of 25-mers (although optimisation techniques can reduce the number required). Other photolithographic systems<sup>17,119</sup> use solid-state micromirror devices<sup>120</sup> in place of chrome masks, thereby alleviating the expense of mask design and complexity of alignment. In these systems, no moving parts are required for photolithographic array fabrication, as synthesis

reagents can be flushed through a chamber sealed to one side of a glass slide, with light directed from the opposite side, through the slide.

Fluid handling is also necessary during hybridisation for delivery of reagents, generally with the array mounted in a flow system. In the micromirror-based system<sup>119</sup>, the same flow system is used for both hybridisation and synthesis. This can be a disadvantage, as the machine is monopolised during hybridisation and cannot be used to make another array. For both the mask-based photolithographic and ink-jet methods, the arrays are diced into chips which are assembled into a custom flow device for hybridisation and processing.

### 5.5.3 Electrochemical Arrays

One advantage of the electrochemical method is that the work piece need not be separated from the tool at any stage. The flow cell described in this thesis allowed positioning of the substrate adjacent to the microelectrode array with an accuracy of about one micron. Although it was necessary to move the substrate further away from the microelectrodes while flushing synthesis reagents through the chamber in this design, there is no inherent reason the fluids could not be delivered through alternative means directly into the gap.

The sealed piston and cylinder used in the work presented here eliminated the need to carefully re-register the lateral position of the substrate each time it was moved back and forth for reagent flushing. Nonetheless, it became apparent that

fluctuations in lateral alignment over the 34 piston movements during 17-mer synthesis confounded the ability to direct electrochemical deprotection at precisely the same location on the substrate each time. As the piston and cylinder apparatus was constructed with PTFE (“Teflon”), a relatively deformable polymer, it is not surprising that there was some horizontal play in the piston; measurement of this misalignment by confocal image analysis of defective probe attachments indicated a possible 40  $\mu\text{m}$  maximum deviation with 34 piston motions, with 5-10  $\mu\text{m}$  generally more typical.

Although this horizontal piston deviation proved irritating, it did not prevent successful synthesis of long probes with a careful reproduction and control of the piston motion from step to step. Furthermore, it may not be necessary to allow such continuous control of the substrate in future designs; recall that the system was designed to explore the effects of substrate-microelectrode gap distances on the deprotection reaction. Subsequent flow-cell designs intended only for array synthesis with these microelectrodes under optimal gap distances could employ 40  $\mu\text{m}$  stoppers attached to the microelectrode array and on which the substrate would rest during deprotection. Precise and accurate substrate alignment in this arrangement would be dependent only on the rigidity of the microscopic stoppers, rather than on the macroscopic fit of the piston and cylinder. In addition, these stoppers could also be configured to limit the horizontal deviation, if this indeed proved significant with smaller microelectrodes.

## 5.6 Simplicity of Fabrication

Though this thesis focuses on the scientific and technical aspects of electrochemical microarray fabrication, discussion is only complete with a brief prediction of difficulties in practice. Although technical advances are rapidly decreasing costs per microarray analysis, very significant research and development expenses and high equipment costs are typical of most means of making arrays at present. Costs are falling, but the high investment required in clean-room construction, mask development, and equipment upkeep and maintenance add significant expense to photolithographic arrays. The difficulty of maintaining the ink-jet head alignment and fluidics over many thousands of runs could likewise prove troublesome. The cDNA libraries or large sets of synthetic oligonucleotides used for spotting arrays are expensive to buy and maintain.

Costs for the electrochemical method could be less than others, given the mechanical simplicity of the fabrication apparatus. Reagents for *in situ* synthesis are relatively inexpensive and the main cost is in the solvents. The most expensive part of the apparatus is the microelectrode set, which can be reused to make many arrays (one electrode set was used in this work over 1,000 times with no sign of deterioration). The microelectrode sets, although customised designs in this work, could be produced more cheaply in higher volumes at conventional microfabrication facilities. The actual oligonucleotide synthesis lends itself to

automation; equipment should be easy to maintain, given its simple design and few moving parts.

## 5.7 Customisation of Probe Design

Some array fabrication techniques are best suited to large-volume production of identical devices. For example, designing and making the many chrome masks used for photolithographic arrays represents a significant expense, so that the method is only reasonable when a known optimum, fixed set of probes is relevant to a wide range of different investigations. Such a prerequisite is not feasible in many applications. It may be necessary to change the probe set from one run to another, for example, in experiments to optimise probe design. Likewise, adding a probe for a newly discovered gene or a mutation in an existing set could require an entirely new set of expensive masks.

The ink-jet and micromirror methods, in contrast, allow complete flexibility; each array made may be different from any other. Changing the design is simply a matter of changing the sequence data that drives the print head or micromirror driver. Conversely, these methods may also be used for large-volume production. However, as throughput is limited in the ink-jet method by the speed of the print head, and in the micromirror method by the total number of pixels on the

micromirror device, these methods may not scale well to higher volumes of fabrication.

The electrochemical method is similar to the ink-jet and micromirror array methods in that the process is directed by a computer instruction set based on the sequence content of the array. A change in design is effected by simply changing the instruction set. This is not to say the method is unsuitable to large-volume processing with multiple electrode sets. In other words, it is as easy to make one thousand different, customised arrays as it is to make one thousand identical arrays.

Many types of surface patterning reactions (other than the conventional oligonucleotide synthesis presented here) could be controlled electrochemically. First, acid may be involved in many other types of reaction on the substrate, for example eliminations, substitutions, rearrangements and chemical etching. Likewise, electrochemically-generated bases could also be used to eliminate base-labile moieties such as 9-fluorenylmethoxycarbonyl (Fmoc) or cyanoethyl groups, particularly relevant for peptide synthesis and peptide-oligonucleotide conjugation chemistry<sup>121,122</sup>. Radicals, halogens, and other reactive intermediaries generated at microelectrodes could be used to elicit other exotic modifications. The large range of possible chemical modifications leaves much room for many types of probe synthesis and modification.



## 5.8 Range of Applications

As discussed in the context of synthesis fidelity and probe length, long probes are more applicable to expression profiling, while short probes are particularly suited to genotyping. Most purposes can be served through ink-jet *in situ* synthesis or spotting pre-synthesised probes at present. Photolithographic arrays are not particularly suited to expression profiling given short probe length, although they have successfully been used for this purpose<sup>123</sup>, and higher coupling yields<sup>124</sup> could increase sensitivity and utility. One original disadvantage of the photolithographic method was that the photolabile protecting group could only be used to block 5' hydroxyls, precluding reverse oligonucleotide synthesis useful for enzymatic extension-based detection methods, although new photocleavable groups<sup>125</sup> may permit such 5' → 3' syntheses.

The work described in this thesis does not push the electrochemical method to its physical limits, but we know probe length and fidelity depends on efficiency of chemical coupling at each base addition. The efficiency was demonstrated to be very high. As the feature sizes are small, the electrochemical method here could in theory combine the high density of photolithographic arrays with the high fidelity of ink-jet arrays. Furthermore, as conventional oligonucleotide synthesis reagents are used (with the exception of the electrochemical step which is only a substitution of one type of acid with another), non-standard or exotic syn-

theses (for example, reverse synthesis) will not require lengthy development of a new photocleavable linker for each application.

## 5.9 Medical Applications

It is beyond the scope of this thesis to review in detail the immense range of biological and clinical microarray applications. For a short review of the recent medical literature, see **Appendix A**.

Most arrays are used in research applications at present, but this will likely change as microfluidics capabilities improve<sup>126-132</sup>. There are two types of clinical diagnostic applications used in research laboratories: detection of molecular lesions associated with disease states, such as cancer, and analysis of gene expression associated with pathological states. These studies can aid in disease classification, prognostic estimates, and help identify targets and biomarkers useful for guiding treatment decisions. Cancer provides a useful example: the tremendous breadth of somatic mutations possible in its initiation and progression can only be captured practically through highly parallel means; arrays are particularly suitable, and have been shown to greatly supplement differential diagnosis, tumour typing, and treatment planning in many human malignancies<sup>133,134</sup>.

At present, however, the cost of each microarray analysis prohibits use in routine clinical diagnostic laboratories. With further development of fabrication

methods, sample preparation techniques, analysis instrumentation, and data analysis algorithms, costs will fall to levels appropriate for widespread use of microarrays in an outpatient clinical setting. It is hoped the electrochemical method described in this work will become a useful tool in the future of genomic medicine.

## Chapter 6

### Discussion II

# Diffusion, Annihilation, and Resolution: Theoretical Considerations and Digital Simulation

*This chapter discusses the results of the electrochemical method in the context of fundamental physical and chemical characteristics. It presents a theoretical framework for the high feature resolution attained, describes a digital simulation used to explore the patterning properties, and discusses theoretical limits to smaller patterned feature sizes. The discussion in this chapter was followed by additional work leading to a brief paper, presented in **Appendix B**.*

## 6.1 Context

As the acid generated at the microelectrode surface reaches the substrate by diffusion, substrate patterning characteristics are affected by diffusive mass trans-

port processes. Thus, not only the shape of the microelectrodes, but also the distribution and motion of acid in the electrolyte would be expected to limit resolution. Diffusion, in acting to homogeneously distribute the highly localised acid generated at the surface of the microelectrodes, tends to spread acid everywhere over the substrate. The edges of the features created in this work, however, were sharper than would be expected from freely diffusing reagents.

The annihilation reaction, chemically characterised in **Chapter 2**, limits the spread of acid in solution. Chemical interaction between the benzoquinone radical anion and proton in the region between the electrodes causes mutual annihilation of these two electrode products. This acts to confine the acid to a zone defined by the cathodes, which flank the anodes and generate the benzoquinone radical anion. The boundary is surprisingly stable; it extends several tens of microns into the electrolyte solution, and is sustained for more than a minute. In short, the annihilation process creates a reactant boundary such that acid can be held in a defined location indefinitely. Although governed by an underlying dynamic process, such a physical state resembles the stable boundaries more typical of solids. Indeed, the strict concentration boundaries of the reactants in solution may be described as “solid state” chemistry in a liquid solution.

Initial attempts to characterise the annihilation reaction system mathematically revealed a relatively complex set of interactions. The rate of acid production at the electrodes, its diffusion in solution, the kinetics of the annihilation reaction,

the chemistry of the deblocking reaction at the surface, the geometry and electrical switching of the electrodes, the substrate-electrode gap, and the nature of the electrolyte all affect the patterning process. Furthermore, these variables are not independent: diffusion depends on the rate of reactant production and its consumption, the annihilation reaction depends on diffusion, the kinetics of acid production depends on diffusion of reactants to the electrodes and their initial concentrations, and so on. This complexity of the overall dynamics of the annihilation reaction obscures any insight gained by observing, for example, diffusion layer boundaries in isolation from other processes.

Although the system's complexity limits the utility (and feasibility) of an analytical approach to its variables, a numerical computer model proved helpful in characterising the patterning process. Based on fundamental physical descriptions of all system reactions and mass transport effects, the digital simulation provided a powerful means of observing the complex physical chemistry behind the delivery of acid to the surface. This section will briefly describe the development of the simulation in the context of other approaches to the diffusion problem in electrochemical patterning, and the annihilation system used in this work.

## 6.2 Electrochemical Patterning

### 6.2.1 Existing Techniques and Limitations

A number of methods using electrochemical systems for patterning surfaces have been described in the literature. Since its introduction more than a decade ago<sup>31</sup>, the typical electrochemical configuration involves moving a small wire tip across an electrically active patterning material. Termed scanning electrochemical microscopy (SECM), electrochemical reactions induced at the probe tip may be used to produce species which etch the patterning material. Although this method has been used to etch features as small as 2.5  $\mu\text{m}$  in size<sup>32</sup>, the etchants generated at the probe reach the surface by diffusion, which also acts to spread the etchant laterally in solution (**Figure 25**). For example, a small 1.7  $\mu\text{m}$  electrode (as arranged as in **Figure 26**) generates a 250  $\mu\text{m}$  pattern after 20 seconds, which grows to an immense 400  $\mu\text{m}$  after 80 seconds<sup>69</sup>.

In general, as dimensions of the electrochemical tool used to create a pattern are decreased, diffusion will become ever more significant in moving reagents away from the tool tip. This can be shown by a simple evaluation of Fick's second law

$$\frac{\partial C}{\partial t} = D \frac{\partial^2 C}{\partial x^2}$$

which relates the concentration of a species in solution  $C$  at location  $x$  as a function of time  $t$  and the diffusion coefficient  $D$ . From this expression, we see that the steeper the change in concentration, the greater the rate of diffusion. As decreasing the dimensions of the tool is analogous to a decrease in  $x$ , we can see that diffusion becomes a problem at small dimensions.

Because of the limits diffusion places on the resolution of any electrochemical patterning process, various means have been devised to control it. One approach is to add a homogeneous scavenger species to the electrolyte solution which acts to actively consume the etchant<sup>135</sup>. Another method, suitable for deep etching, employs very short pulses of a high voltage to limit etchant diffusion time<sup>32,136</sup>. Although both methods increase attainable resolution, one must use extremely short reaction times to maintain sharp resolution. The annihilation reaction system used to control diffusion in this work differs markedly from these approaches.

### 6.2.2 The Utility of Annihilation

The annihilation of protons generated at the anodes by the radical anions generated at the cathodes strictly confines the distribution of acid in the experiments presented in this thesis. This fundamental physical reaction system effectively constrains the action of the acid to a fixed range between the cathodes (**Figure 27**), so that very high definition features may be patterned on the substrate.



These diffusion-confining effects are persistent throughout even long applications of current, indicated by the similarity of patterns produced after 5 and 80 seconds of reaction time. Furthermore, these effects serve to allow very sharp edges at the substrate placed at up to 180  $\mu\text{m}$  from the electrodes (**Figure 35**). A mathematical treatment of the annihilation process itself lends useful insight on the nature of these observations.

### 6.3 Annihilation Physics and Chemistry

Annihilation processes in diffusive motion were first described numerically and analytically by Toussaint and Wiulczek in 1983<sup>137</sup>. The chemical system, termed in the theoretical physics literature an inhomogeneous two species annihilation reaction, exhibits unique properties attributable to the physics of chemical interaction between two distinct species in solution. Consider the two-species annihilation reaction  $A+B \rightarrow 0$ . When particles of type A and B originate from different locations in solution, a stable geometric arrangement of concentrations of A and B will develop over time<sup>138</sup> (**Figure 27**). Thus, although individual particles A and B diffuse freely in solution, the mutual annihilation reaction tends to create

fixed concentration profiles<sup>e</sup>. The rate of the underlying annihilation reaction occurring throughout the reaction zone also varies in space in a similar fashion.

In this dynamic chemical system, the shape of the concentration profile created through the annihilation process is ultimately governed by both (1) the magnitude of flux of species toward one another and (2) the chemical kinetics of the annihilation reaction. In the electrochemical system used in this work, the stream of reactants continuously generated at the microelectrode surface creates the opposing species flux. The free energy of species interaction (in other words, the reaction free energy, ultimately determined by chemical structure, the nature of the solvent, and the background electrolyte) determines the annihilation kinetics.

**Flux.** Hydroquinone oxidation at the anode directly produces protons, one of the mutually annihilating species. At the cathode, the benzoquinone radical anion produced by benzoquinone reduction represents the other species. As the anode and cathode in this system complete an electrical current path, the number of electrons participating in oxidation at the anodes must always equal the number participating in reduction at the cathodes (**Figure 30**). Because the stoichiometry of the two reactions are equivalent (one electron generates one charged product), it follows that the rate of proton and benzoquinone radical an-

---

<sup>e</sup> Given the complexities of the chemical interactions presented in **Chapter 2**, this is a gross simplification, and is used only to illustrate annihilation processes in general. The computer simulations discussed later incorporate the full complexity of the chemical system used in this work.

ion production is always equal, and related to the current  $i$  by Faraday's constant  $F$  and the definition of current,

$$i = \frac{dq}{dt}, \text{ and } \frac{dC_t}{dt} = \frac{i}{F},$$

where  $C_t$  is the total molar quantity of product produced through either oxidation or reduction. Once generated at the surface of the microelectrodes, the species will travel towards each other through diffusion-mediated mass transport, setting up a system similar to the theoretical treatment as shown in **Figure 29**.

**Chemical Kinetics.** Although the process of annihilation is qualitatively described quite simply, sophisticated mathematical approaches, such as the use of quantum-field theory and the Schrödinger equation, have been used to develop full analytical (i.e. generalised, formula-based) solutions to even simple diffusion-limited reactions<sup>139</sup>. Some of this literature, however, is directly relevant here. Ben-Naim and Redner<sup>138</sup> investigated the geometrical properties of the reaction zone (the region where annihilation occurs), when particles are injected at a fixed rate  $j$  from opposite edges of the system (**Figure 28** and **Figure 29**). They describe that the width of the zone in which the annihilation reaction occurs varies inversely with  $j$ . Interestingly, they further categorise the behaviour of the reaction zone width according to whether the flux is large or small. In the limit of large flux, they describe the reaction zone width  $w$  as

$$w \propto \frac{1}{\sqrt[3]{j}},$$

with the concentration within the zone scaling as  $j^{2/3}$ . In the opposite case, with the limit of very low flux, the concentration assumes a nearly constant value of order  $j^{1/2}$  throughout the system, in which the maximum spatial variation is of order  $j$ . The large flux case leads to a sharply localised reaction rate near the domain centre, while in the low flux case, the reaction rate is greatest (but overall quite uniform) near the extremities of the domain (these relationships are depicted in **Figure 28**). Lee and Cardy<sup>140</sup> verify and expand the analysis, confirming that the reaction zone width scales as described in one or two dimensions.

The spatial distribution of the annihilation reaction is critical to the distribution of acid in solution, and is thus worth considering in more detail. For the purposes of confining the acid to a strictly defined boundary, the annihilation reaction should consume all acid beyond the boundary, but none of it within (**Figure 31A**). Of course, such a system would defy the principles of statistical thermodynamics, but the surprisingly sharp and stable boundaries discovered experimentally in this work suggest nearly ideal behaviour with 40  $\mu\text{m}$  electrodes. Cornell and Droz<sup>141</sup> provide a useful theoretical treatment applicable to this discussion. In summary, their findings reiterate the inverse relationship between flux density and annihilation reaction zone width but describe the transition from low-flux to high-flux as a continuous variation as follows:

$$w = \alpha \frac{1}{j} + k ,$$

where  $w$  is the width of the annihilation zone,  $j$  is the flux magnitude, and  $\alpha$  and  $k$  are constants related to the number of dimensions in the system. Thus, there is a continuous variation in reaction zone width with flux. This is important, as it means the annihilation reaction will become less effective in confining acid as flux decreases (**Figure 31**). Ultimately, with very small flux, the acid is distributed almost homogeneously in solution (**Figure 32**). Thus, when the system approaches the low-flux limit, localised surface patterning is impossible.

The obvious experimental variation which will act to reduce flux is reducing the current; this could be caused by decreasing the size of the electrodes with fixed potential. This concept reveals an important implication: if the flux of products into the space between anode and cathode decreases significantly with smaller electrodes, the patterned features become less defined and ultimately indistinguishable. Of course, it seems logical that physics dictates a minimum feature size for this technique. Theoretical analysis reveals a counterintuitive generalisation: only by generating large quantities of acid can one keep it confined.

## 6.4 Limits of Theory

Although the theoretical analysis of annihilation and its variation with flux is useful for a conceptual definition of the electrochemical system used in this work, the exact definition of high flux and low flux under typical experimental condi-

tions is unclear. For example, how do current measurements at the electrode (surface plane) relate to flux across the (orthogonal, vertical) plane in the reaction zone? What magnitude of electrical current induces the annihilation reaction to exhibit typical high-flux behaviour? At what current does the transition to a more low-flux appearance occur? How would the use of much smaller micro-electrodes (sub-micron, for example) alter the distribution and transport of species in solution? Does the physical boundary imposed by the substrate alter annihilation geometry?

Given the dependent relationships between current, the electrolyte, diffusion, and all the other variables important to the electrochemical system used experimentally, an analytical approach to answering these questions was not feasible. A computer simulation incorporating the experimental variables, theoretical relationships, chemical kinetics, and chemical dynamics, however, provided a useful approach. The architecture of the simulation relied on breaking each of the physical processes into separate subroutines; a unified result was obtained by tallying the actual chemical concentrations of all reactants over time. Devised through an iterative development process of progressively increasing complexity, the computer simulation proved helpful not only modelling the chemical processes, but in aiding the process of discovery. With it, one question was most compelling: “What are the theoretical limits to feature densities using this electrochemical patterning method?”

## 6.5 A Computer Simulation

In collaboration with colleagues in our group<sup>f</sup>, a computer model was developed to help describe and interpret the experimental patterning results presented in this thesis. The software used known kinetic rate constants and diffusion coefficients in modelling the following:

- redox reactions at the electrode
- diffusion of redox products in electrolyte solution
- annihilation reactions
- electrical current at the microelectrodes
- deblocking reaction at the substrate

The computer program displayed the distribution of acid and radical anion concentrations graphically, using a colour scheme where blue represented radical anion and red represented acid. The extent of the substrate patterning reaction was also presented as a colour image resembling the format of the fluorescent images generated from confocal microscope scans of patterned substrates. Likewise, the electrical current measurements taken during physical experiments were comparable to the model's theoretical predictions. Thus, the very large number of confocal images and current profiles permitted comparison of experimental data with theory and mathematical description.

---

<sup>f</sup> Based on the physical chemistry principles and experimental data developed in this thesis, J. Elder of our research group wrote the Unix-based computer code used for the simulation, including an accompanying graphical user interface.

In summary, the model used the diffusion and reaction-rate laws to simulate the distribution of acid and other species in solution and its effect on the substrate. A brief description of the computer simulation<sup>g</sup> follows.

### 6.5.1 Setup

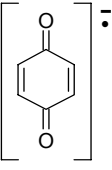
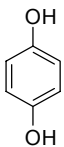
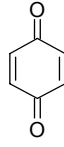
Simulations take place on a grid of variable dimensions up to 800 nodes wide and 120 nodes high, where the width is determined by the positions of left and right boundaries and the height is determined by the position of the substrate. In the simulations shown here, space is assumed to be continuous across the right and left boundaries, which are fixed at the midpoints of two cathodes neighbouring a single anode. This setup models the case of an infinite replication of alternating anodes and cathodes. Each grid node represents a square of side 1000, 500, 250, 100, 50, 25, 10, 5, or 1 nm, as specified by the user. A simulation consists of a series of steps, each of which corresponds to a fixed time interval governed by the diffusion coefficient and the grid size.

There are four species of particle: red, blue, red-grey and blue grey. These colours correspond to the proton, benzoquinone radical anion, hydroquinone, and benzoquinone species as discussed in **Chapter 2** as follows:

---

<sup>g</sup> This section was prepared in close collaboration with J. Elder.



Red	Blue	Red-Grey	Blue-Grey
H <sup>+</sup>			

The model works with the concentrations of these species rather than with particles themselves (i.e. this is not a Monte-Carlo approach). Each grid node records the concentrations of the four species at that position.

At the start of a simulation the grid is populated uniformly with red-grey and blue-grey species only, each typically at a concentration of 25 mmol/l (the experimentally used concentration).

## 6.5.2 Simulation

Each step of a simulation consists of diffusion, activation, annihilation and substrate activity.

### 6.5.2.1 Diffusion

Each of the four species travels by diffusion over the grid area independently of the others according to the diffusion equation

$$\frac{\partial u}{\partial t} = D \left( \frac{\partial^2 u}{\partial x^2} + \frac{\partial^2 u}{\partial y^2} \right)$$

where  $u$  is the species concentration and  $D$  is the diffusion coefficient. Although the system being modelled is three-dimensional, it is assumed to extend uniformly and infinitely in the  $z$ -axis so

$$\frac{\partial^2 u}{\partial z^2} = 0$$

and the above form of the diffusion equation and a two-dimensional grid can be used while continuing to treat concentrations as three-dimensional quantities.

The diffusion equation is solved by the method of finite differences, using forward Euler differencing. The stability criterion for this method applied to the above diffusion equation is

$$\frac{4D\Delta t}{(\Delta x)^2} \leq 1$$

where  $\Delta x = \Delta y$  is the grid spacing. For a typical diffusion coefficient<sup>h</sup> of  $3 \times 10^{-5} \text{ cm}^2/\text{s}$  this gives a time step of  $\Delta t \leq 83 \text{ } \mu\text{s}$  for  $\Delta x = 1000 \text{ nm}$  and  $\Delta t \leq 83 \text{ ps}$  for  $\Delta x = 1 \text{ nm}$ .

Diffusion is subject to the following boundary conditions. The  $x$ -axis and the substrate boundary are treated as non-permeative boundaries by setting  $\partial u / \partial y = 0$  along their lengths. The left and right boundaries are treated similarly by setting  $\partial u / \partial x = 0$ , thus allowing a setup with an infinite series of equispaced

---

<sup>h</sup> Diffusion coefficients were obtained from standard tables. A value of  $3000 \text{ } \mu\text{m}^2\text{s}^{-1}$  was used for both benzoquinone and hydroquinone.

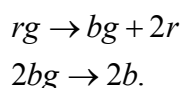
alternating red and blue electrodes to be modelled by single red and blue electrodes.

Each of the four species diffuses according to the diffusion equation by applying one step of the forward differencing method.

### 6.5.2.2 Activation

Red-grey species at each grid node adjacent to a red electrode are converted to red according to a pseudo first-order rate law<sup>142</sup>. Current is calculated from the total amount of matter converted at red electrodes<sup>i</sup>, and for an electrode of dimensions 40 x 7500  $\mu\text{m}$ , rate constant of 700/ms and time step of 1/12 ms is approximately 0.5  $\mu\text{A}$ <sup>j</sup>.

Blue-grey species adjacent to blue electrodes are converted to blue in the same way, subject to the constraint that the total numbers of red-greys and blue-greys converted at each step are equal. The activation reactions are




---

<sup>i</sup> The total rate of oxidation at the anodes and reduction at the cathodes was assumed to be equal (as the current sum must be zero across all electrodes) and governed by a pseudo first-order rate law; current at each electrode was calculated from Faraday's law as charge per unit time.

<sup>j</sup> The rate constant was determined empirically by matching simulation (calculated) current with experimentally measured values under identical conditions.

### 6.5.2.3 Annihilation

Red and blue species partially annihilate each other at each grid node according to the second order integrated rate law for bimolecular reactions<sup>142</sup>

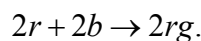
$$\log \frac{B_o}{A_o} \frac{A}{B} = \delta kt ,$$

where  $\delta = A_o - B_o$  and  $k$  is the rate constant (typically 10 l/mol/ns)<sup>k</sup>. For initial concentrations  $A_o$  and  $B_o$ , concentrations  $A$  and  $B$  after time  $t$  are

$$A = \frac{\delta \exp(\delta kt)}{\exp(\delta kt) - (B_o/A_o)}$$

$$B = A - \delta.$$

Red and blue species which are annihilated become red-grey and blue-grey species respectively according to the reaction



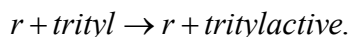
### 6.5.2.4 Substrate

Grid nodes on the substrate surface are initially populated with an inactive species (trityl) of specified monolayer concentration (typically 1000 nmol/m<sup>2</sup>)<sup>l</sup> and

---

<sup>k</sup> The annihilation rate constant was estimated from electrochemiluminescent kinetic studies for a similar annihilation reaction system<sup>138</sup>, and is of sufficient magnitude to indicate the reaction is diffusion-limited (the rate the reactants encounter each other in solution, not thermodynamic considerations, determine the overall reaction rate). The solvent and ionic strength of the electrolyte could alter the free energy of interaction between oppositely-charged reactants, thus affecting this rate constant. For the similar electrochemiluminescent system annihilation reaction, both lowering solvent polarity and decreasing ionic strength act to increase annihilation kinetics<sup>139</sup>.

fixed location. Red species in grid nodes adjacent to the substrate interact with the inactive species according to the second order reaction



The rate constant for this reaction is typically  $10^{-4}$  l/mol/ns<sup>m</sup>.

### 6.5.3 Experimental Verification

Comparison of computer simulations with the theoretical description of annihilation demonstrated good similarity between the two (**Figure 33**). The model usefully recreated the acid concentration and annihilation reaction rate profiles as predicted by theory. The agreement between simulation and theory thus provided evidence that the model accurately predicted experimental results.

Comparison of simulation results with experimental data further supported the accuracy of the model. **Figure 34** shows a computer simulation of the pattern produced on the substrate with the typical 40  $\mu\text{m}$  experimental configuration. There was good agreement between the experimental data recorded from an actual electrochemical oligonucleotide synthesis for multiple time points. Both the model and measured fluorescent images show incomplete acid deblock-

---

<sup>1</sup> This monolayer loading density value was obtained from physical measurements by colleagues in our group<sup>73</sup>.

<sup>m</sup> The detritylation rate constant was estimated based on studies using controlled-pore-glass. As the substrate in these experiments is planar, however, there is likely some error in this estimate. Although a recent paper<sup>140</sup> suggests more sophisticated kinetic modelling may be warranted for surface reactions, the long polyethylene glycol linker to which surface oligonucleotides were tethered justified this approach.

ing up to about 5 seconds, with no pattern definition loss beyond this time point. Furthermore, the model provides added utility not available experimentally: although the completion of the deblocking reaction takes approximately 5 seconds, the concentration profiles (not observable experimentally, of course) stabilise before 3 seconds.

The model also demonstrates accurate prediction of pattern variation with changes in the microelectrode-substrate gap distance. **Figure 35** shows experimental data when varying the gap distance from 2 to 80  $\mu\text{m}$ . Both simulation (not shown) and experiment show the relatively minor importance of gap distance on the resulting pattern. Examination of the acid concentration profiles with varying gap distances shows the likely reason for this independence: annihilation consumes acid mid-way between anode and cathode at any height from the electrode.

In summary, the computer simulation captures the subtleties of the annihilation reaction. Compared to both theory and experimental data, it accurately reproduces expected effects at the 40  $\mu\text{m}$  experimental scale. The concentration and annihilation reaction profiles resemble the theoretical description in the large-flux limit at this scale, presumably because the amount of acid generated with 40  $\mu\text{m}$  electrodes is sufficient to maintain a sharply defined annihilation reaction zone. With the accuracy of the model established for the large set of ex-

perimental data, we now turn to exploring annihilation at the smaller scale not amenable (at least in this work) to experimental investigation.

## 6.6 Fundamental Physical Limits

Simulated proton concentrations in the zone between the anode and cathode with decreasing microelectrode and gap distances demonstrated decreases in edge definition for electrodes less than about 4  $\mu\text{m}$  wide using the same electrochemical parameters as used experimentally. Below 1-2  $\mu\text{m}$ , the annihilation effect ceased to confine the protons, resulting in an indistinct surface pattern (**Figure 36**).

As predicted by theory, increasing the rate of proton generation at small scales increases patterned feature definition. By increasing the current density tenfold from 1.7 to 17  $\text{pA}/\mu\text{m}^2$  at 1  $\mu\text{m}$  electrodes (**Figure 38**), it is possible to increase the rate of annihilation and confine the acid sufficiently enough to maintain sharp sub-micron features. Although simulations predict a minimum feature size near 2  $\mu\text{m}$  using the typical electrolyte, increasing the flux of reactants would increase the annihilation rate and therefore resolution (**Figure 38** shows 1  $\mu\text{m}$  features). Increasing reactant flux could be accomplished by (1) increasing the concentration of hydroquinone and benzoquinone, (2) switching to an electrolyte which more readily liberates acid, (3) adding substituent groups to the base hy-

droquinone moiety to decrease its pKa, or (4) applying higher currents or voltages<sup>n</sup>. As we have discovered that the rate of product generation at the electrodes ultimately controls annihilation, these methods may prove useful in further decreasing feature sizes. Sub-micron features seem reasonable given these findings.

In summary, the computer model of the annihilation reaction, verified by experimental data at a larger scale, predicted a theoretical feature size limit of less than 4  $\mu\text{m}$  using the same chemical system as in the larger-scale experimental investigations. Optimisation of the electrochemical system with the intention of facilitating annihilation would likely aid in pushing the patterning technique to its fundamental physical limits. In the interim, more mundane engineering concerns, such as the ability to make small electrodes and deliver synthesis fluids to small-scale devices, will likely present the most immediate barriers to realising the full potential of this electrochemical patterning technique.

---

<sup>n</sup> Another more complex determinant of flux not directly calculated by the model may be the substrate-electrode gap at any fixed microelectrode dimensions. As the gap decreases, ohmic resistance of the electrolyte increases, since the volume of the electrolyte available to pass current is reduced. This will tend to decrease the maximum rate of acid production. This effect may be counterbalanced, however, by the decreases in ohmic resistance with smaller microelectrodes.



## 6.7 Conclusions

Both theory and computer simulation have proven useful in describing and modelling the annihilation reaction which affords the high resolution capabilities of this electrochemical patterning technique. Results from computer simulations, verified by experimental data at larger scales, indicate a theoretical physical feature definition limit near  $2\text{ }\mu\text{m}$  with the present experimental setup. Below  $2\text{ }\mu\text{m}$  features, the annihilation reaction ceases to confine diffusion of acid throughout the solution. The model provides useful verification of the flux description of the system, and predicts sub-micron features may be possible through alterations in the experimental conditions such as increasing applied current or altering the electrolyte composition. The patterning process presented in this work represents an important new application of physics theory to the practical goals of DNA microarray fabrication.

## 6.8 Figures

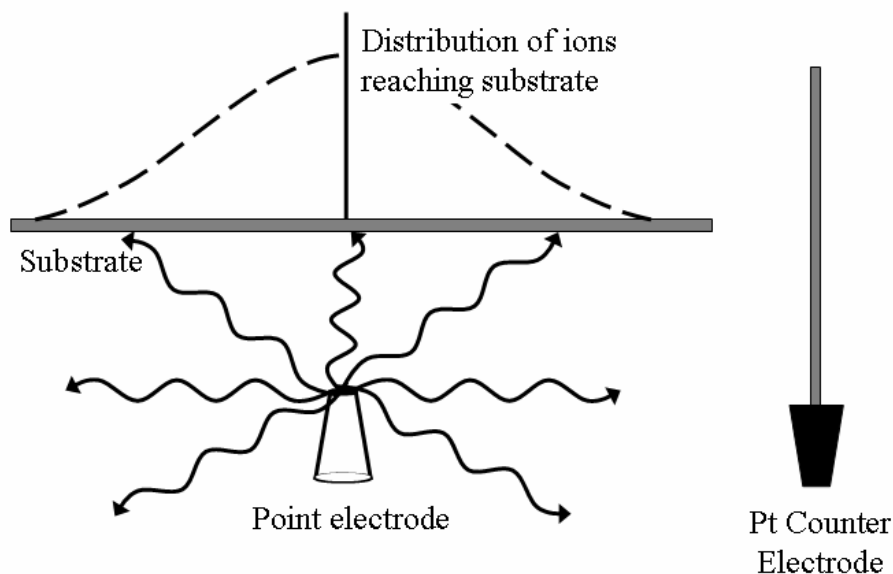


**Figure 25** A typical single-electrode used for surface patterning. This configuration, used in SECM feedback mode surface etching, has the (platinum) counter electrode placed distant to the active patterning electrode. Reagents produced at the point electrode freely diffuse in solution as they travel to the substrate; the diffusion acts to broaden the distribution of ions reaching the substrate, decreasing patterned feature resolution.

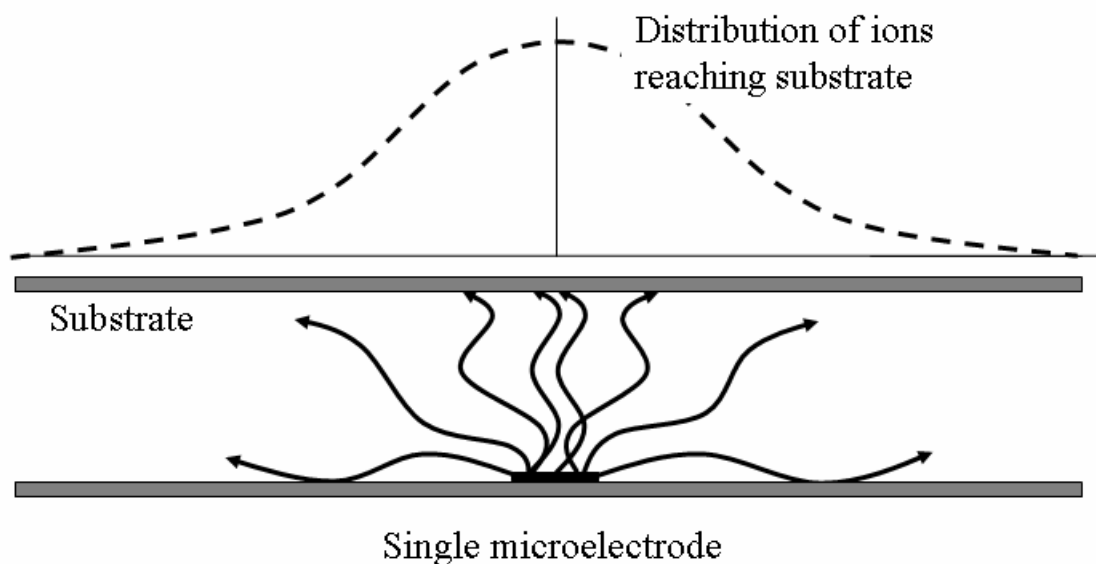


**Figure 26** A single-electrode configuration analogous to **Figure 25**, applied to the adjacent microelectrode-substrate setup used in this work. In this configuration, the width of the pattern produced on the substrate grows with time. For example, experimental data show that a single microelectrode  $1.7\ \mu\text{m}$  in width will produce a macroscopic  $400\ \mu\text{m}$  pattern if current is applied for 80 seconds.

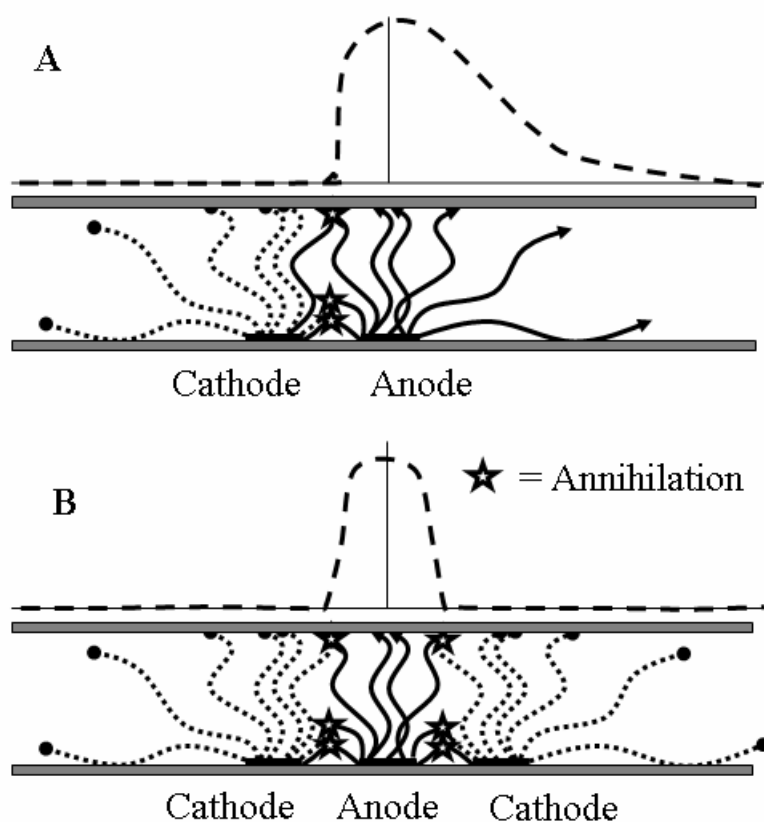


**Figure 27** Placement of the counter electrode (cathode) adjacent to the working electrode (anode). In this configuration, redox products from adjacent electrodes mix in the electrolyte. If the products produced at the anode are reactive with the products produced at the cathode, they will react in the electrolyte. In the electrochemical system used in this work, the two products act to annihilate one another (shown as stars). Panel A shows the annihilation effects induced by a single adjacent cathode. Panel B shows the utility of two confining cathodes surrounding a single anode: the distribution of products in this arrangement is sharply narrowed.

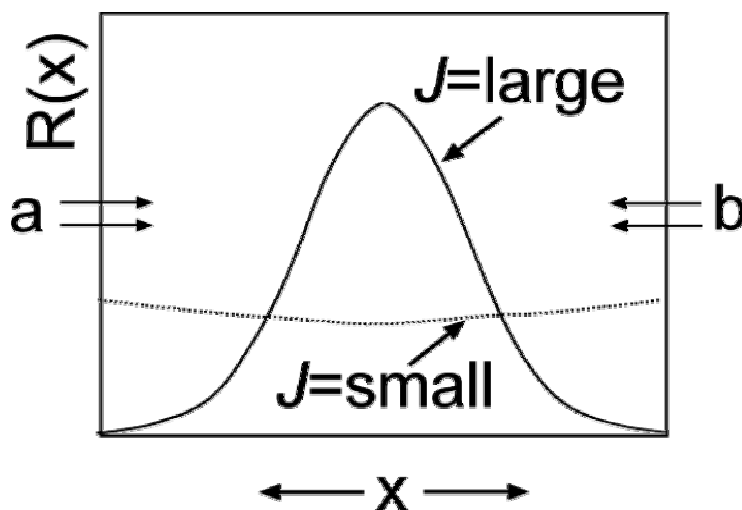


**Figure 28** Analytical solutions describing the rate of annihilation from opposing fluxes of reactive species a and b (adapted from Ben-Naim and Redner<sup>138</sup>). The rate of annihilation reaction varies in space depending on the magnitude of flux  $J$ . In the limit of small flux of a and b, the rate of annihilation is essentially uniform throughout the zone, with maximum rate at the edges. In the limit of high flux, the annihilation reaction occurs maximally in the middle, with very little annihilation at the edges. The high-flux limit may best describe patterning processes using large microelectrodes and substrate-microelectrode gaps, whereas the low-flux limit is more typical of much smaller microelectrodes, where the rate of redox reaction becomes vanishingly small.

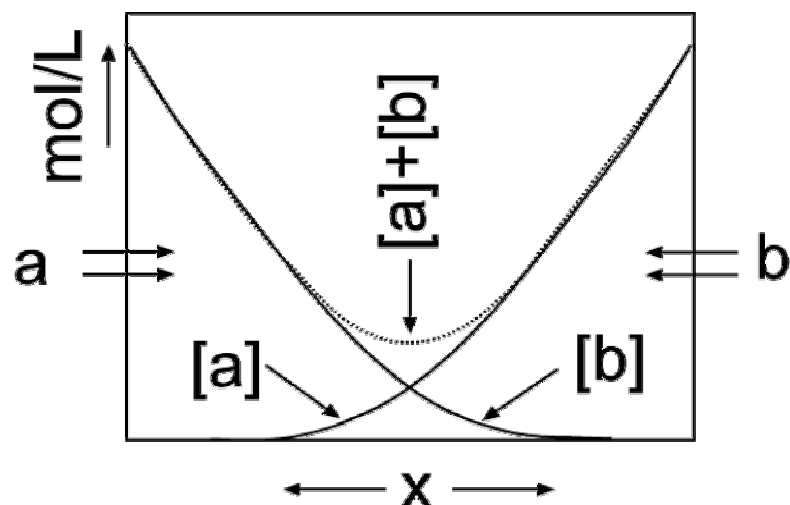


**Figure 29** A stable geometric arrangement of concentrations established upon directing a flux of two annihilating species  $a$  and  $b$  towards one another (adapted from Ben-Naim and Redner<sup>138</sup>). Species  $b$  is injected at a constant rate from the right border of the graph, species  $a$  from the left. The particles react over the length of path  $x$  to annihilate one another completely, so that their concentrations ( $[a]$  and  $[b]$ ) decrease symmetrically across path  $x$ . The total reactant concentration ( $[a] + [b]$ ) reaches a minimum at the midpoint.

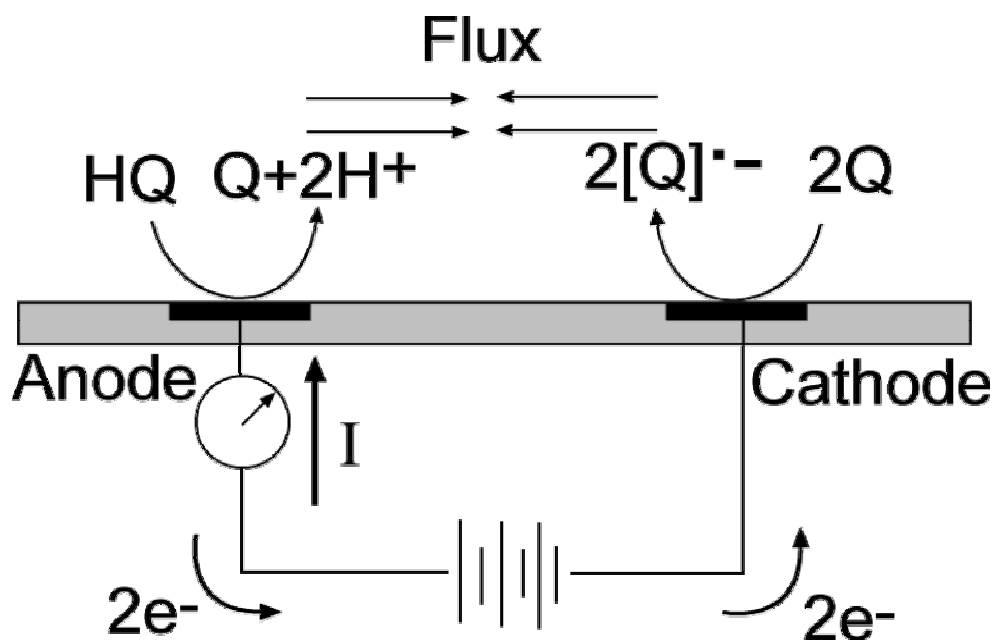


**Figure 30** A simplified two-electrode circuit. As the two electrodes are part of the same current path, the current into the anode is equal to the current out of the cathode. Consequently (ignoring other chemical redox reactions), the rates of proton and benzoquinone radical anion generation are equal. This symmetry (implicit in the experimental system) mirrors the mathematical description of two opposing fluxes of mutually annihilating species shown in **Figure 29**.

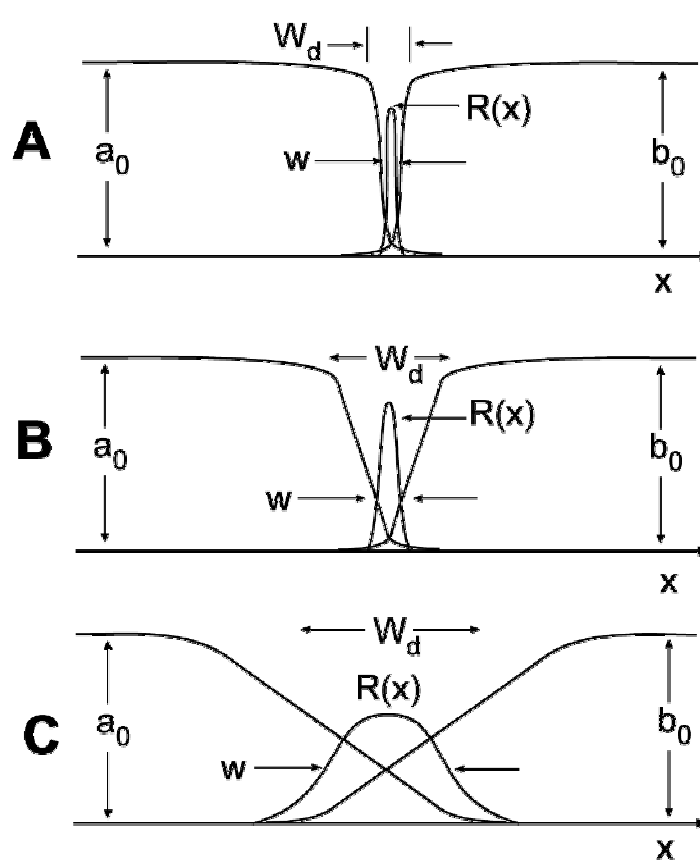


**Figure 31** Variation in the annihilation reaction rate,  $R(x)$ , and concentrations of reactants consumed by the reaction. Species  $a$  and  $b$  are injected from the left and right borders of the graph, with high flux in panel **A**, intermediate flux in **B**, and low flux in panel **C** (classifications are arbitrary). In the context of confining the acid for patterning purposes, the width of the annihilation reaction zone  $w$  is ideally very narrow (panel **A**); the acid concentration  $a_0$  is uniform at the left border (over the anode), but negligible at the right (over the cathode). In actual conditions (panel **B**), the annihilation reaction depletes the acid in a gradual transition over a finite width  $W_d$ . With decreasing flux,  $w$  becomes larger, with corresponding broadening of  $W_d$ . Broadening of  $W_d$  acts to limit the sharpness of features produced by the electrochemical method.



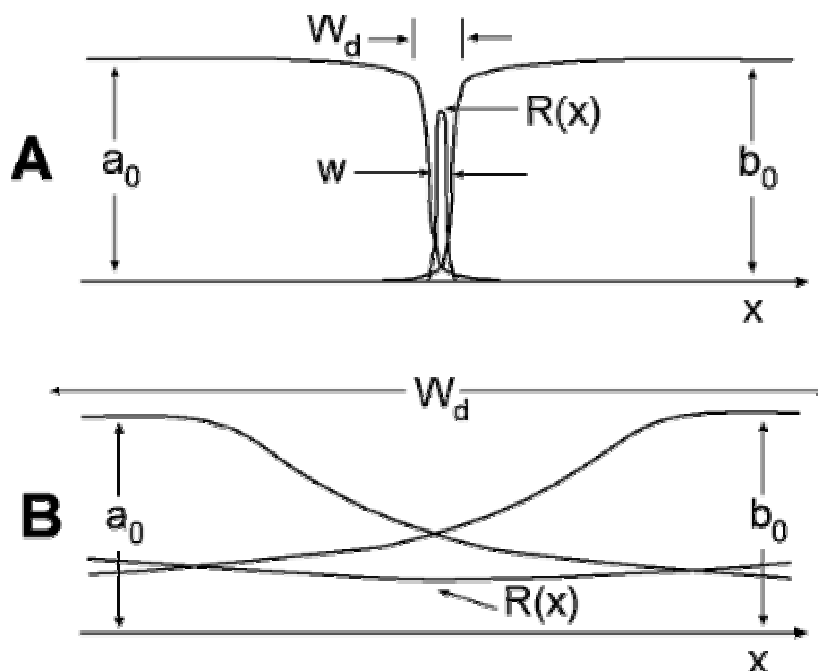


**Figure 32** Variation in the annihilation reaction rate,  $R(x)$ , and concentrations of reactants in the low-flux limit. With very small fluxes of species  $a$  and  $b$ , the annihilation reaction becomes distributed throughout the entire reaction space (panel **B**), rather than being narrowly limited to a defined width  $w$  as in the high-flux limit (panel **A**). As a result, the space over which the reactants are depleted  $W_d$  encompasses the entire region, and there is ineffective confinement of the acid. Substrate patterning under the low-flux conditions as in panel **B** would gain no benefit in resolution from the annihilation reaction.

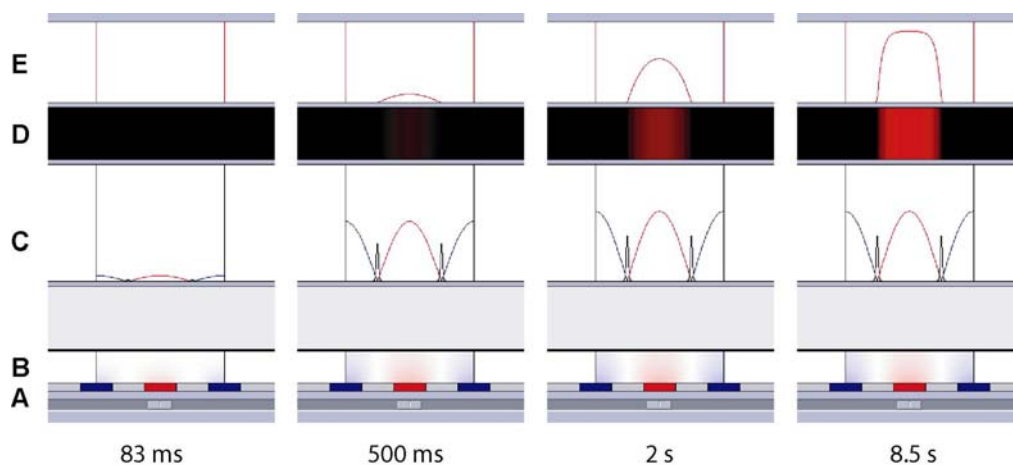


**Figure 33** A computer simulation of the annihilation process. This figure shows a time-course simulation (in cross-section) of an electrochemical patterning run, with a physical setup identical to experimental conditions. Panel **A** shows the geometric arrangement of anode and cathodes ( $40\ \mu\text{m}$  in width). Panel **B** depicts the concentrations of each reactant in space as an intensity-weighted image (the border in the middle of the cathodes is a result of simulation methodology); panel **C** shows a plot of these concentrations (arbitrary scale) at the substrate surface. Panel **D** shows the resulting pattern, as would be generated after using the acid for oligonucleotide synthesis; panel **E** shows a quantitative plot of its fluorescent intensity). The distribution of species in solution and the rate of annihilation closely resemble that of the high-flux theoretical treatment as shown in **Figure 31**. The species concentrations grow initially as the current is applied, and stabilise after about a second.

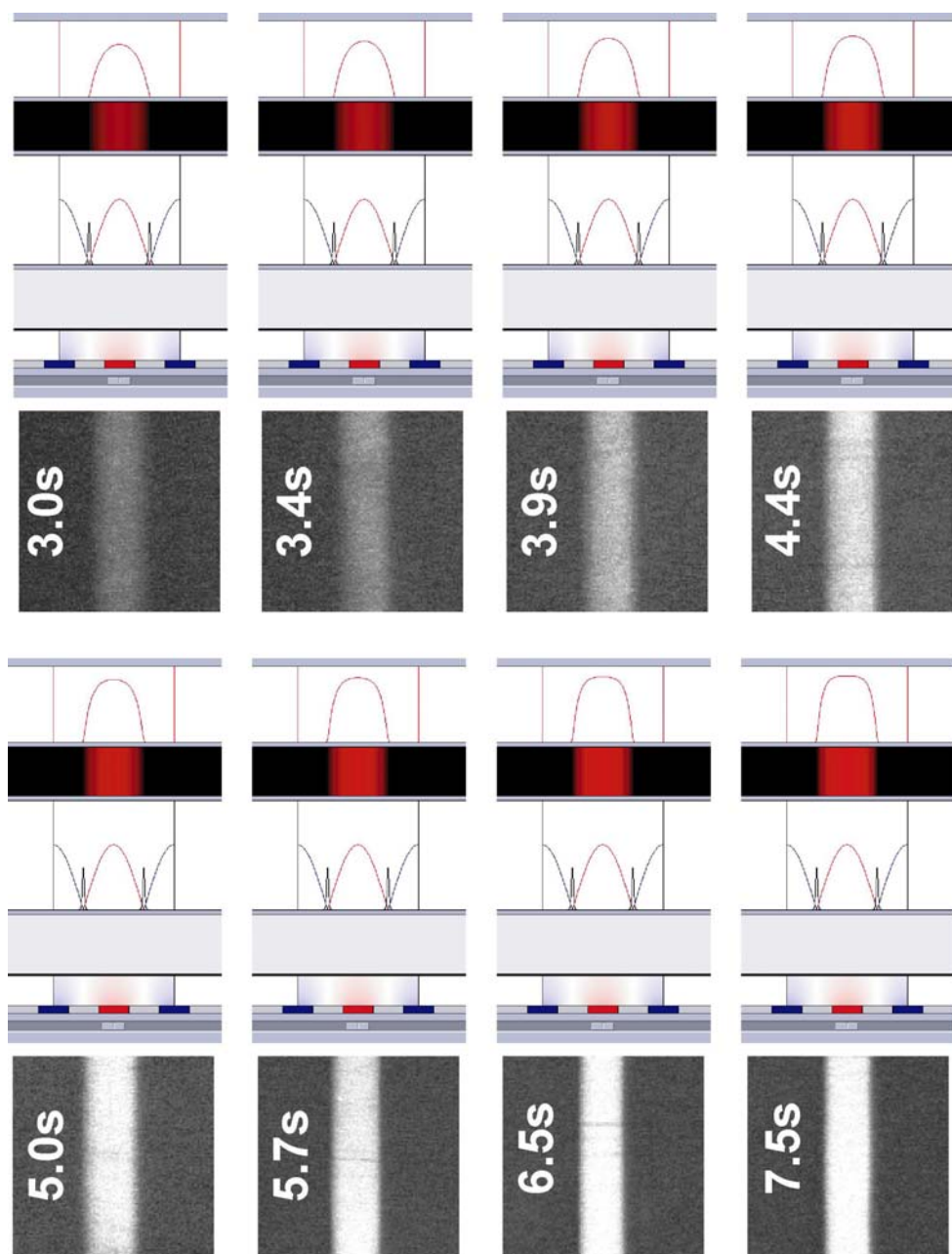


**Figure 34** A computer simulation of the patterning kinetics, compared to experimental data for the same conditions. The reasonable congruence between the model and corresponding experimental observations shown here demonstrated the model's predictive capacity.

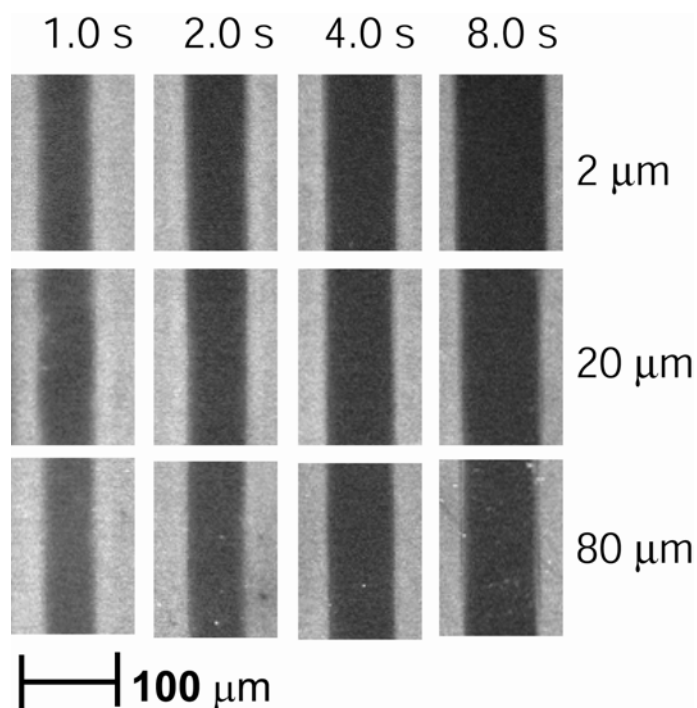


**Figure 35** Demonstration of the effects of different current durations and substrate-microelectrode gaps on substrate pattern. It became clear from many replications of these and similar experiments that substrate-microelectrode gap distance within the range from about 20-80  $\mu\text{m}$  did not significantly affect the pattern, whereas duration of current application time was very important (potential fixed at 1.33 VDC in these experiments). The accuracy of a computer simulation used to model such experiments was tested against similar data. The dark areas in this image represent regions where acid was used to perform a single phosphoramidite deblocking reaction.

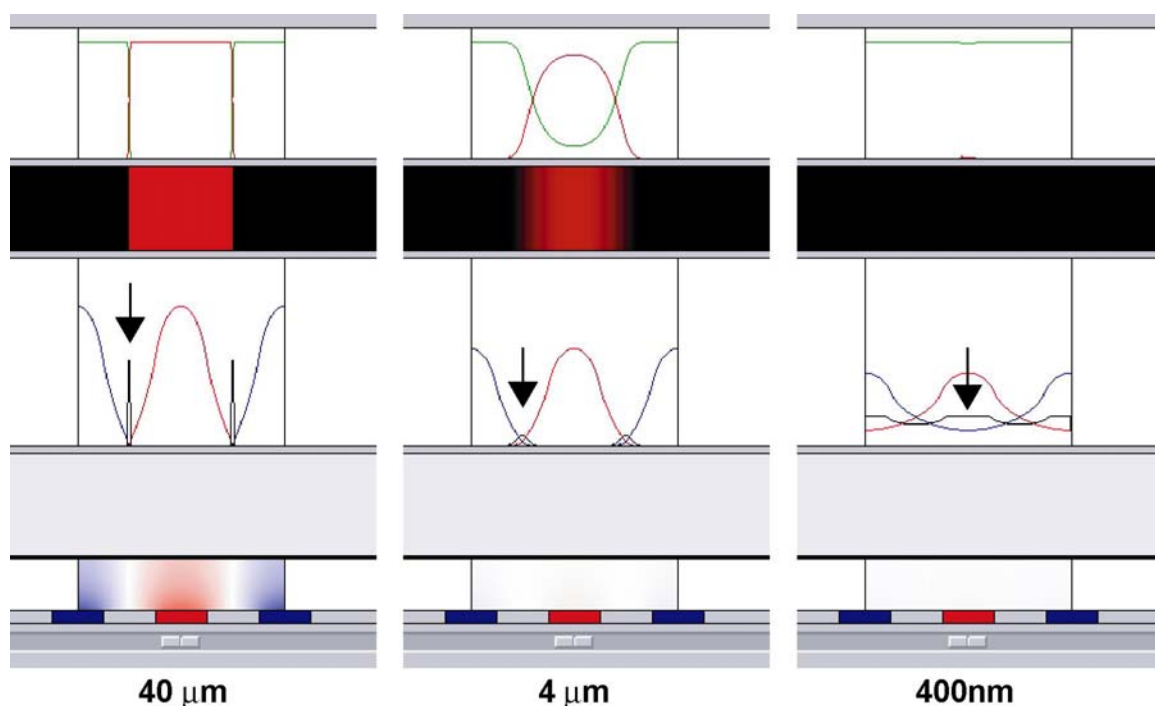


**Figure 36** Computer simulation of annihilation with decreasing microelectrode dimensions. In these simulations, current density scaled with electrode dimensions. Comparing these digital simulations to the theoretical equivalents as described by Ben-Naim and Redner (shown in **Figure 31** and **Figure 32**) reveals striking similarities. Most importantly, the peak of the annihilation (indicated by arrowheads) shifts from the midpoint between electrodes at the large-scale to the midpoint above electrodes in the small scale (the y-axis scales are arbitrary). This congruence suggests the computer model reflects the theoretical descriptions of Ben-Naim and Redner. Image was recorded at 10 s, 2 s, and 28 ms respectively for the 40  $\mu\text{m}$ , 4  $\mu\text{m}$ , and 400 nm sized electrodes; electrical currents were 500 nA, 50 nA, and 5 nA.

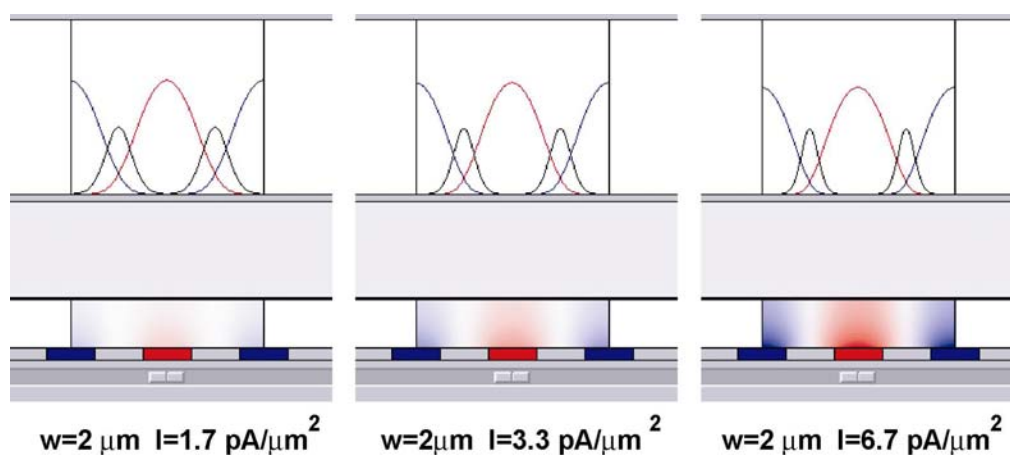


**Figure 37** Effects of current at the microelectrodes on the spread of acid in solution. This series of simulations shows distribution of acid (and rate of annihilation) at three different currents (labeled as current densities). Higher currents are associated with narrower widths over which acid spreads in solution. This effect is predicted by theory (detailed in the text and depicted in **Figure 31**). The microelectrodes used in this simulation were  $2 \mu\text{m}$  in width. The current densities shown here compare to the  $0.3$  to  $3.0 \text{ pA}/\mu\text{m}^2$  values physically measured under experimental conditions at  $40 \mu\text{m}$  electrodes.

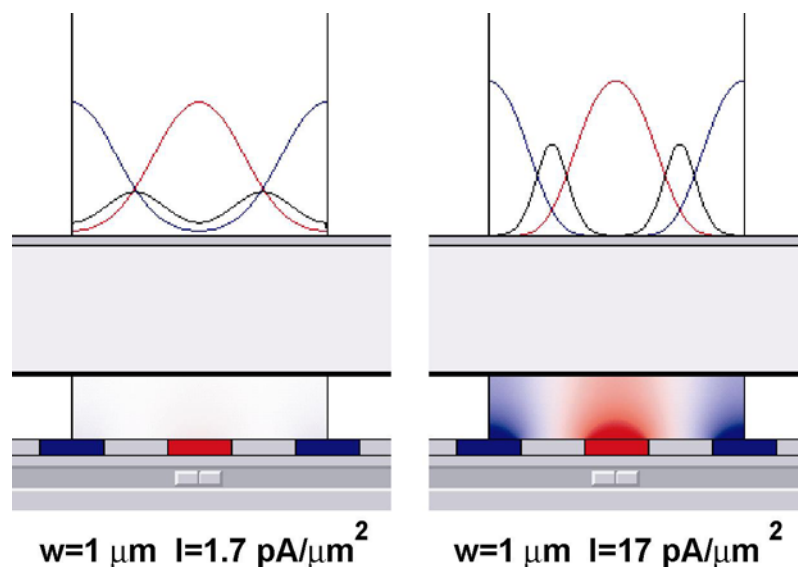


**Figure 38** Computer simulation of small-scale electrochemical patterning at two rates of proton generation. Panel **A** shows the distribution of acid generated by a 1  $\mu\text{m}$  electrode at the same current density as used in physical experiments. Panel **B** shows the same simulation, with the electrical current increased 10 times over that in panel **A**. The higher current increases the rate of proton generation, thus facilitating the annihilation and increased feature resolution as previously described. Current is easily increased in physical experiments by changing the composition of the electrolyte or simply increasing applied voltage. These results suggest that sub-micron feature sizes may be possible with the methods described in this thesis.

## Appendix A

# Microarrays in Biology and Medicine: A Review of Current Progress and Future Prospects

*This section provides an overview of the application of DNA microarrays to biological and medical research. These areas of scientific investigation, although not the explicit focus of this thesis, provide examples of the powerful analyses made available through microarray fabrication research. This section will be submitted as a review article to the journal Pharmacogenomics in September 2003.*

### A.1 Abstract

The analysis of cellular phenomena on a genomic scale requires detection and measurement of thousands or millions of interacting biological variables. Efficient techniques and devices used for performing analyses of this magnitude often rely upon highly-parallel operations. Within this category of methods, DNA microarrays have proven enormously useful. However, the fabrication of mi-



croarrays is technically challenging and not perfected, so genomic and genetic studies applications may be limited and results difficult to interpret. In the past three years, there has been an explosion in reports which have employed microarrays in large-scale biological and medical investigations. The range of topics is immense, and the volume of literature reflects the flood of biological discoveries that often follow revolutionary technology development, in this case of microarrays, a fundamental shift from small-scale or serial examination of nucleic acids to large-scale parallel processing. This review summarises the most important of these discoveries, and discusses future prospects for biological investigations employing microarrays.

## **A.2 Applications**

Since their first introduction a decade ago, microarrays have been rapidly incorporated into biomedical research. In microarray research, technological development, often viewed an enterprise removed from biological discovery, has largely incubated it. Array fabrication techniques, with slow and strenuous development over the years, have broadened experimental possibilities with each improvement in design. Microarrays are now finding uses in almost every area of the medical sciences from characterizing infectious disease and cancer to elucidating unknown pathways, assisting in drug development, and refining notions

of toxicity. The technology is now being used routinely in place of older, often lower throughput or less sensitive techniques such as Northern blotting, comparative genomic hybridisation, and sometimes even gel-based sequencing itself. Indeed the technology promises to produce results faster, on a grander scale, and in more detail than ever before.

### **A.3 Cancer**

One of the earliest and most promising applications of microarrays has been to the study of cancer. Both the expression profiling and resequencing capabilities of microarrays are used in this field.

Expression profiling is capable of typing tumours, allowing the discrimination of both known tumour types and those forms that cannot be differentiated on the basis of the standard techniques<sup>143-145</sup>. Such profiling can help to determine the susceptibility of the tumour to treatment, its metastatic potential, and the survival profile of the patient<sup>144,146-149</sup>. It is also capable of separating normal tissue from cancerous and determining the tissue of origin for a given cancer<sup>144,146,150,151</sup>. Recently microarrays have been used to study the differences between BRCA1 mutant, BRCA2 mutant, and spontaneous breast cancer, early and late stage T Cell lymphoma, and prostate cancer and benign prostatic hyperplasia<sup>152-154</sup>.

Using array-based genotyping it has been possible to detect changes in copy number and loss of heterozygosity, both of which can be used to measure the progression of a cancer, as well as helping to characterise it. A number of techniques have been proposed to measure copy number, most of which use either array-CGH (comparative genomic hybridisation) or some variant of the technique<sup>155-157</sup>. Recently these methods have been used to examine amplification of the 17q23 region, an area that has increased copy number in a variety of cancers, in breast cancer and to determine which genes are amplified in glioblastoma multiforme<sup>158,159</sup>. Additionally, a protocol that allows array-CGH to be applied to standard paraffin embedded sections has been developed, demonstrating that this technique can be adapted for clinical use<sup>160</sup>. Loss of heterozygosity (LOH) can be detected by determining the status of a large collection of single nucleotide polymorphisms (SNPs)<sup>161</sup>. This procedure is made practical by the fact that a sufficiently large microarray can interrogate a collection of SNPs that is quite dense in the genome, making it possible to detect LOH, not only in a specific gene of interest, but throughout the genome. Together, these techniques offer the potential to detect a wide variety of chromosomal disorders simultaneously using a generic method. Such a procedure will allow the detection of unexpected chromosomal alterations and may lead to the discovery of previously unknown alterations that play a role in the disease process.

It is also possible to detect mutations directly in a number of oncogenes and tumour suppressors. The effectiveness of Affymetrix's p53 chip has been validated in two studies. In both it was found to detect more mutations than direct sequencing (although error levels were higher) and was better at detecting single base-pair substitutions, but was not effective in detecting insertions or deletions larger than a base-pair<sup>162,163</sup>. Recently, a new technique that is capable of recognizing such insertions and deletions, which were generally difficult to detect with previous array based genotyping techniques, has been applied to identify a number of mutations found in various cancers<sup>164</sup>. Using PCR/LDR (ligase detection reaction) and a universal (zip code) array, it has been possible to detect K-Ras and BRCA1/2 mutations accurately, apparently more sensitively than standard direct sequencing, including accurately identifying larger insertions and deletions<sup>164-166</sup>. However, this method is limited in that it is designed to detect known mutations, not discover new ones. Other enzymatic techniques such as mini-sequencing promise improved accuracy combined with high sensitivity, but thus far such techniques have not been as successful as was hoped.

The clinical applications of these techniques are readily apparent. Instead of relying on standard histochemical methods alone, pathologists could use microarrays, allowing them to not only confirm initial conclusions, but also to further refine them. This may permit determination of tumour characteristics elusive through traditional pathological examination. This ability to further classify the

tumour could have important implications for treatment, since tumours which appear the same may have vastly different survival profiles and susceptibilities to treatment<sup>144,145</sup>. Knowing the tumour's expression profile and genotype will aid individualised medical care tailored to achieve the most effective treatment while minimizing unnecessary toxicity.

## **A.4 Functional Analysis**

The ability to elucidate the function of unknown genes, and to discover which open reading frames (ORFs) actually represent coding sequences, is one of the most powerful applications of microarrays. This is based on the idea that genes of similar function or involved in the same pathway are co-regulated and thus should group together when cluster analysis is applied to a collection of expression profiles. This notion, often referred to as “guilt by association,” has yielded impressive results in a number of studies, mostly recently Hughes, et al.'s correct prediction of the function of eight previously uncharacterised ORFs in *Saccharomyces Cerevisiae*<sup>167-170</sup>. The successes thus far give hope that this approach may play an important role in the identification of genes of unknown function that will be necessary to complete the annotation of the genome.

## A.5 Drug Development

Microarrays also have the capacity to accelerate the processes of target identification and validation and mechanism determination. This capability has been demonstrated in a number of studies in which microarrays have correctly identified the targets of cyclosporine and FK 506 (FK 506 binding proteins and cyclophilins) and their downstream target (Calcineurin), suggested the target for the anaesthetic dyclonine, revealed possible markers for the susceptibility of tumours to chemotherapeutic agents, and shown that expression levels can be used to measure drug activity<sup>146,167,171,172</sup>. The technology can also be used to detect secondary pathways activated by the compound that may act synergistically or contribute to toxicity<sup>171</sup>. Additionally, expression profiling of current pharmaceuticals may suggest new targets. For example, since isoniazid is effective against mycobacterium tuberculosis, drugs targeted at other genes whose expression levels are altered by isoniazid may yield effective anti-TB therapies as many of these genes are likely to be involved in the same pathway on which isoniazid acts<sup>173</sup>. If these techniques prove successful in pharmaceutical research, they could result in a marked increase in the number of drugs being brought to market each year as well as a decrease in the time and expense required to develop each drug.

## A.6 Toxicology

Microarrays also hold the potential to accelerate toxicity screening greatly in both drug development and environmental testing. A number of arrays specifically for this purpose have been developed in both the public and private sectors. They include ToxChip, developed by NIEHS, ToxBlot, from Syngenta and Astra-Zeneca, and the Merck Drug Safety Chip, which was developed in conjunction with Affymetrix<sup>174-176</sup>. The hope is that this field will ultimately be able to predict which substances are toxic and which are not, as well as their mechanisms of toxicity, based on their expression profiles alone. The hypothesis behind this is that toxins that act through similar mechanisms or act on the same pathway should induce comparable expression profiles in the affected cell, and that with a large enough database of expression profiles, it should eventually be possible to link a given profile to a specific toxic effect. A number of studies measuring gene expression following both in vivo and in vitro treatment with toxins have been performed to explore this possibility<sup>176-179</sup>. So far the results are hopeful and suggest that toxins can be grouped by mechanism based on their expression profiles, but up until this point all the studies have used either a small collection of samples or a limited collection of probes. There has not yet been a study which demonstrates successful unsupervised clustering of several hundred toxins by mechanism, though Waring, et al.'s promising results with a collection of 15 agents suggests that this is just a matter of time<sup>179</sup>. If larger scale studies confirm that this

technique is viable, it will have important implications for drug development since toxicity screening is currently expensive and time consuming<sup>174</sup>. Accelerating this stage would remove a key bottleneck in the drug development process. Additionally, some toxic effects are not revealed until late in the drug development process, or even after the product has reached the market, which can lead to the cancellation of a project or recall of a drug on which significant time, resources, and effort have already been expended. These techniques could also be used to screen environmental and industrial compounds en masse for toxic (including carcinogenic) properties, since it could be done cheaply, without the requirement of expensive, long-term animal studies.

## **A.7 Infectious Disease**

Using microarrays, it is now possible to study expression in both the microbe and the host during infection. A variety of infectious agents including human immunodeficiency virus (HIV), herpesviruses (cytomegalovirus (CMV), human herpes virus 8 (HHV-8), and herpes simplex virus (HSV)), *Listeria monocytogenes*, *Helicobacter pylori*, *Salmonella* (dublin and typhimurium), Hepatitis B and C, and Malaria have been studied with these techniques<sup>180-191</sup>. These studies have explored the sequence of host and microbial gene expression during infection, examined the function of virulence factors, and suggested the function of uncharac-



terised genes in both the host and pathogen. They have helped to clarify such questions as how some microbes, such as herpesviruses, evade the host immune response, how interferon alters macrophage behaviour, how the pathogenesis of hepatitis B and C differ, and what role lipopolysaccharide (LPS, endotoxin) plays in the host response to organisms that display it. Beyond the obvious applications of this knowledge in improving therapy and developing superior pharmaceuticals, this research has more subtle ramifications. For example, understanding the factors which allow certain microorganisms to elude the host immune system may play a crucial role in the development of effective gene therapy vectors, especially since altered HSV is often used in this capacity<sup>184</sup>.

Microarray sequencing techniques have also found applications in this field. Arrays have already been used to identify mycobacteria, not only by determining their species, but also by testing for the presence of drug resistance genes<sup>192,193</sup>. They have also been used to study genetic variation within the species *Mycobacterium Tuberculosis* and among the many BCG vaccine strains (and *M. bovis*). These studies have suggested that genomic deletions tend to decrease the virulence of mycobacteria and that one of the reasons that the BCG vaccines may have declined in effectiveness is due an accumulation of such deletions<sup>194,195</sup>. In addition to mycobacteria, microarrays have also been used to type and to identify virulence and resistance factors in other microbes, including influenza, *Helicobacter Pylori*, and HIV and have been used to rapidly identify the source of bac-

teraemia in unknown blood samples<sup>186,196-199</sup>. Utilizing array-based sequencing will allow physicians to rapidly determine the identity of infectious organisms, even detecting subtle intraspecies variations, such as those contributing to drug resistance and virulence. This should allow them to select effective therapies instead of having to guess to which drugs the disease will be susceptible. These tools should also find use in epidemiology where they can aid in tracking the migration and evolution of specific viral strains and in monitoring outbreaks<sup>195</sup>. Finally, these methods should give a better understanding of how to select effective vaccine strains, which successfully confer immunity while minimizing virulence, and may provide new tests that can differentiate between vaccination and infection (something that cannot be done with the current purified protein derivative of tuberculin (PPD) challenge used for tuberculosis testing)<sup>194</sup>.

Infectious disease research also demonstrates how the genotyping and expression profiling capabilities of microarrays can be fruitfully combined. Microarrays can be used first to explore expression differences in host cells infected by two viral strains, and then to examine their genetic differences in order to assign a role to uncharacterised genes and determine virulence factors<sup>186</sup>. In a variation of this technique the expression profiles induced by a collection of strains of known genotypes can be compared in order to determine the roles of the differing genes in infection. These approaches work best when the two strains are very

similar, such as when one strain is derived from another by the deletion or alteration of a single gene<sup>189</sup>.

## A.8 Further Topics

Microarrays are now being used to study a variety of other topics. The effects of ageing on gene expression have been examined in a number of studies, both on human fibroblasts and in calorie reduced (CR) mice<sup>200-202</sup>. Changes in expression in sleep, waking, and after sleep deprivation have been examined<sup>203-205</sup>. Even alterations in gene expression in alcoholism have been observed<sup>206</sup>. These areas provide just a taste of the myriad fields to which microarrays will be applied in the coming years. As array density increases and more and more of the genome becomes represented on chip, the technology will become ever more powerful and inexpensive, and may one day emerge as a technique as useful and ubiquitous as sequencing itself.

## Appendix B

# Simulation of Electrochemically Activated Confined Chemical Pat- ternning of Surfaces Using an Array of Microband Electrodes

The following abstract was prepared upon conclusion of the work described in this thesis, in collaboration with Stephen W. Feldberg at the Computing Laboratory, University of Oxford and John Elder, Department of Biochemistry. It has been accepted for publication and presentation at the 204th Meeting of The Electrochemical Society, October 12-October 16, 2003. Stephen W. Feldberg and Ryan D. Egeland will be presenters.



## Appendix C

### Tritylisation of Pyrene, Perylene and Coronene: A New Family of Switchable Fluorescent Labels

The following paper was published in *Tetrahedron Letters*. The work described uses the microelectrodes and electrochemical system developed in this thesis to selectively and reversibly switch a new pH-sensitive family of fluorescent labels between a fluorescent and non-fluorescent state. The electrochemical method allowed real-time confocal microscope visualisation of the process on a treated microscope slide.



Pergamon

Tetrahedron Letters 41 (2000) 4943–4948

---

---

TETRAHEDRON  
LETTERS

---

---

## Tritylisation of pyrene, perylene and coronene: a new family of switchable fluorescent labels

Mikhail S. Shchepinov,<sup>a,\*</sup> Vladimir A. Korshun,<sup>b</sup> Ryan D. Egeland<sup>a</sup> and Edwin M. Southern<sup>a</sup>

<sup>a</sup>*Department of Biochemistry, University of Oxford, South Parks Road, Oxford OX1 3QU, UK*

<sup>b</sup>*MRC Laboratory of Molecular Biology, Cambridge CB2 2QH, UK*

Received 31 March 2000; accepted 4 May 2000

---

### Abstract

The synthesis of novel fluorescent labels based on pyrene, perylene and coronene is described. Due to the trityl-type structure, their fluorescence may be reversibly switched on and off by changing the pH. This property can be used to expand the palette of fluorophores available for multicolour DNA detection on DNA chips. Some FRET and surface chemistry applications are also demonstrated. © 2000 Elsevier Science Ltd. All rights reserved.

**Keywords:** polycyclic aromatic compounds; Friedel–Crafts reactions; Grignard reactions; fluorescence; nucleic acids.

---

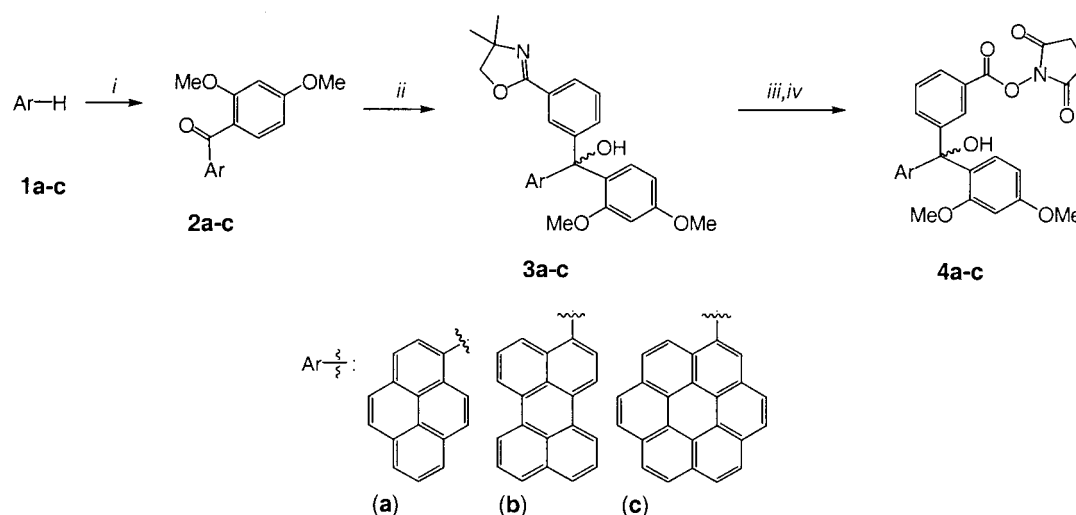
As part of a programme to optimise the manufacture and use of DNA chips we developed a new family of fluorescent tags derived from polycyclic aromatic hydrocarbons (PAHs). Both single fluorophore<sup>1</sup> and energy transfer<sup>2</sup>-based fluorescence detection methods find wide applications in the analysis of nucleic acids. Some PAHs have certain advantages over the fluorophores currently used to label DNA, such as fluorescein: they are less prone to photobleaching and have high molar absorbance and high quantum yields. Furthermore, molecules are available with a range of excitation and emission maxima and large Stokes shifts. We chose pyrene,<sup>3</sup> perylene<sup>4</sup> and coronene<sup>5</sup> as PAHs with useful fluorescent properties. The introduction of a carbinol–carbocation switchable element would allow one to controllably turn the fluorescence on and off by changing the pH. The conversion of these PAHs into trityl-type structures also seems advantageous due to the non-planar conformation of triarylmethanols, which would prevent the  $\pi$ – $\pi$  stacking interactions with a resulting increase in the solubility.

Friedel–Crafts acylation of PAHs with 2,4-dimethoxybenzoyl chloride in presence of  $\text{AlCl}_3$  in DCM for pyrene or chlorobenzene<sup>6</sup> for perylene and coronene gave 1-acylpyrene **2a**, 3-acylperylene **2b** and acylcoronene **2c** (Scheme 1). These ketones were converted into the corresponding

---

\* Corresponding author. Tel: +44 1865 275226; e-mail: misha@bioch.ox.ac.uk

*R,S*-oxazolyltritanols **3a–c** using appropriate phenylmagnesium bromide as a nucleophile in Grignard synthesis. Further conversion<sup>7</sup> yielded *N*-hydroxysuccinimide (NHS)-derivatives **4a** (as pale yellow), **4b** (as dark red) and **4c** as yellow solids.<sup>8</sup> NHS-esters **4a–c** can be used for labelling of biomolecules or for derivatisation of surfaces. The labelling procedure would involve reacting **4a–c** with an amino group(s)-containing analyte; we therefore synthesised<sup>7b,c</sup> the corresponding model butylamides **7–9** (Fig. 1) for fluorescence studies.



Scheme 1. Reagents and conditions: (i) 2,4-dimethoxybenzoylchloride/ $\text{AlCl}_3$  in DCM (a, 86%) or PhCl (b, 53%; c, 48%); (ii) 3-(4,4-dimethyl-1,3-oxazoline-2-yl)phenylmagnesium bromide/THF, reflux; (a, 73%; b, 64%; c, 49%); (iii) 80% AcOH, (or TFA, 72 h, for c), at 70°C, 48 h, then reflux in 20% NaOH in EtOH/ $\text{H}_2\text{O}$ , 3 h; a, 96%; b, 93%, c, 85%; (iv) DCC, NHS, dioxane/THF (a, 91%; b, 87%; c, 79%)

A modified trityl group bearing a pyrenyl residue in place of one of the phenyls has fluorescent properties similar to non-modified pyrene.<sup>9</sup> Triarylmethyl cation derived from tritanol by an acidic treatment (Scheme 2) would have completely different fluorescence properties, while remaining covalently linked to a probe molecule if attached to it through a side-chain.<sup>7</sup> These features are combined in compounds **4a–c**. The pH-threshold for the formation of trityl carbocations (like **6**) from corresponding tritanols at low pH can be controlled by electron withdrawing or donating groups on the aromatic rings.<sup>10</sup> Two methoxy groups and one carboxyl group give **7–9** an acidic stability similar to that of a standard DMTr and MMTr groups.<sup>11</sup> The UV spectra of **7–9** were of the same shape but slightly red-shifted (3–10 nm) as compared to the starting PAHs.<sup>2,3</sup>

Multicolour detection (use of more than one fluorophore in one reaction) is a useful feature of fluorescent dyes; it enables different sequences to be detected simultaneously and has been used to good effect in DNA sequencing,<sup>1</sup> fluorescence in situ hybridisation (FISH)<sup>12</sup> and differential gene expression analysis on DNA chips.<sup>13</sup> The size of the palette is limited by the overlap of the excitation and emission spectra; it has proved difficult to use more than four colours in FISH and two colours are normal in expression analysis. An advantage of trityl-based fluorescent tags is the potential to ‘switch’ the spectra on and off by simply changing the pH. The magnitude of the shifts is very large. For example, moving from neutral or alkaline to acidic pH shifts the excitation maximum of the pyrene-based compound **7** from 346 to 711 nm (Fig. 1), the property earlier used to generate triarylmethyl carbocations with a variety of different colours.<sup>14</sup>



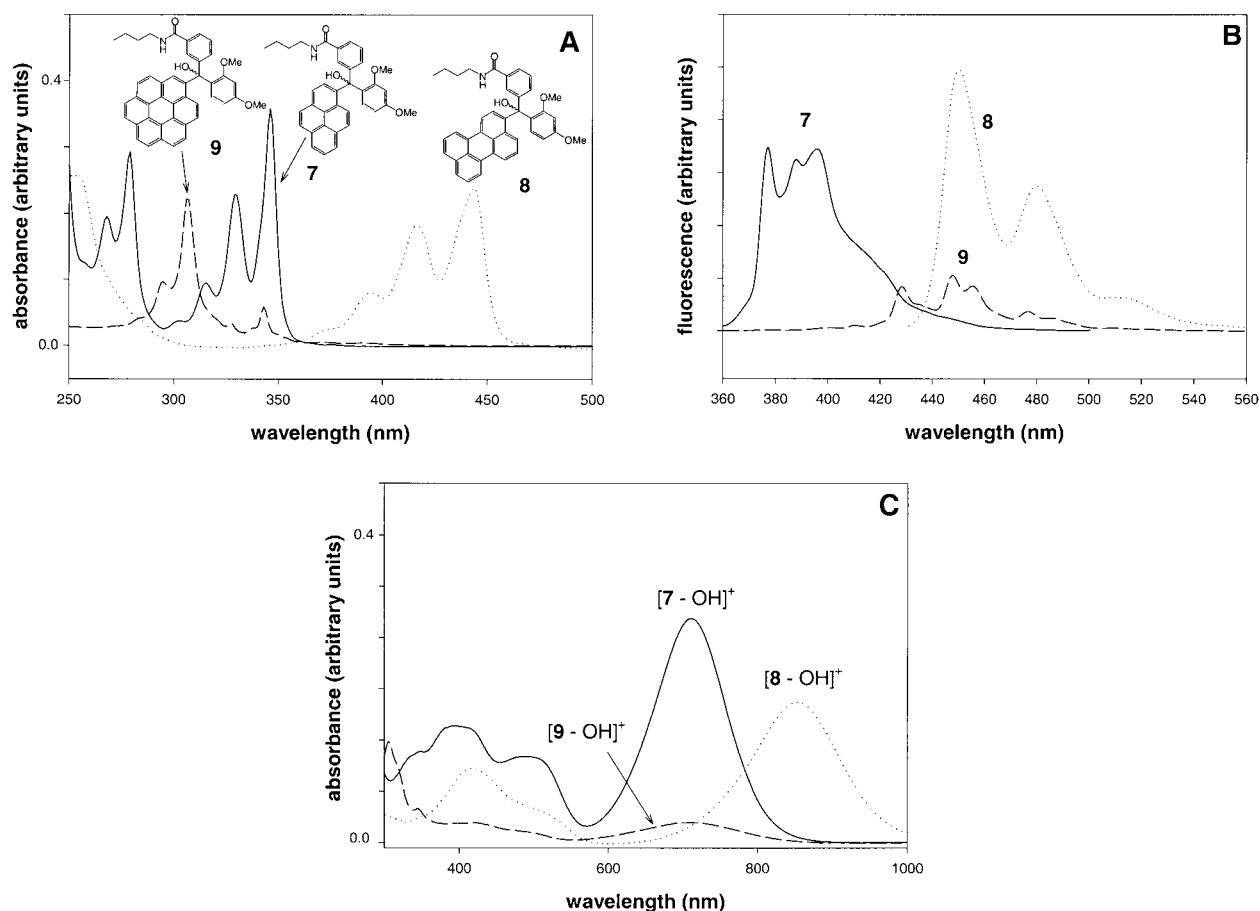
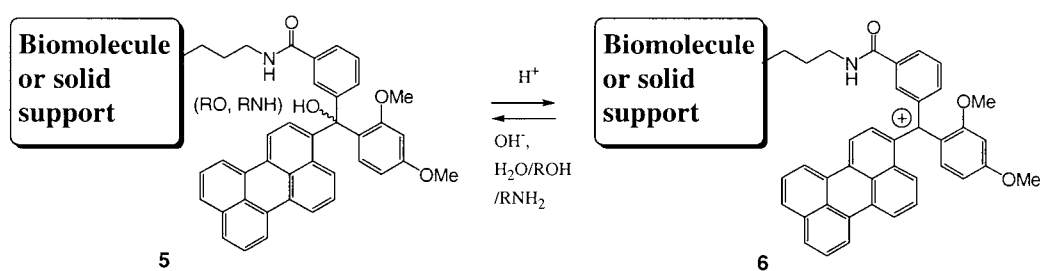


Figure 1. **A.** Absorption spectra of butylamides **7** (solid line), **8** (dotted line) and **9** (dashed line) ( $10^{-5}$  M in DCM). **B.** Fluorescence spectra of butylamides **7–9** ( $10^{-6}$  M in DCM); excitation wavelengths: 330 nm (**7**), 420 nm (**8**), 343 nm (**9**). **C.** Absorption spectra of cations of butylamides **7–9** ( $10^{-5}$  M in 1% TFA/DCM)



Scheme 2.

Trityl carbocations do not fluoresce in the range detected for the corresponding tritanols. This property can be used to improve the discrimination of labels: first by increasing the accuracy of intensity measurements; and, second, increasing the potential number of colours in the palette. For example, targets can be labelled with two fluorophores having similar excitation and emission spectra, but only one of which is switchable by pH change. After hybridisation, measurements are taken at two pH values: under ambient conditions and after exposing the array to acidic vapour, which is enough to switch the emission of fluorescent trityls off immediately, but reversibly. Using

a single excitation source, both fluorophores emit at neutral pH but only one will emit in acid. These two measurements alone would be enough to distinguish the two patterns of hybridisation. But a third measurement, using a source which excites the second fluorophore in acid, can give more analysis. In this way it may be possible to double the number of labels that can be used together.

To evaluate the suitability of our fluorescent labels as components for fluorescence resonance energy transfer (FRET), a model compound **10** was synthesized<sup>8</sup> by the stepwise acylation of 4,7,10-trioxa-1,13-tridecanediamine with **4b** followed by **4a** in DCM. While the absorption spectra for both non-ionised and bis-cationic forms essentially represent a superposition of **7** and **8** (Fig. 2A), **10** fluoresces only at 450, 480 and 515 nm when excited at the pyrene absorption maximum of 330 nm (Fig. 2B), with no detectable fluorescence of pyrene (at 377, 388 or 396 nm). When mixed in equimolar amounts, **7** and **8** retain their own fluorescence properties (data not shown). This suggests a possibility of designing fluorescent labels having increased Stokes' shifts by arranging the necessary fluorophores (perhaps even more than two) in the vicinity of each other.<sup>15</sup> Furthermore, additional control can be achieved by making some of these parts more acid-labile than the others, so that some selected components of the chain may be reversibly switched off by decreasing the pH. Mass-spectrum (LDI-TOF) of **10** (calculated exact mass for C<sub>78</sub>H<sub>70</sub>N<sub>2</sub>O<sub>11</sub>: 1210.50) showed, apart from the molecular ion, two fragments, lacking one (1193.46) and two (1176.47) hydroxyl groups. The fact that the latter flies in mono-charged (mono-cationic) and not in bis-cationic form<sup>7b,c</sup> (the signal for 1176.49/2 = 588.25 was not detected) suggests some unusual interactions, perhaps FRET during the LDI-TOF process, initiated by laser irradiation at 340 nm, which is almost a perfect match with the absorption maximum for **10**.

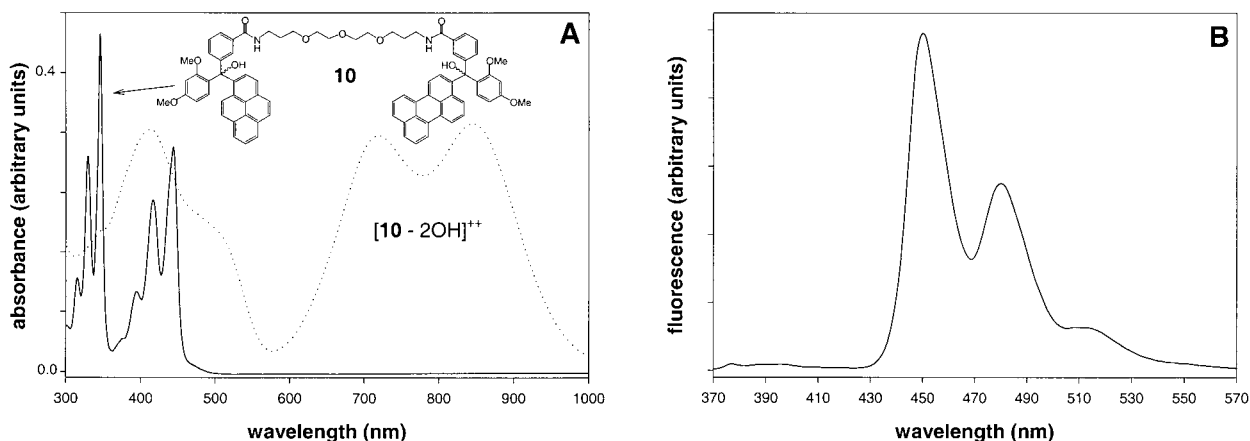


Figure 2. **A.** Absorption spectra of **10** ( $10^{-5}$  M in DCM) in non-ionised (solid line) and bis-cationic (dotted line) forms (in 1% TFA/ DCM). **B.** Fluorescence spectrum of bis-chromophore **10** ( $10^{-6}$  M in DCM); excitation wavelength: 330 nm

To demonstrate the reversibility of the fluorescence in real time, acid was generated using a microelectrode technique. A series of 20 linear iridium microelectrodes 40  $\mu$ m wide (80  $\mu$ m between centres) on a silicon dioxide wafer were manufactured using photolithography methods. A glass microscope slide was silanized with 3-aminopropyltrimethoxysilane and treated overnight with a 0.1 M solution of **4b** in THF. This slide was then washed and placed atop of the microelectrode array, separated by ca. 3  $\mu$ m layer of an electrolyte (hydroquinone in CH<sub>3</sub>CN). Confocal

microscopy was used to examine the fluorescence emission at 520 nm with Ar/Kr laser excitation. Application of voltage across adjacent electrodes generated protons electrochemically at the anodes, resulting in a lower pH and a corresponding decrease in fluorescent emission at 520 nm (Fig. 3). Upon switching off the microelectrodes, the fluorescent emission reverts to the starting, voltage-off condition, demonstrating the reversibility of the acid-catalysed carbocation conformation. Aminated polypropylene can also be used instead of glass (data not shown).

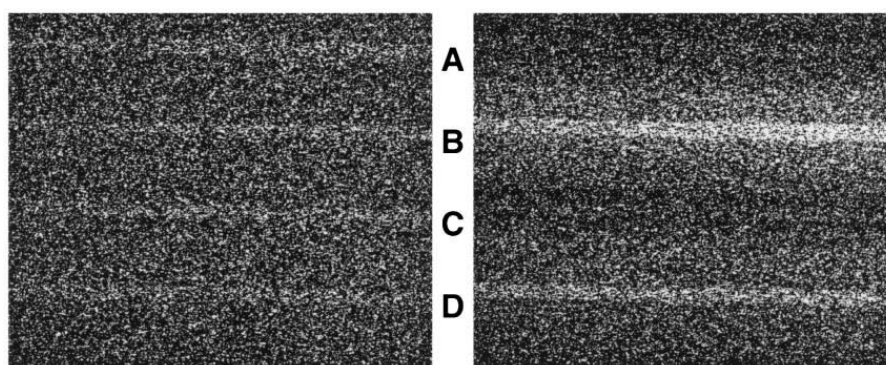


Figure 3. Fluorescent response of an aminated glass surface coated with **4b** (Scheme 2) to acid generated electrochemically above horizontal microelectrodes, observed using confocal microscopy. **Left**, no voltage applied. The signal consists of fluorescence from **4b** on the surface and reflection from iridium-covered electrodes A–D. **Right**, the voltage (1.2 V between cathode B and anode C and 0.8 V between cathode D and anode C) is applied. The acid generated on the anode C leads to conversion of **4b** into cationic form with consequent disappearance of the signal

At present, we are preparing the corresponding phosphoramidite derivatives of **4a–c** to facilitate their incorporation into synthetic oligonucleotides.

## Acknowledgements

The authors would like to express their gratitude to Drs. D. A. Stetsenko for helpful discussions, A. A. Arzumanov for running the fluorescence spectra, R. Chalk for mass-spectra and R. Quarrell for valuable suggestions and comments. M.S.S was supported by an MRC grant.

## References

1. Smith, L. M.; Sanders, J. Z.; Kaiser, R. J.; Hughes, P.; Dodd, C.; Connell, C. R.; Heiner, C.; Kent, S. B. H.; Hood, L. E. *Nature* **1986**, *321*, 674–679.
2. (a) Cardullo, R. A.; Agrawal, S.; Flores, C.; Zamecnic, P. C.; Wolf, D. E., et. al. *Proc. Natl. Acad. Sci. USA* **1988**, *85*, 8790–8794. (b) Tyagi, S.; Kramer, F. R. *Nat. Biotechnol.* **1996**, *14*, 303–308. (c) Lewis, F. D.; Zhang, Y.; Letsinger, R. L. *J. Am. Chem. Soc.* **1997**, *119*, 5451–5452. (d) Masuko, M.; Ohuchi, S.; Sode, K.; Ohtani, H.; Shimadzu, A. *Nucleic Acids Res.* **2000**, *28*, e35. (e) Mao, C. D.; Sun, W. Q.; Shen, Z. Y.; Seeman, N. C. *Nature* **1999**, *397*, 144–146. (f) Dobrikov, M. I.; Gainutdinov, T. I.; Vlassov, V. V. *Nucleosides Nucleotides* **1999**, *18*, 1517–1518.
3. Reines, S. A.; Cantor, C. R. *Nucleic Acids Res.* **1974**, *1*, 767–786.
4. Johansson, L. B.-A.; Molotkovsky, J. G.; Bergelson, L. D. *J. Am. Chem. Soc.* **1987**, *109*, 7374–7381.
5. Rohr, U.; Schlichting, P.; Bohm, A.; Gross, M.; Meerholz, K.; Brauchle, C.; Mullen, K. *Angew. Chem., Int. Ed.* **1998**, *37*, 1434–1437.

6. Zieger, H. E. *J. Org. Chem.* **1966**, *31*, 2977–2981.
7. (a) Gildea, B. D.; Coull, J. M.; Koster, H. *Tetrahedron Lett.* **1990**, *31*, 7095–7098. (b) Shchepinov, M. S.; Chalk, R.; Southern, E. M. *Nucleic Acids Symp. Ser.* **1999**, *42*, 107–108. (c) Shchepinov, M. S.; Chalk, R.; Southern, E. M. *Tetrahedron* **2000**, *56*, 2713–2724.
8. Compound **4a**:  $^1\text{H}$  NMR (200 MHz,  $\text{CDCl}_3$ ,  $\delta$ ): 8.66 (d, 1H,  $J=9.4$  Hz, arom.); 8.25–7.85 (m, 8H, arom.); 7.4–7.15 (m, 4H, arom.); 6.65 (s, 1H, arom.); 6.32 (m, 2H, arom.); 6.12 (s, 1H, OH); 3.77 (s, 3H,  $\text{OCH}_3$ ); 3.74 (s, 3H,  $\text{OCH}_3$ ); 2.85 (br.s, 4H,  $\text{CH}_2$ ). MS (LDI-TOF): 585.3 (MI), 568.3 (MI-OH).  $R_f$  (2% MeOH in  $\text{CDCl}_3$ ): 0.38. Compound **4b**:  $^1\text{H}$  NMR (200 MHz,  $\text{CDCl}_3$ ,  $\delta$ ): 8.27 (d, 1H,  $J=9.6$  Hz, arom.); 8.15 (m, 6H, arom.); 7.95 (d, 1H,  $J=9.4$  Hz, arom.); 7.72–7.4 (m, 7H, arom.); 6.6 (s, 1H, arom.); 6.35 (m, 2H, arom.); 6.22 (br.s, 1H, OH); 3.8 (s, 3H,  $\text{OCH}_3$ ); 3.77 (s, 3H,  $\text{OCH}_3$ ); 2.88 (br.s., 4H,  $\text{CH}_2$ ). MS (LDI-TOF): 635.2 (MI), 618.2 (MI-OH).  $R_f$  (2% MeOH in  $\text{CDCl}_3$ ): 0.55. Compound **4c**:  $^1\text{H}$  NMR (200 MHz,  $\text{CDCl}_3$ ,  $\delta$ ): 8.98–6.55 (m, 18H, arom.); 6.15 (br., 1H, OH); 3.86 (s, 3H,  $\text{OCH}_3$ ); 3.84 (s, 3H,  $\text{OCH}_3$ ); 2.94 (s, 4H,  $\text{CH}_2$ ). MS (LDI-TOF): 683.29 (MI), 666.45 (MI-OH).  $R_f$  (2% MeOH in  $\text{CDCl}_3$ ): 0.26. Compound **10**:  $^1\text{H}$  NMR (300 MHz,  $\text{CDCl}_3$ ,  $\delta$ ): 8.58 (d, 1H,  $J=9.6$  Hz, arom.); 8.41 (br. s, 1H, NH); 8.33–7.96 (m, 12H, arom.); 7.9–7.7 (m, 7H, arom.); 7.5 (m, 2H, arom.); 7.4–7.2 (m, 6H, arom.); 6.78 (d, 2H,  $J=7.9$  Hz, arom.); 6.72–6.63 (m, 3H, 2 arom., 1NH); 6.44 (dd, 2H,  $J_1=2.3$  Hz,  $J_2=8.7$  Hz, arom.); 6.26 (s, 1H, OH); 6.10 (s, 1H, OH); 3.74 (s, 6H, OMe); 3.52 (s, 3H, OMe); 3.45 (s, 3H, OMe); 3.45–3.35 (m, 12H,  $\text{OCH}_2$ ); 3.23 (m, 4H,  $\text{NCH}_2$ ); 1.69 (m, 4H,  $\text{CH}_2\text{CH}_2\text{CH}_2$ ).
9. Fourrey, J. L.; Varenne, J.; Blonski, C.; Dousset, P.; Shire, D. *Tetrahedron Lett.* **1987**, *28*, 5157–5160.
10. Smith, M.; Rammler, D. H.; Goldberg, I. H.; Khorana, H. G. *J. Am. Chem. Soc.* **1961**, *84*, 430–440.
11. The acidic stability of **7–9** (2% TsOH/ $\text{CH}_2\text{Cl}_2$ ) was as follows: DMTrOH < **7** < **9** ~ MMTrOH < **8** < TrOH.
12. Klinger, K. W.; Landes, G.; Dackowski, W.; Leverone, B.; Lopez, L.; Locke, P.; Ward, D.; Ried, T. *Cytogenet. Cell Genet.* **1991**, *58*, 2149.
13. Schena, M.; Shalon, D.; Davis, R. W.; Brown, P. O. *Science* **1995**, *270*, 467–470.
14. Fisher, E. F.; Caruthers, M. H. *Nucleic Acids Res.* **1983**, *11*, 1589–1599.
15. Lee, L. G.; Spurgeon, S. L.; Heiner, C. R.; Benson, S. C.; Rosenblum, B. B.; Menchen, S. M.; Graham, R. J.; Constantinescu, A.; Upadhyaya, K. G.; Cassel, J. M. *Nucleic Acids Res.* **1997**, *25*, 2816–2822.

# Appendix D

## Supplementary Confocal Image Data

Given the value of brevity in published works, the fluorescent images presented in **Chapters 2-5** represent a small subset of the large number of confocal images generated during the course of this research. As most of the oligonucleotide synthesis results are in the form of image-based data, the full data set from all experiments is overwhelming. However, some of the images not presented in manuscript form are shown here. Selected to show interesting electrochemical effects, negative results, preliminary experiments, and various other uncategorised findings, the images shown here provide a reasonably good sampling of the fluorescent data generated throughout the course of this work. Many of these and similar images were used in the formulation of ongoing theoretical hypotheses and improvements in apparatus and technique.

Brief descriptions of the included data follow the images. The annotations are concise, but provide further examples for reference. The images are presented in chronological order. Each image represents an area of  $1\text{ mm}^2$  (1 mm width and height) unless otherwise noted.

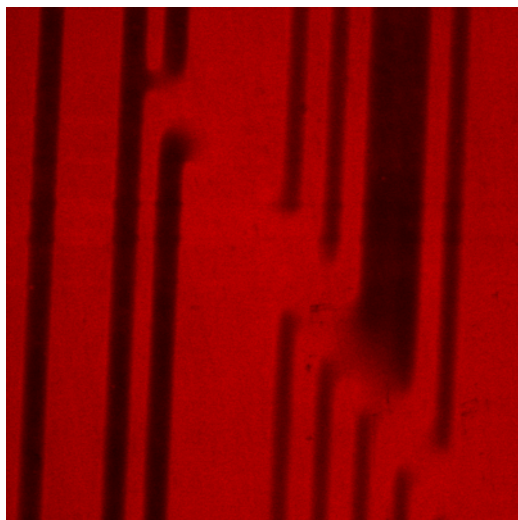


Figure 39 Patterning produced by damaged microelectrodes. Black represents area where acid reached the surface. The diagonal interruption in the lines shows where the microelectrodes were scratched. Interestingly, the acid spills out in areas without apparent adjacent cathodes. This experiment provided some evidence for the confining effect of the cathodes.

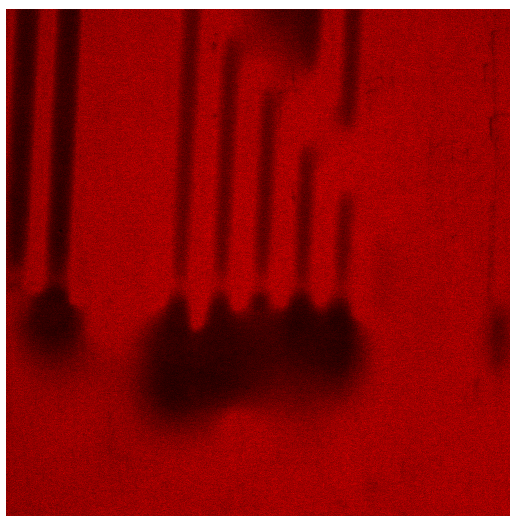


Figure 40 Spread of acid at the edges of the electrodes. Black represents acid distribution. The black plumes at the bottom of the image are areas where acid could escape the confining cathodes, as the linear electrodes ended just above that point.

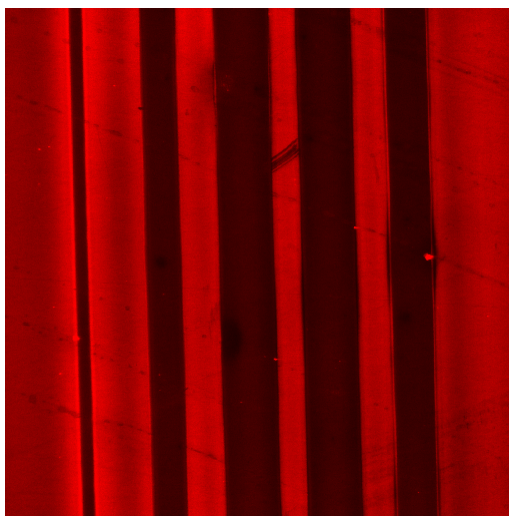


Figure 41 “Cy5 destruction” experiment. One of the first series of experiments designed to determine the spread of acid used a glass substrate entirely coated with fluorescent label. Held adjacent to the microelectrodes during application of current, very low pH caused covalent rearrangement (and “killed” fluorescence) of the fluorophore. Confocal analysis subsequently revealed black lines as regions where the acid had reached the substrate. The above image shows the results from five voltages, from 1.10 V on the left to 1.90 V on the right (30 s at 40  $\mu\text{m}$  gap). Note the *higher* fluorescence on the edges of the leftmost line. This was likely due to very high fluorescent loading density and a non-linear fluorophore self-quenching effect. Because this effect is difficult to interpret, these “Cy5 destruction” experiments were abandoned for the “capping” experiments as used in Chapter 2.

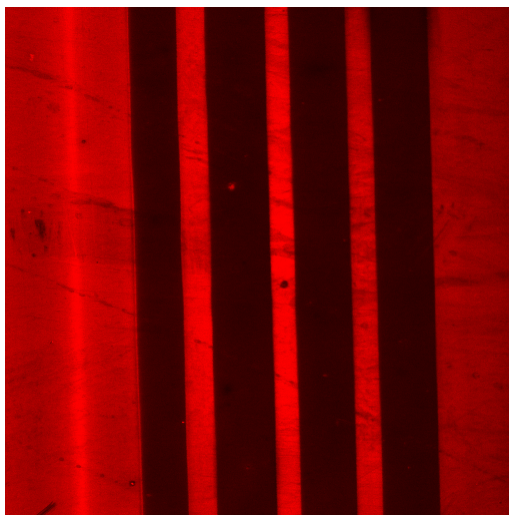


Figure 42 Another Cy5 destruction experiment. This result shows an example of the irritating self-quenching behaviour. The brighter left line actually represents fluorophore *destruction*, which then causes a slightly lower fluorescent molecule density, and reduction in self-quenching. Nonetheless, the very sharp edges on the lines provided promising evidence that the electrochemical method could produce high-resolution features.





Figure 43 Acid streams beyond edges of the microelectrodes. At the end of the microelectrodes, the unconfined anode produces acid which streams out elsewhere. The above images show such acid streaming at 1.9 V. The relatively straight jet or stream at the edge of the electrode appeared like an electrokinetic effect, in that diffusion alone would have produced a cloud pattern.



Figure 44 Acid spilling into undefined areas. This is a lower magnification of results as shown in the previous figure. A darker shaded region between all the electrodes as compared to the control substrate fluorescence (the edges of the image) seems to indicate unconfined acid leaking across cathodes. This image uses the self-quenching Cy5 destruction test, and comparatively high voltages (up to 2.1V).

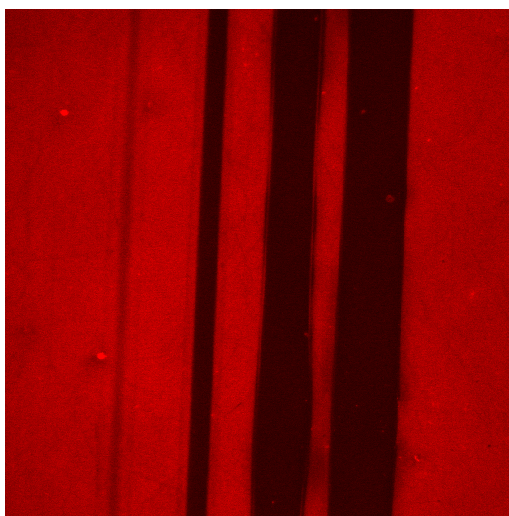


Figure 45 Capping method. This is the first result demonstrating the use of the capping method of detection, which was used in Chapter 2. The capping method suffers none of the self-quenching artefacts, and verifies acidic deblocking of the dimethoxy-trityl group was successful.

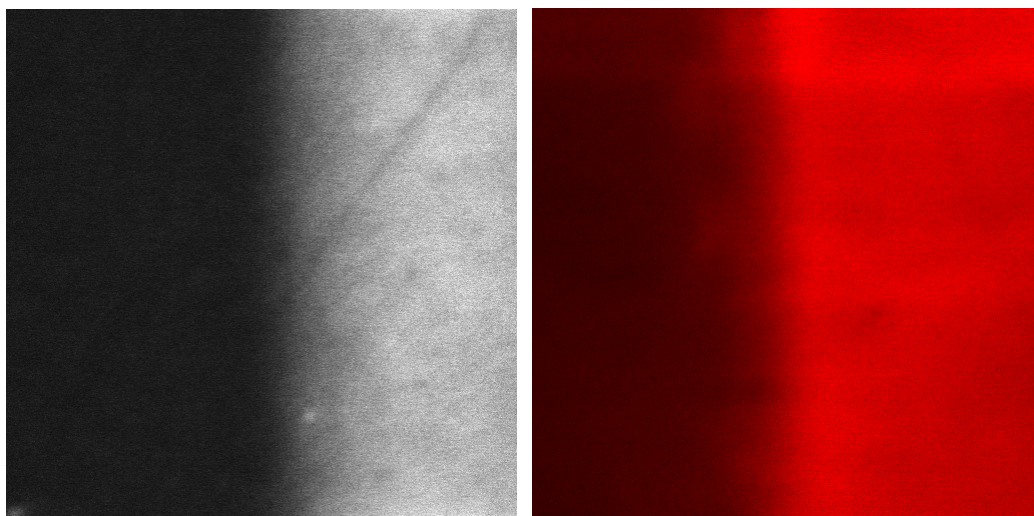


Figure 46 Patterned edge magnification. This image shows a high power magnification of the edges of the lines produced using early variations of the electrochemical patterning method. The entire frame is  $25\text{ }\mu\text{m}$  wide, and the transition from patterned region (dark) to unpatterned occurs over about  $5\text{ }\mu\text{m}$ . These features were patterned at a gap distance of  $120\text{ }\mu\text{m}$ . Subsequent refinement in the method allowed even sharper edge definition. The left-hand image shows results from the capping method, and the right-hand from the Cy5 destruction method.

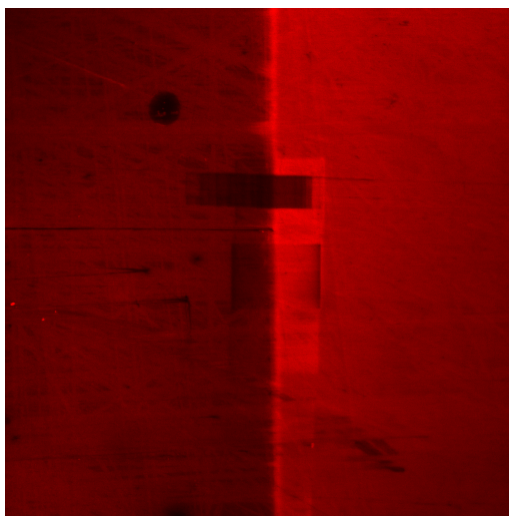


Figure 47 Fluorescence bleaching. When repeatedly scanned for long durations at high laser power under confocal microscopy, the fluorophore undergoes photobleaching. The dark rectangles in the middle of the sample show areas where the substrate was scanned for several minutes at high power. The brightest rectangles, in the middle of the micrograph, show evidence of the self-quenching behaviour as previously described.

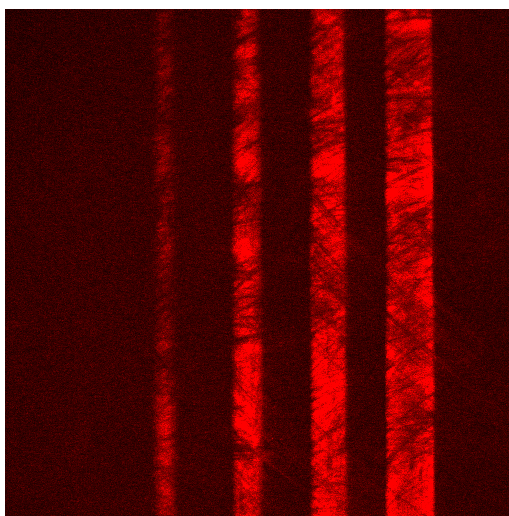


Figure 48 Incomplete substrate derivatisation. The vapour-phase glass derivatisation procedure used to prepare the substrate for covalent attachment of DNA was usually reliable. However, this image shows the results of DNA synthesis after failure in the temperature cycle for the derivatisation procedure; the oligonucleotides do not adhere well to the glass.

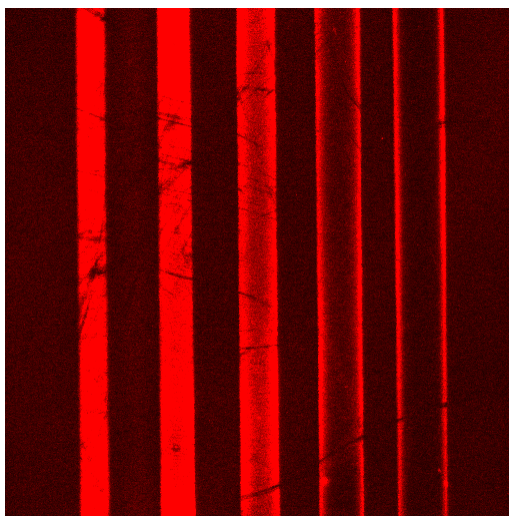


Figure 49 Early range-finding experiments. This image shows single-step base additions using a range of acid exposure times (all at 1.33 V and 40  $\mu\text{m}$  gap distance). The stripe on the far left was exposed to acid for 4 seconds, and the one on the far right for 128 seconds. The dark area in the middle of the stripes shows the effects of acid overexposure, which causes depurination as discussed in detail in Chapter 4.

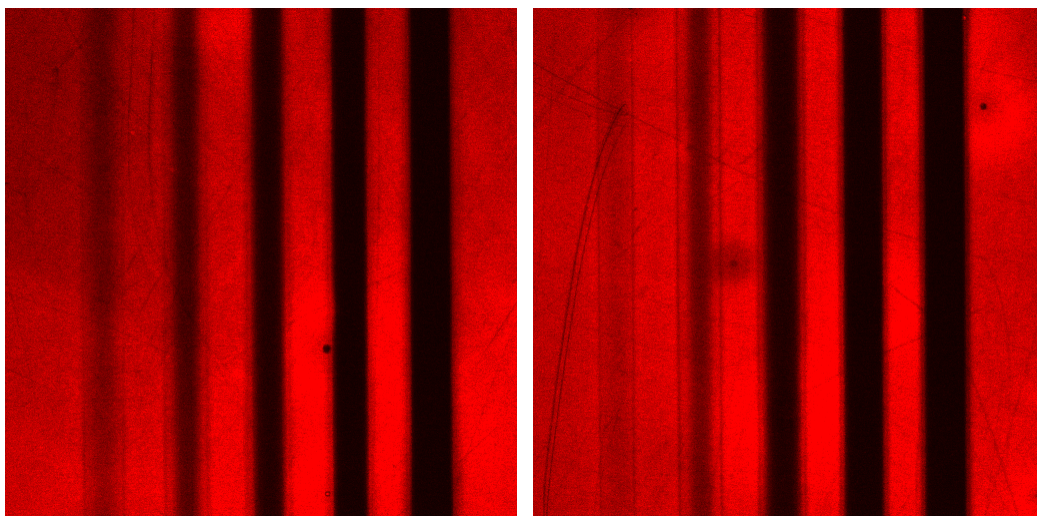


Figure 50 An example of the patterns produced during early range-finding experiments. The ability to address single electrodes and vary the gap distance during single experimental runs proved enormously useful in completing large numbers of range finding experiments quickly. The above images show the results obtained in parallel from a single synthetic run: acid exposure times were 8 s, 16 s, 32 s, 64 s, and 128 s (from left to right, all at 1.33 V) at 20  $\mu\text{m}$  gap distance (left image) and 40  $\mu\text{m}$  gap distance (right image). The capping method was used here, producing dark areas upon acid exposure.



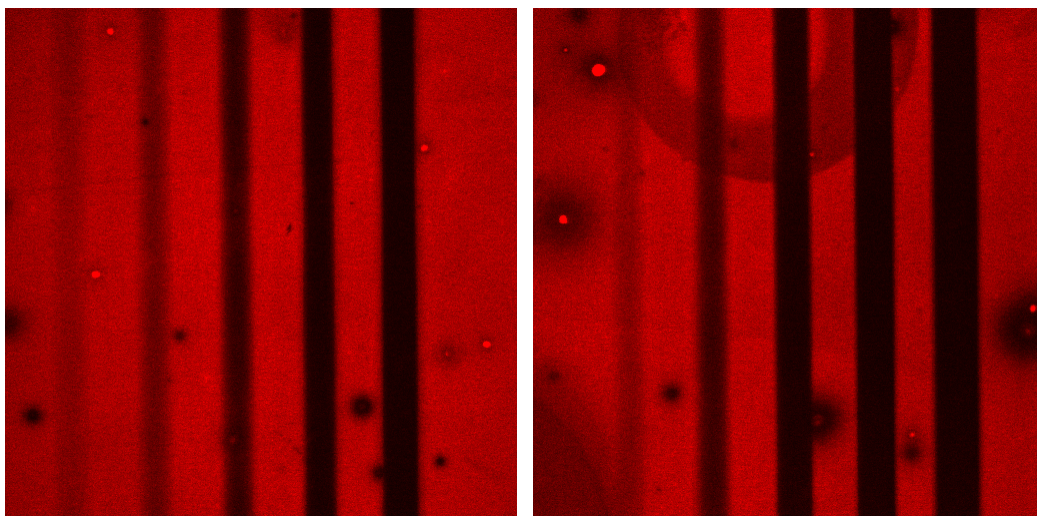


Figure 51 A further example of range-finding experiments conducted in parallel. These images show the variation in acid reaching the substrate with various voltages applied to the microelectrodes (1.08, 1.15, 1.22, 1.28, 1.36 V from left to right), at two different durations (4 seconds left image, 8 seconds right). Gap distance was 40  $\mu\text{m}$  for both images.

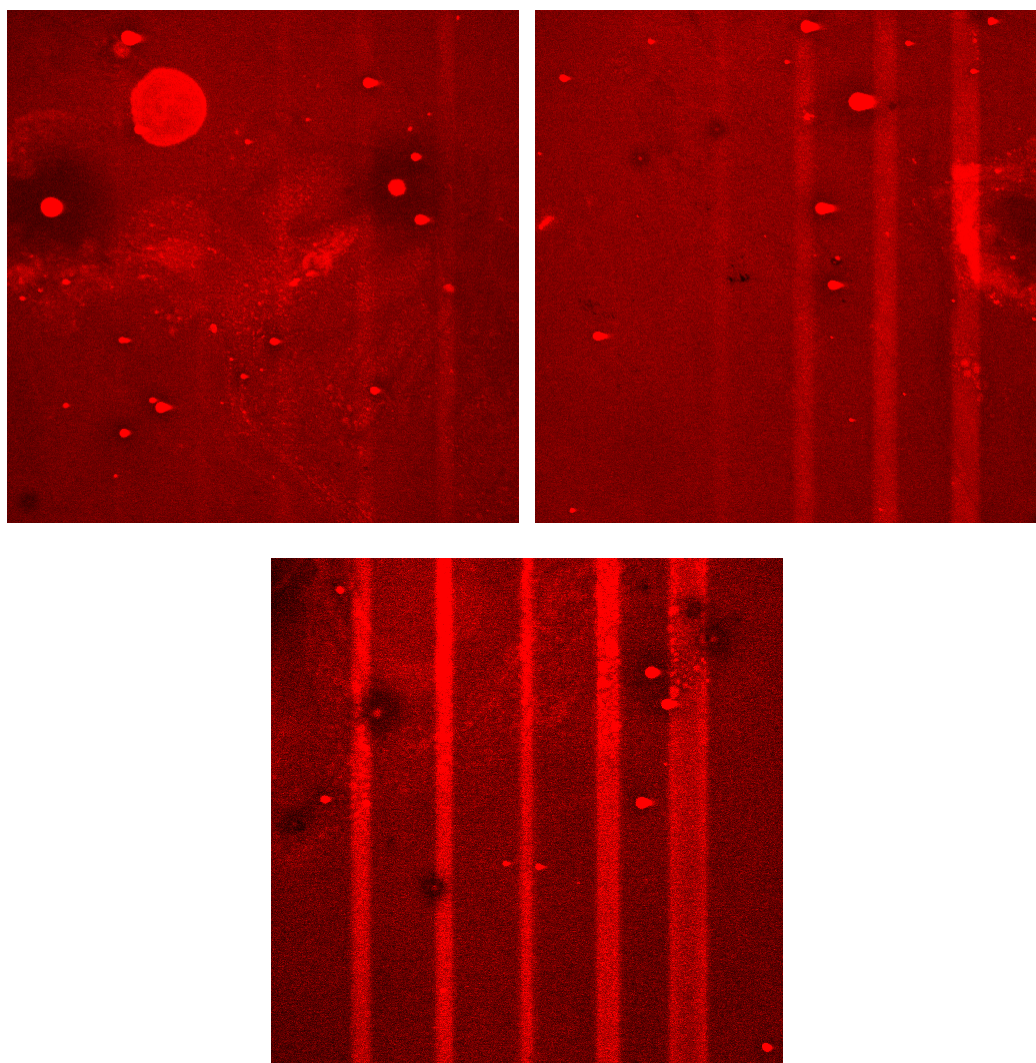


Figure 52 Demonstration of synthesis failure. The entire system used for DNA synthesis in these experiments was complex. Failure in any one of its component parts (electronics, software, flow-cell, micrometer housing, synthesiser, or chemical reagents) would result in poor or no DNA synthesis. The above images show the results from one such failure; the substrate became detached from its carrier during synthesis, and was left floating in the flow cell. Real-time current measurements during this run were abnormal, so the problem was quickly detected and corrected.



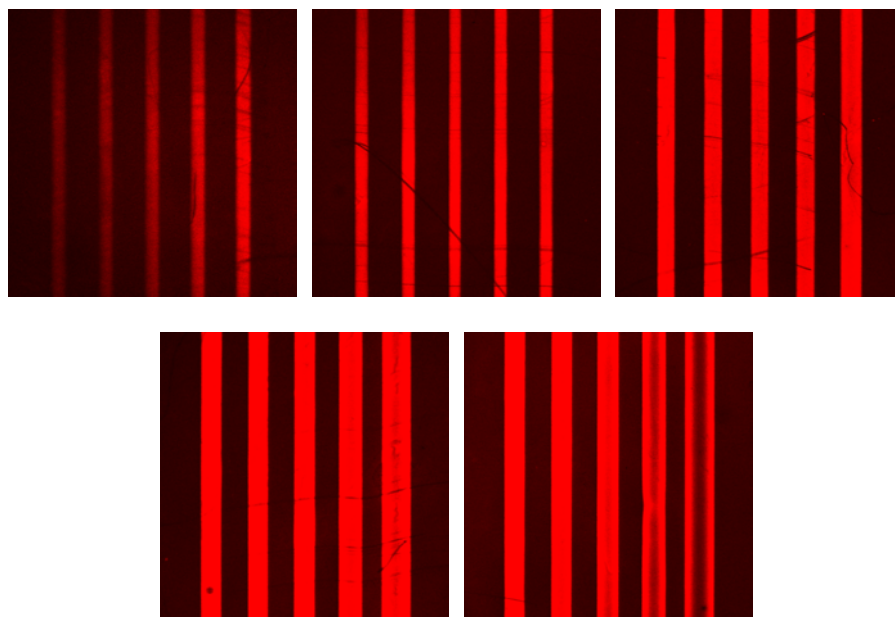


Figure 53 Further demonstration of large-scale parallel range finding. For optimising yields in this work, a two-phase approach was generally practised. In the first phase, multiple variables were altered in large increments with the goal of exploring as wide of a range of parameters as possible. Subsequent second phase experiments varied a single parameter, with the goal of fine-tuning the system. The above images show the results from a single synthetic run of the second-phase fine-tuning variety, in this case varying exposure times from 3.0 seconds (left line on top left image) to 41 seconds (right line on bottom right image). Chapter 4 presents and discusses results from experiments similar to these.

## Appendix E

# An Electrochemical Redox Couple Activated by Microelectrodes for Confined Chemical Patterning of Surfaces

The following paper was published in *Analytical Chemistry* in 2002 and presented in Chapter 2 with changes only in formatting.

# An Electrochemical Redox Couple Activitated by Microelectrodes for Confined Chemical Patterning of Surfaces

Ryan D. Egeland,<sup>\*,†</sup> Frank Marken,<sup>‡</sup> and Edwin M. Southern<sup>†</sup>

Department of Biochemistry, University of Oxford, South Parks Road, Oxford, OX1 3DR, United Kingdom, and  
Department of Chemistry, Loughborough University, Loughborough, Leics, LE11 3TU, United Kingdom

**Microelectrodes, printed as an array on the surface of a silicon chip, generate chemically active species in a solution of electrolyte held between the electrode array and a glass plate. The active species induce chemical change in molecules coupled to the surface of the glass plate, which is separated from the electrode array by a gap of several micrometers. This paper explores the nature and pattern of the induced chemical change. The patterning is discussed with respect to the electrolyte composition and the magnitude and duration of current applied to the microelectrodes. We show that under suitable conditions the active species is confined to micrometer-sized features and diffusion does not obscure the surface pattern produced.**

The techniques that revolutionized the manufacture of electronic components have recently been applied to biological and chemical systems. Small devices carrying molecules of DNA<sup>1–6</sup> or peptides<sup>7</sup> have been fabricated on glass, silicon, and plastic substrates. These chemical and biological “chips” have been used in genomic analysis,<sup>8,9</sup> gene expression profiling,<sup>10</sup> drug analysis,<sup>11,12</sup> and environmental and biological sample analysis.<sup>13–17</sup>

Although several in situ fabrication techniques have been used to make these devices, there remain many significant technical challenges.<sup>18,19</sup>

There are two requirements for any in situ molecular fabrication method. First, it must be able to apply the methods of chemical synthesis to make molecules of defined structure on a solid substrate. Second, it must be capable of creating the molecular features in spatially defined regions. Many organic syntheses follow a stepwise path in which an active group is exposed by removal of a protecting group and then coupled with an active reagent.<sup>20–22</sup> Nucleic acid and peptide syntheses are examples of this approach;<sup>23</sup> these chemistries were first adapted to solid-state synthesis and then to patterned synthesis on planar substrates. In these and other syntheses, protecting groups are typically removed by acid or base.

Methods that have been used for patterned in situ synthesis include ink-jet application of deprotection agents,<sup>24</sup> application of precursors by physical masking<sup>25,26</sup> or ink-jet printing,<sup>27–30</sup> application of physical masks by photolithography,<sup>31</sup> and removal of photolabile protecting groups by photomasking.<sup>18,32</sup> Although these methods have proven useful, each has certain disadvantages. Physical masking is only suitable when the synthetic pattern may be formed by overlapping placements of the mask; the resolution of the ink-jet method is limited by the accuracy in aiming droplets of reagents and by their spread when they hit the surface; the

\* Corresponding author: (e-mail) ryan@egeland.net; (fax) +44 (8701) 312592.

<sup>†</sup> University of Oxford.

<sup>‡</sup> Loughborough University.

- (1) Case-Green, S. C.; Mir, K. U.; Pritchard, C. E.; Southern, E. M. *Curr. Opin. Chem. Biol.* **1998**, *2*, 404–410.
- (2) Gao, X. L.; Yu, P. L.; LeProust, E.; Sonigo, L.; Pellois, J. P.; Zhang, H. *J. Am. Chem. Soc.* **1998**, *120*, 12698–12699.
- (3) Hashimoto, K.; Ito, K.; Ishimori, Y. *Anal. Chem.* **1994**, *66*, 3830–3833.
- (4) Livache, T.; Bazin, H.; Caillat, P.; Roget, A. *Biosens. Bioelectron.* **1998**, *13*, 629–634.
- (5) Millan, K. M.; Spurmanis, A. J.; Mikkelsen, S. R. *Electroanalysis* **1992**, *4*, 929–932.
- (6) Zhao, Y. D.; Pang, D. W.; Wang, Z. L.; Cheng, J. K.; Qi, Y. P. *J. Electroanal. Chem.* **1997**, *431*, 203–209.
- (7) Fodor, S. P. A.; Read, J. L.; Pirrung, M. C.; Stryer, L.; Lu, A. T.; Solas, D. *Science* **1991**, *251*, 767–773.
- (8) Hacia, J. G.; Brody, L. C.; Collins, F. S. *Mol. Psychiatr.* **1998**, *3*, 483–492.
- (9) Cheng, J.; Sheldon, E. L.; Wu, L.; Uribe, A.; Gerrue, L. O.; Carrino, J.; Heller, M. J.; O'Connell, J. P. *Nat. Biotechnol.* **1998**, *16*, 541–546.
- (10) Hughes, T. R.; Shoemaker, D. D. *Curr. Opin. Chem. Biol.* **2001**, *5*, 21–25.
- (11) Manz, A. *Chimia* **1996**, *50*, 140–143.
- (12) Wang, J. J. *Pharm. Biomed.* **1999**, *19*, 47–53.
- (13) Cheng, J.; Sheldon, E. L.; Wu, L.; Heller, M. J.; O'Connell, J. P. *Anal. Chem.* **1998**, *70*, 2321–2326.
- (14) Suzuki, H. *Electroanalysis* **2000**, *12*, 703–715.
- (15) Fiaccabrino, G. C.; Koudelka-Hep, M. *Electroanalysis* **1998**, *10*, 217–222.
- (16) Liu, C. C.; Zhang, Z. R. *Sel. Electron. Rev.* **1992**, *14*, 147–167.

- (17) Wise, K. D.; Najafi, K. *Science* **1991**, *254*, 1335–1342.
- (18) Singh-Gasson, S.; Green, R. D.; Yue, Y. J.; Nelson, C.; Blattner, F.; Sussman, M. R.; Cerrina, F. *Nat. Biotechnol.* **1999**, *17*, 974–978.
- (19) McGall, G. H.; Barone, A. D.; Diggelmann, M.; Fodor, S. P. A.; Gentelen, E.; Ngo, N. *J. Am. Chem. Soc.* **1997**, *119*, 5081–5090.
- (20) Schreiber, S. L. *Science* **2000**, *287*, 1964–1969.
- (21) Dolle, R. E.; Nelson, K. H. *J. Comb. Chem.* **1999**, *1*, 235–282.
- (22) Osborn, H. M. I.; Khan, T. H. *Tetrahedron* **1999**, *55*, 1807–1850.
- (23) *Oligonucleotide Synthesis: A Practical Approach*; Gait, M. J., Ed.; IRL Press: Oxford, U.K., 1984; pp 83–116.
- (24) Hughes, T. R.; et al. *Nat. Biotechnol.* **2001**, *19*, 342–347.
- (25) Southern, E. M.; Maskos, U.; Elder, J. K. *Genomics* **1992**, *13*, 1008–1017.
- (26) Southern, E. M.; Maskos, U. *J. Biotechnol.* **1994**, *35*, 217–227.
- (27) Stanton, L.; et al. *Am. J. Hum. Genet.* **2000**, *67*, 1463.
- (28) Okamoto, T.; Suzuki, T.; Yamamoto, N. *Nat. Biotechnol.* **2000**, *18*, 438–441.
- (29) Roda, A.; Guardigli, M.; Russo, C.; Pasini, P.; Baralini, M. *Biotechniques* **2000**, *28*, 492–496.
- (30) Stimpson, D. I.; Cooley, P. W.; Knepper, S. M.; Wallace, D. B. *Biotechniques* **1998**, *25*, 886–890.
- (31) McGall, G.; Labadie, J.; Brock, P.; Wallraff, G.; Nguyen, T.; Hinsberg, W. P. *Natl. Acad. Sci. U.S.A.* **1996**, *93*, 13555–13560.
- (32) Fodor, S. P. A. *Science* **1997**, *277*, 393–395.

photolithographic methods require special photosensitive reagents and expensive fabrication of mask sets for each pattern produced.

In this work, we explore a method of patterning a surface using electrochemically generated reagents. Reagents that can be produced electrochemically include acids, bases, radicals, reactive gases or ions, metals, and many types of reducing and oxidizing species.<sup>33–39</sup> The amount and reactivity of reagents can be controlled by the choice of electrolyte solution or the applied voltage. This fine regulation of the chemical conditions may thus permit a degree of control of the reaction not possible with other fabrication methods.

Electrochemical methods described previously used single active electrodes<sup>37</sup> and are not suitable for creating large numbers of small features. We describe a new approach which uses an array of individually addressable electrodes placed a short distance from the surface to be treated. The electrodes generate active reagent that reacts with molecules on the surface. In the examples described here, active reagent is an acid, generated at anodes.

The elements of the microelectrode array are individually addressable, so independent features of the pattern can be generated in parallel. Furthermore, using anodes and cathodes in close proximity introduces a means of controlling diffusion of the reactants. In systems that use a single isolated electrode to generate an active species, such as scanning electrochemical microscopy, reactants diffuse rapidly from the vicinity of the electrode. A number of electrical and chemical means have been used to confine the reagents generated at the microelectrode,<sup>40,41</sup> but diffusion is intrinsic to any reagent in solution. For example, a small 1.7- $\mu\text{m}$  electrode generates a 250- $\mu\text{m}$  pattern after 20 s which grows to the relatively macroscopic dimension of 400  $\mu\text{m}$  after 80 s.<sup>42</sup> We have designed a chemical system that limits these effects.

A “quenching” reagent generated at the cathodes destroys acid everywhere but in regions close to the anode that generated it. This constraining effect of the counter electrodes creates features that approach the size of the microelectrodes themselves. Unlike methods such as scanning electrochemical microscopy patterning, where the tool must be manipulated to “write” a surface feature, this method allows “printing” on a surface, with printed pattern determined simply by the microelectrode arrangement.

## EXPERIMENTAL SECTION

**Materials.** Silicon wafers were used for creating the microelectrodes and as the solid supports for the electrochemical

patterning. Wafers were purchased from Aurel GmbH (Landsberg, Germany) as P-type (boron doped),  $\langle 100 \rangle$  orientation, 7–21  $\Omega\text{ cm}$  resistivity, 100-mm diameter, 518–532  $\mu\text{m}$  thick, CZ Silicon Prime Wafers, SEMI standard. The wafers were thermally oxidized to yield a  $124 \pm 0.4\text{-nm}$  surface thickness of silicon dioxide. (Glycidoxypyril)trimethoxysilane (Sigma-Aldrich, Poole, England) was used as supplied. Poly(ethylene glycol) (200 average molecular weight, Sigma-Aldrich) was used without further purification. Benzoquinone, hydroquinone, and tetrabutylammonium hexafluorophosphate (Sigma-Aldrich) were dissolved in anhydrous acetonitrile (supplied as “phosphoramidite diluent”, Cruachem, Glasgow, Scotland) under dry argon immediately before use. Dimethoxytrityl (DMT) was attached to the substrate as a thymidine  $\beta$ -cyanoethyl phosphoramidite (Cruachem) using standard DNA synthesis reagents (Cruachem). Equal volumes of acetic anhydride and (dimethylamino)pyridine (Cruachem) were used in solution for the acetylation. “Cy5 phosphoramidite” used for fluorescent reporting was purchased from Amersham Pharmacia Biotech (Buckinghamshire, England) and diluted with anhydrous acetonitrile (100 mg/mL) before use. Iridium metal used for microelectrodes was 99.9% purity (Johnson Matthey Noble Metals, London, England).

**Microelectrode Array.** The fabrication of an array of microelectrodes resistant to reduction, oxidation, chemical attack, and mechanical destruction presented special challenges and will be described in detail elsewhere. Briefly, 96 linear electrodes were fabricated by electron beam evaporation of 50-nm iridium metal onto silicon wafers previously patterned with an organic photoresist using conventional UV light photolithography. After the photoresist was removed in acetone, the iridium was annealed by heating at 350  $^{\circ}\text{C}$  for 30 min in air and then cleaned by reactive ion etching (in oxygen and argon). The resulting microelectrodes, each measuring  $40 \pm 0.1\text{ }\mu\text{m}$  wide by 7500  $\mu\text{m}$  long and separated by 40- $\mu\text{m}$  gaps, were connected to separate printed circuit board tracks via 20- $\mu\text{m}$  gold wire bonds.

**Preparation of Glass Substrate.** Polished, oxidized silicon wafers were used as the patterned surface supports. Before electrochemical patterning, the wafer surface was functionalized with a linker molecule to which the organic reagents were attached.<sup>43</sup> Wafers were placed in a 18.1-L vacuum furnace chamber with an ampule containing 5 mL of (glycidoxypyril)trimethoxysilane. After the furnace was heated to 185  $^{\circ}\text{C}$ , the ampule was heated to 205  $^{\circ}\text{C}$  and the chamber evacuated to 25–30 mBar. After  $\sim 2.5$  mL of the silane had evaporated, the chamber was allowed to cool under vacuum ( $10^{-3}$  Torr). A “linker molecule” was attached by immersing the (glycidoxypyril)trimethoxysilane-derivatized wafers in 200 mL of poly(ethylene glycol) containing 100  $\mu\text{L}$  of sulfuric acid. DMT-containing phosphoramidite was then covalently attached to the free hydroxyl on the poly(ethylene glycol) by conventional oligonucleotide synthesis techniques<sup>23,44</sup> employing 3% dichloroacetic acid deblocking. The wafer substrate surface thus prepared was cut into 1-cm squares for use in patterning.

**Reagent Delivery and Substrate Positioning.** Reagents used for the electrochemically directed synthetic steps were flushed across the entire substrate surface in an apparatus designed to

(33) Lund, H.; Baizer, M. M. *Organic Electrochemistry: An Introduction and Guide*; (3rd revision and expand edition); M. Dekker: New York, 1991.

(34) Kyriacou, D. K. *Basics of Electroorganic Synthesis*; Wiley: New York, 1981.

(35) Kyriacou, D. K. *Modern Electroorganic Chemistry*; Springer-Verlag: New York, 1994.

(36) Covington, A. K.; Dickinson, T. *Physical Chemistry of Organic Solvent Systems*; Plenum Press: New York, 1973.

(37) Volke, J.; Liska, F. *Electrochemistry in Organic Synthesis*; Springer-Verlag: London, 1994.

(38) Zuman, P. *The Elucidation of Organic Electrode Processes*; Academic Press: New York, 1969.

(39) Zuman, P.; Patel, R. *Techniques in Organic Reaction Kinetics*; Wiley: New York, 1984.

(40) Kirchner, V.; Xia, X. H.; Schuster, R. *Acc. Chem. Res.* **2001**, *34*, 371–377.

(41) Zu, Y. B.; Xie, L.; Mao, B. W.; Tian, Z. W. *Electrochim. Acta* **1998**, *43*, 1683–1690.

(42) Shiku, H.; Takeda, T.; Yamada, H.; Matsue, T.; Uchida, I. *Anal. Chem.* **1995**, *67*, 312–317.

(43) Gray, D. E.; Case-Green, S. C.; Fell, T. S.; Dobson, P. J.; Southern, E. M. *Langmuir* **1997**, *13*, 2833–2842.

(44) Beaucage, S. L.; Iyer, R. P. *Tetrahedron* **1992**, *48*, 2223–2311.

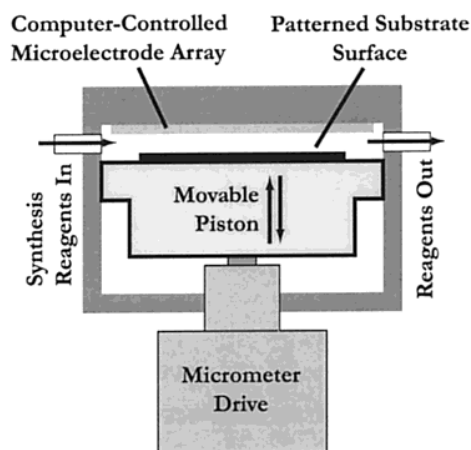


Figure 1. Chemical patterning reactions on a surface carried out in an enclosed chamber through which appropriate reagents could be delivered. A digital micrometer head precisely manipulated a gap between a microelectrode array and the surface so that chemical products generated at the microelectrodes could diffuse to the patterned surface, where synthetic chemical steps were performed. A specially designed computer control board controlled the flow of reagents, applied external potentials to each of 96 individual microelectrodes, and measured the resulting currents.

hold the substrate a specified distance ( $20 \pm 1 \mu\text{m}$  in these experiments) from the microelectrode set (Figure 1). This distance could be increased by adjusting a digital micrometer head piston to allow large volumes of solvent or other reagent through the system as appropriate and then reestablished during the electrochemical acid generation.

**Acid Generation and Current Measurement.** A custom electronic circuit applied current in a parallel fashion to each of the electrodes independently and is described in detail elsewhere. Any electrode could be disconnected from the voltage source (made "floating") by analog multiplex switch integrated circuits. Voltages were applied at the anodes with respect to the cathodes (the electrochemical system is a "two-electrode cell"). As the current delivered to each individual electrode was very small (nanoamps), instrumentation amplifiers were employed in its measurement. A computer software program controlled this electronic circuit and also automated delivery of reagents to the substrate.

**Acetylation and Fluorescent Reporter.** The loss of the acid-sensitive trityl protecting group on conventional phosphoramidites indicated regions where acid reached the substrate during the electrochemical deblocking step. After electrochemical patterning of a microscope slide coated with trityl-containing phosphoramidite, the entire surface was treated with a mixture of equal volumes of acetic anhydride and (dimethylamino)pyridine using an ABI 394 DNA synthesizer. This reagent renders the regions previously subject to acids unreactive toward further chemical modification. Remaining trityl groups were removed by treating the whole surface with DCA, and a subsequent final modification of the entire surface with Cy5 phosphoramidite resulted in fluorescence everywhere except those regions patterned by electrochemically generated acids.

**Fluorescence Detection.** Fluorescent molecules were detected using a Leica TCS NT confocal microscope. Confocal microscopy allowed examination of fluorescence in a single focal

plane, thus eliminating background fluorescence while the monolayer was observed. Before each measurement, the focal plane was adjusted to the height of the substrate on the microscope stage and the photomultiplier tube (PMT) voltage adjusted to maximum sensitivity without saturation. The fluorescent units recorded for each image are arbitrary and not directly comparable across experiments, as microscope adjustments were independent for each sample.

**Cyclic Voltammetry.** Voltammetric experiments were performed with an Autolab potentiostat system (Eco Chemie) in a conventional three-electrode cell with a platinum gauze counter electrode and a saturated calomel (SCE) reference electrode. The cyclic voltammograms were obtained for the reduction and oxidation of an acetonitrile solution (0.1 M  $\text{NBu}_4\text{PF}_6$ ) of 2.5 mM benzoquinone and 2.5 mM hydroquinone at a 1-mm platinum disk electrode ( $T = 22^\circ\text{C}$ ).

## RESULTS AND DISCUSSION

**Interaction of Acid at the Surface.** As an example of a step used widely in organic synthesis, we chose to study the thermodynamically and kinetically favorable removal of a DMT group by mild acid to form a primary hydroxyl (an overall depiction of the process is shown in Figure 2). A glass chip was first derivatized with a linker to which a deoxyribothymidine (dT) phosphotriester was attached by conventional phosphoramidite coupling.<sup>23</sup> The dT carried a DMT group on the 5'-hydroxyl. We had previously verified that the DMT group could be efficiently removed by dilute sulfuric acid in acetonitrile.

The objective was to remove this group using acid generated at the anodes of a microelectrode array placed against the glass chip by a substrate positioning apparatus allowing fine control of the distance between the electrodes and chip (Figure 1) and to acetylate the hydroxyl groups in the exposed regions by treatment of the whole surface with acetic anhydride. The DMT groups not removed by the electrochemical step were then removed by treating the whole surface with a solution of dichloroacetic acid in dichloromethane. The hydroxyl groups thus exposed were coupled to Cy5, a fluorescent dye, so that the pattern produced by the electrochemical generation of acid was revealed by observing the fluorescence of the Cy5 in a confocal microscope.

In the following sections, we discuss the processes that generate active species at the electrodes, the reaction that takes place on the substrate, and the interactions that take place in the solution between the electrodes to destroy the species generated at the anode and cathode. We discuss the stoichiometry and kinetics of these processes.

**Acid Generation.** We have explored the effects of varying the electrolyte solution, and the results presented here were obtained with an electrolyte system optimized for the acetylation patterning process. Acid was generated at the anode by the oxidation of hydroquinone (HQ) to benzoquinone (Q) in acetonitrile. Although the mechanism was subject to some controversy in the early literature,<sup>45–50</sup> the oxidation half-reaction yields a clean source of protons at the anodes, as shown below:

(45) Parker, V. D. *J. Chem. Soc. D* **1969**, 716–717.

(46) Eggins, B. R. *J. Chem. Soc. D* **1969**, 1267–1268.

(47) Eggins, B. R.; Chambers, J. Q. *Chem. Commun.* **1969**, 232–233.

(48) Parker, V. D.; Eberson, L. *J. Chem. Soc. D* **1970**, 1289–1290.

(49) Eggins, B. R. *J. Chem. Soc., Chem. Commun.* **1972**, 427.

(50) Parker, V. D. *Electrochim. Acta* **1973**, 18, 519–524.



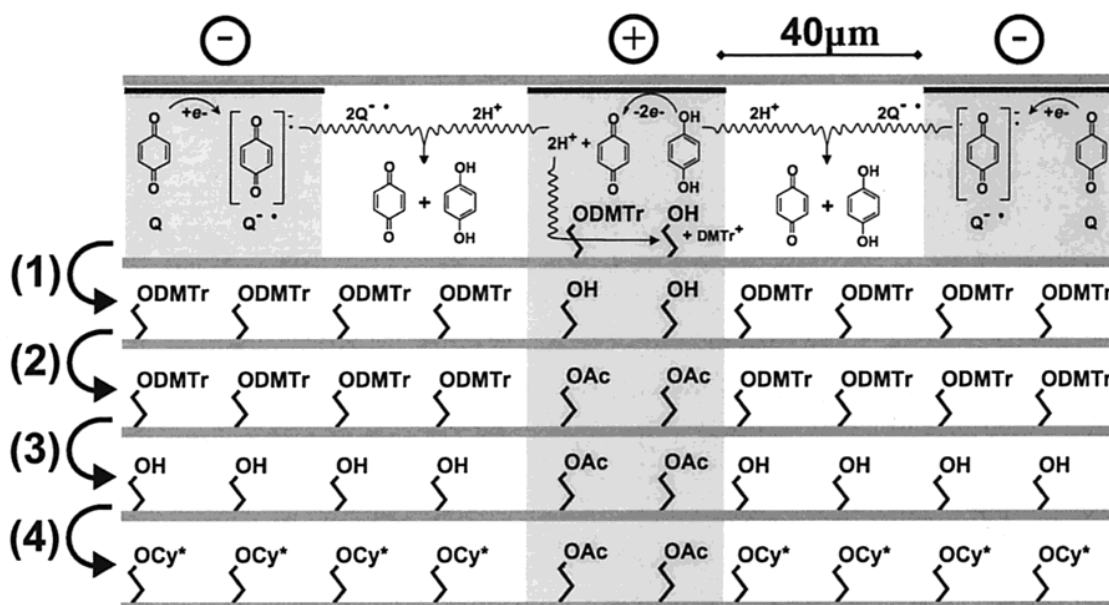
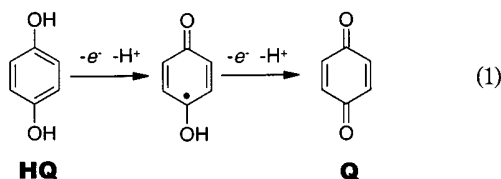
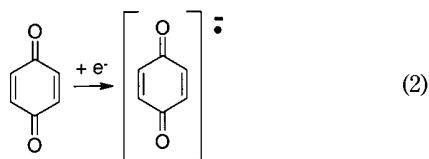


Figure 2. Oxidation process, Electrochemical oxidation of hydroquinone at the anodes (+) on an array of microelectrodes delivers acid to localized regions on a surface (the gray shading symbolizes surface regions near the anode). The acid removes a dimethoxytrityl (DMTr) group (1) to expose a primary hydroxyl (OH), which is then exposed to an acetylating reagent (2) to attach an acetyl group (Ac). Subsequent treatment of the entire surface with an acid solution (3) followed by coupling of a fluorescent (Cy\*) dye (4) allows imaging by confocal microscopy so that regions of acetylation are revealed by diminished fluorescence. The counter electrode process at the adjacent cathodes (−) is the reduction of benzoquinone, which yields a radical anion reactive with protons, thus acting to deplete acid in the cathode region and regenerate hydroquinone.



This oxidation of hydroquinone and the reduction of benzoquinone in these experiments was characterized by cyclic voltammetry in bulk electrolyte solution (see Figure 3). The two main processes detected under these conditions are the oxidation of hydroquinone ( $P2_{ox}$ ) at +1.2 V versus SCE peak potential (eq 1) and the reduction of benzoquinone ( $P1_{red}$ , eq 2) at −0.47 V vs



SCE peak potential. Two minor signals in the voltammogram may be attributed to the oxidation of hydroquinone in the deprotonated state ( $P4_{ox}$ ) and the reduction of benzoquinone in the presence of electrogenerated acid ( $P3_{red}$ ). Overall, the reaction scheme is complex but in agreement with previous reports.<sup>50</sup>

The process at the cathodes is the reduction of benzoquinone and yields a radical anion as shown in eq 2.<sup>51</sup> The radical anion is relatively stable but may undergo followup chemical reactions in the presence of protons. We therefore speculated that acid in

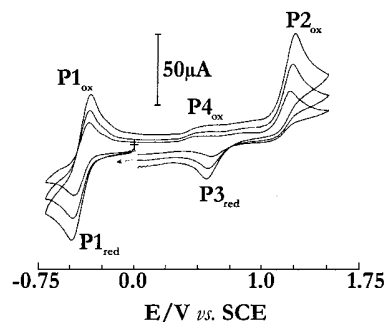
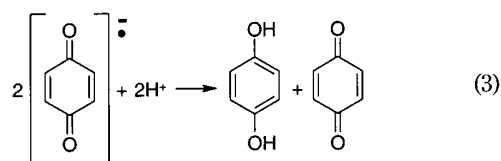


Figure 3. Reversible oxidation of hydroquinone and reduction of benzoquinone. The chemical system comprising this process generates well-defined, electrochemically induced pH gradients, with proton generation at the anode and proton consumption at the cathode. This figure shows cyclic voltammograms for the reduction and oxidation of an acetonitrile solution (0.1 M  $\text{NBu}_4\text{PF}_6$ ) of 2.5 mM benzoquinone and 2.5 mM hydroquinone at a 1-mm platinum disk electrode (scan rates 200, 500, and 1000 mV/s,  $T = 22^\circ\text{C}$ ). The peak  $P1_{red}$  corresponds to the reversible reduction of benzoquinone to yield a radical anion, and  $P2_{ox}$  corresponds to the oxidation of hydroquinone. Minor signals  $P4_{ox}$  and  $P3_{red}$  have been assigned tentatively to the oxidation of deprotonated hydroquinone and the reduction of protonated benzoquinone, respectively.

solution would be consumed by the cathodic radical anion as shown in eq 3. As the radical anion and proton are of opposite



(51) Bauscher, M.; Maentele, W. *J. Phys. Chem.* **1992**, *96*, 11101–11108.

charge, we considered that electric field effects in depleted concentrations of supporting electrolyte may also act to enhance the annihilation of acid.<sup>52</sup>

We speculated that the acid generated in the anodic process (P2) would be strong enough to remove the acid-labile DMT group. The voltage (applied at the anodes with respect to the cathodes) required to establish the pH gradient was expected to be between 0.9 (difference between potentials for reduction P1 and oxidation P4) and 1.67 V (difference between reduction P1 and oxidation P2). Observations described below support this prediction and demonstrate that the rate of production of acid at the anodes and the rate of diffusion across the gap to the surface leads to complete removal of the DMT in a few seconds.

**Stoichiometry and Kinetics.** The rate of the patterning reaction is determined by the probability that protons in solution reach the immobilized DMT at the surface. We therefore found it instructive to compare the total number of hydroquinone molecules in solution to the number of DMT groups on the surface.

Before voltage is applied, the amount of DMT on the glass chip is  $\sim 10$  pmol/mm<sup>2</sup> surface area.<sup>53</sup> The quantity of hydroquinone in a 20- $\mu$ m depth of electrolyte solution overlying the surface is 500 pmol/mm<sup>2</sup>. Thus, oxidation of all the hydroquinone in this area would result in a 100-fold molar excess of acid, assuming all protons transverse the electrode-surface gap and arrive evenly over the chip surface.

A true estimate of the number of protons generated at the anode can be obtained from measurement of the current. The number of protons ( $N_p$ ) produced during patterning of duration  $t$  is equal to the number of electrons ( $N_e$ ) removed from the anodes by the external voltage source and was calculated from the applied current ( $i$ ) as follows:

$$N_p = N_e = \frac{\int_0^t i \, dt}{F} \quad (4)$$

where  $F$  is Faraday's constant (we assumed 100% current efficiency for these calculations). We designed an amplifier circuit to record current at each of the microelectrodes to nanoampere precision, with negligible measured background current. We then used the electrodes to generate patterns and considered the amount of acid produced under various conditions.

We applied a range of dc potentials to anodes (with respect to cathodes) which were 7.5 mm long by 40  $\mu$ m wide and separated from adjacent cathodes by 40  $\mu$ m (the significance of the electrode arrangement is discussed later), with a depth of solution of 20  $\mu$ m between the electrode array and substrate. The rate of protons generated is very small at cell potentials below 1.2 V and increases exponentially above 1.3 V (Figure 4), with a corresponding increase in the rate of the patterning at the substrate (Figure 5). The current is high directly after the voltage is applied while the hydroquinone near the anodes is oxidized (as in a potential step experiment). It then reaches a diffusion-limited steady state near 1  $\mu$ A for a cell potential of 1.33 V after  $\sim 2$  s, when the rate of

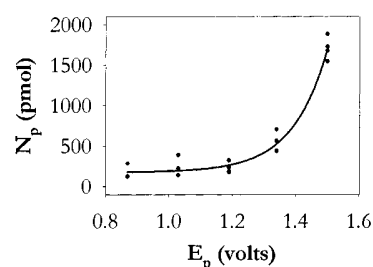


Figure 4. Total protons liberated after 20 s as a function of the applied electrical potential ( $E_p$ ). The number of protons ( $N_p$ ) produced was calculated from electrical current measurements. The voltage and microelectrode geometry for these experiments is as shown in Figure 5. The plot shows that  $N_p$  varies exponentially with potential. Thus, the rate of acid production and therefore surface patterning may be manipulated by small changes in applied potential. The total number of protons liberated at high voltages exceeds 1000 pmol (the maximum amount that can be generated without regeneration of reactant), thus demonstrating the regeneration of hydroquinone from benzoquinone and free protons in solution.

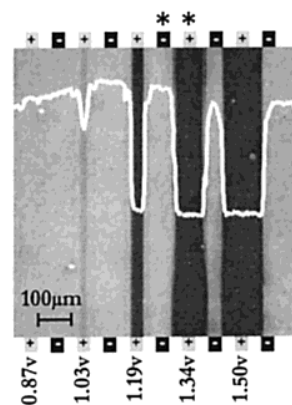


Figure 5. Fluorescent image of a surface after patterning with electrochemically generated acid. White (fluorescence) appears where the surface was left unchanged by the acid generated at the anodes; dark areas represent formation of an ester bond at the surface where the dimethoxytrityl was removed. The active patterning reagents are generated at the anodes (+) and confined by the cathodes (−). The potential applied to the microelectrodes greatly affects the surface patterning reaction. Five different potentials were applied for 20 s to electrodes 20  $\mu$ m from the surface. A potential of 0.87 V generated insufficient quantities of acid for reaction at the surface. At 1.03 V, reaction is detectable but incomplete. In contrast, at 1.50 V, reaction is complete everywhere inside the flanking cathodes. The overlying white plot indicates average fluorescent intensity (arbitrary units) across the image.

anodic hydroquinone oxidation is balanced by its regeneration from benzoquinone and protons at the cathode.

We consider here the total amount of acid generated over an anode versus the amount required to pattern the surface in a time course experiment where the electrodes were 7500  $\mu$ m long by 40  $\mu$ m wide and separated from adjacent cathodes by 40  $\mu$ m, with a depth of solution of 20  $\mu$ m between the electrode array and the substrate. At 1.33 V,  $2.0 \pm 0.1$  pmol of protons are generated at each anode in 0.2 s, rising to  $800 \pm 40$  pmol in 80 s. This total quantity of acid generated after 80 s is in vast excess to the DMT groups in the region of the substrate opposite the anode.

Analysis of the reaction at the surface of the substrate shows that reaction is essentially complete after  $\sim 4$  s at 1.33 V, resulting in a 75- $\mu$ m-wide pattern (Figure 6) and the complete detritylation

(52) Yamanuki, M.; Hoshino, T.; Oyama, M.; Okazaki, S. *J. Electroanal. Chem.* **1998**, *458*, 191–198.

(53) Maskos, U.; Southern, E. M. *Nucleic Acids Res.* **1992**, *20*, 1679–1684.

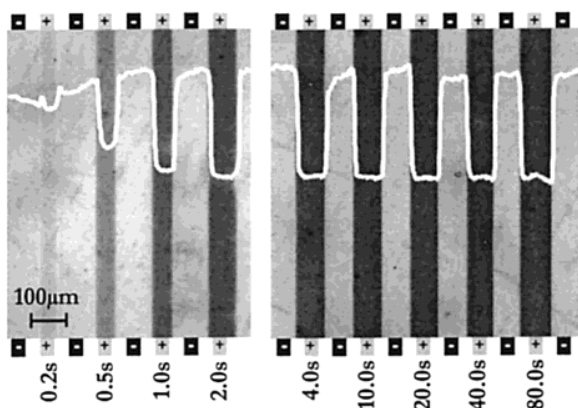


Figure 6. Surface reaction following timed applications of current. The extent of reaction at the surface may be controlled and investigated by delivering timed applications of current to the electrodes; the patterning reagent is confined to the anodic region over very long times. This image shows the patterns formed over a time course, using a fixed potential of 1.33 V applied to electrodes 20  $\mu\text{m}$  from the surface. Diffusion does not blur the edges of the stripe formed after 80 s. Instead, the sharply defined stripes are limited to regions between the cathodes and show that patterning reagents may be directed to strictly confined areas. After 0.2 s, detritylation is incomplete; it is near completion at 1.0 s and complete by 2.0 s. With longer times, the width of the stripe increases slightly until it is stable at  $\sim 10$  s. There is no detectable change between 10 and 80 s, when the reaction was terminated.

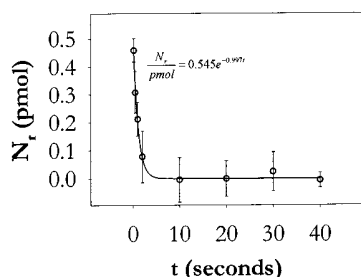


Figure 7. Initial extent and rate of the chemical reaction at the surface determined by the amount of acid reaching the surface. This plot shows the rate of patterning reaction, measured as the consumption of unreacted surface molecules ( $N_i$ ), and is taken from area measurements of the stripes in replicates of the experiment shown in Figure 6. In these experiments, protons were liberated at the anode at a measured, constant rate of 10 pmol/s. The reaction rate at the surface is determined by both this rate of proton production and the proportion of these protons that reach the patterned surface. If the protons reach the surface, they act to remove remaining DMT groups; if they travel elsewhere, they are consumed by the cathodic products (reaction shown in Figure 2). The plot shows that reaction is complete by  $\sim 4$  s (additional protons liberated after this time elicit no further chemical change).

of 30 pmol of DMT. Figure 7 shows stoichiometry calculated from replicates of the experiment in Figure 6, where  $N_i$  was calculated by measuring the surface area of the completely reacted stripe and multiplying by the known initial density of unreacted DMT on the surface, as described above. The amount of acid generated after 4 s is  $40 \pm 2$  pmol. Some of this acid does not reach the substrate because it is consumed by an interaction with products diffusing locally from the cathode into the region between the electrodes.

**Diffusion and Proton Neutralization.** We believe the electrode arrangement presented in this paper causes consumption

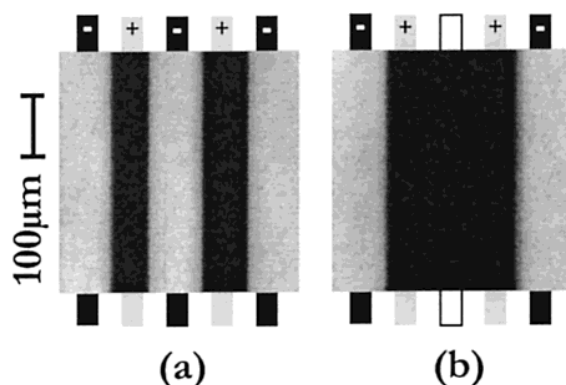


Figure 8. Ability of the cathodes to confine the acid. (a) Current (fixed at 1.33 V for 16 s) applied to two anodes and three cathodes produced two dark stripes. (b) Without a cathode separating the anodes (outline  $\square$  shows where the cathode was disconnected from the circuit), anodic products flood the middle area, resulting in a single, wide stripe. The patterned surface was 40  $\mu\text{m}$  from the electrodes in this experiment.

of anode-generated protons near the cathodes by the reaction shown in eq 3. Because we used cathodes situated only 40  $\mu\text{m}$  from the anodes, the products liberated at the cathodes diffuse rapidly to mix with the protons generated at the anodes allowing regeneration of hydroquinone and benzoquinone in the solution between the electrodes (complete reaction system as mentioned previously in Figure 2). These products can then diffuse into the region of the electrodes where they will take place in further electrochemical reactions.

Figure 8 is a dramatic demonstration of this effect; a single cathode placed between two adjacent anodes prevents any acid from reaching the surface in its vicinity upon application of 1.33 V for 20 s. Subsequent removal of the cathode allows protons to flood the area.

That the width of the line in Figure 6 does not increase with prolonged generation of acid demonstrates the confinement of protons over very long time periods. As the patterning technique presented here utilizes free protons in solution, the lines generated at the surface would become wider if protons were free to diffuse over time. For example, an unconfined collection of 40 pmol of protons released from the 40- $\mu\text{m}$ -wide anodes would reach the surface to produce a stripe over 400  $\mu\text{m}$  wide after 40 s. Figure 6 shows that this does not occur; the radical anions near the cathode consume protons in this region and thus limit the stripe to  $\sim 75$   $\mu\text{m}$ , and even after 80 s the width of the stripe is unchanged.

The ability to deliver sharp pH gradients over a long time period provides significant advantages in inducing chemical reactions to completion on a surface. Although this particular reaction was relatively fast so that the surface was patterned after  $\sim 4$  s, less kinetically favorable reactions may be driven to completion by delivering anodic products to confined regions for any duration required, without diffusion outside the regions.

## CONCLUSIONS

In this work, we have demonstrated a number of advantages of the use of arrays of microelectrodes for performing synthetic reactions on a surface.

First, the proximity of anodes and cathodes restricts diffusion of the active species generated at one electrode by interaction



with the products of the electrode of opposite charge. Thus, the pattern of change induced on the substrate closely mirrors the pattern of the electrode array, and features with dimensions of a few micrometers are readily generated.

Second, fine control of the reaction is permitted by regulating the voltage and duration of the pulse and by measurement of current.

Third, a high degree of parallelism permits many different reaction conditions to be applied to different regions of the substrate surface; the number is limited only by the number of electrodes in the array.

We illustrate the method by the removal of an acid-labile protecting group that is commonly used in organic synthesis. Elsewhere we will describe the extension of this reaction to the synthesis of oligonucleotides, but the method has wider potential. Electrochemical methods can be used to generate acids and bases or other reactants of different strengths by changing the electrolyte, solvent, or applied potential. There are many examples of

organic synthesis steps that use acids, bases, or other reactants that could be generated at electrodes. Thus, the method could be applied to a very diverse collection of chemical syntheses.

#### ACKNOWLEDGMENT

We especially thank Prof. P. Dobson and Dr. P. Leigh of Oxford Department of Engineering for invaluable fabrication advice and resources. Mr. M. Johnson helped with apparatus construction, and Drs. M. Shchepinov and K. Mir provided kind encouragement. R.D.E. thanks the Rhodes Scholarship for enabling his Oxford tenure. F.M. thanks the Royal Society for the award of a University Research Fellowship. This work was supported by the U.K. Medical Research Council.

Received for review August 27, 2001. Accepted January 25, 2002.

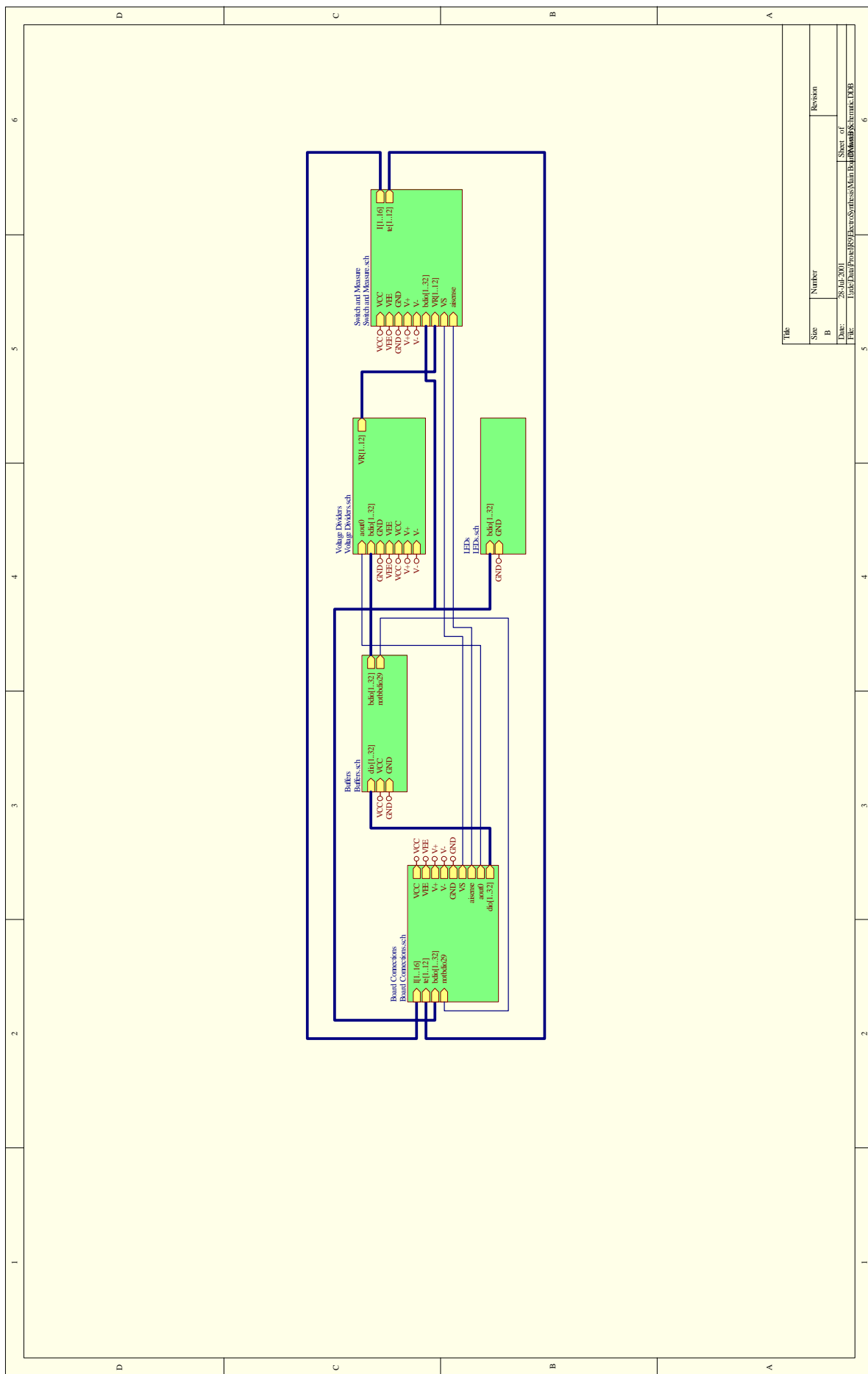
AC010953V

# Appendix F

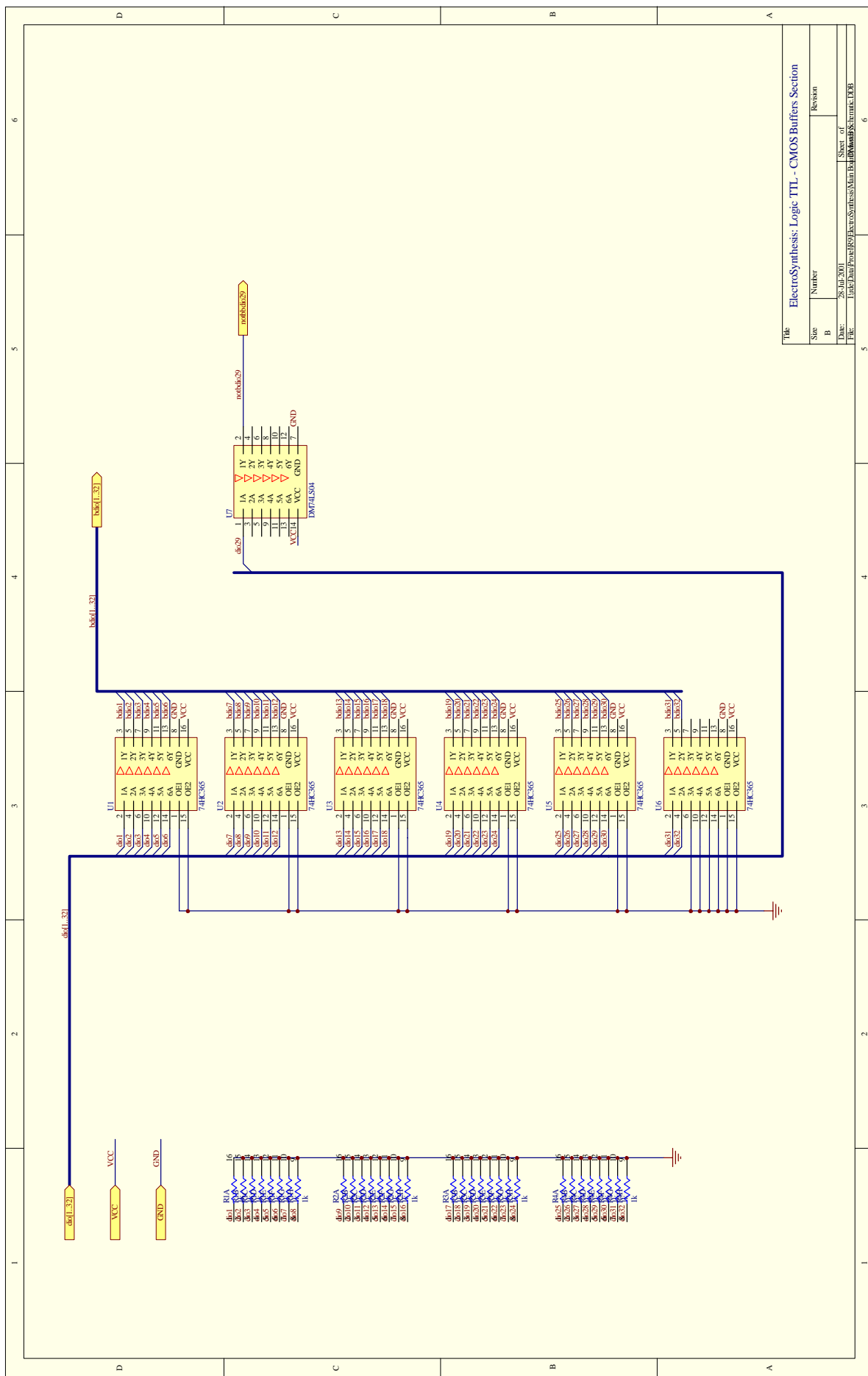
## Microelectronics

The following is the final schematic of the microelectronic circuit built in this work to regulate the voltage applied to the microelectrodes, control their switching, and measure resulting current. Thirty-two CMOS-level digital lines from a computer interface board controlled the multiplexer switching and various other functions in the circuit. The same interface board delivered two analogue voltage outputs, and allowed for 16 simultaneous analogue voltage inputs.

The computer software program used for schematic layout also aided in designing a printed circuit board (PCB) for building the device. The last page shows the multi-layer layout for the schematic as constructed.



Title		
Size	Number	Revision
B		
Date: 28-Jul-2001		
File: \\pda\proj\99\Exec\Synthesis\Main\Bsp\BspMain18g.Temut.DDB		
Sheet of		



ElectroSynthesis: Logic TTL - CMOS Buffers Section



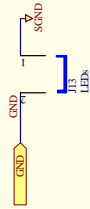
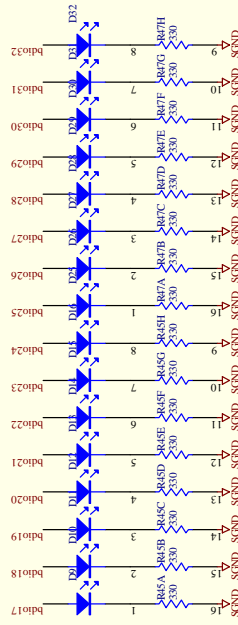
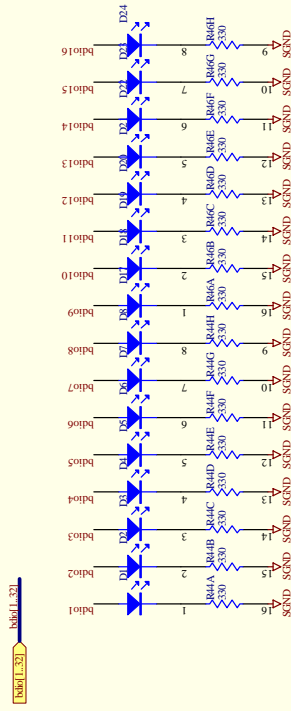
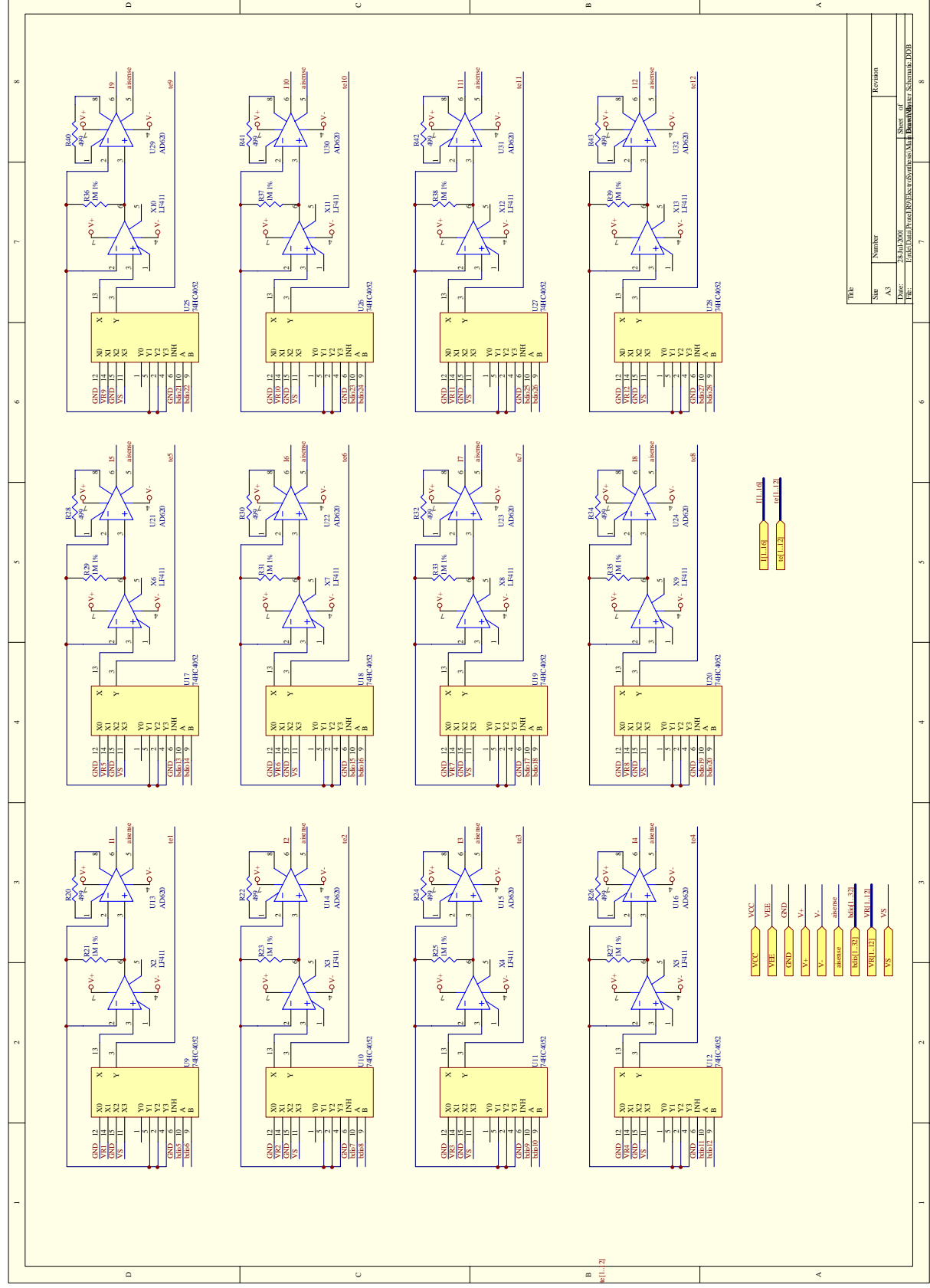
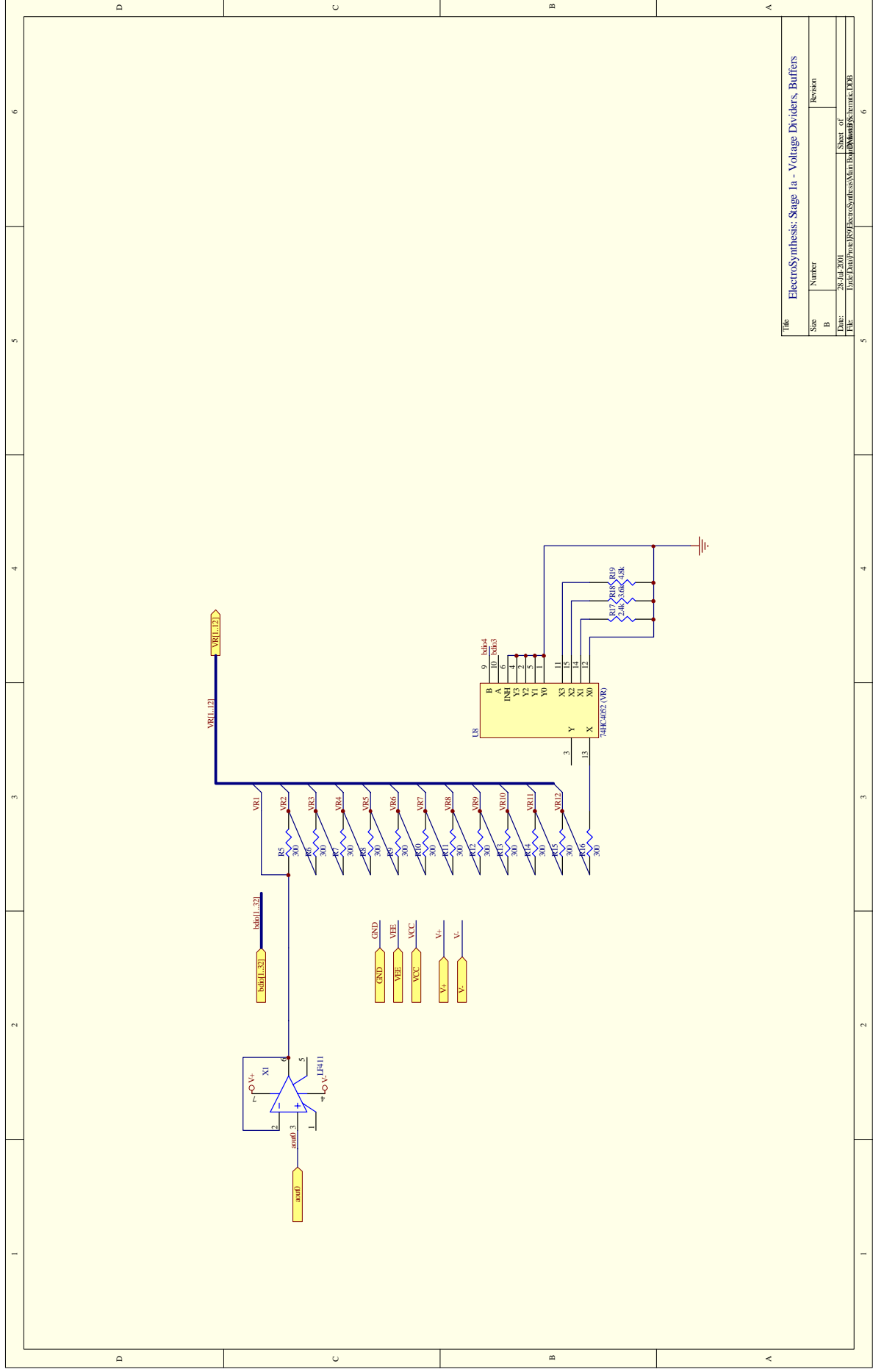
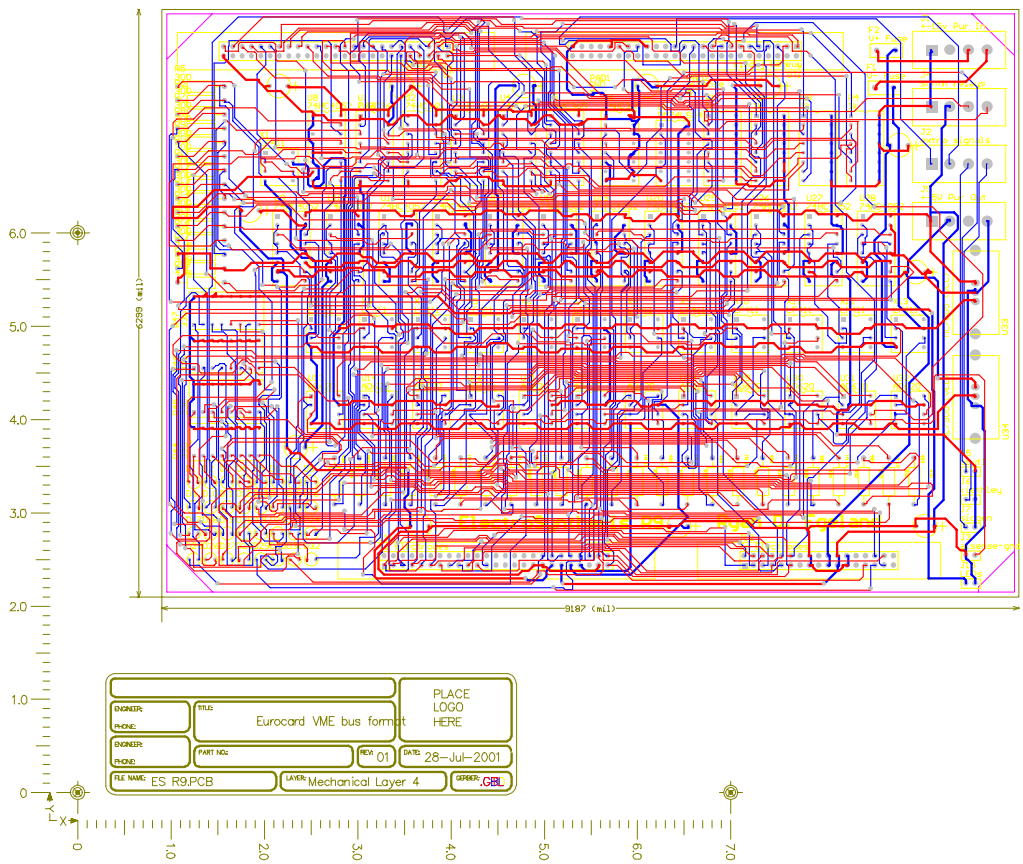


Table		ElectroSynthesis: LED Driver Section	
Size	Number		Revision
A	B		
Date:	28 Jul 2001		Sheet of
File:	Link'DrPrjCt/ElectroSynthesis/Main Page/LEDs/LEDs.html: PCB		6









## Appendix G

### Mechanical Diagrams

The following diagrams illustrate mechanical characteristics of reaction chambers used for delivery of reagents to the gap between the microelectrodes and the substrate. A number of designs were constructed to refine tolerances of gap alignment, ensure good seal between components, and resist chemical attack or swelling upon contact with the reagents and organic solvents used for synthesis. Some of the earlier designs are included for illustration of the design process.

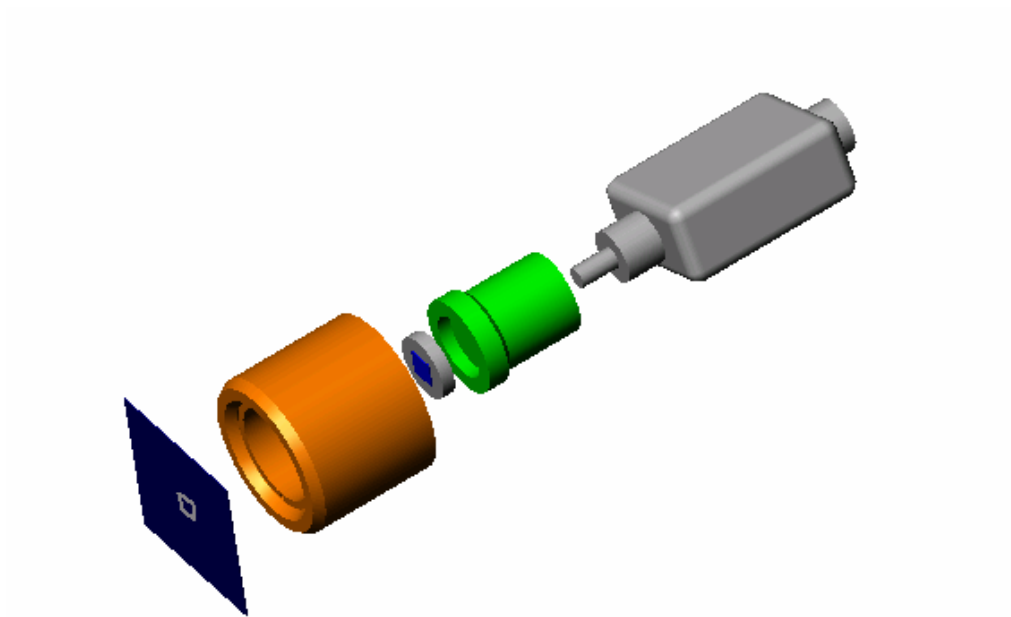


**Figure 54** A 3D CAD Reconstruction of the flow-cell device as presented in Chapter 3.

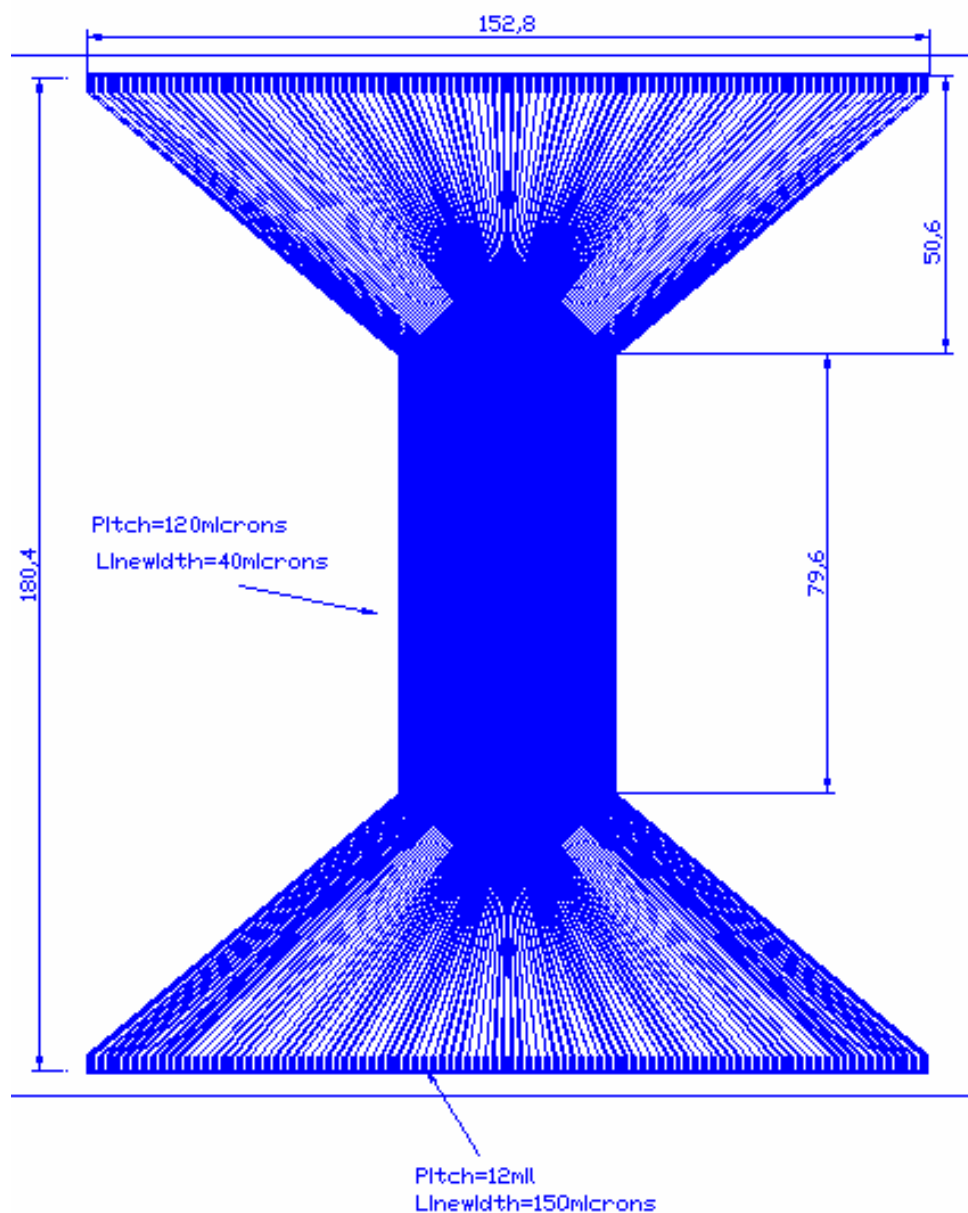


**Figure 55** General specifications and dimensions for the microelectrodes used for most of the oligonucleotide syntheses in this work. The microelectrodes (in the middle, not individually distinguishable in this picture) fan out to bonding pads (top and bottom of the image).

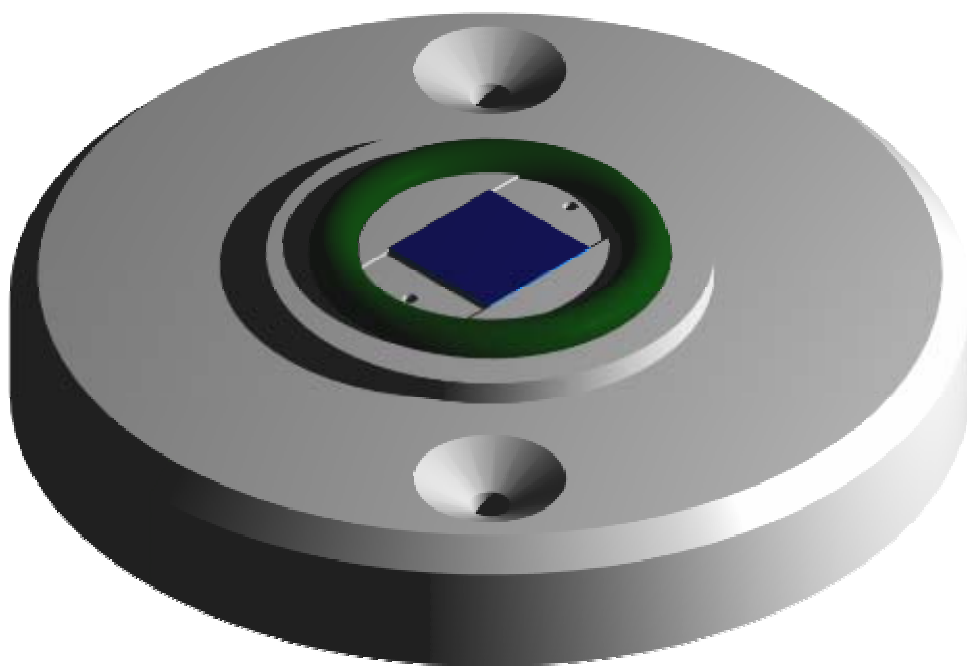
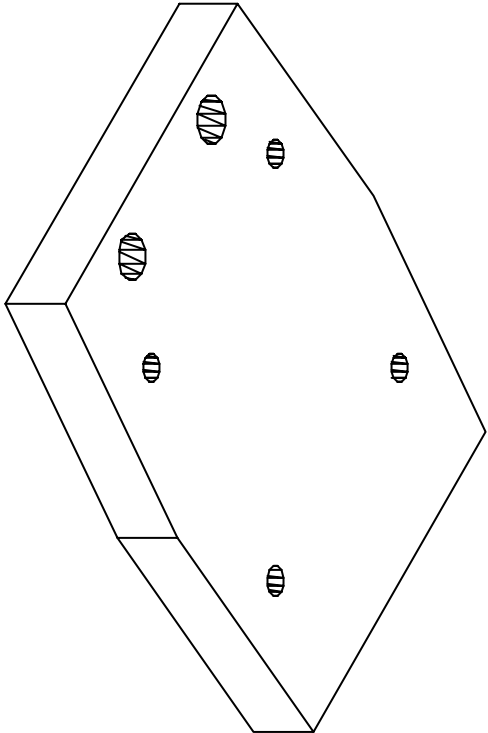
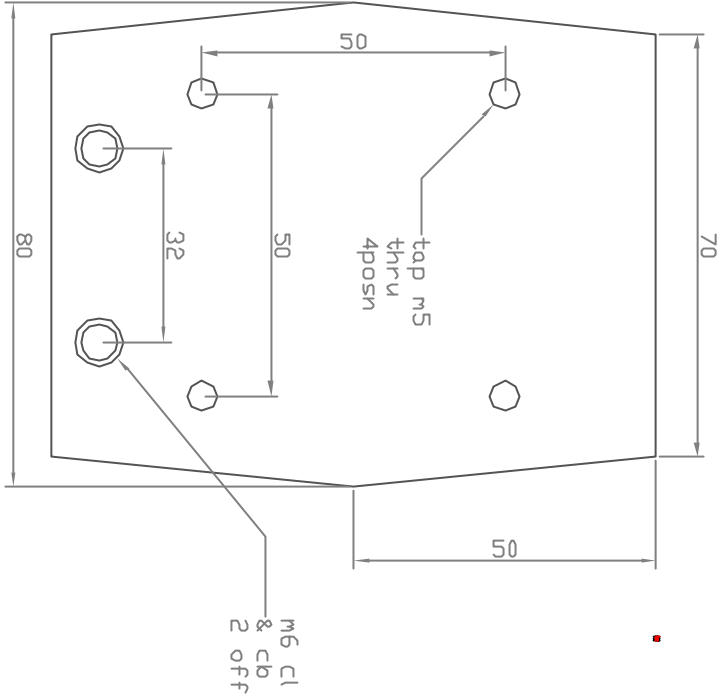
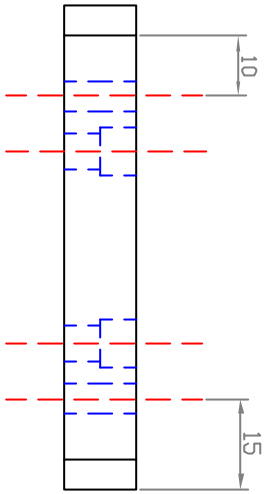


**Figure 56** An earlier O-ring based flow cell.  
The DNA substrate is shown in blue.

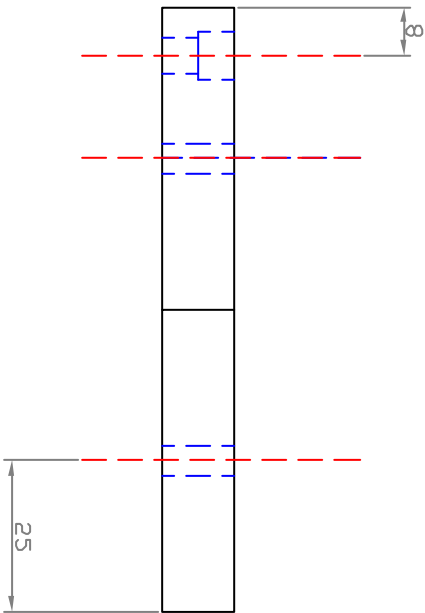
Top View



Front View



Side View



## Appendix H

# Oligonucleotide Synthesiser Modification and Control

Applied Biosystems 394 and 392 oligonucleotide synthesisers were adapted to the electrochemical patterning processes developed in this work. As these machines were designed specifically for reaction conditions in small synthesiser columns, the larger fluidics chamber used for the electrochemical application required modification of the synthesiser program.

The primary modifications included increased reagent delivery time, and more vigorous rinses between synthesis steps. In addition, the synthesisers were programmed to synchronise reagent delivery with application of current to microelectrode switching and the micrometer motions required to flush the reaction chamber. In addition, software controlled and logged the synthesiser status for each reagent delivery procedure, enabling quality control for long oligonucleotide syntheses.

The following cycles (selected from many hundreds tried and used experimentally) were the primary cycles developed for the work described in this thesis. The tables use a numerical code to represent each reagent bottle, and function numbers to identify reagent delivery steps. The cycles were discussed briefly in Chapter 3. A key to reagent bottle numbers is shown in **Figure 57**. These tables are reasonably complex, and presented here only for a complete record of procedural details.



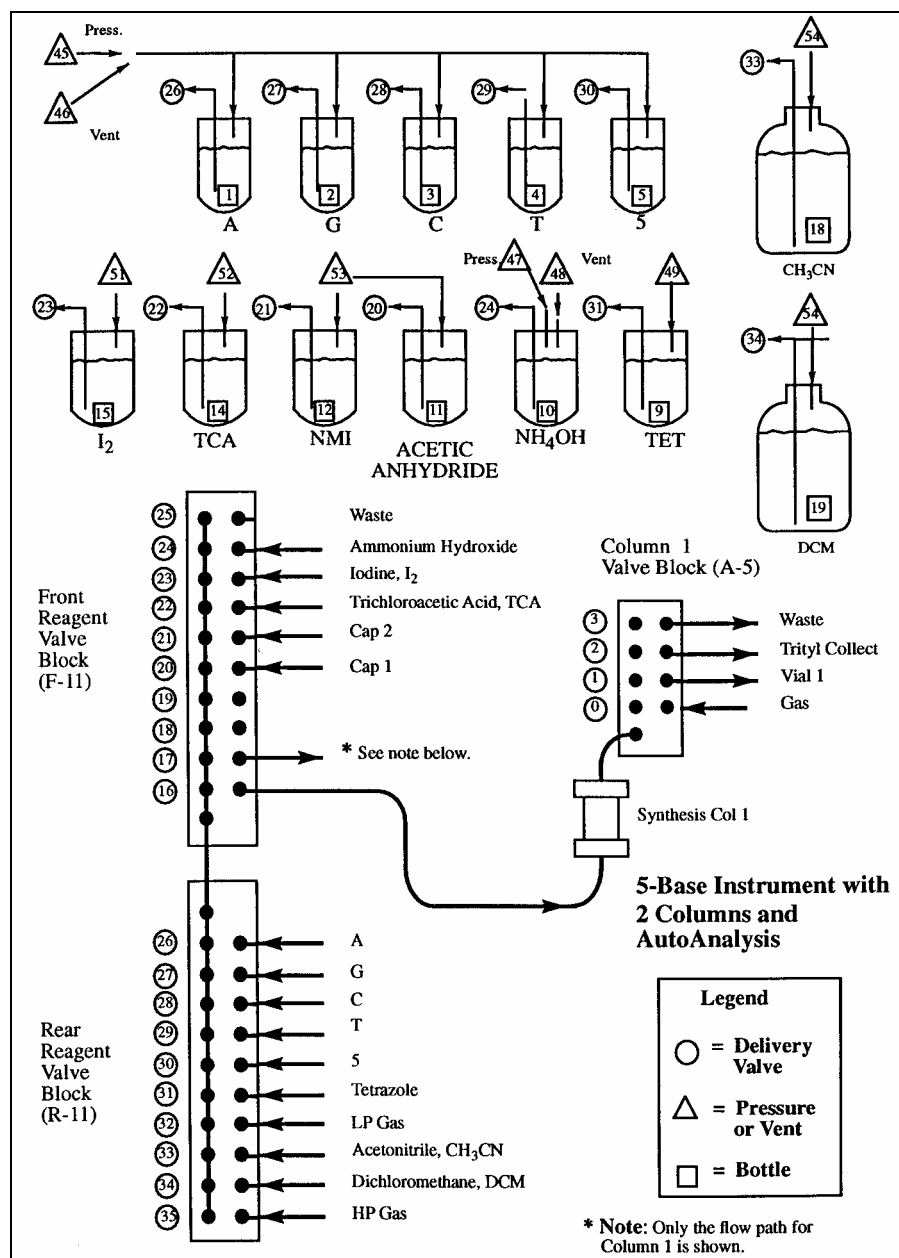


**Figure 57** ABI Synthesiser block diagram and reagent number key. Reagents are represented as “bottle numbers” and referred to as such in the following customized synthesiser function chart. (Reprinted from ABI Synthesiser manual.)

**“ElectroAdd.” This cycle was use for the 6-mer and 17-mer syntheses as described in Chapter 4:**

- 392 Cycle Listing -

(Version 2.00)

Name : ElectroAdd  
Steps: 73

5:26:15P, 8/ 8/ 0

Step Number	Function # Name	Step Time	Step Active for Bases								Safe Step
			A	G	C	T	5	6	7	8	
1	106 Begin										Yes
2	133 Relay 5 On										Yes
3	103 Wait	1.0	Yes	Yes	Yes	Yes	Yes	No	No	No	Yes
4	134 Relay 5 Off										Yes
5	42 18 to Column	20.0	Yes	Yes	Yes	Yes	Yes	No	No	No	Yes
6	2 Reverse Flush	15.0	Yes	Yes	Yes	Yes	Yes	No	No	No	Yes
7	1 Block Flush	4.0	Yes	Yes	Yes	Yes	Yes	No	No	No	Yes
8	42 18 to Column	20.0	Yes	Yes	Yes	Yes	Yes	No	No	No	Yes
9	2 Reverse Flush	15.0	Yes	Yes	Yes	Yes	Yes	No	No	No	Yes
10	1 Block Flush	4.0	Yes	Yes	Yes	Yes	Yes	No	No	No	Yes
11	202 Phos Prep	3.0	Yes	Yes	Yes	Yes	Yes	No	No	No	Yes
12	30 6 to Column	20.0	Yes	Yes	Yes	Yes	Yes	No	No	No	Yes
13	103 Wait	5.0	Yes	Yes	Yes	Yes	Yes	No	No	No	Yes
14	30 6 to Column	20.0	Yes	Yes	Yes	Yes	Yes	No	No	No	Yes
15	132 Relay 4 Pulse										Yes
16	104 Interrupt										Yes
17	132 Relay 4 Pulse										Yes
18	111 Block Vent	30.0	Yes	Yes	Yes	Yes	Yes	No	No	No	Yes
19	103 Wait	145.0	Yes	Yes	Yes	Yes	Yes	No	No	No	Yes
20	132 Relay 4 Pulse										Yes
21	104 Interrupt										Yes
22	132 Relay 4 Pulse										Yes
23	111 Block Vent	30.0	Yes	Yes	Yes	Yes	Yes	No	No	No	Yes
24	1 Block Flush	4.0	Yes	Yes	Yes	Yes	Yes	No	No	No	Yes
25	42 18 to Column	60.0	Yes	Yes	Yes	Yes	Yes	No	No	No	Yes
26	2 Reverse Flush	15.0	Yes	Yes	Yes	Yes	Yes	No	No	No	Yes
27	1 Block Flush	4.0	Yes	Yes	Yes	Yes	Yes	No	No	No	Yes
28	42 18 to Column	20.0	Yes	Yes	Yes	Yes	Yes	No	No	No	Yes
29	2 Reverse Flush	15.0	Yes	Yes	Yes	Yes	Yes	No	No	No	Yes
30	1 Block Flush	4.0	Yes	Yes	Yes	Yes	Yes	No	No	No	Yes
31	42 18 to Column	20.0	Yes	Yes	Yes	Yes	Yes	No	No	No	Yes
32	2 Reverse Flush	15.0	Yes	Yes	Yes	Yes	Yes	No	No	No	Yes
33	1 Block Flush	4.0	Yes	Yes	Yes	Yes	Yes	No	No	No	Yes
34	42 18 to Column	20.0	Yes	Yes	Yes	Yes	Yes	No	No	No	Yes
35	2 Reverse Flush	15.0	Yes	Yes	Yes	Yes	Yes	No	No	No	Yes
36	1 Block Flush	4.0	Yes	Yes	Yes	Yes	Yes	No	No	No	Yes
37	202 Phos Prep	3.0	Yes	Yes	Yes	Yes	Yes	No	No	No	Yes
38	111 Block Vent	2.0	Yes	Yes	Yes	Yes	Yes	No	No	No	Yes
39	204 Tet to Waste	1.7	Yes	Yes	Yes	Yes	Yes	No	No	No	Yes
40	33 B+Tet to Column	3.0	Yes	Yes	Yes	Yes	Yes	No	No	No	Yes
41	34 Tet to Column	1.5	Yes	Yes	Yes	Yes	Yes	No	No	No	Yes
42	33 B+Tet to Column	3.0	Yes	Yes	Yes	Yes	Yes	No	No	No	Yes
43	34 Tet to Column	1.5	Yes	Yes	Yes	Yes	Yes	No	No	No	Yes
44	33 B+Tet to Column	3.0	Yes	Yes	Yes	Yes	Yes	No	No	No	Yes
45	34 Tet to Column	1.5	Yes	Yes	Yes	Yes	Yes	No	No	No	Yes
46	33 B+Tet to Column	3.0	Yes	Yes	Yes	Yes	Yes	No	No	No	Yes

---

## APPENDIX H: OLIGONUCLEOTIDE SYNTHESISER MODIFICATION AND CONTROL

---

47	34 Tet to Column	1.5	Yes	Yes	Yes	Yes	Yes	No	No	No	Yes
48	103 Wait	30.0	Yes	Yes	Yes	Yes	Yes	No	No	No	Yes
49	205 Push to Column	1.0	Yes	Yes	Yes	Yes	Yes	No	No	No	Yes
50	103 Wait	30.0	Yes	Yes	Yes	Yes	Yes	No	No	No	Yes
51	2 Reverse Flush	15.0	Yes	Yes	Yes	Yes	Yes	No	No	No	Yes
52	1 Block Flush	4.0	Yes	Yes	Yes	Yes	Yes	No	No	No	Yes
53	42 18 to Column	20.0	Yes	Yes	Yes	Yes	Yes	No	No	No	Yes
54	2 Reverse Flush	15.0	Yes	Yes	Yes	Yes	Yes	No	No	No	Yes
55	1 Block Flush	4.0	Yes	Yes	Yes	Yes	Yes	No	No	No	Yes
56	41 15 to Column	15.0	Yes	Yes	Yes	Yes	Yes	No	No	No	Yes
57	103 Wait	5.0	Yes	Yes	Yes	Yes	Yes	No	No	No	Yes
58	41 15 to Column	15.0	Yes	Yes	Yes	Yes	Yes	No	No	No	Yes
59	103 Wait	5.0	Yes	Yes	Yes	Yes	Yes	No	No	No	Yes
60	2 Reverse Flush	15.0	Yes	Yes	Yes	Yes	Yes	No	No	No	Yes
61	201 18 to Waste	4.0	Yes	Yes	Yes	Yes	Yes	No	No	No	Yes
62	1 Block Flush	4.0	Yes	Yes	Yes	Yes	Yes	No	No	No	Yes
63	42 18 to Column	20.0	Yes	Yes	Yes	Yes	Yes	No	No	No	Yes
64	2 Reverse Flush	15.0	Yes	Yes	Yes	Yes	Yes	No	No	No	Yes
65	1 Block Flush	4.0	Yes	Yes	Yes	Yes	Yes	No	No	No	Yes
66	42 18 to Column	20.0	Yes	Yes	Yes	Yes	Yes	No	No	No	Yes
67	2 Reverse Flush	15.0	Yes	Yes	Yes	Yes	Yes	No	No	No	Yes
68	1 Block Flush	4.0	Yes	Yes	Yes	Yes	Yes	No	No	No	Yes
69	42 18 to Column	60.0	No	No	No	No	No	No	No	Yes	Yes
70	2 Reverse Flush	60.0	No	No	No	No	No	No	No	Yes	Yes
71	1 Block Flush	4.0	No	No	No	No	No	No	No	Yes	Yes
72	105 Start Detrityl										Yes
73	107 End										Yes

**“Cap.” This cycle was used for capping deblocked nucleotides as described in Chapter 2.**

- 392 Cycle Listing -

(Version 2.00)

Name : Cap

7:44:01P, 3/24/ 0

Steps: 20

Step Number	Function # Name	Step Time	Step Active for Bases								Safe Step
			A	G	C	T	5	6	7	8	
1	106 Begin										Yes
2	64 18 to Waste	5.0									Yes
3	1 Block Flush	4.0	Yes	Yes	Yes	Yes	Yes	Yes	Yes	Yes	Yes
4	42 18 to Column	17.0	Yes	Yes	Yes	Yes	Yes	Yes	Yes	Yes	Yes
5	2 Reverse Flush	12.0	Yes	Yes	Yes	Yes	Yes	Yes	Yes	Yes	Yes
6	4 Flush to Waste	4.0	Yes	Yes	Yes	Yes	Yes	Yes	Yes	Yes	Yes
7	102 Cap Prep	5.0									Yes
8	39 Cap to Column	17.0	Yes	Yes	Yes	Yes	Yes	Yes	Yes	Yes	Yes
9	103 Wait	10.0	Yes	Yes	Yes	Yes	Yes	Yes	Yes	Yes	Yes
10	64 18 to Waste	5.0									Yes
11	2 Reverse Flush	18.0	Yes	Yes	Yes	Yes	Yes	Yes	Yes	Yes	Yes
12	1 Block Flush	4.0	Yes	Yes	Yes	Yes	Yes	Yes	Yes	Yes	Yes
13	42 18 to Column	17.0	Yes	Yes	Yes	Yes	Yes	Yes	Yes	Yes	Yes
14	2 Reverse Flush	12.0	Yes	Yes	Yes	Yes	Yes	Yes	Yes	Yes	Yes
15	42 18 to Column	17.0	Yes	Yes	Yes	Yes	Yes	Yes	Yes	Yes	Yes
16	2 Reverse Flush	14.0	Yes	Yes	Yes	Yes	Yes	Yes	Yes	Yes	Yes
17	42 18 to Column	17.0	Yes	Yes	Yes	Yes	Yes	Yes	Yes	Yes	Yes
18	2 Reverse Flush	14.0	Yes	Yes	Yes	Yes	Yes	Yes	Yes	Yes	Yes
19	1 Block Flush	4.0	Yes	Yes	Yes	Yes	Yes	Yes	Yes	Yes	Yes
20	107 End										Yes

**“Fast Syn.”** This cycle was used for DNA synthesis with conventional dichloroacetic acid deblocking (used to make control oligonucleotides). The reagent delivery cycles and washing times were highly optimised for the flow cell as described in Chapter 3.

- 392 Cycle Listing -

(Version 2.00)

Name : Fast Syn

7:43:45P, 3/24/ 0

Steps: 49

Step Number	Function # Name	Step Time	Step Active for Bases								Safe Step
			A	G	C	T	5	6	7	8	
1	106 Begin										Yes
2	64 18 to Waste	4.0									Yes
3	42 18 to Column	12.0	Yes	Yes	Yes	Yes	Yes	Yes	Yes	Yes	Yes
4	2 Reverse Flush	6.0	Yes	Yes	Yes	Yes	Yes	Yes	Yes	Yes	Yes
5	1 Block Flush	4.0	Yes	Yes	Yes	Yes	Yes	Yes	Yes	Yes	Yes
6	101 Phos Prep	3.0									Yes
7	140 Column 1 On										Yes
8	111 Block Vent	2.0	Yes	Yes	Yes	Yes	Yes	Yes	Yes	Yes	Yes
9	58 Tet to Waste	1.7									Yes
10	33 B+Tet to Column	2.0	Yes	Yes	Yes	Yes	Yes	Yes	Yes	Yes	Yes
11	34 Tet to Column	0.5	Yes	Yes	Yes	Yes	Yes	Yes	Yes	Yes	Yes
12	33 B+Tet to Column	2.0	Yes	Yes	Yes	Yes	Yes	Yes	Yes	Yes	Yes
13	34 Tet to Column	0.5	Yes	Yes	Yes	Yes	Yes	Yes	Yes	Yes	Yes
14	33 B+Tet to Column	1.5	Yes	Yes	Yes	Yes	Yes	Yes	Yes	Yes	Yes
15	103 Wait	15.0	Yes	Yes	Yes	Yes	Yes	Yes	Yes	Yes	Yes
16	43 Push to Column										Yes
17	141 Column 1 Off										Yes
18	103 Wait	15.0	Yes	Yes	Yes	Yes	Yes	Yes	Yes	Yes	Yes
19	2 Reverse Flush	6.0	Yes	Yes	Yes	Yes	Yes	Yes	Yes	Yes	Yes
20	1 Block Flush	4.0	Yes	Yes	Yes	Yes	Yes	Yes	Yes	Yes	Yes
21	41 15 to Column	10.0	Yes	Yes	Yes	Yes	Yes	Yes	Yes	Yes	Yes
22	103 Wait	10.0	Yes	Yes	Yes	Yes	Yes	Yes	Yes	Yes	Yes
23	41 15 to Column	10.0	Yes	Yes	Yes	Yes	Yes	Yes	Yes	Yes	Yes
24	64 18 to Waste	4.0									Yes
25	42 18 to Column	12.0	Yes	Yes	Yes	Yes	Yes	Yes	Yes	Yes	Yes
26	2 Reverse Flush	6.0	Yes	Yes	Yes	Yes	Yes	Yes	Yes	Yes	Yes
27	42 18 to Column	12.0	Yes	Yes	Yes	Yes	Yes	Yes	Yes	Yes	Yes
28	2 Reverse Flush	6.0	Yes	Yes	Yes	Yes	Yes	Yes	Yes	Yes	Yes
29	1 Block Flush	3.0	Yes	Yes	Yes	Yes	Yes	Yes	Yes	Yes	Yes
30	105 Start Detrityl										Yes
31	103 Wait	20.0	Yes	Yes	Yes	Yes	Yes	Yes	Yes	Yes	Yes
32	40 14 to Column	6.0	Yes	Yes	Yes	Yes	Yes	Yes	Yes	Yes	Yes
33	103 Wait	2.0	Yes	Yes	Yes	Yes	Yes	Yes	Yes	Yes	Yes
34	40 14 to Column	6.0	Yes	Yes	Yes	Yes	Yes	Yes	Yes	Yes	Yes
35	103 Wait	2.0	Yes	Yes	Yes	Yes	Yes	Yes	Yes	Yes	Yes
36	40 14 to Column	6.0	Yes	Yes	Yes	Yes	Yes	Yes	Yes	Yes	Yes
37	103 Wait	2.0	Yes	Yes	Yes	Yes	Yes	Yes	Yes	Yes	Yes
38	40 14 to Column	6.0	Yes	Yes	Yes	Yes	Yes	Yes	Yes	Yes	Yes
39	103 Wait	2.0	Yes	Yes	Yes	Yes	Yes	Yes	Yes	Yes	Yes
40	42 18 to Column	12.0	Yes	Yes	Yes	Yes	Yes	Yes	Yes	Yes	Yes
41	2 Reverse Flush	6.0	Yes	Yes	Yes	Yes	Yes	Yes	Yes	Yes	Yes
42	42 18 to Column	12.0	Yes	Yes	Yes	Yes	Yes	Yes	Yes	Yes	Yes
43	2 Reverse Flush	6.0	Yes	Yes	Yes	Yes	Yes	Yes	Yes	Yes	Yes

---

## APPENDIX H: OLIGONUCLEOTIDE SYNTHESISER MODIFICATION AND CONTROL

---

44	42 18 to Column	12.0	Yes	Yes	Yes	Yes	Yes	Yes	Yes	Yes	Yes	Yes
45	2 Reverse Flush	6.0	Yes	Yes	Yes	Yes	Yes	Yes	Yes	Yes	Yes	Yes
46	42 18 to Column	12.0	Yes	Yes	Yes	Yes	Yes	Yes	Yes	Yes	Yes	Yes
47	2 Reverse Flush	6.0	Yes	Yes	Yes	Yes	Yes	Yes	Yes	Yes	Yes	Yes
48	1 Block Flush	4.0	Yes	Yes	Yes	Yes	Yes	Yes	Yes	Yes	Yes	Yes
49	107 End											Yes
7	End									Yes		

**“10 um CE” This cycle was used for conventional DNA synthesis in Cruachem-supplied “10 micromolar” columns, and was used to synthesise some of the targets as described in Chapter 4.**

- 392 Cycle Listing -

(Version 2.00)

Name : 10 um CE

12:50:29P, 4/17/ 0

Steps: 66

Step Number	Function # Name	Step Time	Step Active for Bases								Safe Step
			A	G	C	T	5	6	7	8	
1	106 Begin										Yes
2	64 18 to Waste	4.0									Yes
3	42 18 to Column	80.0	Yes	Yes	Yes	Yes	Yes	Yes	Yes	Yes	Yes
4	2 Reverse Flush	35.0	Yes	Yes	Yes	Yes	Yes	Yes	Yes	Yes	Yes
5	1 Block Flush	4.0	Yes	Yes	Yes	Yes	Yes	Yes	Yes	Yes	Yes
6	101 Phos Prep	3.0									Yes
7	140 Column 1 On										Yes
8	34 Tet to Column	1.0	Yes	Yes	Yes	Yes	Yes	Yes	Yes	Yes	Yes
9	33 B+Tet to Column	30.0	Yes	Yes	Yes	Yes	Yes	Yes	Yes	Yes	Yes
10	141 Column 1 Off										Yes
11	142 Column 2 On										Yes
12	64 18 to Waste	5.0									Yes
13	1 Block Flush	4.0	Yes	Yes	Yes	Yes	Yes	Yes	Yes	Yes	Yes
14	34 Tet to Column	1.0	Yes	Yes	Yes	Yes	Yes	Yes	Yes	Yes	Yes
15	33 B+Tet to Column	30.0	Yes	Yes	Yes	Yes	Yes	Yes	Yes	Yes	Yes
16	143 Column 2 Off										Yes
17	103 Wait	40.0	Yes	Yes	Yes	Yes	Yes	Yes	Yes	Yes	Yes
18	64 18 to Waste	5.0									Yes
19	42 18 to Column	30.0	Yes	Yes	Yes	Yes	Yes	Yes	Yes	Yes	Yes
20	2 Reverse Flush	35.0	Yes	Yes	Yes	Yes	Yes	Yes	Yes	Yes	Yes
21	1 Block Flush	4.0	Yes	Yes	Yes	Yes	Yes	Yes	Yes	Yes	Yes
22	102 Cap Prep	5.0									Yes
23	39 Cap to Column	55.0	Yes	Yes	Yes	Yes	Yes	Yes	Yes	Yes	Yes
24	103 Wait	10.0	Yes	Yes	Yes	Yes	Yes	Yes	Yes	Yes	Yes
25	64 18 to Waste	5.0									Yes
26	2 Reverse Flush	35.0	Yes	Yes	Yes	Yes	Yes	Yes	Yes	Yes	Yes
27	1 Block Flush	4.0	Yes	Yes	Yes	Yes	Yes	Yes	Yes	Yes	Yes
28	41 15 to Column	50.0	Yes	Yes	Yes	Yes	Yes	Yes	Yes	Yes	Yes
29	103 Wait	20.0	Yes	Yes	Yes	Yes	Yes	Yes	Yes	Yes	Yes
30	64 18 to Waste	5.0									Yes
31	1 Block Flush	4.0	Yes	Yes	Yes	Yes	Yes	Yes	Yes	Yes	Yes
32	42 18 to Column	50.0	Yes	Yes	Yes	Yes	Yes	Yes	Yes	Yes	Yes
33	2 Reverse Flush	35.0	Yes	Yes	Yes	Yes	Yes	Yes	Yes	Yes	Yes
34	42 18 to Column	50.0	Yes	Yes	Yes	Yes	Yes	Yes	Yes	Yes	Yes
35	2 Reverse Flush	35.0	Yes	Yes	Yes	Yes	Yes	Yes	Yes	Yes	Yes
36	42 18 to Column	50.0	Yes	Yes	Yes	Yes	Yes	Yes	Yes	Yes	Yes
37	2 Reverse Flush	35.0	Yes	Yes	Yes	Yes	Yes	Yes	Yes	Yes	Yes
38	42 18 to Column	50.0	Yes	Yes	Yes	Yes	Yes	Yes	Yes	Yes	Yes
39	2 Reverse Flush	35.0	Yes	Yes	Yes	Yes	Yes	Yes	Yes	Yes	Yes
40	1 Block Flush	4.0	Yes	Yes	Yes	Yes	Yes	Yes	Yes	Yes	Yes
41	105 Start Detrityl										Yes
42	64 18 to Waste	5.0									Yes
43	42 18 to Column	30.0	Yes	Yes	Yes	Yes	Yes	Yes	Yes	Yes	Yes
44	2 Reverse Flush	35.0	Yes	Yes	Yes	Yes	Yes	Yes	Yes	Yes	Yes
45	1 Block Flush	4.0	Yes	Yes	Yes	Yes	Yes	Yes	Yes	Yes	Yes

---

## APPENDIX H: OLIGONUCLEOTIDE SYNTHESISER MODIFICATION AND CONTROL

---

46	167 If Monitoring											Yes
47	44 19 to Column	50.0	Yes	Yes	Yes	Yes	Yes	Yes	Yes	Yes	Yes	Yes
48	40 14 to Column	5.0	Yes	Yes	Yes	Yes	Yes	Yes	Yes	Yes	Yes	Yes
49	135 Monitor trityls											Yes
50	40 14 to Column	140.0	Yes	Yes	Yes	Yes	Yes	Yes	Yes	Yes	Yes	Yes
51	136 Monitor noise											Yes
52	40 14 to Column	10.0	Yes	Yes	Yes	Yes	Yes	Yes	Yes	Yes	Yes	Yes
53	137 Stop monitor											Yes
54	42 18 to Column	10.0	Yes	Yes	Yes	Yes	Yes	Yes	Yes	Yes	Yes	Yes
55	2 Reverse Flush	8.0	Yes	Yes	Yes	Yes	Yes	Yes	Yes	Yes	Yes	Yes
56	168 If not Montring											Yes
57	40 14 to Column	140.0	Yes	Yes	Yes	Yes	Yes	Yes	Yes	Yes	Yes	No
58	169 End Monitoring											Yes
59	1 Block Flush	4.0	Yes	Yes	Yes	Yes	Yes	Yes	Yes	Yes	Yes	No
60	64 18 to Waste	5.0										No
61	42 18 to Column	30.0	Yes	Yes	Yes	Yes	Yes	Yes	Yes	Yes	Yes	No
62	2 Reverse Flush	35.0	Yes	Yes	Yes	Yes	Yes	Yes	Yes	Yes	Yes	No
63	42 18 to Column	30.0	Yes	Yes	Yes	Yes	Yes	Yes	Yes	Yes	Yes	No
64	2 Reverse Flush	35.0	Yes	Yes	Yes	Yes	Yes	Yes	Yes	Yes	Yes	No
65	1 Block Flush	4.0	Yes	Yes	Yes	Yes	Yes	Yes	Yes	Yes	Yes	Yes
66	107 End											Yes



**“DCA.” This cycle was specifically used to deliver dichloroacetic acid to the chamber, for control experiments comparing conventional deblocking to the electrochemical method.**

- 392 Cycle Listing -

(Version 2.00)

Name : DCA

11:54:32P, 7/22/ 0

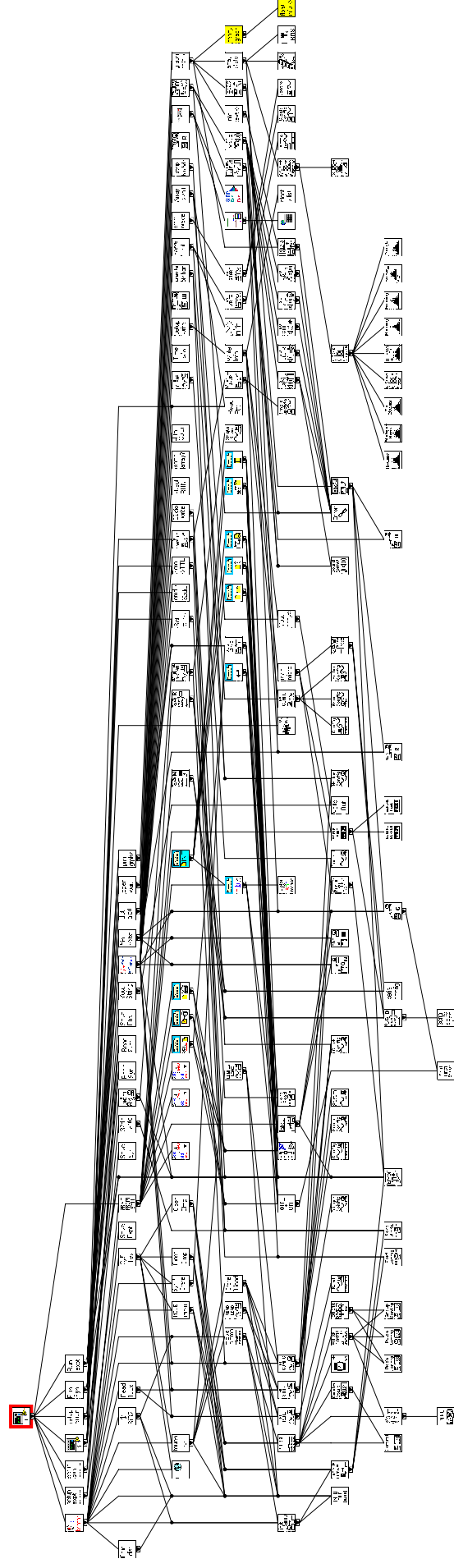
Steps: 36

Step Number	Function # Name	Step Time	Step Active for Bases								Safe Step
			A	G	C	T	5	6	7	8	
1	106 Begin										Yes
2	133 Relay 5 On										Yes
3	103 Wait	1.0	Yes	Yes	Yes	Yes	Yes	Yes	Yes	Yes	Yes
4	134 Relay 5 Off										Yes
5	64 18 to Waste	4.0									Yes
6	42 18 to Column	15.0	Yes	Yes	Yes	Yes	Yes	Yes	Yes	Yes	Yes
7	2 Reverse Flush	15.0	Yes	Yes	Yes	Yes	Yes	Yes	Yes	Yes	Yes
8	1 Block Flush	4.0	Yes	Yes	Yes	Yes	Yes	Yes	Yes	Yes	Yes
9	42 18 to Column	15.0	Yes	Yes	Yes	Yes	Yes	Yes	Yes	Yes	Yes
10	2 Reverse Flush	15.0	Yes	Yes	Yes	Yes	Yes	Yes	Yes	Yes	Yes
11	1 Block Flush	4.0	Yes	Yes	Yes	Yes	Yes	Yes	Yes	Yes	Yes
12	42 18 to Column	15.0	Yes	Yes	Yes	Yes	Yes	Yes	Yes	Yes	Yes
13	2 Reverse Flush	15.0	Yes	Yes	Yes	Yes	Yes	Yes	Yes	Yes	Yes
14	1 Block Flush	4.0	Yes	Yes	Yes	Yes	Yes	Yes	Yes	Yes	Yes
15	42 18 to Column	15.0	Yes	Yes	Yes	Yes	Yes	Yes	Yes	Yes	Yes
16	2 Reverse Flush	15.0	Yes	Yes	Yes	Yes	Yes	Yes	Yes	Yes	Yes
17	1 Block Flush	4.0	Yes	Yes	Yes	Yes	Yes	Yes	Yes	Yes	Yes
18	42 18 to Column	15.0	Yes	Yes	Yes	Yes	Yes	Yes	Yes	Yes	Yes
19	2 Reverse Flush	15.0	Yes	Yes	Yes	Yes	Yes	Yes	Yes	Yes	Yes
20	1 Block Flush	4.0	Yes	Yes	Yes	Yes	Yes	Yes	Yes	Yes	Yes
21	40 14 to Column	25.0	Yes	Yes	Yes	Yes	Yes	Yes	Yes	Yes	Yes
22	103 Wait	5.0	Yes	Yes	Yes	Yes	Yes	Yes	Yes	Yes	Yes
23	40 14 to Column	25.0	Yes	Yes	Yes	Yes	Yes	Yes	Yes	Yes	Yes
24	103 Wait	5.0	Yes	Yes	Yes	Yes	Yes	Yes	Yes	Yes	Yes
25	2 Reverse Flush	20.0	Yes	Yes	Yes	Yes	Yes	Yes	Yes	Yes	Yes
26	40 14 to Column	25.0	Yes	Yes	Yes	Yes	Yes	Yes	Yes	Yes	Yes
27	103 Wait	5.0	Yes	Yes	Yes	Yes	Yes	Yes	Yes	Yes	Yes
28	40 14 to Column	25.0	Yes	Yes	Yes	Yes	Yes	Yes	Yes	Yes	Yes
29	103 Wait	5.0	Yes	Yes	Yes	Yes	Yes	Yes	Yes	Yes	Yes
30	2 Reverse Flush	20.0	Yes	Yes	Yes	Yes	Yes	Yes	Yes	Yes	Yes
31	64 18 to Waste	4.0									Yes
32	1 Block Flush	4.0	Yes	Yes	Yes	Yes	Yes	Yes	Yes	Yes	Yes
33	42 18 to Column	15.0	Yes	Yes	Yes	Yes	Yes	Yes	Yes	Yes	Yes
34	2 Reverse Flush	15.0	Yes	Yes	Yes	Yes	Yes	Yes	Yes	Yes	Yes
35	1 Block Flush	4.0	Yes	Yes	Yes	Yes	Yes	Yes	Yes	Yes	Yes
36	107 End										Yes

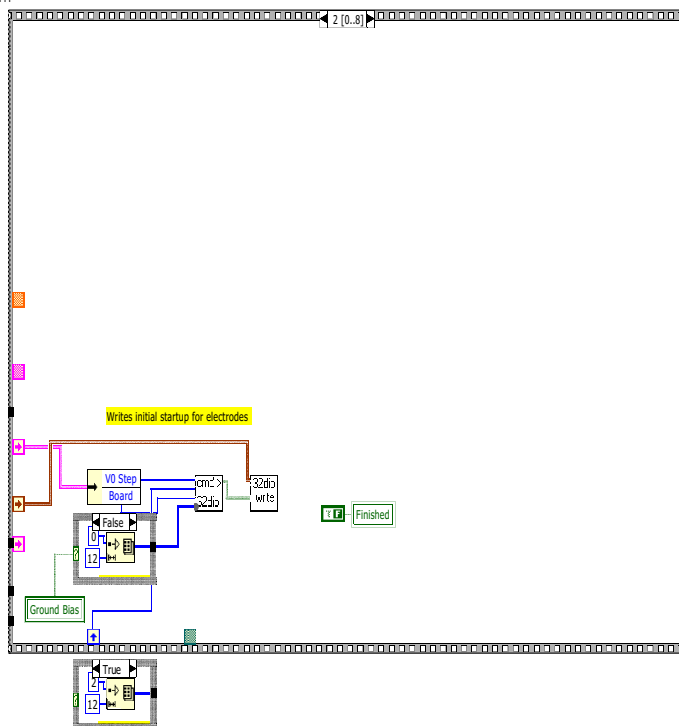
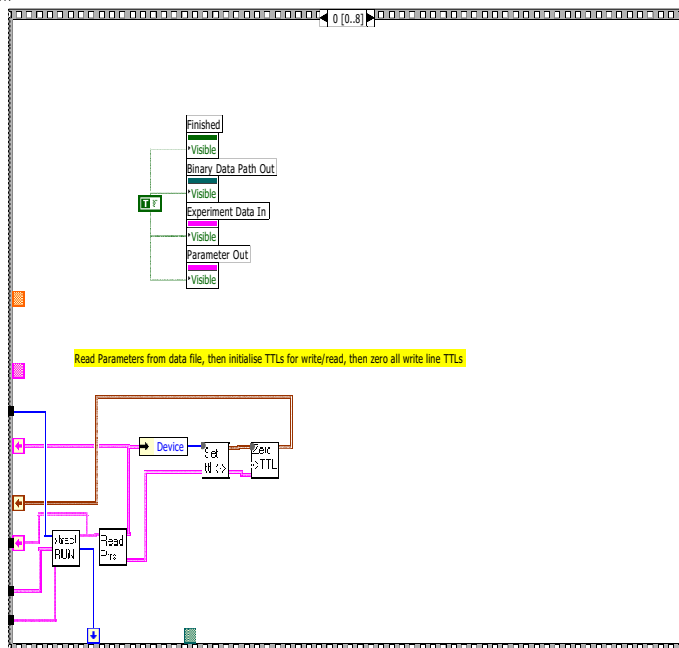
# Appendix I

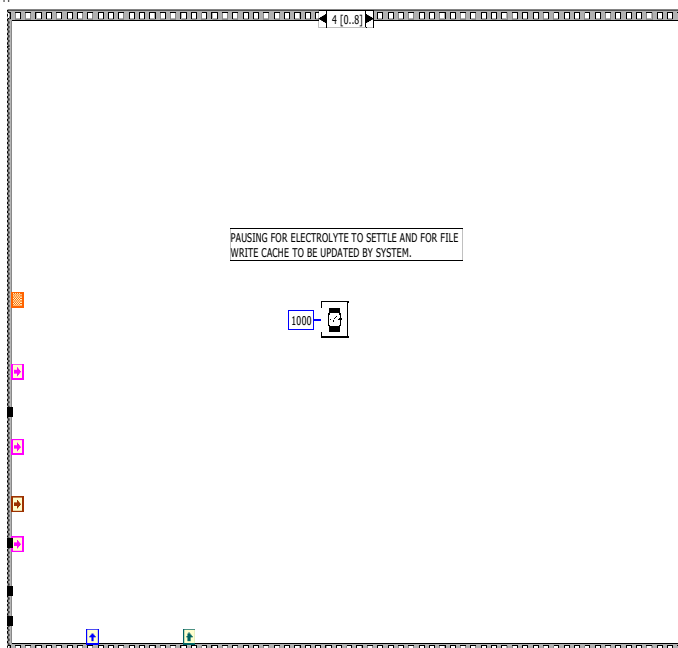
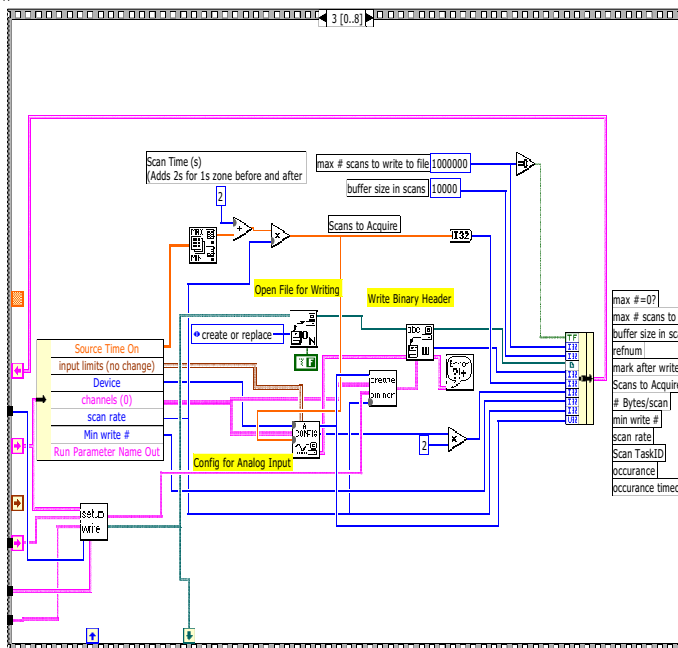
## Software

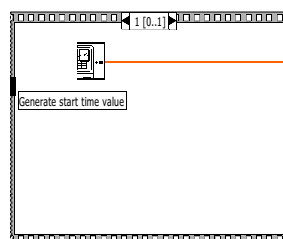
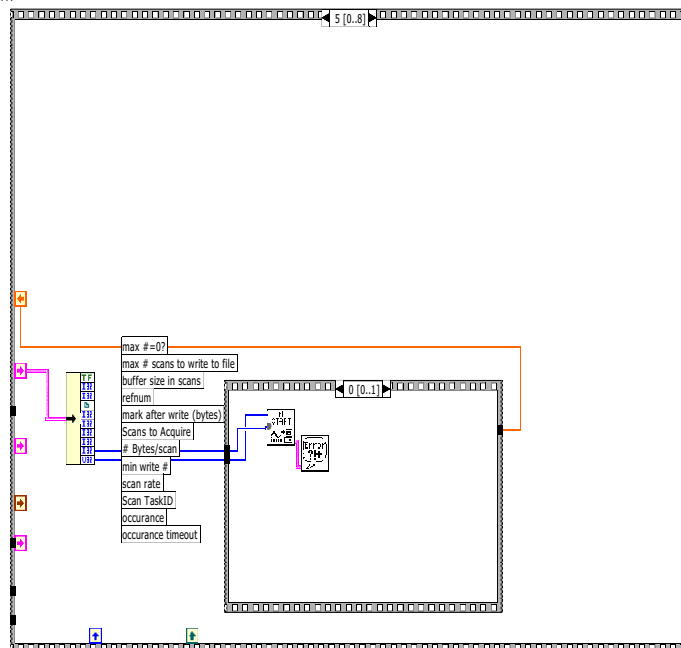
Software controlled all components required for oligonucleotide syntheses including the electronics, data acquisition, the synthesiser, micrometer movements and measurements, and reaction chamber movement and sealing. The software was written using a graphical user interface language (Labview). The full software programme is too long to reprint here, but the following selected pages show brief block diagrams of the important parts.

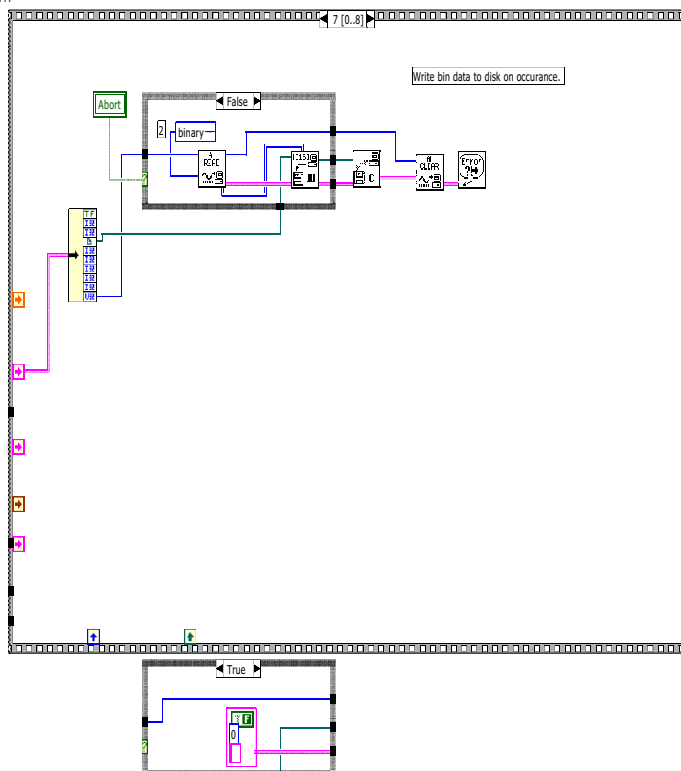
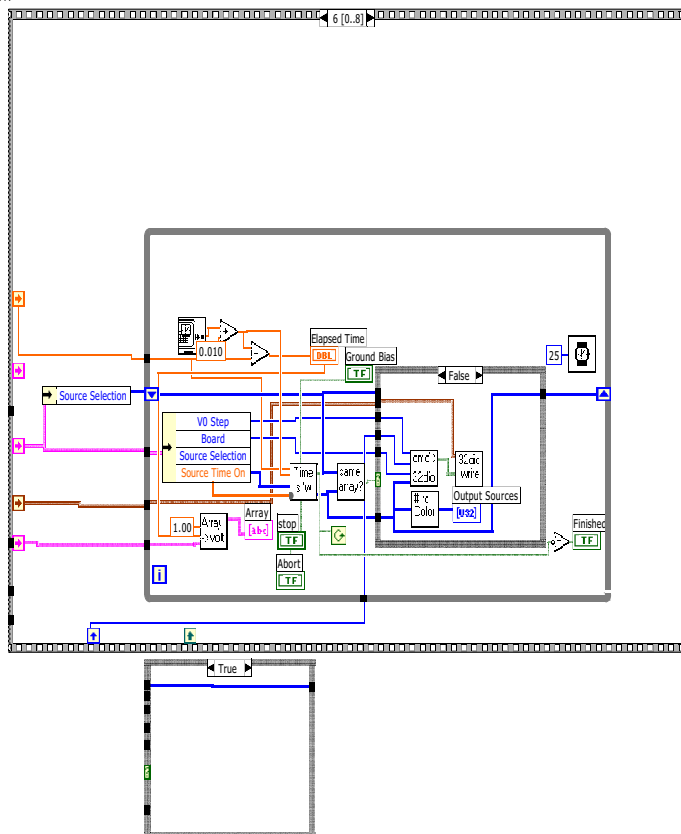








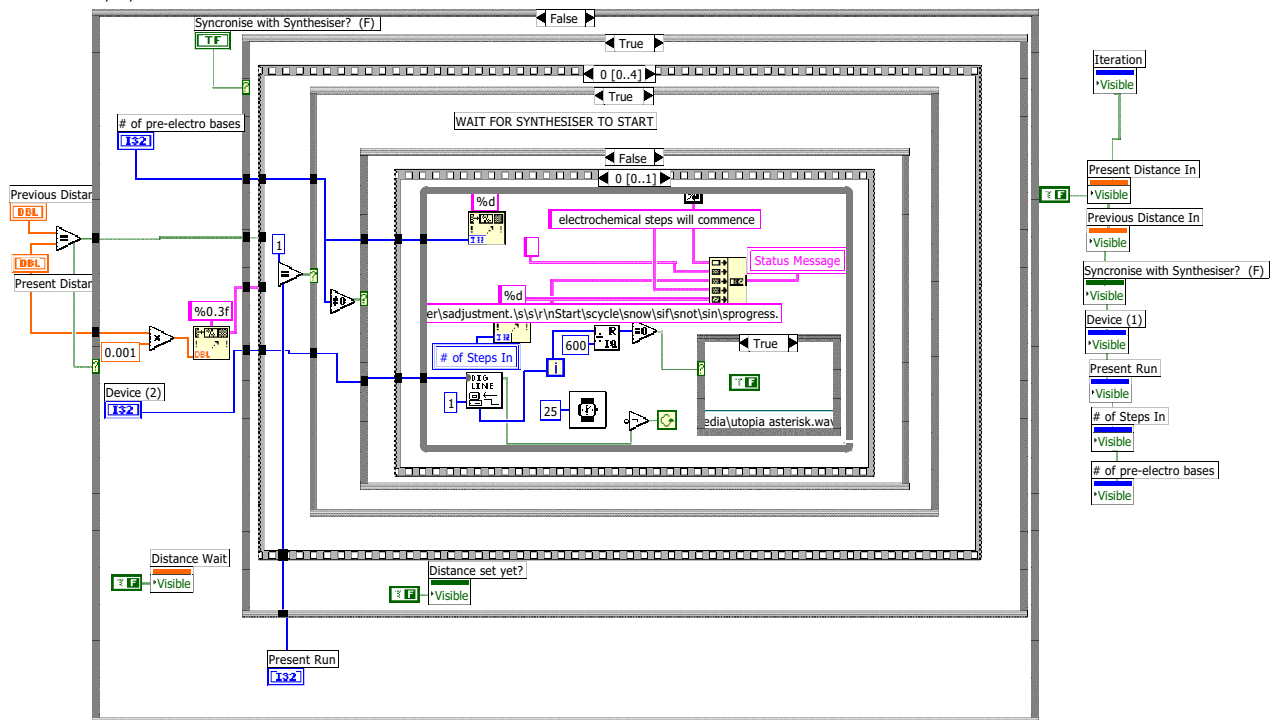




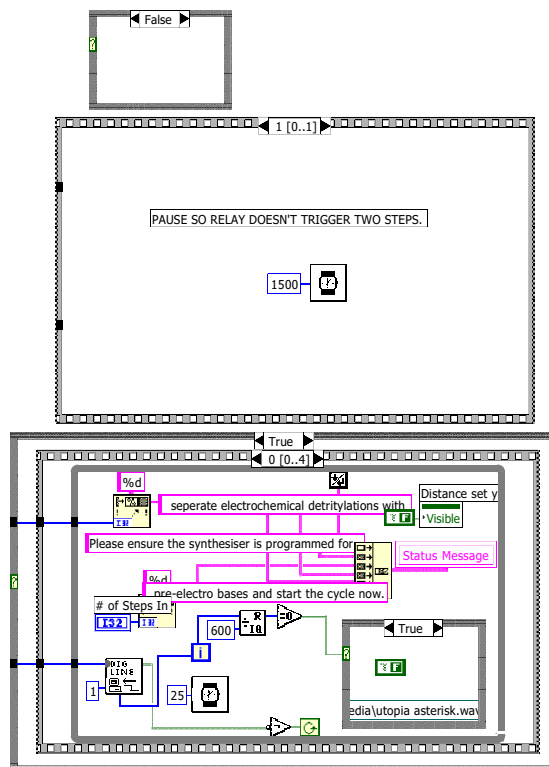




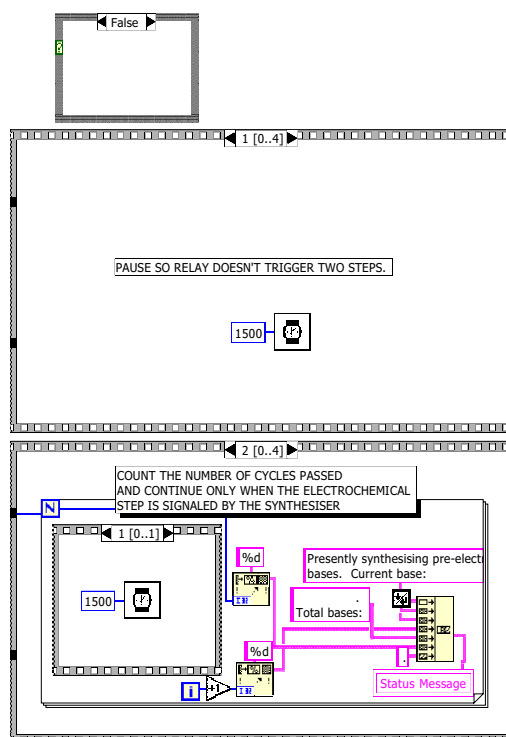
Distance Alert.vi  
D:\Data Archive\Labview\ElectroSynthesis\Labview Code\Distance Alert.vi  
Last modified on 05/08/2000 at 2:30 PM  
Printed on 14/05/2003 at 8:12 PM



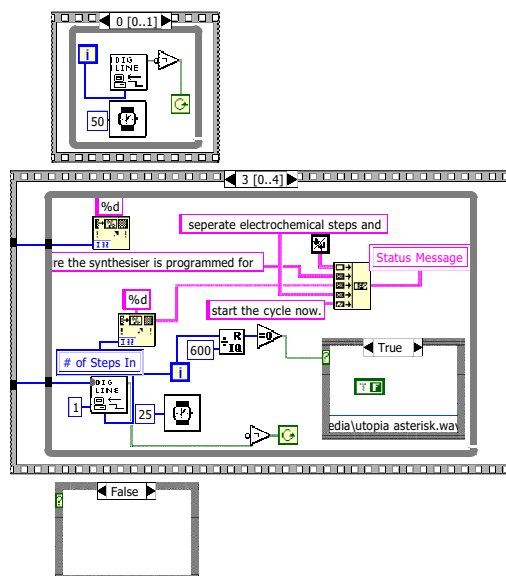
Distance Alert.vi  
D:\Data Archive\Labview\ElectroSynthesis\Labview Code\Distance Alert.vi  
Last modified on 05/08/2000 at 2:30 PM  
Printed on 14/05/2003 at 8:12 PM



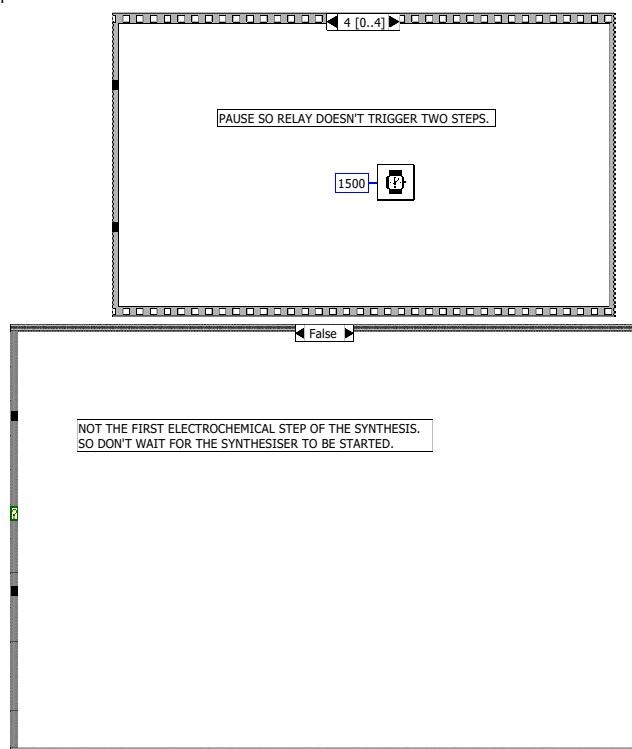
Distance Alert.vi  
D:\Data Archive\Labview\ElectroSynthesis\Labview Code\Distance Alert.vi  
Last modified on 05/08/2000 at 2:30 PM  
Printed on 14/05/2003 at 8:12 PM



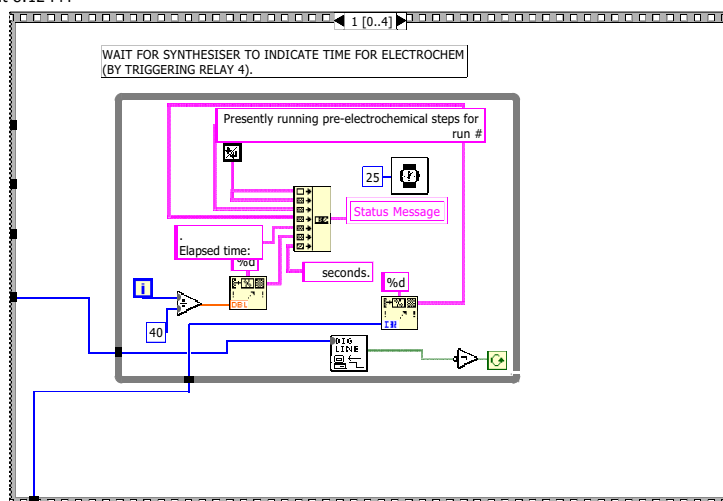
Distance Alert.vi  
D:\Data Archive\Labview\ElectroSynthesis\Labview Code\Distance Alert.vi  
Last modified on 05/08/2000 at 2:30 PM  
Printed on 14/05/2003 at 8:12 PM



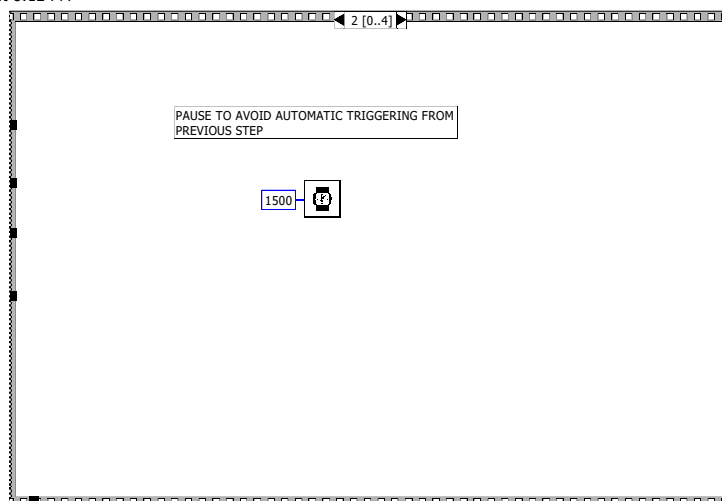
Distance Alert.vi  
D:\Data Archive\Labview\ElectroSynthesis\Labview Code\Distance Alert.vi  
Last modified on 05/08/2000 at 2:30 PM  
Printed on 14/05/2003 at 8:12 PM



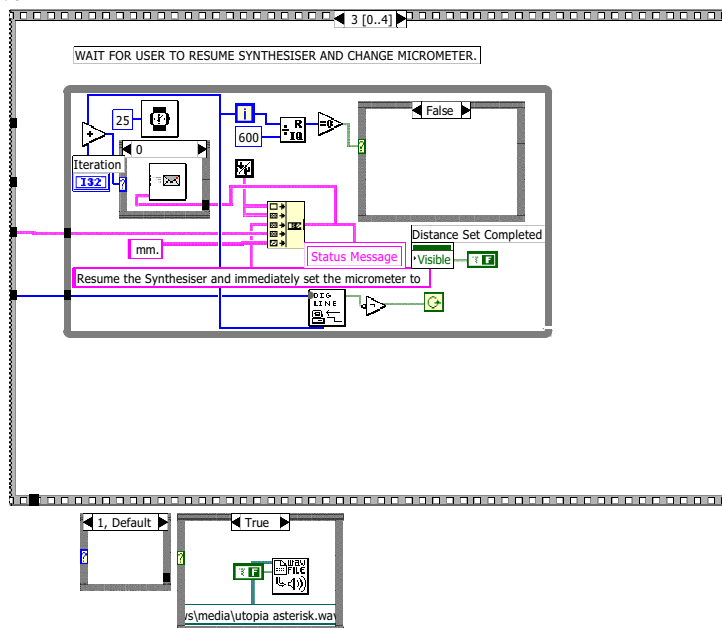
Distance Alert.vi  
D:\Data Archive\Labview\ElectroSynthesis\Labview Code\Distance Alert.vi  
Last modified on 05/08/2000 at 2:30 PM  
Printed on 14/05/2003 at 8:12 PM



Distance Alert.vi  
D:\Data Archive\Labview\ElectroSynthesis\Labview Code\Distance Alert.vi  
Last modified on 05/08/2000 at 2:30 PM  
Printed on 14/05/2003 at 8:12 PM



Distance Alert.vi  
D:\Data Archive\Labview\ElectroSynthesis\Labview Code\Distance Alert.vi  
Last modified on 05/08/2000 at 2:30 PM  
Printed on 14/05/2003 at 8:12 PM

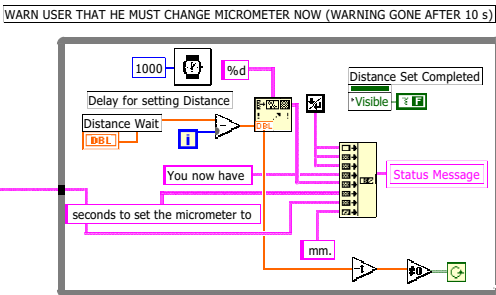


Distance Alert.vi

D:\Data Archive\Labview\ElectroSynthesis\Labview Code\Distance Alert.vi

Last modified on 05/08/2000 at 2:30 PM

Printed on 14/05/2003 at 8:12 PM

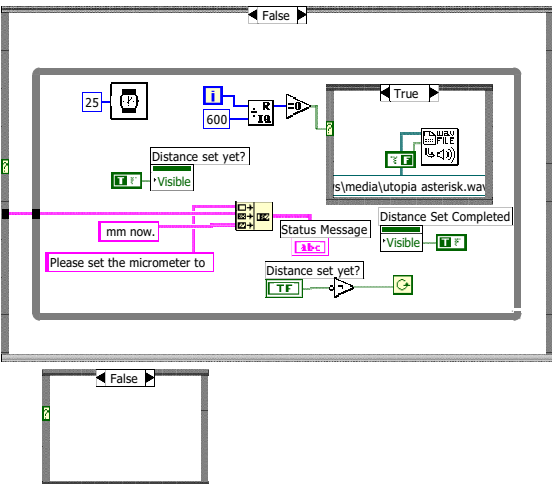


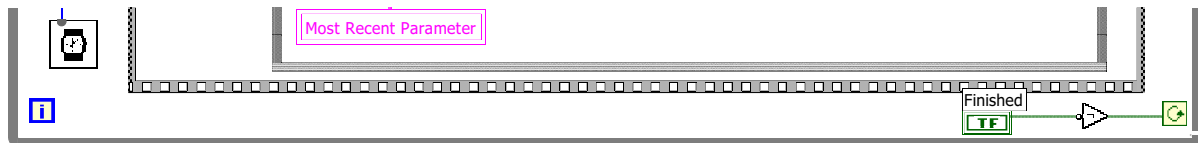
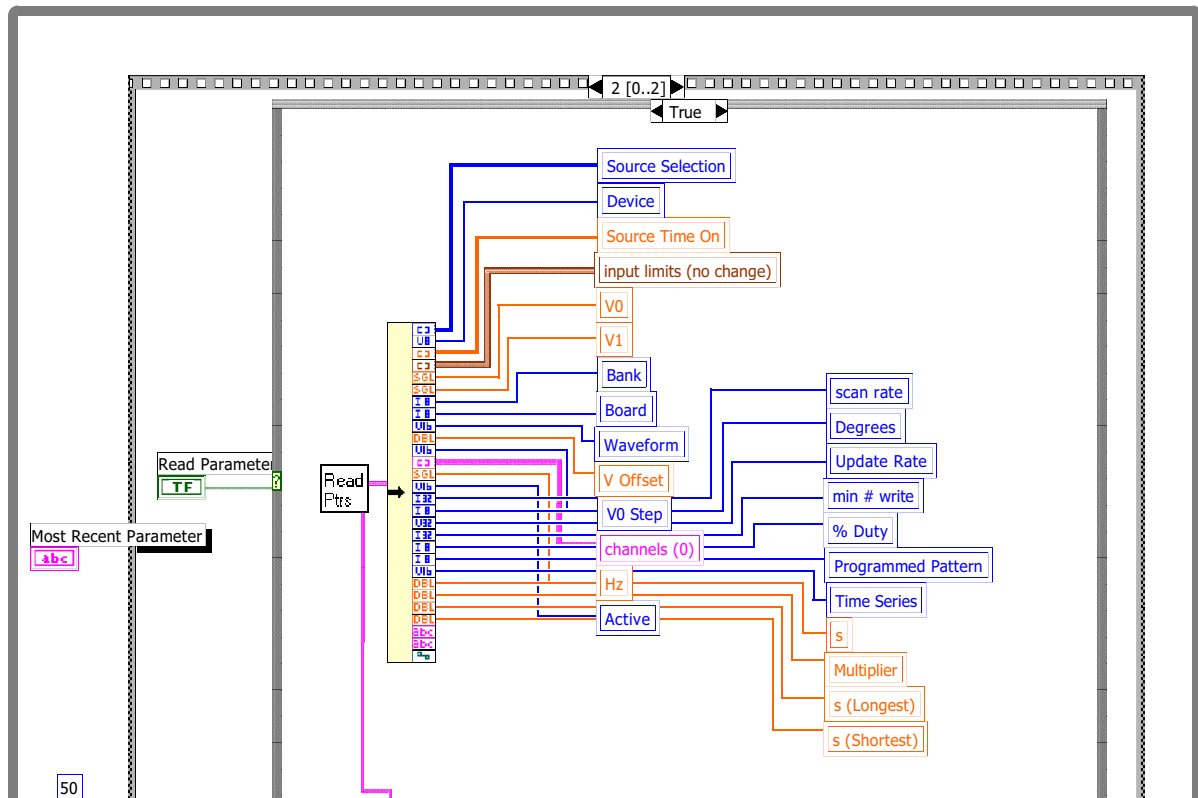
Distance Alert.vi

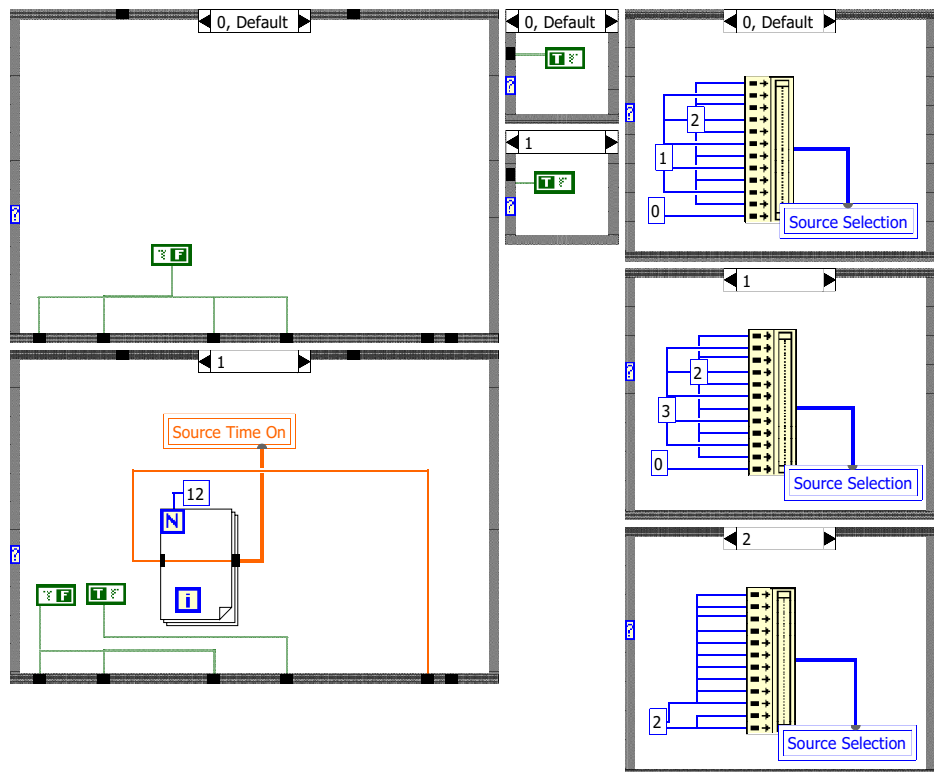
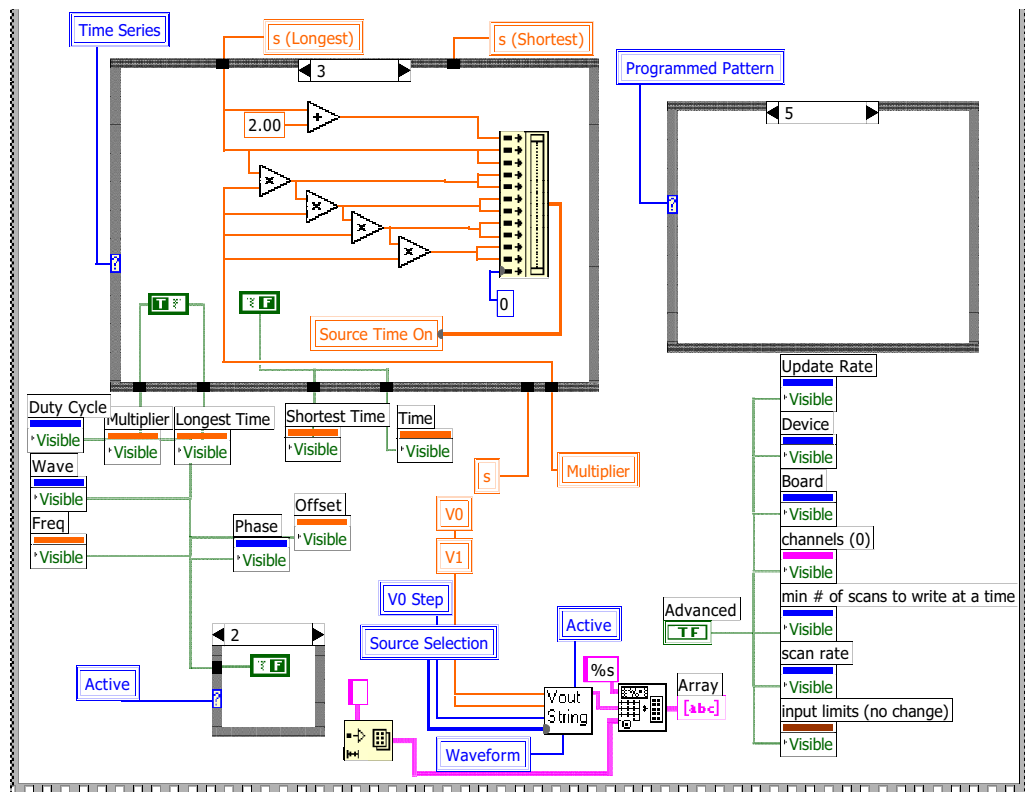
D:\Data Archive\Labview\ElectroSynthesis\Labview Code\Distance Alert.vi

Last modified on 05/08/2000 at 2:30 PM

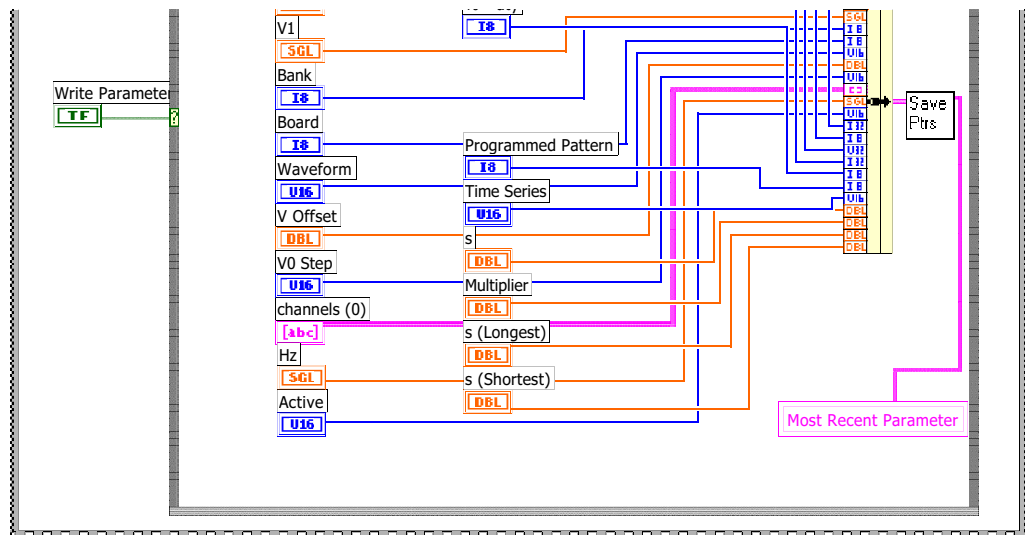
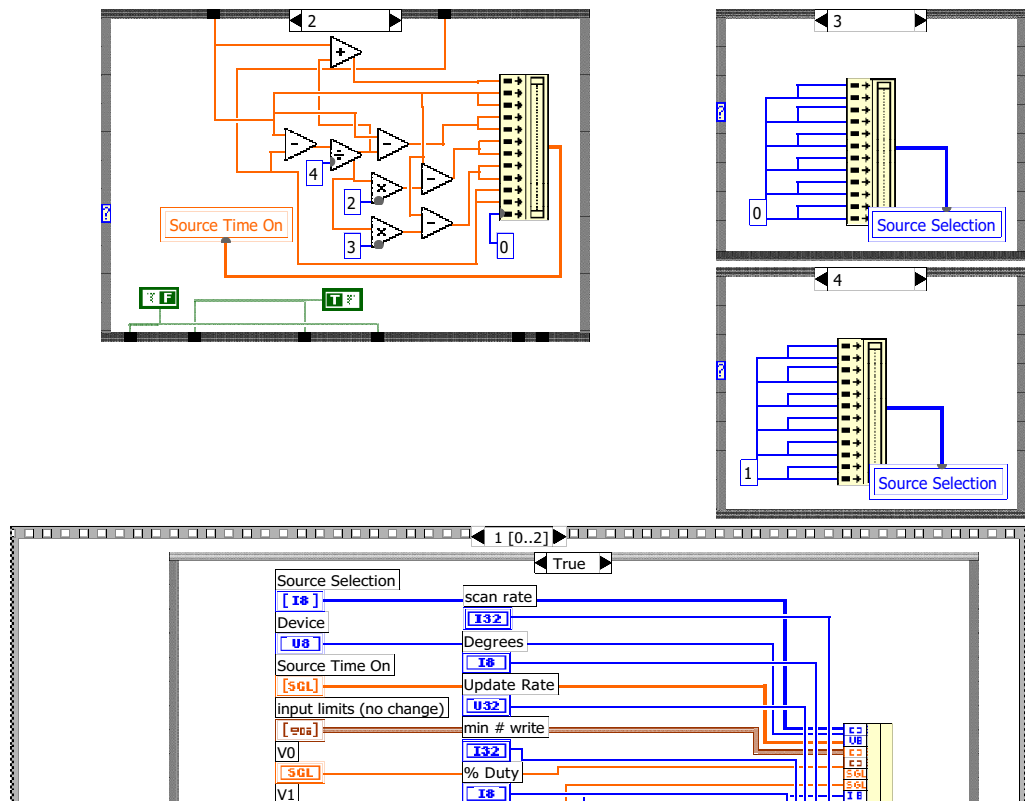
Printed on 14/05/2003 at 8:12 PM

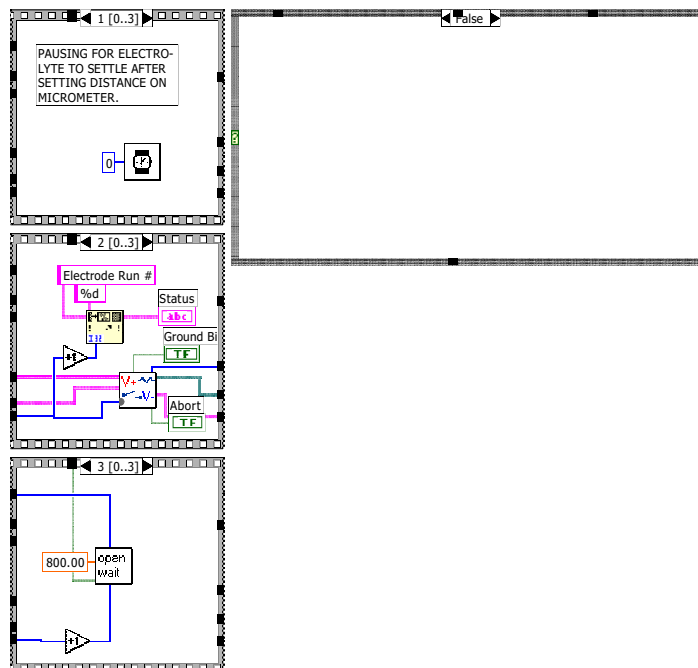
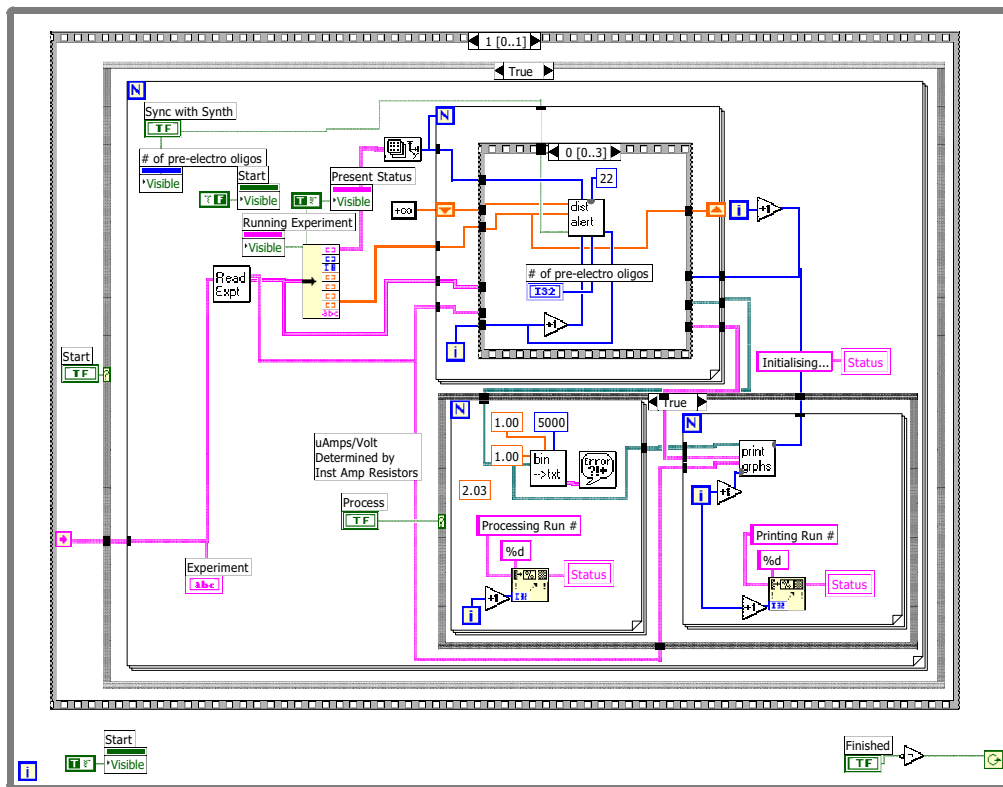


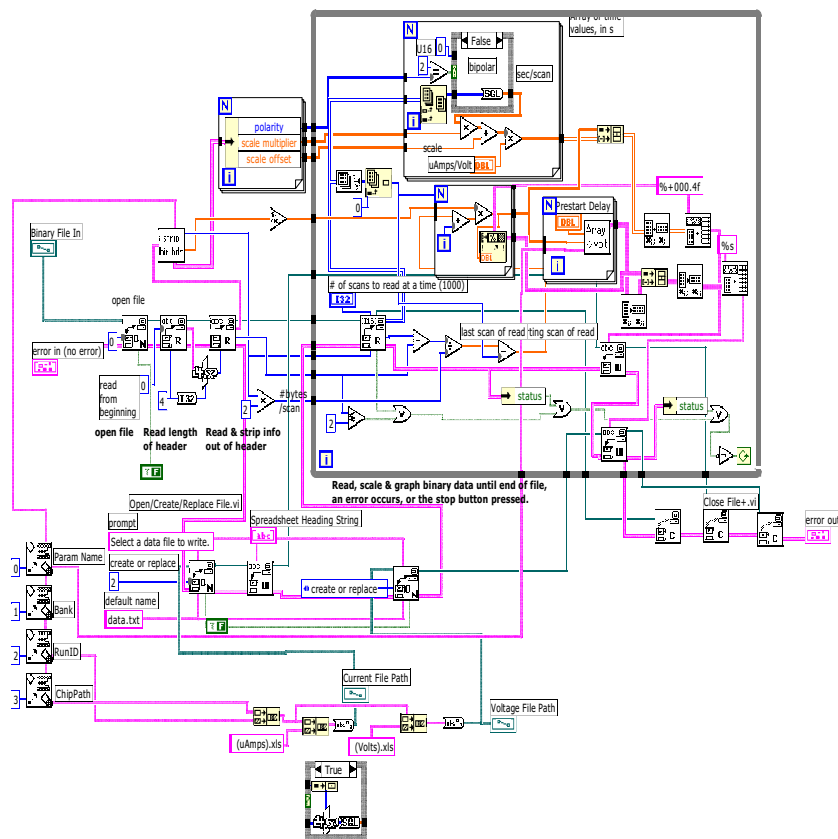
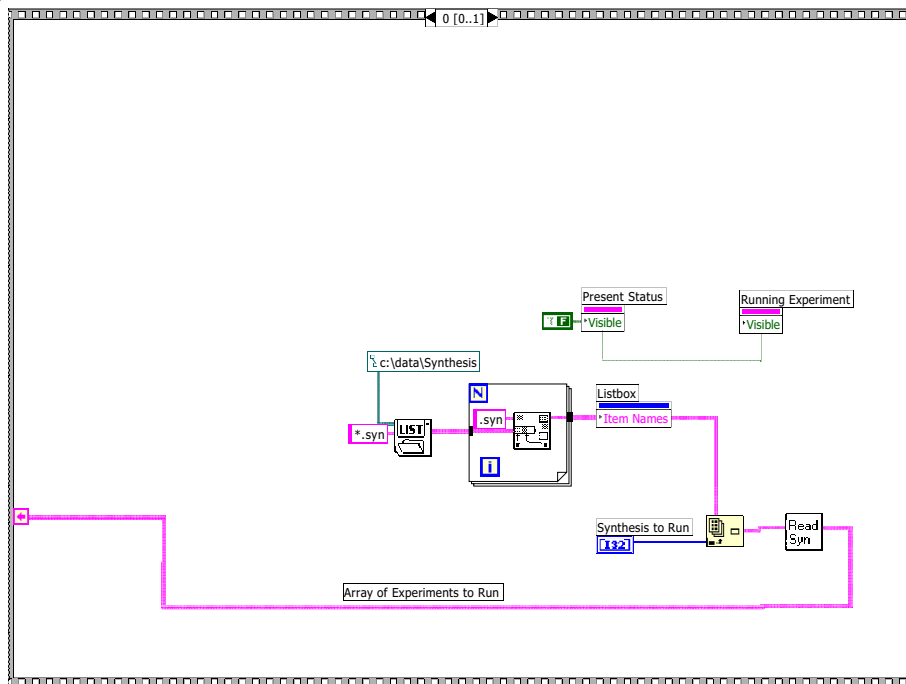


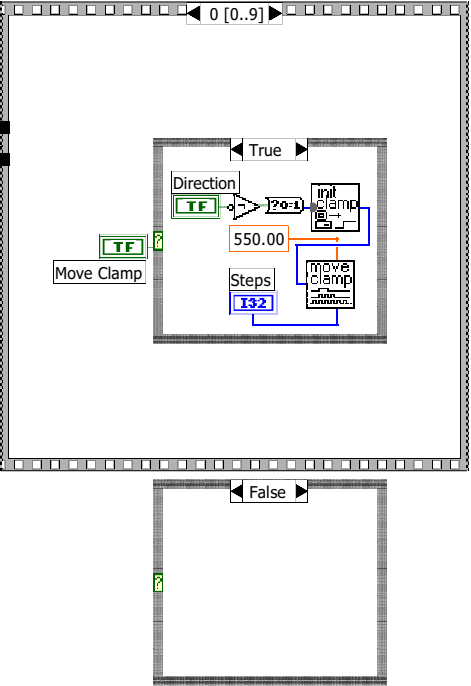
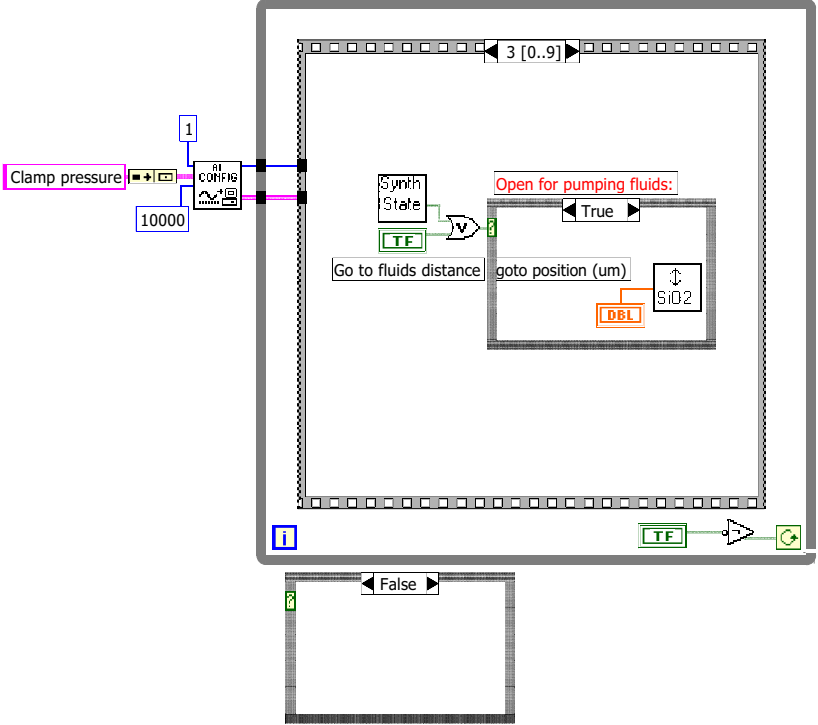




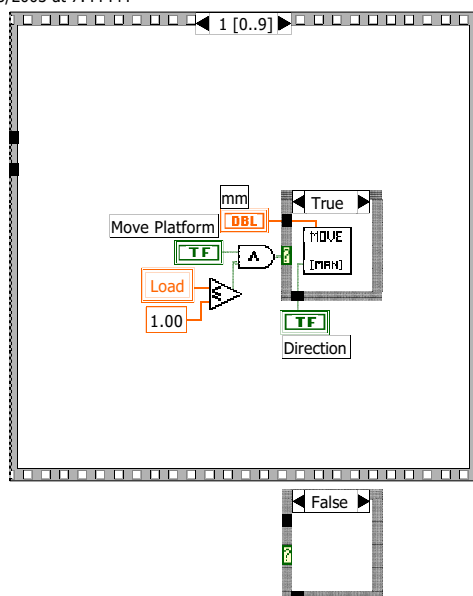




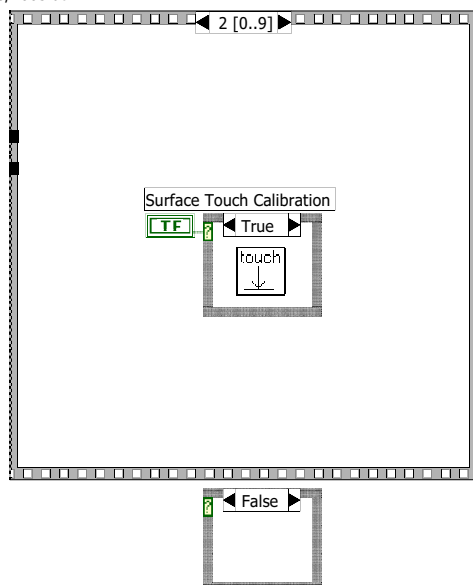




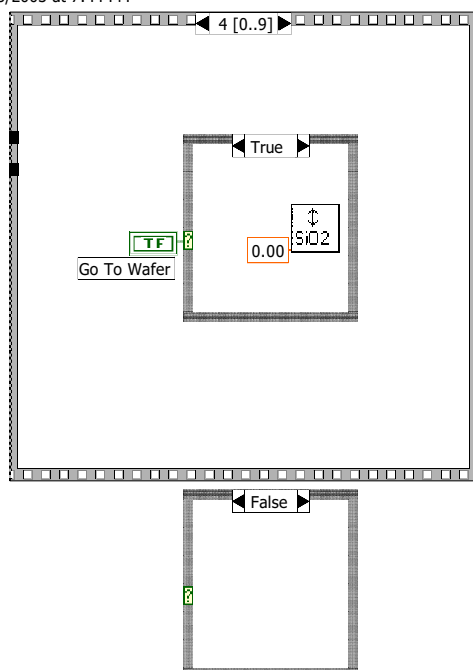
Operate Motors.vi  
D:\Data Archive\Labview\ElectroSynthesis\Labview Code\Operate Motors.vi  
Last modified on 22/06/2000 at 4:54 PM  
Printed on 14/05/2003 at 7:44 PM



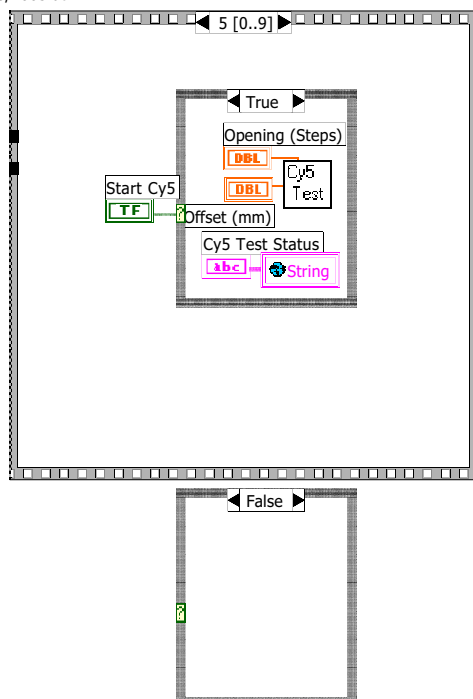
Operate Motors.vi  
D:\Data Archive\Labview\ElectroSynthesis\Labview Code\Operate Motors.vi  
Last modified on 22/06/2000 at 4:54 PM  
Printed on 14/05/2003 at 7:44 PM



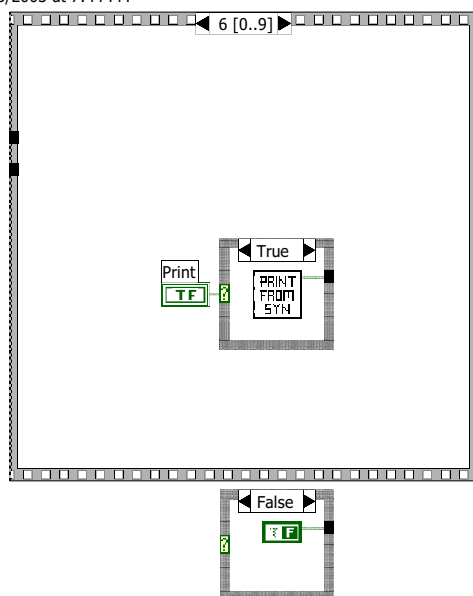
Operate Motors.vi  
D:\Data Archive\Labview\ElectroSynthesis\Labview Code\Operate Motors.vi  
Last modified on 22/06/2000 at 4:54 PM  
Printed on 14/05/2003 at 7:44 PM



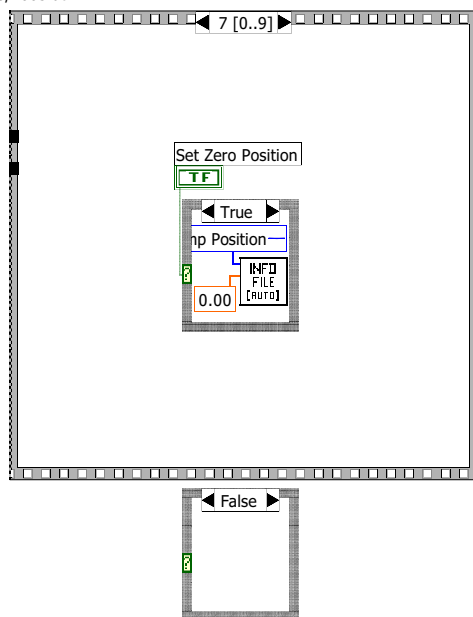
Operate Motors.vi  
D:\Data Archive\Labview\ElectroSynthesis\Labview Code\Operate Motors.vi  
Last modified on 22/06/2000 at 4:54 PM  
Printed on 14/05/2003 at 7:44 PM



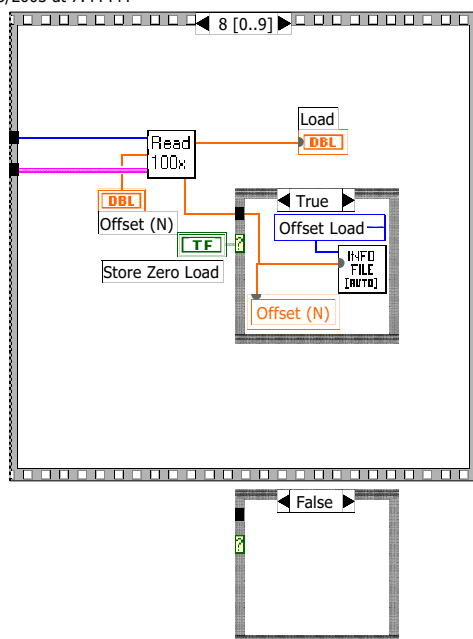
Operate Motors.vi  
D:\Data Archive\Labview\ElectroSynthesis\Labview Code\Operate Motors.vi  
Last modified on 22/06/2000 at 4:54 PM  
Printed on 14/05/2003 at 7:44 PM



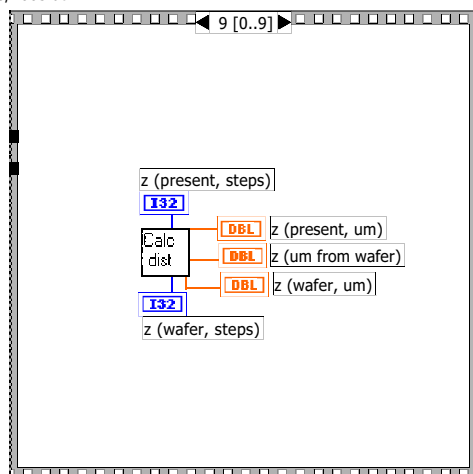
Operate Motors.vi  
D:\Data Archive\Labview\ElectroSynthesis\Labview Code\Operate Motors.vi  
Last modified on 22/06/2000 at 4:54 PM  
Printed on 14/05/2003 at 7:44 PM



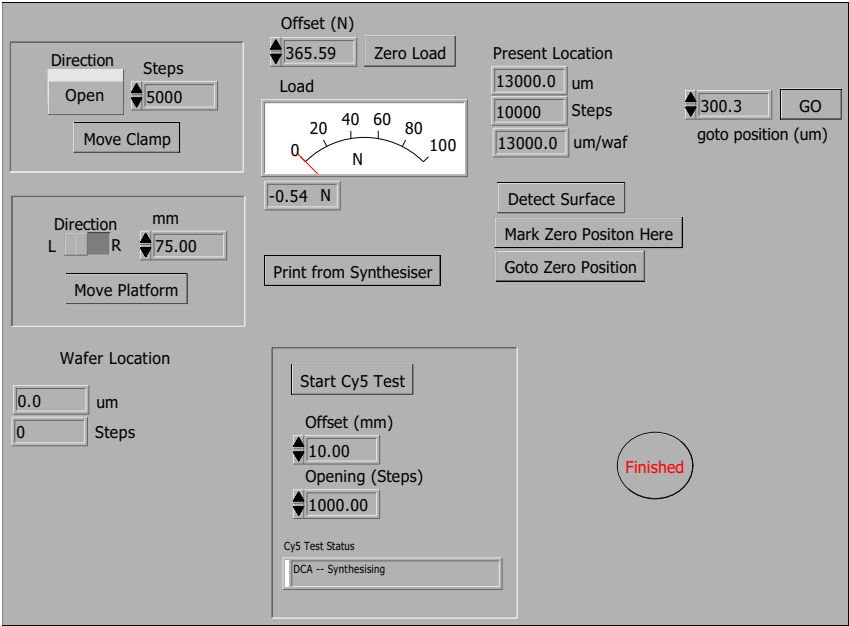
Operate Motors.vi  
D:\Data Archive\Labview\ElectroSynthesis\Labview Code\Operate Motors.vi  
Last modified on 22/06/2000 at 4:54 PM  
Printed on 14/05/2003 at 7:44 PM



Operate Motors.vi  
D:\Data Archive\Labview\ElectroSynthesis\Labview Code\Operate Motors.vi  
Last modified on 22/06/2000 at 4:54 PM  
Printed on 14/05/2003 at 7:44 PM







[illegible]

ed (no change) Update Rate

limit 200 scan rate 1000 min # write 1000

limit 10 der 10 Ground 11 Float 12

VDC 25.00 Gnd 25.00 Flt 25.00

# Appendix J

## Current Measurements

The electronics and software systems were designed to allow current measurement at each of the microelectrodes during each electrochemical deprotection step. Throughout the course of this work, over 3,000 current profiles were collected during syntheses. Often, the profiles proved useful in diagnosing circuit or microelectrode faults, or ensuring accuracy of synthesis.

The current data presented in **Chapter 2** and **Chapter 3** was obtained directly from spreadsheet data collected by sampling each microelectrode at 50 Hz. In addition, the software program output all electrode current profiles to a printer immediately following each run for quick checks of system integrity. The following pages show a few examples of the generated current profiles. For each of the relevant results as discussed in the body of the thesis, current data was obtained from current profiles similar to those shown here.

## References

1. Lockhart DJ, Dong HL, Byrne MC, Follettie MT, Gallo MV, Chee MS, Mittmann M, Wang CW, Kobayashi M, Horton H, et al.: **Expression monitoring by hybridization to high-density oligonucleotide arrays.** *Nature Biotechnology* 1996, **14**:1675-1680.
2. Schena M, Shalon D, Heller R, Chai A, Brown PO, Davis RW: **Parallel human genome analysis: microarray-based expression monitoring of 1000 genes.** *Proceedings of the National Academy of Sciences of the United States of America* 1996, **93**:10614-10619.
3. Schena M, Shalon D, Davis RW, Brown PO: **Quantitative monitoring of gene expression patterns with a complementary DNA microarray.** *Science* 1995, **270**:467-470.
4. Mir KU, Southern EM: **Sequence variation in genes and genomic DNA: methods for large-scale analysis.** *Annual Review of Genomics and Human Genetics* 2000, **1**:329-360.
5. Wang W, Montgomery D: **Electrochemically mediated Michael additions for carbon-carbon bond formation on microchips.** *Abstracts of Papers of the American Chemical Society* 1998, **216**:184.
6. Southern EM, Milner N, Mir KU: **Discovering antisense reagents by hybridization of RNA to oligonucleotide arrays.** *Ciba Foundation Symposium* 1997, **209**:38-44.
7. Southern E, Mir K, Shchepinov M: **Molecular interactions on microarrays.** *Nature Genetics* 1999, **21**:5-9.
8. Southern EM, Case-Green SC, Elder JK, Johnson M, Mir KU, Wang L, Williams JC: **Arrays of complementary oligonucleotides for analysing**

- the hybridisation behaviour of nucleic acids. *Nucleic Acids Research* 1994, **22**:1368-1373.
9. Chee M, Yang R, Hubbell E, Berno A, Huang XC, Stern D, Winkler J, Lockhart DJ, Morris MS, Fodor SPA: **Accessing genetic information with high-density DNA arrays.** *Science* 1996, **274**:610-614.
  10. Cargill M, Altshuler D, Ireland J, Sklar P, Ardlie K, Patil N, Shaw N, Lane CR, Lim EP, Kalyanaraman N, et al.: **Characterization of single-nucleotide polymorphisms in coding regions of human genes.** *Nature Genetics* 1999, **22**:231-238.
  11. Halushka MK, Fan JB, Bentley K, Hsie L, Shen N, Weder A, Cooper R, Lipshutz R, Chakravarti A: **Patterns of single-nucleotide polymorphisms in candidate genes for blood-pressure homeostasis.** *Nature Genetics* 1999, **22**:239-247.
  12. Bulyk ML, Gentalen E, Lockhart DJ, Church GM: **Quantifying DNA-protein interactions by double-stranded DNA arrays.** *Nature Biotechnology* 1999, **17**:573-577.
  13. Pirrung MC: **Spatially addressable combinatorial libraries.** *Chemical Reviews* 1997, **97**:473-488.
  14. Pirrung MC: **How to make a DNA chip.** *Angewandte Chemie-International Edition* 2002, **41**:1277-1289.
  15. Blohm DH, Guiseppi-Elie A: **New developments in microarray technology.** *Current Opinion in Biotechnology* 2001, **12**:41-47.
  16. Brenner S, Johnson M, Bridgham J, Golda G, Lloyd DH, Johnson D, Luo SJ, McCurdy S, Foy M, Ewan M, et al.: **Gene expression analysis by massively parallel signature sequencing (MPSS) on microbead arrays.** *Nature Biotechnology* 2000, **18**:630-634.
  17. Singh-Gasson S, Green RD, Yue YJ, Nelson C, Blattner F, Sussman MR, Cerrina F: **Maskless fabrication of light-directed oligonucleotide microarrays using a digital micromirror array.** *Nature Biotechnology* 1999, **17**:974-978.

18. Fodor SPA: **DNA sequencing - Massively parallel genomics.** *Science* 1997, **277**:393.
19. Gao XL, Yu PL, LeProust E, Sonigo L, Pellois JP, Zhang H: **Oligonucleotide synthesis using solution photogenerated acids.** *Journal of the American Chemical Society* 1998, **120**:12698-12699.
20. Hughes TR, Linsley P, Marton M, Roberts C, Jones A, Stoughton R, Shoemaker D, Blanchard A, Phillips J, Ziman M, et al.: **Large-scale discovery of gene functions using an ink-jet oligonucleotide synthesizer and a compendium of DNA microarray expression profiles.** *American Journal of Human Genetics* 2000, **67**:212.
21. Ferguson J, Steemers F, Schauer C, Michael K, Taylor L, Walt DR: **Randomly ordered, high-density, fiber-optic, microsensor-array sensors.** *Abstracts of Papers of the American Chemical Society* 2000, **219**:235.
22. Giegrich H, Eisele-Buhler S, Hermann C, Kvasnyuk E, Charubala R, Pfeleiderer W: **New photolabile protecting groups in nucleoside and nucleotide chemistry -- Synthesis, cleavage mechanisms and applications.** *Nucleosides & Nucleotides* 1998, **17**:1987-1996.
23. McGall GH, Barone AD, Diggelmann M, Fodor SPA, Gentalen E, Ngo N: **The efficiency of light-directed synthesis of DNA arrays on glass substrates.** *Journal of the American Chemical Society* 1997, **119**:5081-5090.
24. Southern EM, Maskos U, Elder JK: **Analyzing and comparing nucleic acid sequences by hybridization to arrays of oligonucleotides: Evaluation using experimental models.** *Genomics* 1992, **13**:1008-1017.
25. Case-Green SC, Mir KU, Pritchard CE, Southern EM: **Analysing genetic information with DNA arrays.** *Current Opinion in Biotechnology* 1998, **2**:404-410.
26. Stimpson DI, Cooley PW, Knepper SM, Wallace DB: **Parallel production of oligonucleotide arrays using membranes and reagent jet printing.** *Biotechniques* 1998, **25**:886-890.

27. Okamoto T, Suzuki T, Yamamoto N: **Microarray fabrication with covalent attachment of DNA using Bubble Jet technology.** *Nature Biotechnology* 2000, **18**:438-441.
28. Hughes TR, Mao M, Jones AR, Burchard J, Marton M, Shannon KW, Lefkowitz SM, Ziman M, Schelter J: **Expression profiling using microarrays fabricated by an ink-jet oligonucleotide synthesizer.** *Nature Biotechnology* 2001, **19**:342-347.
29. Bond AM: **200 years of practical electroanalytical chemistry: Past, present and future directions illustrated by reference to the on-line, on-stream and off-line determination of trace metals in zinc plant electrolyte by voltammetric and potentiometric techniques.** *Analytica Chimica Acta* 1999, **400**:333-379.
30. Kyriacou DK: *Basics of Electroorganic Synthesis*. New York: Wiley; 1981.
31. Bard AJ, Denuault G, Lee C, Mandler D, Wipf DO: **Scanning electrochemical microscopy - a new technique for the characterization and modification of surfaces.** *Accounts of Chemical Research* 1990, **23**:357-363.
32. Schuster R, Kirchner V, Allongue P, Ertl G: **Electrochemical micro-machining.** *Science* 2000, **289**:98-101.
33. Livache T, Roget A, Dejean E, Barthet C, Bidan G, Teoule R: **Preparation of a DNA matrix via an electrochemically directed copolymerization of pyrrole and oligonucleotides bearing a pyrrole group.** *Nucleic Acids Research* 1994, **22**:2915-2921.
34. Livache T, Fouque B, Roget A, Marchand J, Bidan G, Teoule R, Mathis G: **Polypyrrole DNA chip on a silicon device: Example of hepatitis C virus genotyping.** *Analytical Biochemistry* 1998, **255**:188-194.
35. Bu HZ, Mikkelsen SR, English AM: **NAD(P)H sensors based on enzyme entrapment in ferrocene-containing polyacrylamide-based redox gels.** *Analytical Chemistry* 1998, **70**:4320-4325.

36. Livache T, Bazin H, Caillat P, Roget A: **Electroconducting polymers for the construction of DNA or peptide arrays on silicon chips.** *Bio-sensors & Bioelectronics* 1998, **13**:629-634.
37. Montgomery D: **Electrochemical solid phase synthesis of polymers.** US Patent 1998, PCT/US97/11463.
38. Montgomery D, Undem BL: **CombiMatrix' customizable DNA microarrays -- Tutorial: In situ computer-aided synthesis of custom oligo microarrays.** *Genetic Engineering News* 2002, **22**:32-33.
39. Kyriacou DK: *Modern Electroorganic Chemistry*. Berlin ; New York: Springer-Verlag; 1994.
40. Volke J, Liska, F.: *Electrochemistry in Organic Synthesis*. London: Springer-Verlag; 1994.
41. Hashimoto K, Ito K, Ishimori Y: **Sequence-specific gene detection with a gold electrode modified with DNA probes and an electrochemically active dye.** *Analytical Chemistry* 1994, **66**:3830-3833.
42. Millan KM, Spurmanis AJ, Mikkelsen SR: **Covalent immobilization of DNA onto glassy-carbon electrodes.** *Electroanalysis* 1992, **4**:929-932.
43. Zhao YD, Pang DW, Wang ZL, Cheng JK, Qi YP: **DNA-modified electrodes 2: Electrochemical characterization of gold electrodes modified with DNA.** *Journal of Electroanalytical Chemistry* 1997, **431**:203-209.
44. Fodor SPA, Read JL, Pirrung MC, Stryer L, Lu AT, Solas D: **Light-directed, spatially addressable parallel chemical synthesis.** *Science* 1991, **251**:767-773.
45. Hacia JG, Brody LC, Collins FS: **Applications of DNA chips for genomic analysis.** *Molecular Psychiatry* 1998, **3**:483-492.
46. Cheng J, Sheldon EL, Wu L, Uribe A, Gerrue LO, Carrino J, Heller MJ, O'Connell JP: **Preparation and hybridization analysis of DNA/RNA**



- from E-coli on microfabricated bioelectronic chips.** *Nature Biotechnology* 1998, **16**:541-546.
47. Hughes TR, Shoemaker DD: **DNA microarrays for expression profiling.** *Current Opinion in Chemical Biology* 2001, **5**:21-25.
48. Manz A: **What can chips technology offer for next century's chemistry and life sciences?** *Chimia* 1996, **50**:140-143.
49. Wang J: **Amperometric biosensors for clinical and therapeutic drug monitoring: A review.** *Journal of Pharmaceutical and Biomedical Analysis* 1999, **19**:47-53.
50. Cheng J, Sheldon EL, Wu L, Heller MJ, O'Connell JP: **Isolation of cultured cervical carcinoma cells mixed with peripheral blood cells on a bioelectronic chip.** *Analytical Chemistry* 1998, **70**:2321-2326.
51. Suzuki H: **Advances in the microfabrication of electrochemical sensors and systems.** *Electroanalysis* 2000, **12**:703-715.
52. Fiaccabrino GC, Koudelka-Hep M: **Thin-film microfabrication of electrochemical transducers.** *Electroanalysis* 1998, **10**:217-222.
53. Liu CC, Zhang ZR: **Research-and-Development of Chemical Sensors Using Microfabrication Techniques.** *Selective Electrode Reviews* 1992, **14**:147-167.
54. Wise KD, Najafi K: **Microfabrication Techniques for Integrated Sensors and Microsystems.** *Science* 1991, **254**:1335-1342.
55. Schreiber SL: **Target-oriented and diversity-oriented organic synthesis in drug discovery.** *Science* 2000, **287**:1964-1969.
56. Dolle RE, Nelson KH: **Comprehensive survey of combinatorial library synthesis: 1998.** *Journal of Combinatorial Chemistry* 1999, **1**:235-282.

57. Osborn HMI, Khan TH: **Recent developments in polymer supported syntheses of oligosaccharides and glycopeptides.** *Tetrahedron* 1999, **55**:1807-1850.
  58. Gait MJ: *Oligonucleotide Synthesis : A Practical Approach*. Oxford: IRL Press; 1984.
  59. Southern EM, Maskos U: **Parallel synthesis and analysis of large numbers of related chemical compounds: applications to oligonucleotides.** *Journal of Biotechnology* 1994, **35**:217-227.
  60. Stanton L, Bruhn L, Weist D, Lightfoot S, Villaneuva H, Collins S, Sum C, Ilsley-Tyree D, Webb P, Westall M, et al.: **Performance characterization of cDNA microarrays produced by thermal ink-jet (TIJ) deposition.** *American Journal of Human Genetics* 2000, **67**:1463.
  61. Roda A, Guardigli M, Russo C, Pasini P, Baraldini M: **Protein microdeposition using a conventional ink-jet printer.** *Biotechniques* 2000, **28**:492-496.
  62. McGall G, Labadie J, Brock P, Wallraff G, Nguyen T, Hinsberg W: **Light-directed synthesis of high-density oligonucleotide arrays using semiconductor photoresists.** *Proceedings of the National Academy of Sciences of the United States of America* 1996, **93**:13555-13560.
  63. Lund H, Baizer MM: *Organic Electrochemistry: An Introduction and Guide* edn 3, rev. and expanded. New York: M. Dekker; 1991.
  64. Covington AK, Dickinson T: *Physical Chemistry of Organic Solvent Systems*, vol x: Plenum Press; 1973.
  65. Zuman P, Polytechnic Institute of Brooklyn.: *The Elucidation of Organic Electrode Processes*. New York,: Academic Press; 1969.
  66. Zuman P, Patel R: *Techniques in Organic Reaction Kinetics*. New York: Wiley; 1984.
-

- 67. Kirchner V, Xia XH, Schuster R: **Electrochemical nanostructuring with ultrashort voltage pulses.** *Accounts of Chemical Research* 2001, **34**:371-377.
- 68. Zu YB, Xie L, Mao BW, Tian ZW: **Studies on silicon etching using the confined etchant layer technique.** *Electrochimica Acta* 1998, **43**:1683-1690.
- 69. Shiku H, Takeda T, Yamada H, Matsue T, Uchida I: **Microfabrication and characterization of diaphorase-patterned surfaces by scanning electrochemical microscopy.** *Analytical Chemistry* 1995, **67**:312-317.
- 70. Gray DE, Case-Green SC, Fell TS, Dobson PJ, Southern EM: **Ellipsometric and interferometric characterization of DNA probes immobilized on a combinatorial array.** *Langmuir* 1997, **13**:2833-2842.
- 71. Beaucage SL, Iyer RP: **Advances in the synthesis of oligonucleotides by the phosphoramidite approach.** *Tetrahedron* 1992, **48**:2223-2311.
- 72. Parker VD: **Hydroquinone-quinone redox behavior in acetonitrile.** *Journal of the Chemical Society: D* 1969:716-717.
- 73. Parker VD: **Anodic oxidation of hydroquinone in acetonitrile. Possible one electron intermediate.** *Electrochimica Acta* 1973, **18**:519-524.
- 74. Parker VD, Eberson L: **Anodic oxidation of hydroquinone in acetonitrile.** *Journal of the Chemical Society: D* 1970:1289-1290.
- 75. Eggins BR: **Interpretation of electrochemical reduction and oxidation waves of quinone-hydroquinone system in acetonitrile.** *Journal of the Chemical Society: D* 1969:1267-1268.
- 76. Eggins BR: **One-electron intermediate in the anodic oxidation of hydroquinone in acetonitrile.** *Journal of the Chemistry Society, Chemical Communications* 1972:427.
- 77. Eggins BR, Chambers JQ: **Electrochemical oxidation of hydroquinone in acetonitrile.** *Chemical Communications* 1969:232-233.

78. Bauscher M, Maentele W: **Electrochemical and infrared-spectroscopic characterization of redox reactions of p-quinones.** *Journal of Physical Chemistry* 1992, **96**:11101-11108.
79. Yamanuki M, Hoshino T, Oyama M, Okazaki S: **Thin layer electrochemical Raman study of ion pair formation between the tetrachlorobenzoquinone anion radical and alkaline earth metal cations.** *Journal of Electroanalytical Chemistry* 1998, **458**:191-198.
80. Maskos U, Southern EM: **Oligonucleotide hybridizations on glass supports: A novel linker for oligonucleotide synthesis and hybridization properties of oligonucleotides synthesised in situ.** *Nucleic Acids Research* 1992, **20**:1679-1684.
81. Blanchard AP, Kaiser RJ, Hood LE: **High-density oligonucleotide arrays.** *Biosensors & Bioelectronics* 1996, **11**:687-690.
82. Forster AH, Krihak M, Swanson PD, Young TC, Ackley DE: **A laminated, flex structure for electronic transport and hybridization of DNA.** *Biosensors & Bioelectronics* 2001, **16**:187-194.
83. Bond AM: **Past, present and future contributions of microelectrodes to analytical studies employing voltammetric detection -- A review.** *Analyst* 1994, **119**:R1-R21.
84. Alden JA, Feldman MA, Hill E, Prieto F, Oyama M, Coles BA, Compton RG, Dobson PJ, Leigh PA: **Channel microband electrode arrays for mechanistic electrochemistry. Two dimensional voltammetry: Transport-limited currents.** *Analytical Chemistry* 1998, **70**:1707-1720.
85. Mitchelson KR, Cheng J, Kricka LJ: **The use of capillary electrophoresis for point-mutation screening.** *Trends in Biotechnology* 1997, **15**:448-458.
86. Huang Y, Ewalt KL, Tirado M, Haigis TR, Forster A, Ackley D, Heller MJ, O'Connell JP, Krihak M: **Electric manipulation of bioparticles and macromolecules on microfabricated electrodes.** *Analytical Chemistry* 2001, **73**:1549-1559.

87. Gilles PN, Wu DJ, Foster CB, Dillon PJ, Chanock SJ: **Single nucleotide polymorphic discrimination by an electronic dot blot assay on semiconductor microchips.** *Nature Biotechnology* 1999, **17**:365-370.
  88. Pividori MI, Merkoci A, Alegret S: **Electrochemical genosensor design: immobilisation of oligonucleotides onto transducer surfaces and detection methods.** *Biosensors & Bioelectronics* 2000, **15**:291-303.
  89. Dill K, Montgomery DD, Wang W, Tsai JC: **Antigen detection using microelectrode array microchips.** *Analytica Chimica Acta* 2001, **444**:69-78.
  90. Huber M, Heiduschka P, Kienle S, Pavlidis C, Mack J, Walk T, Jung G, Thanos S: **Modification of glassy carbon surfaces with synthetic laminin-derived peptides for nerve cell attachment and neurite growth.** *Journal of Biomedical Materials Research* 1998, **41**:278-288.
  91. Khan GF, Kobatake E, Shinohara H, Ikariyama Y, Aizawa M: **Voltage-assisted peptide synthesis in aqueous solution by alpha-chymotrypsin immobilized in polypyrrole matrix.** *Journal of the American Chemical Society* 1996, **118**:1824-1830.
  92. Zhang Z, Lei CH, Deng JQ: **Electrochemical fabrication of amperometric glucose enzyme electrode by immobilizing glucose oxidase in electropolymerized poly(3,3'-diaminobenzidine) film on palladinized glassy carbon electrode.** *Analyst* 1996, **121**:971-975.
  93. Sadik OA: **Bioaffinity sensors based on conducting polymers: A short review.** *Electroanalysis* 1999, **11**:839-844.
  94. Egeland RD, Marken F, Southern EM: **An electrochemical redox couple activated by microelectrodes for confined chemical patterning of surfaces.** *Analytical Chemistry* 2002, **74**:1590-1596.
  95. Kounaves SP, Deng W, Hallock PR, Kovacs GTA, Stormont CW: **Iridium-based ultramicroelectrode array fabricated by microlithography.** *Analytical Chemistry* 1994, **66**:418-423.
-

96. Caruthers MH: **Chemical synthesis of DNA and DNA analogs.** *Accounts of Chemical Research* 1991, **24**:278-284.
97. Oivanen M, Lonnberg H: **Kinetics and mechanisms for reactions of adenosine 2'- and 3'- monophosphates in aqueous acid -- Competition between phosphate migration, dephosphorylation, and depurination.** *Journal of Organic Chemistry* 1989, **54**:2556-2560.
98. Butkus VV, Kayushin AL, Berlin YA, Kolosov MN, Smirnov IV: **Cleavage of 5'-O-protecting trityl groups in oligodeoxynucleotide synthesis -- Effect of substrate structure and reaction conditions on the detritylation and depurination rates.** *Bioorganicheskaya Khimiya* 1983, **9**:1518-1530.
99. Wang DG, Fan JB, Siao CJ, Berno A, Young P, Sapolsky R, Ghandour G, Perkins N, Winchester E, Spencer J, et al.: **Large-scale identification, mapping, and genotyping of single-nucleotide polymorphisms in the human genome.** *Science* 1998, **280**:1077-1082.
100. Hecker KH, Green SM, Kobayashi K: **Analysis and purification of nucleic acids by ion-pair reversed-phase high-performance liquid chromatography.** *Journal of Biochemical and Biophysical Methods* 2000, **46**:83-93.
101. Septak M: **Kinetic studies on depurination and detritylation of CPG-bound intermediates during oligonucleotide synthesis.** *Nucleic Acids Research* 1996, **24**:3053-3058.
102. Meyer H, Drewer H, Grundig B, Cammann K, Kakerow R, Manoli Y, Mokwa W, Rospert M: **2-Dimensional imaging of O<sub>2</sub>, H<sub>2</sub>O<sub>2</sub>, and glucose distributions by an array of 400 individually addressable microelectrodes.** *Analytical Chemistry* 1995, **67**:1164-1170.
103. Polushin NN, Morochko AM, Chen BC, Cohen JS: **On the rapid deprotection of synthetic oligonucleotides and analogs.** *Nucleic Acids Research* 1994, **22**:639-645.
104. Duggan DJ, Bittner M, Chen YD, Meltzer P, Trent JM: **Expression profiling using cDNA microarrays.** *Nature Genetics* 1999, **21**:10-14.

105. Yang YH, Dudoit S, Luu P, Lin DM, Peng V, Ngai J, Speed TP: **Normalization for cDNA microarray data: a robust composite method addressing single and multiple slide systematic variation.** *Nucleic Acids Research* 2002, **30**:art. no. e15.
106. Brown CS, Goodwin PC, Sorger PK: **Image metrics in the statistical analysis of DNA microarray data.** *Proceedings of the National Academy of Sciences of the United States of America* 2001, **98**:8944-8949.
107. Freeman TC, Lee K, Richardson PJ: **Analysis of gene expression in single cells.** *Current Opinion in Biotechnology* 1999, **10**:579-582.
108. Everts EM, Au-Young J, Ruvolo MV, Lim AC, Reynolds MA: **Hybridization cross-reactivity within homologous gene families on glass cDNA microarrays.** *Biotechniques* 2001, **31**:1182,1184,1186.
109. Hoyt PR, Tack L, Jones BH, Van Dinther J, Staat S, Doktycz MJ: **Automated high-throughput probe production for DNA microarray analysis.** *Biotechniques* 2003, **34**:402-407.
110. Clark MD, Panopoulou GD, Cahill DJ, Bussow K, Lehrach H: **DUPLICATE Construction and analysis of arrayed cDNA libraries.** In *Cdna Preparation and Characterization*. Edited by: Academic Press Inc; 1999:205-233. Methods in Enzymology, vol 303.]
111. Drmanac R, Drmanac S: **cDNA screening by array hybridization.** In *cDNA Preparation and Characterization*. Edited by: Academic Press Inc; 1999:165-178. Methods in Enzymology, vol 303.]
112. Jobs M, Fredriksson S, Brookes AJ, Landegren U: **Effect of oligonucleotide truncation on single-nucleotide distinction by solid-phase hybridization.** *Analytical Chemistry* 2002, **74**:199-202.
113. Trabesinger W, Schutz GJ, Gruber HJ, Schindler H, Schmidt T: **Detection of individual oligonucleotide pairing by single-molecule microscopy.** *Analytical Chemistry* 1999, **71**:279-283.
114. Vercoutere W, Akeson M: **Biosensors for DNA sequence detection.** *Current Opinion in Chemical Biology* 2002, **6**:816-822.

115. Selinger DW, Cheung KJ, Mei R, Johansson EM, Richmond CS, Blattner FR, Lockhart DJ, Church GM: **RNA expression analysis using a 30 base pair resolution Escherichia coli genome array.** *Nature Biotechnology* 2000, **18**:1262-1268.
116. Heller MJ, Forster AH, Tu E: **Active microelectronic chip devices which utilize controlled electrophoretic fields for multiplex DNA hybridization and other genomic applications.** *Electrophoresis* 2000, **21**:157-164.
117. Swanson P, Gelbart R, Atlas E, Yang L, Grogan T, Butler WF, Ackley DE, Sheldon E: **A fully multiplexed CMOS biochip for DNA analysis.** *Sensors and Actuators B-Chemical* 2000, **64**:22-30.
118. Pease AC, Solas D, Sullivan EJ, Cronin MT, Holmes CP, Fodor SPA: **Light-generated oligonucleotide arrays for rapid DNA-sequence analysis.** *Proceedings of the National Academy of Sciences of the United States of America* 1994, **91**:5022-5026.
119. Cerrina F, Blattner F, Huang W, Hue Y, Green R, Singh-Gasson S, Sussman M: **Biological lithography: Development of a maskless microarray synthesizer for DNA chips.** *Microelectronic Engineering* 2002, **61**:2:33-40.
120. Sampsell JB: **Digital micromirror device and its application to projection displays.** *Journal of Vacuum Science & Technology B* 1994, **12**:3242-3246.
121. Stetsenko DA, Gait MJ: **Efficient conjugation of peptides to oligonucleotides by "native ligation".** *Journal of Organic Chemistry* 2000, **65**:4900-4908.
122. Stetsenko DA, Malakhov AD, Gait MJ: **Total stepwise solid-phase synthesis of oligonucleotide-(3' --> N)-peptide conjugates.** *Organic Letters* 2002, **4**:3259-3262.
123. Nuwaysir EF, Huang W, Albert TJ, Singh J, Nuwaysir K, Pitas A, Richmond T, Gorski T, Berg JP, Ballin J, et al.: **Gene expression analysis**



- using oligonucleotide arrays produced by maskless photolithography. *Genome Research* 2002, **12**:1749-1755.
124. Beier M, Baum M, Rebscher H, Mauritz R, Wixmerten A, Stahler CF, Muller M, Stahler PF: **Exploring nature's plasticity with a flexible probing tool, and finding new ways for its electronic distribution.** *Biochemical Society Transactions* 2002, **30**:78-82.
125. Beier M, Stephan A, Hoheisel JD: **Synthesis of photolabile 5'-O-phosphoramidites for the photolithographic production of microarrays of inversely oriented oligonucleotides.** *Helvetica Chimica Acta* 2001, **84**:2089-2095.
126. Yang JN, Liu YJ, Rauch CB, Stevens RL, Liu RH, Lenigk R, Grodzinski P: **High sensitivity PCR assay in plastic micro reactors.** *Lab on a Chip* 2002, **2**:179-187.
127. Weston DF, Smekal T, Rhine DB, Blackwell J: **Fabrication of microfluidic devices in silicon and plastic using plasma etching.** *Journal of Vacuum Science & Technology B* 2001, **19**:2846-2851.
128. Shi WM, Reed MR, Liu YB, Cheung LN, Wu RJ, Asatourians A, Park G, Coty WA: **Cystic fibrosis carrier screening using electrochemical detection on the eSensor (TM) DNA detection platform.** *Clinical Chemistry* 2002, **48**:12.
129. Ramakrishnan R, Dorris D, Lublinsky A, Nguyen A, Domanus M, Prokhorova A, Gieser L, Touma E, Lockner R, Tata M, et al.: **An assessment of Motorola CodeLink (TM) microarray performance for gene expression profiling applications.** *Nucleic Acids Research* 2002, **30**:art. no.-e30.
130. Liu YJ, Rauch CB, Stevens RL, Lenigk R, Yang JN, Rhine DB, Grodzinski P: **DNA amplification and hybridization assays in integrated plastic monolithic devices.** *Analytical Chemistry* 2002, **74**:3063-3070.
131. Lenigk R, Liu RH, Rhine D, Singhal P, Athavale M, Chen ZJ, Grodzinski P: **Optimization of DNA hybridization kinetics in microfluidic**
-

- channels using electronic on-line detection.** *Abstracts of Papers of the American Chemical Society* 2002, **224**:027-BIOT.
132. Dorris DR, Ramakrishnan R, Trakas D, Dudzik F, Belval R, Zhao C, Nguyen A, Domanus M, Mazumder A: **A highly reproducible, linear, and automated sample preparation method for DNA microarrays.** *Genome Research* 2002, **12**:976-984.
133. Macoska JA: **The progressing clinical utility of DNA microarrays.** *Ca: a Cancer Journal for Clinicians.* 2002, **52**:50-59.
134. Van't Veer LJ, De Jong D: **The microarray way to tailored cancer treatment.** *Nature Medicine* 2002, **8**:13-14.
135. Tian ZW, Fen ZD, Tian ZQ, Zhuo XD, Mu JQ, Li CZ, Lin HS, Ren B, Xie ZX, Hu WL: **Confined etchant layer technique for 2-dimensional lithography at high-resolution using electrochemical scanning-tunneling microscopy.** *Faraday Discussions* 1992:37-44.
136. Schuster R, Kirchner V, Xia XH, Bittner AM, Ertl G: **Nanoscale electrochemistry.** *Physical Review Letters* 1998, **80**:5599-5602.
137. Toussaint D, Wilczek F: **Particle antiparticle annihilation in diffusive motion.** *Journal of Chemical Physics* 1983, **78**:2642-2647.
138. Ben-Naim E, Redner S: **Inhomogeneous 2-species annihilation in the steady-state.** *Journal of Physics A-Mathematical and General* 1992, **25**:L575-L583.
139. Mattis DC, Glasser ML: **The uses of quantum field theory in diffusion-limited reactions.** *Reviews of Modern Physics* 1998, **70**:979-1001.
140. Lee BP, Cardy J: **Scaling of reaction zones in the  $A+B \rightarrow 0$  diffusion-limited reaction.** *Physical Review E* 1994, **50**:R3287-R3290.
141. Cornell S, Droz M: **Steady-state reaction-diffusion front scaling for  $Ma+Nb \rightarrow [\text{inert}]$ .** *Physical Review Letters* 1993, **70**:3824-3827.

- 142. Atkins PW: *Physical Chemistry* edn 5. Oxford: Oxford University Press; 1994.
- 143. Golub TR, Slonim DK, Tamayo P, Huard C, Gaasenbeek M, Mesirov JP, Coller H, Loh ML, Downing JR, Caligiuri MA, et al.: **Molecular classification of cancer: Class discovery and class prediction by gene expression monitoring.** *Science* 1999, **286**:531-537.
- 144. Alizadeh AA, Eisen MB, Davis RE, Ma C, Lossos IS, Rosenwald A, Boldrick JC, Sabet H, Tran T, Yu X, et al.: **Distinct types of diffuse large B-cell lymphoma identified by gene expression profiling.** *Nature* 2000, **403**:503-511.
- 145. Perou CM, Sorlie T, Eisen MB, van de Rijn M, Jeffrey SS, Rees CA, Pollack JR, Ross DT, Johnsen H, Akslen LA, et al.: **Molecular portraits of human breast tumours.** *Nature* 2000, **406**:747-752.
- 146. Scherf U, Ross DT, Waltham M, Smith LH, Lee JK, Tanabe L, Kohn KW, Reinhold WC, Myers TG, Andrews DT, et al.: **A gene expression database for the molecular pharmacology of cancer.** *Nature Genetics* 2000, **24**:236-244.
- 147. Bittner M, Meltzer P, Chen Y, Jiang Y, Seftor E, Hendrix M, Radmacher M, Simon R, Yakhini Z, Ben-Dor A, et al.: **Molecular classification of cutaneous malignant melanoma by gene expression profiling.** *Nature* 2000, **406**:536-540.
- 148. Khanna C, Khan J, Nguyen P, Prehn J, Caylor J, Yeung C, Trepel J, Meltzer P, Helman L: **Metastasis-associated differences in gene expression in a murine model of osteosarcoma.** *Cancer Research* 2001, **61**:3750-3759.
- 149. Clark EA, Golub TR, Lander ES, Hynes RO: **Genomic analysis of metastasis reveals an essential role for RhoC.** *Nature* 2000, **406**:532-535.
- 150. Alon U, Barkai N, Notterman DA, Gish K, Ybarra S, Mack D, Levine AJ: **Broad patterns of gene expression revealed by clustering analysis of tumor and normal colon tissues probed by oligonucleotide ar-**

- rays.** *Proceedings of the National Academy of Sciences of the United States of America* 1999, **96**:6745-6750.
151. Ross DT, Scherf U, Eisen MB, Perou CM, Rees C, Spellman P, Iyer V, Jeffrey SS, Van de Rijn M, Waltham M, et al.: **Systematic variation in gene expression patterns in human cancer cell lines.** *Nature Genetics* 2000, **24**:227-235.
  152. Hedenfalk I, Duggan D, Chen Y, Radmacher M, Bittner M, Simon R, Meltzer P, Gusterson B, Esteller M, Kallioniemi OP, et al.: **Gene-expression profiles in hereditary breast cancer.** *New England Journal of Medicine* 2001, **344**:539-548.
  153. Li S, Ross DT, Kadin ME, Brown PO, Wasik MA: **Comparative genome-scale analysis of gene expression profiles in T cell lymphoma cells during malignant progression using a complementary DNA microarray.** *American Journal of Pathology* 2001, **158**:1231-1237.
  154. Luo J, Duggan DJ, Chen Y, Sauvageot J, Ewing CM, Bittner ML, Trent JM, Isaacs WB: **Human prostate cancer and benign prostatic hyperplasia: molecular dissection by gene expression profiling.** *Cancer Research* 2001, **61**:4683-4688.
  155. Pinkel D, Segraves R, Sudar D, Clark S, Poole I, Kowbel D, Collins C, Kuo WL, Chen C, Zhai Y, et al.: **High resolution analysis of DNA copy number variation using comparative genomic hybridization to microarrays.** *Nature Genetics* 1998, **20**:207-211.
  156. Pollack JR, Perou CM, Alizadeh AA, Eisen MB, Pergamenschikov A, Williams CF, Jeffrey SS, Botstein D, Brown PO: **Genome-wide analysis of DNA copy-number changes using cDNA microarrays.** *Nature Genetics* 1999, **23**:41-46.
  157. Lucito R, West J, Reiner A, Alexander J, Esposito D, Mishra B, Powers S, Norton L, Wigler M: **Detecting gene copy number fluctuations in tumor cells by microarray analysis of genomic representations.** *Genome Research* 2000, **10**:1726-1736.
-

- 158. Monni O, Barlund M, Mousses S, Kononen J, Sauter G, Heiskanen M, Paavola P, Avela K, Chen Y, Bittner ML, et al.: **Comprehensive copy number and gene expression profiling of the 17q23 amplicon in human breast cancer.** *Proceedings of the National Academy of Sciences of the United States of America* 2001, **98**:5711-5716.
- 159. Hui AB, Lo KW, Yin XL, Poon WS, Ng HK: **Detection of multiple gene amplifications in glioblastoma multiforme using array-based comparative genomic hybridization.** *Laboratory Investigation* 2001, **81**:717-723.
- 160. Daigo Y, Chin SF, Gorringer KL, Bobrow LG, Ponder BA, Pharoah PD, Caldas C: **Degenerate oligonucleotide primed-polymerase chain reaction-based array comparative genomic hybridization for extensive amplicon profiling of breast cancers: A new approach for the molecular analysis of paraffin-embedded cancer tissue.** *American Journal of Pathology* 2001, **158**:1623-1631.
- 161. Mei R, Galipeau PC, Prass C, Berno A, Ghandour G, Patil N, Wolff RK, Chee MS, Reid BJ, Lockhart DJ: **Genome-wide detection of allelic imbalance using human SNPs and high-density DNA arrays.** *Genome Research* 2000, **10**:1126-1137.
- 162. Wen WH, Bernstein L, Lescallett J, Beazer-Barclay Y, Sullivan-Halley J, White M, Press MF: **Comparison of TP53 mutations identified by oligonucleotide microarray and conventional DNA sequence analysis.** *Cancer Research* 2000, **60**:2716-2722.
- 163. Ahrendt SA, Halachmi S, Chow JT, Wu L, Halachmi N, Yang SC, Wehage S, Jen J, Sidransky D: **Rapid p53 sequence analysis in primary lung cancer using an oligonucleotide probe array.** *Proceedings of the National Academy of Sciences of the United States of America* 1999, **96**:7382-7387.
- 164. Favis R, Barany F: **Mutation detection in K-ras, BRCA1, BRCA2, and p53 using PCR/LDR and a universal DNA microarray.** *Annals of the New York Academy of Sciences* 2000, **906**:39-43.
- 165. Favis R, Day JP, Gerry NP, Phelan C, Narod S, Barany F: **Universal DNA array detection of small insertions and deletions in BRCA1 and BRCA2.** *Nature Biotechnology* 2000, **18**:561-564.

166. Khanna M, Park P, Zirvi M, Cao W, Picon A, Day J, Paty P, Barany F: **Multiplex PCR/LDR for detection of K-ras mutations in primary colon tumors.** *Oncogene* 1999, **18**:27-38.
167. Hughes TR, Marton MJ, Jones AR, Roberts CJ, Stoughton R, Armour CD, Bennett HA, Coffey E, Dai H, He YD, et al.: **Functional discovery via a compendium of expression profiles.** *Cell* 2000, **102**:109-126.
168. Eisen MB, Spellman PT, Brown PO, Botstein D: **Cluster analysis and display of genome-wide expression patterns.** *Proceedings of the National Academy of Sciences of the United States of America* 1998, **95**:14863-14868.
169. Iyer VR, Eisen MB, Ross DT, Schuler G, Moore T, Lee JC, Trent JM, Staudt LM, Hudson J, Jr., Boguski MS, et al.: **The transcriptional program in the response of human fibroblasts to serum.** *Science* 1999, **283**:83-87.
170. Gachotte D, Eckstein J, Barbuch R, Hughes T, Roberts C, Bard M: **A novel gene conserved from yeast to humans is involved in sterol biosynthesis.** *Journal of Lipid Research* 2001, **42**:150-154.
171. Marton MJ, DeRisi JL, Bennett HA, Iyer VR, Meyer MR, Roberts CJ, Stoughton R, Burchard J, Slade D, Dai HY, et al.: **Drug target validation and identification of secondary drug target effects using DNA microarrays.** *Nature Medicine* 1998, **4**:1293-1301.
172. Gray NS, Wodicka L, Thunnissen AM, Norman TC, Kwon S, Espinoza FH, Morgan DO, Barnes G, LeClerc S, Meijer L, et al.: **Exploiting chemical libraries, structure, and genomics in the search for kinase inhibitors.** *Science* 1998, **281**:533-538.
173. Wilson M, DeRisi J, Kristensen HH, Imboden P, Rane S, Brown PO, Schoolnik GK: **Exploring drug-induced alterations in gene expression in Mycobacterium tuberculosis by microarray hybridization.** *Proceedings of the National Academy of Sciences of the United States of America* 1999, **96**:12833-12838.

174. Nuwaysir EF, Bittner M, Trent J, Barrett JC, Afshari CA: **Microarrays and toxicology: The advent of toxicogenomics.** *Molecular Carcinogenesis* 1999, **24**:153-159.
175. Pennie WD, Woodyatt NJ, Aldridge TC, Orphanides G: **Application of genomics to the definition of the molecular basis for toxicity.** *Toxicology Letters* 2001, **120**:353-358.
176. Gerhold D, Lu M, Xu J, Austin C, Caskey CT, Rushmore T: **Monitoring expression of genes involved in drug metabolism and toxicology using DNA microarrays.** *Physiological Genomics* 2001, **5**:161-170.
177. Bartosiewicz MJ, Jenkins D, Penn S, Emery J, Buckpitt A: **Unique gene expression patterns in liver and kidney associated with exposure to chemical toxicants.** *The Journal of Pharmacology and Experimental Therapeutics* 2001, **297**:895-905.
178. Burczynski ME, McMillian M, Ciervo J, Li L, Parker JB, Dunn RT, 2nd, Hicken S, Farr S, Johnson MD: **Toxicogenomics-based discrimination of toxic mechanism in HepG2 human hepatoma cells.** *Toxicological Sciences* 2000, **58**:399-415.
179. Waring JF, Ciurlionis R, Jolly RA, Heindel M, Ulrich RG: **Microarray analysis of hepatotoxins in vitro reveals a correlation between gene expression profiles and mechanisms of toxicity.** *Toxicology Letters* 2001, **120**:359-368.
180. Geiss GK, Bumgarner RE, An MC, Agy MB, van 't Wout AB, Hammersmark E, Carter VS, Upchurch D, Mullins JI, Katze MG: **Large-scale monitoring of host cell gene expression during HIV-1 infection using cDNA microarrays.** *Virology* 2000, **266**:8-16.
181. Chambers J, Angulo A, Amaratunga D, Guo H, Jiang Y, Wan JS, Bittner A, Frueh K, Jackson MR, Peterson PA, et al.: **DNA microarrays of the complex human cytomegalovirus genome: Profiling kinetic class with drug sensitivity of viral gene expression.** *Journal of Virology* 1999, **73**:5757-5766.

182. Zhu H, Cong JP, Mamtora G, Gingeras T, Shenk T: **Cellular gene expression altered by human cytomegalovirus: Global monitoring with oligonucleotide arrays.** *Proceedings of the National Academy of Sciences of the United States of America* 1998, **95**:14470-14475.
  183. Paulose-Murphy M, Ha NK, Xiang C, Chen Y, Gillim L, Yarchoan R, Meltzer P, Bittner M, Trent J, Zeichner S: **Transcription program of human herpesvirus 8 (kaposi's sarcoma-associated herpesvirus).** *Journal of Virology* 2001, **75**:4843-4853.
  184. Mossman KL, Macgregor PF, Rozmus JJ, Goryachev AB, Edwards AM, Smiley JR: **Herpes simplex virus triggers and then disarms a host antiviral response.** *Journal of Virology* 2001, **75**:750-758.
  185. Cohen P, Bouaboula M, Bellis M, Baron V, Jbilo O, Poinot-Chazel C, Galiegue S, Hadibi EH, Casellas P: **Monitoring cellular responses to *Listeria monocytogenes* with oligonucleotide arrays.** *Journal of Biological Chemistry* 2000, **275**:11181-11190.
  186. Israel DA, Salama N, Arnold CN, Moss SF, Ando T, Wirth HP, Tham KT, Camorlinga M, Blaser MJ, Falkow S, et al.: ***Helicobacter pylori* strain-specific differences in genetic content, identified by microarray, influence host inflammatory responses.** *The Journal of Clinical Investigation* 2001, **107**:611-620.
  187. Eckmann L, Smith JR, Housley MP, Dwinell MB, Kagnoff MF: **Analysis by high density cDNA arrays of altered gene expression in human intestinal epithelial cells in response to infection with the invasive enteric bacteria *Salmonella*.** *Journal of Biological Chemistry* 2000, **275**:14084-14094.
  188. Rosenberger CM, Scott MG, Gold MR, Hancock RE, Finlay BB: ***Salmonella typhimurium* infection and lipopolysaccharide stimulation induce similar changes in macrophage gene expression.** *Journal of Immunology* 2000, **164**:5894-5904.
  189. Detweiler CS, Cunanan DB, Falkow S: **Host microarray analysis reveals a role for the *Salmonella* response regulator phoP in human macrophage cell death.** *Proceedings of the National Academy of Sciences of the United States of America* 2001, **98**:5850-5855.
-



190. Honda M, Kaneko S, Kawai H, Shirota Y, Kobayashi K: **Differential gene expression between chronic hepatitis B and C hepatic lesion.** *Gastroenterology* 2001, **120**:955-966.
191. Ben Mamoun C, Gluzman IY, Hott C, MacMillan SK, Amarakone AS, Anderson DL, Carlton JM, Dame JB, Chakrabarti D, Martin RK, et al.: **Co-ordinated programme of gene expression during asexual intraerythrocytic development of the human malaria parasite *Plasmodium falciparum* revealed by microarray analysis.** *Molecular Microbiology* 2001, **39**:26-36.
192. Troesch A, Nguyen H, Miyada CG, Desvarenne S, Gingeras TR, Kaplan PM, Cros P, Mabilat C: **Mycobacterium species identification and rifampin resistance testing with high-density DNA probe arrays.** *Journal of Clinical Microbiology* 1999, **37**:49-55.
193. Gingeras TR, Ghandour G, Wang E, Berno A, Small PM, Drobniewski F, Alland D, Desmond E, Holodniy M, Drenkow J: **Simultaneous genotyping and species identification using hybridization pattern recognition analysis of generic Mycobacterium DNA arrays.** *Genome Research* 1998, **8**:435-448.
194. Behr MA, Wilson MA, Gill WP, Salamon H, Schoolnik GK, Rane S, Small PM: **Comparative genomics of BCG vaccines by whole-genome DNA microarray.** *Science* 1999, **284**:1520-1523.
195. Kato-Maeda M, Rhee JT, Gingeras TR, Salamon H, Drenkow J, Smittipat N, Small PM: **Comparing genomes within the species *Mycobacterium tuberculosis*.** *Genome Research* 2001, **11**:547-554.
196. Li J, Chen S, Evans DH: **Typing and subtyping influenza virus using DNA microarrays and multiplex reverse transcriptase PCR.** *Journal of Clinical Microbiology* 2001, **39**:696-704.
197. Salama N, Guillemin K, McDaniel TK, Sherlock G, Tompkins L, Falkow S: **A whole-genome microarray reveals genetic diversity among *Helicobacter pylori* strains.** *Proceedings of the National Academy of Sciences of the United States of America* 2000, **97**:14668-14673.

198. Kozal MJ, Shah N, Shen N, Yang R, Fucini R, Merigan TC, Richman DD, Morris D, Hubbell E, Chee M, et al.: **Extensive polymorphisms observed in HIV-1 clade B protease gene using high-density oligonucleotide arrays.** *Nature Medicine* 1996, **2**:753-759.
199. Anthony RM, Brown TJ, French GL: **Rapid diagnosis of bacteremia by universal amplification of 23S ribosomal DNA followed by hybridization to an oligonucleotide array.** *Journal of Clinical Microbiology* 2000, **38**:781-788.
200. Lee CK, Klopp RG, Weindruch R, Prolla TA: **Gene expression profile of aging and its retardation by caloric restriction.** *Science* 1999, **285**:1390-1393.
201. Lee CK, Weindruch R, Prolla TA: **Gene-expression profile of the ageing brain in mice.** *Nature Genetics* 2000, **25**:294-297.
202. Weindruch R, Kayo T, Lee CK, Prolla TA: **Microarray profiling of gene expression in aging and its alteration by caloric restriction in mice.** *The Journal of Nutrition* 2001, **131**:918S-923S.
203. Cirelli C, Tononi G: **Differences in brain gene expression between sleep and waking as revealed by mRNA differential display and cDNA microarray technology.** *Journal of Sleep Research* 1999, **8 Suppl** 1:44-52.
204. Cirelli C, Tononi G: **Gene expression in the brain across the sleep-waking cycle.** *Brain Research* 2000, **885**:303-321.
205. Cirelli C, Tononi G: **Differential expression of plasticity-related genes in waking and sleep and their regulation by the noradrenergic system.** *The Journal of Neuroscience* 2000, **20**:9187-9194.
206. Lewohl JM, Dodd PR, Mayfield RD, Harris RA: **Application of DNA microarrays to study human alcoholism.** *Journal of Biomedical Science* 2001, **8**:28-36.

# An Electrochemical System for DNA Microarray Fabrication

## REFERENCES GUIDE

Ryan David Egeland  
Lincoln College  
University of Oxford

*This guide is provided as a convenience to the reader in reviewing citations in the main thesis.  
A full references list is included, and a CD-ROM contains full-text references for many of the  
thesis citations.*

*For University of Oxford academic and scholarly use only.*



## References Guide

*The following duplicate references list is provided as a convenience to the reader. In addition to listing all citations in the thesis, this reference list also contains a final underlined filename field for most references. If this underlined filename is present, the full-text of the article is available on the accompanying CD-ROM. The full-text reference may be accessed by opening the appropriate filename on the CD-ROM with Adobe Acrobat or other PDF viewer. References which do not have a PDF filename listed were not available from University of Oxford online resources.*

*Please note copyright restrictions permit using the full-text references for University of Oxford scholarly and academic pursuits only.*

1. Lockhart DJ, Dong HL, Byrne MC, Follettie MT, Gallo MV, Chee MS, Mittmann M, Wang CW, Kobayashi M, Horton H, et al.: **Expression monitoring by hybridization to high-density oligonucleotide arrays.** *Nature Biotechnology* 1996, **14**:1675-1680.
2. Schena M, Shalon D, Heller R, Chai A, Brown PO, Davis RW: **Parallel human genome analysis: microarray-based expression monitoring of 1000 genes.** *Proceedings of the National Academy of Sciences of the United States of America* 1996, **93**:10614-10619. [SchenaM-PNASUSA-96-10614.pdf](#)
3. Schena M, Shalon D, Davis RW, Brown PO: **Quantitative monitoring of gene expression patterns with a complementary DNA microarray.** *Science* 1995, **270**:467-470. [SchenaM-S-95-467.pdf](#)
4. Mir KU, Southern EM: **Sequence variation in genes and genomic DNA: methods for large-scale analysis.** *Annual Review of Genomics and Human Genetics* 2000, **1**:329-360. [MirKU-ARGHG-00-329.pdf](#)
5. Wang W, Montgomery D: **Electrochemically mediated Michael additions for carbon-carbon bond formation on microchips.** *Abstracts of Papers of the American Chemical Society* 1998, **216**:184.

6. Southern EM, Milner N, Mir KU: **Discovering antisense reagents by hybridization of RNA to oligonucleotide arrays.** *Ciba Foundation Symposium* 1997, **209**:38-44.
7. Southern E, Mir K, Shchepinov M: **Molecular interactions on microarrays.** *Nature Genetics* 1999, **21**:5-9. [SouthernE-NG-99-5.pdf](#)
8. Southern EM, Case-Green SC, Elder JK, Johnson M, Mir KU, Wang L, Williams JC: **Arrays of complementary oligonucleotides for analysing the hybridisation behaviour of nucleic acids.** *Nucleic Acids Research* 1994, **22**:1368-1373.
9. Chee M, Yang R, Hubbell E, Berno A, Huang XC, Stern D, Winkler J, Lockhart DJ, Morris MS, Fodor SPA: **Accessing genetic information with high-density DNA arrays.** *Science* 1996, **274**:610-614. [CheeM-S-96.610.pdf](#)
10. Cargill M, Altshuler D, Ireland J, Sklar P, Ardlie K, Patil N, Shaw N, Lane CR, Lim EP, Kalyanaraman N, et al.: **Characterization of single-nucleotide polymorphisms in coding regions of human genes.** *Nature Genetics* 1999, **22**:231-238. [CargillM-NG-99-231.pdf](#)
11. Halushka MK, Fan JB, Bentley K, Hsie L, Shen N, Weder A, Cooper R, Lipshutz R, Chakravarti A: **Patterns of single-nucleotide polymorphisms in candidate genes for blood-pressure homeostasis.** *Nature Genetics* 1999, **22**:239-247. [HalushkaMK-NG-99-239.pdf](#)
12. Bulyk ML, Gentalen E, Lockhart DJ, Church GM: **Quantifying DNA-protein interactions by double-stranded DNA arrays.** *Nature Biotechnology* 1999, **17**:573-577. [BulykML-NB-99-573.pdf](#)
13. Pirrung MC: **Spatially addressable combinatorial libraries.** *Chemical Reviews* 1997, **97**:473-488. [PirrungMC-CR-97-473.pdf](#)
14. Pirrung MC: **How to make a DNA chip.** *Angewandte Chemie-International Edition* 2002, **41**:1277-1289. [PirrungMC-ACIE-02-1276.pdf](#)
15. Blohm DH, Guiseppi-Elie A: **New developments in microarray technology.** *Current Opinion in Biotechnology* 2001, **12**:41-47.
16. Brenner S, Johnson M, Bridgham J, Golda G, Lloyd DH, Johnson D, Luo SJ, McCurdy S, Foy M, Ewan M, et al.: **Gene expression analysis by massively parallel signature sequencing (MPSS) on microbead arrays.** *Nature Biotechnology* 2000, **18**:630-634. [BrennerS-NB-00-630.pdf](#)
17. Singh-Gasson S, Green RD, Yue YJ, Nelson C, Blattner F, Sussman MR, Cerrina F: **Maskless fabrication of light-directed oligonucleotide mi-**

- croarrays using a digital micromirror array.** *Nature Biotechnology* 1999, **17**:974-978. [SinghGassonS-NB-99-974.pdf](#)
18. Fodor SPA: **DNA sequencing - Massively parallel genomics.** *Science* 1997, **277**:393. [FodorSPA-S-97-393.pdf](#)
  19. Gao XL, Yu PL, LeProust E, Sonigo L, Pellois JP, Zhang H: **Oligonucleotide synthesis using solution photogenerated acids.** *Journal of the American Chemical Society* 1998, **120**:12698-12699. [GaoXL-JACS-98-12698.pdf](#)
  20. Hughes TR, Linsley P, Marton M, Roberts C, Jones A, Stoughton R, Shoemaker D, Blanchard A, Phillips J, Ziman M, et al.: **Large-scale discovery of gene functions using an ink-jet oligonucleotide synthesizer and a compendium of DNA microarray expression profiles.** *American Journal of Human Genetics* 2000, **67**:212.
  21. Ferguson J, Steemers F, Schauer C, Michael K, Taylor L, Walt DR: **Randomly ordered, high-density, fiber-optic, microsensor-array sensors.** *Abstracts of Papers of the American Chemical Society* 2000, **219**:235.
  22. Gieglich H, Eisele-Buhler S, Hermann C, Kvasnyuk E, Charubala R, Pfeleiderer W: **New photolabile protecting groups in nucleoside and nucleotide chemistry -- Synthesis, cleavage mechanisms and applications.** *Nucleosides & Nucleotides* 1998, **17**:1987-1996.
  23. McGall GH, Barone AD, Diggelmann M, Fodor SPA, Gentalen E, Ngo N: **The efficiency of light-directed synthesis of DNA arrays on glass substrates.** *Journal of the American Chemical Society* 1997, **119**:5081-5090. [McgallGH-JACS-97-5081.pdf](#)
  24. Southern EM, Maskos U, Elder JK: **Analyzing and comparing nucleic acid sequences by hybridization to arrays of oligonucleotides: Evaluation using experimental models.** *Genomics* 1992, **13**:1008-1017.
  25. Case-Green SC, Mir KU, Pritchard CE, Southern EM: **Analysing genetic information with DNA arrays.** *Current Opinion in Biotechnology* 1998, **2**:404-410. [CaseGreenSC-COCB-98-404.pdf](#)
  26. Stimpson DI, Cooley PW, Knepper SM, Wallace DB: **Parallel production of oligonucleotide arrays using membranes and reagent jet printing.** *Biotechniques* 1998, **25**:886-890.
  27. Okamoto T, Suzuki T, Yamamoto N: **Microarray fabrication with covalent attachment of DNA using Bubble Jet technology.** *Nature Biotechnology* 2000, **18**:438-441. [OkamotoT-NB-00-438.pdf](#)
-

28. Hughes TR, Mao M, Jones AR, Burchard J, Marton M, Shannon KW, Lefkowitz SM, Ziman M, Schelter J: **Expression profiling using microarrays fabricated by an ink-jet oligonucleotide synthesizer.** *Nature Biotechnology* 2001, **19**:342-347. [HughesTR-NB-01-342.pdf](#)
29. Bond AM: **200 years of practical electroanalytical chemistry: Past, present and future directions illustrated by reference to the on-line, on-stream and off-line determination of trace metals in zinc plant electrolyte by voltammetric and potentiometric techniques.** *Analytica Chimica Acta* 1999, **400**:333-379. [BondAM-ACA-99-333.pdf](#)
30. Kyriacou DK: *Basics of Electroorganic Synthesis*. New York: Wiley; 1981.
31. Bard AJ, Denuault G, Lee C, Mandler D, Wipf DO: **Scanning electrochemical microscopy - a new technique for the characterization and modification of surfaces.** *Accounts of Chemical Research* 1990, **23**:357-363. [BardAJ-ACR-90-357.pdf](#)
32. Schuster R, Kirchner V, Allongue P, Ertl G: **Electrochemical micro-machining.** *Science* 2000, **289**:98-101. [SchusterR-S-00-98.pdf](#)
33. Livache T, Roget A, Dejean E, Barthet C, Bidan G, Teoule R: **Preparation of a DNA matrix via an electrochemically directed copolymerization of pyrrole and oligonucleotides bearing a pyrrole group.** *Nucleic Acids Research* 1994, **22**:2915-2921.
34. Livache T, Fouque B, Roget A, Marchand J, Bidan G, Teoule R, Mathis G: **Polypyrrole DNA chip on a silicon device: Example of hepatitis C virus genotyping.** *Analytical Biochemistry* 1998, **255**:188-194. [LivacheT-AB-98-165.pdf](#)
35. Bu HZ, Mikkelsen SR, English AM: **NAD(P)H sensors based on enzyme entrapment in ferrocene-containing polyacrylamide-based redox gels.** *Analytical Chemistry* 1998, **70**:4320-4325. [BuHZ-AC-98-4320.pdf](#)
36. Livache T, Bazin H, Caillat P, Roget A: **Electroconducting polymers for the construction of DNA or peptide arrays on silicon chips.** *Biosensors & Bioelectronics* 1998, **13**:629-634. [LivacheT-BB-98-629.pdf](#)
37. Montgomery D: **Electrochemical solid phase synthesis of polymers.** US Patent 1998, PCT/US97/11463.
38. Montgomery D, Udem BL: **CombiMatrix' customizable DNA microarrays -- Tutorial: In situ computer-aided synthesis of custom oligo microarrays.** *Genetic Engineering News* 2002, **22**:32-33.
39. Kyriacou DK: *Modern Electroorganic Chemistry*. Berlin ; New York: Springer-Verlag; 1994.



40. Volke J, Liska, F.: *Electrochemistry in Organic Synthesis*. London: Springer-Verlag; 1994.
41. Hashimoto K, Ito K, Ishimori Y: **Sequence-specific gene detection with a gold electrode modified with DNA probes and an electrochemically active dye**. *Analytical Chemistry* 1994, **66**:3830-3833. [HashimotoK-AC-94-3830.pdf](#)
42. Millan KM, Spurmanis AJ, Mikkelsen SR: **Covalent immobilization of DNA onto glassy-carbon electrodes**. *Electroanalysis* 1992, **4**:929-932.
43. Zhao YD, Pang DW, Wang ZL, Cheng JK, Qi YP: **DNA-modified electrodes 2: Electrochemical characterization of gold electrodes modified with DNA**. *Journal of Electroanalytical Chemistry* 1997, **431**:203-209. [ZhaoYD-JEC-97-203.pdf](#)
44. Fodor SPA, Read JL, Pirrung MC, Stryer L, Lu AT, Solas D: **Light-directed, spatially addressable parallel chemical synthesis**. *Science* 1991, **251**:767-773. [FodorSPA-S-91-767.pdf](#)
45. Hacia JG, Brody LC, Collins FS: **Applications of DNA chips for genomic analysis**. *Molecular Psychiatry* 1998, **3**:483-492. [HaciaJG-MP-98-483.pdf](#)
46. Cheng J, Sheldon EL, Wu L, Uribe A, Gerrue LO, Carrino J, Heller MJ, O'Connell JP: **Preparation and hybridization analysis of DNA/RNA from E-coli on microfabricated bioelectronic chips**. *Nature Biotechnology* 1998, **16**:541-546.
47. Hughes TR, Shoemaker DD: **DNA microarrays for expression profiling**. *Current Opinion in Chemical Biology* 2001, **5**:21-25. [HughesTR-COCB-01-21.pdf](#)
48. Manz A: **What can chips technology offer for next century's chemistry and life sciences?** *Chimia* 1996, **50**:140-143. [Not found](#)
49. Wang J: **Amperometric biosensors for clinical and therapeutic drug monitoring: A review**. *Journal of Pharmaceutical and Biomedical Analysis* 1999, **19**:47-53. [WangJ-JPBA-99-47.pdf](#)
50. Cheng J, Sheldon EL, Wu L, Heller MJ, O'Connell JP: **Isolation of cultured cervical carcinoma cells mixed with peripheral blood cells on a bioelectronic chip**. *Analytical Chemistry* 1998, **70**:2321-2326. [ChengJ-AC-98-2321.pdf](#)
51. Suzuki H: **Advances in the microfabrication of electrochemical sensors and systems**. *Electroanalysis* 2000, **12**:703-715. [SuzukiH-E-00-703.pdf](#)

52. Fiaccabrino GC, Koudelka-Hep M: **Thin-film microfabrication of electrochemical transducers.** *Electroanalysis* 1998, **10**:217-222. [FiaccabrinoGC-E-98-217.pdf](#)
  53. Liu CC, Zhang ZR: **Research-and-Development of Chemical Sensors Using Microfabrication Techniques.** *Selective Electrode Reviews* 1992, **14**:147-167.
  54. Wise KD, Najafi K: **Microfabrication Techniques for Integrated Sensors and Microsystems.** *Science* 1991, **254**:1335-1342. [WiseKD-S-91-5036.pdf](#)
  55. Schreiber SL: **Target-oriented and diversity-oriented organic synthesis in drug discovery.** *Science* 2000, **287**:1964-1969. [SchreiberSL-S-00-1964.pdf](#)
  56. Dolle RE, Nelson KH: **Comprehensive survey of combinatorial library synthesis: 1998.** *Journal of Combinatorial Chemistry* 1999, **1**:235-282. [DolleRE-JCC-99-235.pdf](#)
  57. Osborn HMI, Khan TH: **Recent developments in polymer supported syntheses of oligosaccharides and glycopeptides.** *Tetrahedron* 1999, **55**:1807-1850. [OsbornHMI-T-99-1807.pdf](#)
  58. Gait MJ: *Oligonucleotide Synthesis : A Practical Approach*. Oxford: IRL Press; 1984.
  59. Southern EM, Maskos U: **Parallel synthesis and analysis of large numbers of related chemical compounds: applications to oligonucleotides.** *Journal of Biotechnology* 1994, **35**:217-227.
  60. Stanton L, Bruhn L, Weist D, Lightfoot S, Villaneuva H, Collins S, Sum C, Ilsley-Tyree D, Webb P, Westall M, et al.: **Performance characterization of cDNA microarrays produced by thermal ink-jet (TIJ) deposition.** *American Journal of Human Genetics* 2000, **67**:1463.
  61. Roda A, Guardigli M, Russo C, Pasini P, Baraldini M: **Protein microdeposition using a conventional ink-jet printer.** *Biotechniques* 2000, **28**:492-496.
  62. McGall G, Labadie J, Brock P, Wallraff G, Nguyen T, Hinsberg W: **Light-directed synthesis of high-density oligonucleotide arrays using semiconductor photoresists.** *Proceedings of the National Academy of Sciences of the United States of America* 1996, **93**:13555-13560. [McGallG-PNAS-96-13555.pdf](#)
  63. Lund H, Baizer MM: *Organic Electrochemistry: An Introduction and Guide* edn 3, rev. and expanded. New York: M. Dekker; 1991.
-

64. Covington AK, Dickinson T: *Physical Chemistry of Organic Solvent Systems*, vol x: Plenum Press; 1973.
65. Zuman P, Polytechnic Institute of Brooklyn.: *The Elucidation of Organic Electrode Processes*. New York,: Academic Press; 1969.
66. Zuman P, Patel R: *Techniques in Organic Reaction Kinetics*. New York: Wiley; 1984.
67. Kirchner V, Xia XH, Schuster R: **Electrochemical nanostructuring with ultrashort voltage pulses**. *Accounts of Chemical Research* 2001, **34**:371-377. [KirchnerV-ACR-01-371.pdf](#)
68. Zu YB, Xie L, Mao BW, Tian ZW: **Studies on silicon etching using the confined etchant layer technique**. *Electrochimica Acta* 1998, **43**:1683-1690. [ZuYB-EA-98-1683.pdf](#)
69. Shiku H, Takeda T, Yamada H, Matsue T, Uchida I: **Microfabrication and characterization of diaphorase-patterned surfaces by scanning electrochemical microscopy**. *Analytical Chemistry* 1995, **67**:312-317. [ShikuH-AC-95-312.pdf](#)
70. Gray DE, Case-Green SC, Fell TS, Dobson PJ, Southern EM: **Ellipsometric and interferometric characterization of DNA probes immobilized on a combinatorial array**. *Langmuir* 1997, **13**:2833-2842. [GrayDE-L-97-2833.pdf](#)
71. Beaucage SL, Iyer RP: **Advances in the synthesis of oligonucleotides by the phosphoramidite approach**. *Tetrahedron* 1992, **48**:2223-2311. [BeaucageSL-T-92-2223.pdf](#)
72. Parker VD: **Hydroquinone-quinone redox behavior in acetonitrile**. *Journal of the Chemical Society: D* 1969:716-717.
73. Parker VD: **Anodic oxidation of hydroquinone in acetonitrile. Possible one electron intermediate**. *Electrochimica Acta* 1973, **18**:519-524.
74. Parker VD, Ebersson L: **Anodic oxidation of hydroquinone in acetonitrile**. *Journal of the Chemical Society: D* 1970:1289-1290.
75. Eggins BR: **Interpretation of electrochemical reduction and oxidation waves of quinone-hydroquinone system in acetonitrile**. *Journal of the Chemical Society: D* 1969:1267-1268.
76. Eggins BR: **One-electron intermediate in the anodic oxidation of hydroquinone in acetonitrile**. *Journal of the Chemistry Society, Chemical Communications* 1972:427.

77. Eggins BR, Chambers JQ: **Electrochemical oxidation of hydroquinone in acetonitrile.** *Chemical Communications* 1969:232-233.
78. Bauscher M, Maentele W: **Electrochemical and infrared-spectroscopic characterization of redox reactions of p-quinones.** *Journal of Physical Chemistry* 1992, **96**:11101-11108. [BauscherM-JPC-92-11101.pdf](#)
79. Yamanuki M, Hoshino T, Oyama M, Okazaki S: **Thin layer electrochemical Raman study of ion pair formation between the tetrachlorobenzoquinone anion radical and alkaline earth metal cations.** *Journal of Electroanalytical Chemistry* 1998, **458**:191-198. [YamanukiM-JEC-98-191.pdf](#)
80. Maskos U, Southern EM: **Oligonucleotide hybridizations on glass supports: A novel linker for oligonucleotide synthesis and hybridization properties of oligonucleotides synthesised in situ.** *Nucleic Acids Research* 1992, **20**:1679-1684.
81. Blanchard AP, Kaiser RJ, Hood LE: **High-density oligonucleotide arrays.** *Biosensors & Bioelectronics* 1996, **11**:687-690. [BlanchardAP-BB-96-687.pdf](#)
82. Forster AH, Krihak M, Swanson PD, Young TC, Ackley DE: **A laminated, flex structure for electronic transport and hybridization of DNA.** *Biosensors & Bioelectronics* 2001, **16**:187-194. [ForsterAH-BB-01-187.pdf](#)
83. Bond AM: **Past, present and future contributions of microelectrodes to analytical studies employing voltammetric detection -- A review.** *Analyst* 1994, **119**:R1-R21.
84. Alden JA, Feldman MA, Hill E, Prieto F, Oyama M, Coles BA, Compton RG, Dobson PJ, Leigh PA: **Channel microband electrode arrays for mechanistic electrochemistry. Two dimensional voltammetry: Transport-limited currents.** *Analytical Chemistry* 1998, **70**:1707-1720.
85. Mitchelson KR, Cheng J, Kricka LJ: **The use of capillary electrophoresis for point-mutation screening.** *Trends in Biotechnology* 1997, **15**:448-458. [MitchelsonKR-TB-97-448.pdf](#)
86. Huang Y, Ewalt KL, Tirado M, Haigis TR, Forster A, Ackley D, Heller MJ, O'Connell JP, Krihak M: **Electric manipulation of bioparticles and macromolecules on microfabricated electrodes.** *Analytical Chemistry* 2001, **73**:1549-1559. [HuangY-AC-01-1549.pdf](#)
87. Gilles PN, Wu DJ, Foster CB, Dillon PJ, Chanock SJ: **Single nucleotide polymorphic discrimination by an electronic dot blot assay on semi-**

- conductor microchips.** *Nature Biotechnology* 1999, **17**:365-370. [GillesPN-NB-99-365](#)
88. Pividori MI, Merkoci A, Alegret S: **Electrochemical genosensor design: immobilisation of oligonucleotides onto transducer surfaces and detection methods.** *Biosensors & Bioelectronics* 2000, **15**:291-303. [PividoriMI-BB-00-291.pdf](#)
89. Dill K, Montgomery DD, Wang W, Tsai JC: **Antigen detection using microelectrode array microchips.** *Analytica Chimica Acta* 2001, **444**:69-78. [DillK-ACA-01-69.pdf](#)
90. Huber M, Heiduschka P, Kienle S, Pavlidis C, Mack J, Walk T, Jung G, Thanos S: **Modification of glassy carbon surfaces with synthetic laminin-derived peptides for nerve cell attachment and neurite growth.** *Journal of Biomedical Materials Research* 1998, **41**:278-288. [HuberM-JBMR-98-278.pdf](#)
91. Khan GF, Kobatake E, Shinohara H, Ikariyama Y, Aizawa M: **Voltage-assisted peptide synthesis in aqueous solution by alpha-chymotrypsin immobilized in polypyrrole matrix.** *Journal of the American Chemical Society* 1996, **118**:1824-1830. [KhanGF-JACS-96-1824.pdf](#)
92. Zhang Z, Lei CH, Deng JQ: **Electrochemical fabrication of amperometric glucose enzyme electrode by immobilizing glucose oxidase in electropolymerized poly(3,3'-diaminobenzidine) film on palladinized glassy carbon electrode.** *Analyst* 1996, **121**:971-975.
93. Sadik OA: **Bioaffinity sensors based on conducting polymers: A short review.** *Electroanalysis* 1999, **11**:839-844. [SadikOA-E-99-839.pdf](#)
94. Egeland RD, Marken F, Southern EM: **An electrochemical redox couple activitated by microelectrodes for confined chemical patterning of surfaces.** *Analytical Chemistry* 2002, **74**:1590-1596. [EgelandRD-AC-02-1590.pdf](#)
95. Kounaves SP, Deng W, Hallock PR, Kovacs GTA, Storment CW: **Iridium-based ultramicroelectrode array fabricated by microlithography.** *Analytical Chemistry* 1994, **66**:418-423. [KounavesSP-AC-94-418.pdf](#)
96. Caruthers MH: **Chemical synthesis of DNA and DNA analogs.** *Accounts of Chemical Research* 1991, **24**:278-284. [CaruthersMH-ACR-91-278.pdf](#)
97. Oivanen M, Lonnberg H: **Kinetics and mechanisms for reactions of adenosine 2'- and 3'- monophosphates in aqueous acid -- Competition between phosphate migration, dephosphorylation, and depuri-**

- nation. *Journal of Organic Chemistry* 1989, **54**:2556-2560. [OivanenM-JOC-89-2556.pdf](#)
98. Butkus VV, Kayushin AL, Berlin YA, Kolosov MN, Smirnov IV: **Cleavage of 5'-O-protecting trityl groups in oligodeoxynucleotide synthesis -- Effect of substrate structure and reaction conditions on the de-tritylation and depurination rates.** *Bioorganicheskaya Khimiya* 1983, **9**:1518-1530.
99. Wang DG, Fan JB, Siao CJ, Berno A, Young P, Sapolsky R, Ghandour G, Perkins N, Winchester E, Spencer J, et al.: **Large-scale identification, mapping, and genotyping of single-nucleotide polymorphisms in the human genome.** *Science* 1998, **280**:1077-1082. [WangDG-S-98-1077.pdf](#)
100. Hecker KH, Green SM, Kobayashi K: **Analysis and purification of nucleic acids by ion-pair reversed-phase high-performance liquid chromatography.** *Journal of Biochemical and Biophysical Methods* 2000, **46**:83-93. [HeckerKH-JBBM-00-83.pdf](#)
101. Septak M: **Kinetic studies on depurination and detritylation of CPG-bound intermediates during oligonucleotide synthesis.** *Nucleic Acids Research* 1996, **24**:3053-3058. [SeptakM-NAR-96-3053.pdf](#)
102. Meyer H, Drewer H, Grundig B, Cammann K, Kakerow R, Manoli Y, Mokwa W, Rospert M: **2-Dimensional imaging of O<sub>2</sub>, H<sub>2</sub>O<sub>2</sub>, and glucose distributions by an array of 400 individually addressable micro-electrodes.** *Analytical Chemistry* 1995, **67**:1164-1170. [MeyerH-AC-95-1164.pdf](#)
103. Polushin NN, Morocho AM, Chen BC, Cohen JS: **On the rapid deprotection of synthetic oligonucleotides and analogs.** *Nucleic Acids Research* 1994, **22**:639-645.
104. Duggan DJ, Bittner M, Chen YD, Meltzer P, Trent JM: **Expression profiling using cDNA microarrays.** *Nature Genetics* 1999, **21**:10-14. [DugganDJ-NG-99-10.pdf](#)
105. Yang YH, Dudoit S, Luu P, Lin DM, Peng V, Ngai J, Speed TP: **Normalization for cDNA microarray data: a robust composite method addressing single and multiple slide systematic variation.** *Nucleic Acids Research* 2002, **30**:art. no. e15. [YangYH-NAR-02-e15.pdf](#)
106. Brown CS, Goodwin PC, Sorger PK: **Image metrics in the statistical analysis of DNA microarray data.** *Proceedings of the National Academy of Sciences of the United States of America* 2001, **98**:8944-8949. [BrownCS-PNAS-01-8944.pdf](#)
-

107. Freeman TC, Lee K, Richardson PJ: **Analysis of gene expression in single cells.** *Current Opinion in Biotechnology* 1999, **10**:579-582. [FreemanTC-COB-99-579.pdf](#)
108. Evertsz EM, Au-Young J, Ruvolo MV, Lim AC, Reynolds MA: **Hybridization cross-reactivity within homologous gene families on glass cDNA microarrays.** *Biotechniques* 2001, **31**:1182,1184,1186.
109. Hoyt PR, Tack L, Jones BH, Van Dinther J, Staat S, Doktycz MJ: **Automated high-throughput probe production for DNA microarray analysis.** *Biotechniques* 2003, **34**:402-407.
110. Clark MD, Panopoulou GD, Cahill DJ, Bussow K, Lehrach H: **DUPLICATE Construction and analysis of arrayed cDNA libraries.** In *Cdna Preparation and Characterization*. Edited by: Academic Press Inc; 1999:205-233. Methods in Enzymology, vol 303.]
111. Drmanac R, Drmanac S: **cDNA screening by array hybridization.** In *cDNA Preparation and Characterization*. Edited by: Academic Press Inc; 1999:165-178. Methods in Enzymology, vol 303.]
112. Jobs M, Fredriksson S, Brookes AJ, Landegren U: **Effect of oligonucleotide truncation on single-nucleotide distinction by solid-phase hybridization.** *Analytical Chemistry* 2002, **74**:199-202. [JobsM-AC-02-199.pdf](#)
113. Trabesinger W, Schutz GJ, Gruber HJ, Schindler H, Schmidt T: **Detection of individual oligonucleotide pairing by single-molecule microscopy.** *Analytical Chemistry* 1999, **71**:279-283. [TrabesingerW-AC-99-279.pdf](#)
114. Vercoutere W, Akeson M: **Biosensors for DNA sequence detection.** *Current Opinion in Chemical Biology* 2002, **6**:816-822. [VercoutereW-COCB-02-816.pdf](#)
115. Selinger DW, Cheung KJ, Mei R, Johansson EM, Richmond CS, Blattner FR, Lockhart DJ, Church GM: **RNA expression analysis using a 30 base pair resolution Escherichia coli genome array.** *Nature Biotechnology* 2000, **18**:1262-1268. [SelingerDW-NB-00-1262.pdf](#)
116. Heller MJ, Forster AH, Tu E: **Active microelectronic chip devices which utilize controlled electrophoretic fields for multiplex DNA hybridization and other genomic applications.** *Electrophoresis* 2000, **21**:157-164. [HellerMJ-E-00-157.pdf](#)
117. Swanson P, Gelbart R, Atlas E, Yang L, Grogan T, Butler WF, Ackley DE, Sheldon E: **A fully multiplexed CMOS biochip for DNA analysis.** *Sensors and Actuators B-Chemical* 2000, **64**:22-30. [SwansonP-SABC-00-22.pdf](#)

118. Pease AC, Solas D, Sullivan EJ, Cronin MT, Holmes CP, Fodor SPA: **Light-generated oligonucleotide arrays for rapid DNA-sequence analysis.** *Proceedings of the National Academy of Sciences of the United States of America* 1994, **91**:5022-5026. [PeaseAC-PNASUSA-94-5022.pdf](#)
119. Cerrina F, Blattner F, Huang W, Hue Y, Green R, Singh-Gasson S, Sussman M: **Biological lithography: Development of a maskless microarray synthesizer for DNA chips.** *Microelectronic Engineering* 2002, **61-2**:33-40. [CerrinaF-ME-02-33.pdf](#)
120. Sampsell JB: **Digital micromirror device and its application to projection displays.** *Journal of Vacuum Science & Technology B* 1994, **12**:3242-3246. [SampsellJB-JVSTB-94-3242.pdf](#)
121. Stetsenko DA, Gait MJ: **Efficient conjugation of peptides to oligonucleotides by "native ligation".** *Journal of Organic Chemistry* 2000, **65**:4900-4908.
122. Stetsenko DA, Malakhov AD, Gait MJ: **Total stepwise solid-phase synthesis of oligonucleotide-(3' --> N)-peptide conjugates.** *Organic Letters* 2002, **4**:3259-3262.
123. Nuwaysir EF, Huang W, Albert TJ, Singh J, Nuwaysir K, Pitas A, Richmond T, Gorski T, Berg JP, Ballin J, et al.: **Gene expression analysis using oligonucleotide arrays produced by maskless photolithography.** *Genome Research* 2002, **12**:1749-1755. [NuwaysirEF-GR-02-1749.pdf](#)
124. Beier M, Baum M, Rebscher H, Mauritz R, Wixmerten A, Stahler CF, Muller M, Stahler PF: **Exploring nature's plasticity with a flexible probing tool, and finding new ways for its electronic distribution.** *Biochemical Society Transactions* 2002, **30**:78-82. [BeierM-BST-02-78.pdf](#)
125. Beier M, Stephan A, Hoheisel JD: **Synthesis of photolabile 5'-O-phosphoramidites for the photolithographic production of microarrays of inversely oriented oligonucleotides.** *Helvetica Chimica Acta* 2001, **84**:2089-2095. [BeierM-HCA-01-2089.pdf](#)
126. Yang JN, Liu YJ, Rauch CB, Stevens RL, Liu RH, Lenigk R, Grodzinski P: **High sensitivity PCR assay in plastic micro reactors.** *Lab on a Chip* 2002, **2**:179-187. [YangJN-LC-02-179.pdf](#)
127. Weston DF, Smekal T, Rhine DB, Blackwell J: **Fabrication of microfluidic devices in silicon and plastic using plasma etching.** *Journal of Vacuum Science & Technology B* 2001, **19**:2846-2851. [WestonDF-JVSTB-01-2846.pdf](#)



128. Shi WM, Reed MR, Liu YB, Cheung LN, Wu RJ, Asatourians A, Park G, Coty WA: **Cystic fibrosis carrier screening using electrochemical detection on the eSensor (TM) DNA detection platform.** *Clinical Chemistry* 2002, **48**:12.
  129. Ramakrishnan R, Dorris D, Lublinsky A, Nguyen A, Domanus M, Prokhorova A, Gieser L, Touma E, Lockner R, Tata M, et al.: **An assessment of Motorola CodeLink (TM) microarray performance for gene expression profiling applications.** *Nucleic Acids Research* 2002, **30**:art. no.-e30. [RamakrishnanR-NAR-02-e30.pdf](#)
  130. Liu YJ, Rauch CB, Stevens RL, Lenigk R, Yang JN, Rhine DB, Grodzinski P: **DNA amplification and hybridization assays in integrated plastic monolithic devices.** *Analytical Chemistry* 2002, **74**:3063-3070. [LiuYJ-AC-02-3063.pdf](#)
  131. Lenigk R, Liu RH, Rhine D, Singhal P, Athavale M, Chen ZJ, Grodzinski P: **Optimization of DNA hybridization kinetics in microfluidic channels using electronic on-line detection.** *Abstracts of Papers of the American Chemical Society* 2002, **224**:027-BIOT.
  132. Dorris DR, Ramakrishnan R, Trakas D, Dudzik F, Belval R, Zhao C, Nguyen A, Domanus M, Mazumder A: **A highly reproducible, linear, and automated sample preparation method for DNA microarrays.** *Genome Research* 2002, **12**:976-984. [DorrisDR-GR-02-976.pdf](#)
  133. Macoska JA: **The progressing clinical utility of DNA microarrays.** *Ca: a Cancer Journal for Clinicians*. 2002, **52**:50-59. [MacoskaJA-CCJC-02-50.pdf](#)
  134. Van't Veer LJ, De Jong D: **The microarray way to tailored cancer treatment.** *Nature Medicine* 2002, **8**:13-14. [van'tVeerLJ-NM-02-13.pdf](#)
  135. Tian ZW, Fen ZD, Tian ZQ, Zhuo XD, Mu JQ, Li CZ, Lin HS, Ren B, Xie ZX, Hu WL: **Confined etchant layer technique for 2-dimensional lithography at high-resolution using electrochemical scanning-tunneling microscopy.** *Faraday Discussions* 1992:37-44.
  136. Schuster R, Kirchner V, Xia XH, Bittner AM, Ertl G: **Nanoscale electrochemistry.** *Physical Review Letters* 1998, **80**:5599-5602. [SchusterR-PRL-98-5599.pdf](#)
  137. Toussaint D, Wilczek F: **Particle antiparticle annihilation in diffusive motion.** *Journal of Chemical Physics* 1983, **78**:2642-2647. [ToussaintD-JCP-83-2642.pdf](#)
-

138. Ben-Naim E, Redner S: **Inhomogeneous 2-species annihilation in the steady-state.** *Journal of Physics A-Mathematical and General* 1992, **25**:L575-L583. [BennaimE-JPAMG-92-L575.pdf](#)
139. Mattis DC, Glasser ML: **The uses of quantum field theory in diffusion-limited reactions.** *Reviews of Modern Physics* 1998, **70**:979-1001. [MattisDC-RMP-98-979.pdf](#)
140. Lee BP, Cardy J: **Scaling of reaction zones in the  $A+B \rightarrow 0$  diffusion-limited reaction.** *Physical Review E* 1994, **50**:R3287-R3290. [LeeBP-PRE-94-R3287.pdf](#)
141. Cornell S, Droz M: **Steady-state reaction-diffusion front scaling for  $Ma+Nb \rightarrow [\text{inert}]$ .** *Physical Review Letters* 1993, **70**:3824-3827. [CornellS-PRL-93-3824.pdf](#)
142. Atkins PW: *Physical Chemistry* edn 5. Oxford: Oxford University Press; 1994.
143. Golub TR, Slonim DK, Tamayo P, Huard C, Gaasenbeek M, Mesirov JP, Coller H, Loh ML, Downing JR, Caligiuri MA, et al.: **Molecular classification of cancer: Class discovery and class prediction by gene expression monitoring.** *Science* 1999, **286**:531-537. [GolubTR-S-99-531.pdf](#)
144. Alizadeh AA, Eisen MB, Davis RE, Ma C, Lossos IS, Rosenwald A, Boldrick JC, Sabet H, Tran T, Yu X, et al.: **Distinct types of diffuse large B-cell lymphoma identified by gene expression profiling.** *Nature* 2000, **403**:503-511. [AlizadehAA-N-00-503.pdf](#)
145. Perou CM, Sorlie T, Eisen MB, van de Rijn M, Jeffrey SS, Rees CA, Pollack JR, Ross DT, Johnsen H, Akslen LA, et al.: **Molecular portraits of human breast tumours.** *Nature* 2000, **406**:747-752. [PerouCM-N-00-747.pdf](#)
146. Scherf U, Ross DT, Waltham M, Smith LH, Lee JK, Tanabe L, Kohn KW, Reinhold WC, Myers TG, Andrews DT, et al.: **A gene expression database for the molecular pharmacology of cancer.** *Nature Genetics* 2000, **24**:236-244. [ScherfU-NG-00-236.pdf](#)
147. Bittner M, Meltzer P, Chen Y, Jiang Y, Seftor E, Hendrix M, Radmacher M, Simon R, Yakhini Z, Ben-Dor A, et al.: **Molecular classification of cutaneous malignant melanoma by gene expression profiling.** *Nature* 2000, **406**:536-540. [BittnerM-N-00-536.pdf](#)
148. Khanna C, Khan J, Nguyen P, Prehn J, Caylor J, Yeung C, Trepel J, Meltzer P, Helman L: **Metastasis-associated differences in gene expression**

- in a murine model of osteosarcoma.** *Cancer Research* 2001, **61**:3750-3759. [KhannaC-CR-01-3750.pdf](#)
149. Clark EA, Golub TR, Lander ES, Hynes RO: **Genomic analysis of metastasis reveals an essential role for RhoC.** *Nature* 2000, **406**:532-535. [ClarkEA-N-00-532.pdf](#)
150. Alon U, Barkai N, Notterman DA, Gish K, Ybarra S, Mack D, Levine AJ: **Broad patterns of gene expression revealed by clustering analysis of tumor and normal colon tissues probed by oligonucleotide arrays.** *Proceedings of the National Academy of Sciences of the United States of America* 1999, **96**:6745-6750. [AlonU-PNASUSA-99-6745.pdf](#)
151. Ross DT, Scherf U, Eisen MB, Perou CM, Rees C, Spellman P, Iyer V, Jeffrey SS, Van de Rijn M, Waltham M, et al.: **Systematic variation in gene expression patterns in human cancer cell lines.** *Nature Genetics* 2000, **24**:227-235. [RossDT-NG-00-227.pdf](#)
152. Hedenfalk I, Duggan D, Chen Y, Radmacher M, Bittner M, Simon R, Meltzer P, Gusterson B, Esteller M, Kallioniemi OP, et al.: **Gene-expression profiles in hereditary breast cancer.** *New England Journal of Medicine* 2001, **344**:539-548. [Hedenfalk-NEJM-01-539.pdf](#)
153. Li S, Ross DT, Kadin ME, Brown PO, Wasik MA: **Comparative genome-scale analysis of gene expression profiles in T cell lymphoma cells during malignant progression using a complementary DNA microarray.** *American Journal of Pathology* 2001, **158**:1231-1237. [LiS-AJP-01-1231.pdf](#)
154. Luo J, Duggan DJ, Chen Y, Sauvageot J, Ewing CM, Bittner ML, Trent JM, Isaacs WB: **Human prostate cancer and benign prostatic hyperplasia: molecular dissection by gene expression profiling.** *Cancer Research* 2001, **61**:4683-4688. [LuoJ-CR-01-4683.pdf](#)
155. Pinkel D, Segraves R, Sudar D, Clark S, Poole I, Kowbel D, Collins C, Kuo WL, Chen C, Zhai Y, et al.: **High resolution analysis of DNA copy number variation using comparative genomic hybridization to microarrays.** *Nature Genetics* 1998, **20**:207-211. [PinkelD-NG-98-207.pdf](#)
156. Pollack JR, Perou CM, Alizadeh AA, Eisen MB, Pergamenschikov A, Williams CF, Jeffrey SS, Botstein D, Brown PO: **Genome-wide analysis of DNA copy-number changes using cDNA microarrays.** *Nature Genetics* 1999, **23**:41-46. [PollackJR-NG-99-41.pdf](#)
157. Lucito R, West J, Reiner A, Alexander J, Esposito D, Mishra B, Powers S, Norton L, Wigler M: **Detecting gene copy number fluctuations in tu-**

- mor cells by microarray analysis of genomic representations. *Genome Research* 2000, **10**:1726-1736. [Lucitor-GR-00-1726.pdf](#)
158. Monni O, Barlund M, Mousses S, Kononen J, Sauter G, Heiskanen M, Paavola P, Avela K, Chen Y, Bittner ML, et al.: **Comprehensive copy number and gene expression profiling of the 17q23 amplicon in human breast cancer.** *Proceedings of the National Academy of Sciences of the United States of America* 2001, **98**:5711-5716. [MonniO-PNASUSA-01-5711.pdf](#)
159. Hui AB, Lo KW, Yin XL, Poon WS, Ng HK: **Detection of multiple gene amplifications in glioblastoma multiforme using array-based comparative genomic hybridization.** *Laboratory Investigation* 2001, **81**:717-723. [HuiAB-LI-01-717.pdf](#)
160. Daigo Y, Chin SF, Gorringer KL, Bobrow LG, Ponder BA, Pharoah PD, Caldas C: **Degenerate oligonucleotide primed-polymerase chain reaction-based array comparative genomic hybridization for extensive amplicon profiling of breast cancers: A new approach for the molecular analysis of paraffin-embedded cancer tissue.** *American Journal of Pathology* 2001, **158**:1623-1631. [DaigoY-AJP-01-1623.pdf](#)
161. Mei R, Galipeau PC, Prass C, Berno A, Ghandour G, Patil N, Wolff RK, Chee MS, Reid BJ, Lockhart DJ: **Genome-wide detection of allelic imbalance using human SNPs and high-density DNA arrays.** *Genome Research* 2000, **10**:1126-1137. [MeiR-GR-00-1126.pdf](#)
162. Wen WH, Bernstein L, Lescallett J, Beazer-Barclay Y, Sullivan-Halley J, White M, Press MF: **Comparison of TP53 mutations identified by oligonucleotide microarray and conventional DNA sequence analysis.** *Cancer Research* 2000, **60**:2716-2722. [WenWH-CR-00-2716.pdf](#)
163. Ahrendt SA, Halachmi S, Chow JT, Wu L, Halachmi N, Yang SC, Wehage S, Jen J, Sidransky D: **Rapid p53 sequence analysis in primary lung cancer using an oligonucleotide probe array.** *Proceedings of the National Academy of Sciences of the United States of America* 1999, **96**:7382-7387. [AhrendtSA-PNASUSA-99-7382.pdf](#)
164. Favis R, Barany F: **Mutation detection in K-ras, BRCA1, BRCA2, and p53 using PCR/LDR and a universal DNA microarray.** *Annals of the New York Academy of Sciences* 2000, **906**:39-43.
165. Favis R, Day JP, Gerry NP, Phelan C, Narod S, Barany F: **Universal DNA array detection of small insertions and deletions in BRCA1 and BRCA2.** *Nature Biotechnology* 2000, **18**:561-564. [FavisR-NB-00-561.pdf](#)
-

166. Khanna M, Park P, Zirvi M, Cao W, Picon A, Day J, Paty P, Barany F: **Multiplex PCR/LDR for detection of K-ras mutations in primary colon tumors.** *Oncogene* 1999, **18**:27-38. [KhannaM-O-99-27.pdf](#)
167. Hughes TR, Marton MJ, Jones AR, Roberts CJ, Stoughton R, Armour CD, Bennett HA, Coffey E, Dai H, He YD, et al.: **Functional discovery via a compendium of expression profiles.** *Cell* 2000, **102**:109-126. [HughesTR-C-00-109.pdf](#)
168. Eisen MB, Spellman PT, Brown PO, Botstein D: **Cluster analysis and display of genome-wide expression patterns.** *Proceedings of the National Academy of Sciences of the United States of America* 1998, **95**:14863-14868. [EisenMB-PNASUSA-98-14863.pdf](#)
169. Iyer VR, Eisen MB, Ross DT, Schuler G, Moore T, Lee JC, Trent JM, Staudt LM, Hudson J, Jr., Boguski MS, et al.: **The transcriptional program in the response of human fibroblasts to serum.** *Science* 1999, **283**:83-87. [IyerVR-S-99-83.pdf](#)
170. Gachotte D, Eckstein J, Barbuch R, Hughes T, Roberts C, Bard M: **A novel gene conserved from yeast to humans is involved in sterol biosynthesis.** *Journal of Lipid Research* 2001, **42**:150-154. [GachotteD-JLR-01-150.pdf](#)
171. Marton MJ, DeRisi JL, Bennett HA, Iyer VR, Meyer MR, Roberts CJ, Stoughton R, Burchard J, Slade D, Dai HY, et al.: **Drug target validation and identification of secondary drug target effects using DNA microarrays.** *Nature Medicine* 1998, **4**:1293-1301. [MartonMJ-NM-98-1293.pdf](#)
172. Gray NS, Wodicka L, Thunnissen AM, Norman TC, Kwon S, Espinoza FH, Morgan DO, Barnes G, LeClerc S, Meijer L, et al.: **Exploiting chemical libraries, structure, and genomics in the search for kinase inhibitors.** *Science* 1998, **281**:533-538. [GrayNS-S-98-533.pdf](#)
173. Wilson M, DeRisi J, Kristensen HH, Imboden P, Rane S, Brown PO, Schoolnik GK: **Exploring drug-induced alterations in gene expression in Mycobacterium tuberculosis by microarray hybridization.** *Proceedings of the National Academy of Sciences of the United States of America* 1999, **96**:12833-12838. [WilsonM-PNASUSA-99-12833.pdf](#)
174. Nuwaysir EF, Bittner M, Trent J, Barrett JC, Afshari CA: **Microarrays and toxicology: The advent of toxicogenomics.** *Molecular Carcinogenesis* 1999, **24**:153-159. [NuwaysirEF-MC-99-153.pdf](#)
175. Pennie WD, Woodyatt NJ, Aldridge TC, Orphanides G: **Application of genomics to the definition of the molecular basis for toxicity.** *Toxicology Letters* 2001, **120**:353-358. [PennieWD-TL-01-353.pdf](#)

176. Gerhold D, Lu M, Xu J, Austin C, Caskey CT, Rushmore T: **Monitoring expression of genes involved in drug metabolism and toxicology using DNA microarrays.** *Physiological Genomics* 2001, **5**:161-170. [GerholdD-PG-01-161.pdf](#)
  177. Bartosiewicz MJ, Jenkins D, Penn S, Emery J, Buckpitt A: **Unique gene expression patterns in liver and kidney associated with exposure to chemical toxicants.** *The Journal of Pharmacology and Experimental Therapeutics* 2001, **297**:895-905. [BartosiewiczMJ-JPET-01-895](#)
  178. Burczynski ME, McMillian M, Ciervo J, Li L, Parker JB, Dunn RT, 2nd, Hicken S, Farr S, Johnson MD: **Toxicogenomics-based discrimination of toxic mechanism in HepG2 human hepatoma cells.** *Toxicological Sciences* 2000, **58**:399-415. [BurczynskiME-TS-00-399](#)
  179. Waring JF, Ciurlionis R, Jolly RA, Heindel M, Ulrich RG: **Microarray analysis of hepatotoxins in vitro reveals a correlation between gene expression profiles and mechanisms of toxicity.** *Toxicology Letters* 2001, **120**:359-368. [WaringJF-TL-01-359.pdf](#)
  180. Geiss GK, Bumgarner RE, An MC, Agy MB, van 't Wout AB, Hammersmark E, Carter VS, Upchurch D, Mullins JI, Katze MG: **Large-scale monitoring of host cell gene expression during HIV-1 infection using cDNA microarrays.** *Virology* 2000, **266**:8-16. [GeissGK-V-00-8.pdf](#)
  181. Chambers J, Angulo A, Amaratunga D, Guo H, Jiang Y, Wan JS, Bittner A, Frueh K, Jackson MR, Peterson PA, et al.: **DNA microarrays of the complex human cytomegalovirus genome: Profiling kinetic class with drug sensitivity of viral gene expression.** *Journal of Virology* 1999, **73**:5757-5766. [ChambersJ-JV-99-5757.pdf](#)
  182. Zhu H, Cong JP, Mamtora G, Gingeras T, Shenk T: **Cellular gene expression altered by human cytomegalovirus: Global monitoring with oligonucleotide arrays.** *Proceedings of the National Academy of Sciences of the United States of America* 1998, **95**:14470-14475. [ZhuH-PNASUSA-98-14470.pdf](#)
  183. Paulose-Murphy M, Ha NK, Xiang C, Chen Y, Gillim L, Yarchoan R, Meltzer P, Bittner M, Trent J, Zeichner S: **Transcription program of human herpesvirus 8 (kaposi's sarcoma-associated herpesvirus).** *Journal of Virology* 2001, **75**:4843-4853. [PauloseMurphyM-JV-01-4843.pdf](#)
  184. Mossman KL, Macgregor PF, Rozmus JJ, Goryachev AB, Edwards AM, Smiley JR: **Herpes simplex virus triggers and then disarms a host antiviral response.** *Journal of Virology* 2001, **75**:750-758. [MossmanKL-JV-01-750.pdf](#)
-

185. Cohen P, Bouaboula M, Bellis M, Baron V, Jbilo O, Poinot-Chazel C, Galiegue S, Hadibi EH, Casellas P: **Monitoring cellular responses to *Listeria monocytogenes* with oligonucleotide arrays.** *Journal of Biological Chemistry* 2000, **275**:11181-11190. [CohenP-JBC-00-11181.pdf](#)
186. Israel DA, Salama N, Arnold CN, Moss SF, Ando T, Wirth HP, Tham KT, Camorlinga M, Blaser MJ, Falkow S, et al.: ***Helicobacter pylori* strain-specific differences in genetic content, identified by microarray, influence host inflammatory responses.** *The Journal of Clinical Investigation* 2001, **107**:611-620. [IsraelDA-JCI-01-611.pdf](#)
187. Eckmann L, Smith JR, Housley MP, Dwinell MB, Kagnoff MF: **Analysis by high density cDNA arrays of altered gene expression in human intestinal epithelial cells in response to infection with the invasive enteric bacteria *Salmonella*.** *Journal of Biological Chemistry* 2000, **275**:14084-14094. [EckmannL-JBC-00-14084.pdf](#)
188. Rosenberger CM, Scott MG, Gold MR, Hancock RE, Finlay BB: ***Salmonella typhimurium* infection and lipopolysaccharide stimulation induce similar changes in macrophage gene expression.** *Journal of Immunology* 2000, **164**:5894-5904. [RosenbergerCM-JI-00-5894.pdf](#)
189. Detweiler CS, Cunanan DB, Falkow S: **Host microarray analysis reveals a role for the *Salmonella* response regulator *phoP* in human macrophage cell death.** *Proceedings of the National Academy of Sciences of the United States of America* 2001, **98**:5850-5855. [DetweilerCS-PNASUSA-01-5850.pdf](#)
190. Honda M, Kaneko S, Kawai H, Shirota Y, Kobayashi K: **Differential gene expression between chronic hepatitis B and C hepatic lesion.** *Gastroenterology* 2001, **120**:955-966. [HondaM-G-01-955.pdf](#)
191. Ben Mamoun C, Gluzman IY, Hott C, MacMillan SK, Amarakone AS, Anderson DL, Carlton JM, Dame JB, Chakrabarti D, Martin RK, et al.: **Co-ordinated programme of gene expression during asexual intraerythrocytic development of the human malaria parasite *Plasmodium falciparum* revealed by microarray analysis.** *Molecular Microbiology* 2001, **39**:26-36. [BenMamounC-MM-01-26.pdf](#)
192. Troesch A, Nguyen H, Miyada CG, Desvarenne S, Gingeras TR, Kaplan PM, Cros P, Mabilat C: ***Mycobacterium* species identification and rifampin resistance testing with high-density DNA probe arrays.** *Journal of Clinical Microbiology* 1999, **37**:49-55. [TroeschA-JCM-99-49.pdf](#)
193. Gingeras TR, Ghandour G, Wang E, Berno A, Small PM, Drobniowski F, Alland D, Desmond E, Holodniy M, Drenkow J: **Simultaneous genotyping and species identification using hybridization pattern recogni-**

- tion analysis of generic Mycobacterium DNA arrays.** *Genome Research* 1998, **8**:435-448. [GingerasTR-GR-98-435.pdf](#)
194. Behr MA, Wilson MA, Gill WP, Salamon H, Schoolnik GK, Rane S, Small PM: **Comparative genomics of BCG vaccines by whole-genome DNA microarray.** *Science* 1999, **284**:1520-1523. [BehrMA-S-99-1520.pdf](#)
  195. Kato-Maeda M, Rhee JT, Gingeras TR, Salamon H, Drenkow J, Smittipat N, Small PM: **Comparing genomes within the species Mycobacterium tuberculosis.** *Genome Research* 2001, **11**:547-554. [KatoMaedaM-GR-01-547.pdf](#)
  196. Li J, Chen S, Evans DH: **Typing and subtyping influenza virus using DNA microarrays and multiplex reverse transcriptase PCR.** *Journal of Clinical Microbiology* 2001, **39**:696-704. [Lij-JCM-01-696.pdf](#)
  197. Salama N, Guillemin K, McDaniel TK, Sherlock G, Tompkins L, Falkow S: **A whole-genome microarray reveals genetic diversity among Helicobacter pylori strains.** *Proceedings of the National Academy of Sciences of the United States of America* 2000, **97**:14668-14673. [SalamaN-PNASUSA-00-14668.pdf](#)
  198. Kozal MJ, Shah N, Shen N, Yang R, Fucini R, Merigan TC, Richman DD, Morris D, Hubbell E, Chee M, et al.: **Extensive polymorphisms observed in HIV-1 clade B protease gene using high-density oligonucleotide arrays.** *Nature Medicine* 1996, **2**:753-759.
  199. Anthony RM, Brown TJ, French GL: **Rapid diagnosis of bacteremia by universal amplification of 23S ribosomal DNA followed by hybridization to an oligonucleotide array.** *Journal of Clinical Microbiology* 2000, **38**:781-788. [AnthonyRM-JCM-00-781.pdf](#)
  200. Lee CK, Klopp RG, Weindruch R, Prolla TA: **Gene expression profile of aging and its retardation by caloric restriction.** *Science* 1999, **285**:1390-1393. [LeeCK-S-99-1390.pdf](#)
  201. Lee CK, Weindruch R, Prolla TA: **Gene-expression profile of the ageing brain in mice.** *Nature Genetics* 2000, **25**:294-297. [LeeCK-NG-00-294.pdf](#)
  202. Weindruch R, Kayo T, Lee CK, Prolla TA: **Microarray profiling of gene expression in aging and its alteration by caloric restriction in mice.** *The Journal of Nutrition* 2001, **131**:918S-923S. [WeindruchR-JN-01-918S.pdf](#)
  203. Cirelli C, Tononi G: **Differences in brain gene expression between sleep and waking as revealed by mRNA differential display and**



- cDNA microarray technology.** *Journal of Sleep Research* 1999, **8 Suppl 1**:44-52. [CirelliC-JSR-99-44.pdf](#)
204. Cirelli C, Tononi G: **Gene expression in the brain across the sleep-waking cycle.** *Brain Research* 2000, **885**:303-321. [CirelliC-BR-00-303.pdf](#)
205. Cirelli C, Tononi G: **Differential expression of plasticity-related genes in waking and sleep and their regulation by the noradrenergic system.** *The Journal of Neuroscience* 2000, **20**:9187-9194. [CirelliC-JN-00-9187.pdf](#)
206. Lewohl JM, Dodd PR, Mayfield RD, Harris RA: **Application of DNA microarrays to study human alcoholism.** *Journal of Biomedical Science* 2001, **8**:28-36.